doi : 10.17596/0003145

Preliminary Cruise Report

MR11-02

11 February - 9 March 2011

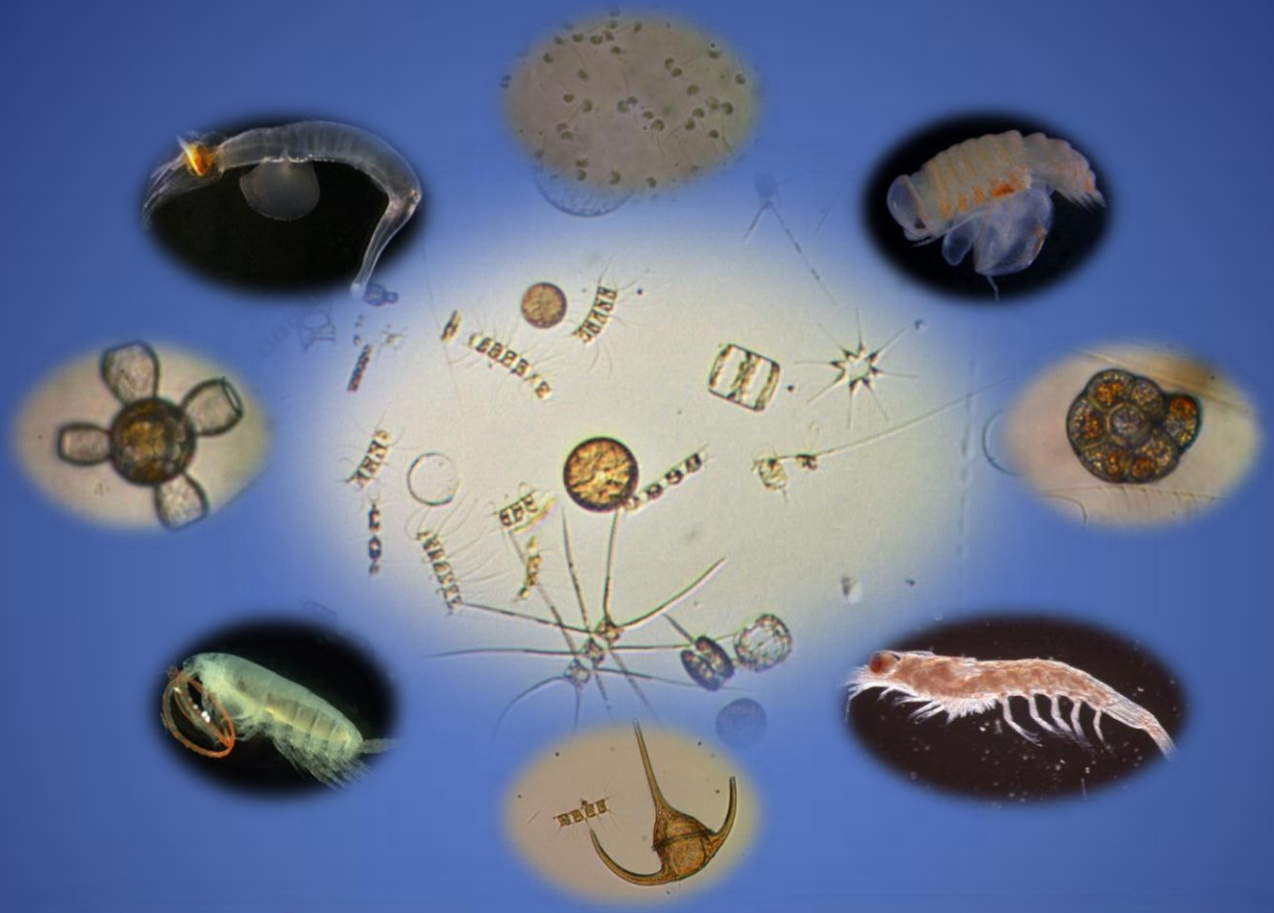

March 2011
JAMSTEC

Note

This cruise report is a preliminary documentation published in approximately a month after the end of this cruise. It may not be corrected even if changes on contents are found after publication. It may also be changed without notice. Data on the cruise report may be raw or not processed. Please ask the principal investigator and parsons in charge of respective observations for the latest information and permission before using. Users of data are requested to submit their results to JAMSTEC Data Integration and Analysis Group (DIAG).

31 March 2011

Principal Investigator of MR11-02

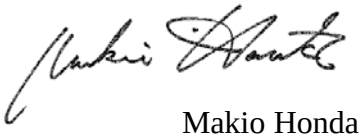

Makio Honda
JAMSTEC

Cruise Report ERRATA of the Nutrients part

page	Error	Correction
62	potassium nitrate CAS No. 7757-91-1	potassium nitrate CAS No. 7757-79-1
60	1N H2SO4	1M H2SO4

Cruise Report ERRATA of the Photosynthetic Pigments part

page	Error	Correction
90	Ethyl-apo-8'-carotenoate	trans-β-Apo-8'-carotenal

Contents of MR11-02 Preliminary Cruise Report

Cover sheet: the first prize of “MR11-02 CRUISE REPORT COVER SHEET CONTEST” by MR11-02 biology team (Kobari, Isami: Kagoshima Univ., Kitamura: JAMSTEC, Kawachi: NIES, Yubuki: Univ. of British Columbia)

A. Cruise summary

1. Cruise information

(1) Cruise designation (research vessel)
MR11-02 (R/V MIRAI)

(2) Cruise title (principal science proposal) and introduction
Change in material cycles and ecosystem by the climate change and its feedback
Introduction

Some disturbing effects are progressively coming to the fore in the ocean by climate change, such as rising water temperature, intensification of upper ocean stratification and ocean acidification. It is supposed that these effects result in serious damage to the ocean ecosystems. Disturbed ocean ecosystems will change a material cycle through the change of biological pump efficiency, and it will be fed back into the climate. We are aimed at clarifying the mechanisms of changes in the ocean structure in ocean ecosystems derived from the climate change,

We arranged the time-series observation stations in the subarctic gyre (K2: 47°N 160°E) and the subtropical gyre (S1: 30°N, 145°E) in the western North Pacific. In general, biological pump is more efficient in the subarctic gyre than the subtropical gyre because large size phytoplankton (diatom) is abundant in the subarctic gyre by its eutrophic oceanic condition. It is suspected that the responses against climate change are different for respective gyres. To elucidate the oceanic structures in ocean ecosystems and material cycles at both gyres is important to understand the relationship between ecosystem, material cycle and climate change in the global ocean.

There are significant seasonal variations in the ocean environments in both gyres. The seasonal variability of oceanic structures will be estimated by the mooring systems and by the seasonally repetitive ship observations scheduled for next several years.

(3) Principal Investigator (PI)
Makio Honda
Research Institute for Global Change (RIGC)
Japan Agency for Marine-Earth Science and Technology (JAMSTEC)

(4) Science proposals of cruise

Affiliation	PI	Proposal titles
AORI / The Univ. Tokyo	Koji HAMASAKI	Studies on the microbial-geochemical processes that regulate the operation of the biological pump in the subarctic and subtropical regions of the western North Pacific
Kagoshima Univ.	Toru KOBARI	Effects of meso-zooplankton on food web and vertical flux
Nagoya Univ.	Osamu ABE	An evaluation of past change of primary productivity at the region of NPIW formation using oxygen triple isotopes, O_2, N_2 and noble gases.
NIES	Masanobu KAWACHI	Taxonomy and genome analysis of eukaryotic picophytoplankton originated from cryopreserved marine environmental specimens
JAMSTEC	Makio HONDA	Research and development of optical measurement of marine snow

Okayama Univ.	Osamu TSUKAMOTO	Onboard continuous air-sea eddy flux measurement
Nagoya Univ,	Yoshihisa MINO	Settling velocity of particles in the twilight zone
JAMSTEC	Hisanori TAKASHIMA	Tropospheric aerosol and gas profile observations by MAX-DOAS on a research vessel
MRI	Michio AOYAMA	Long-term study on nutrients in global ocean
Toyama Univ.	Kazuma AOKI	Maritime aerosol optical properties from measurements of Ship-borne sky radiometer
JAMSTEC	Toshio SUGA	Study of ocean circulation and heat and freshwater transport and their variability, and experimental comprehensive study of physical, chemical, and biochemical processes in the western North Pacific by the deployment of Argo floats and using Argo data
NIES	Nobuo SUGIMOTO	Study of distribution and optical characteristics of ice/water clouds and marine aerosols
Chiba Univ.	Masao NAKANISHI	Tectonics of the mid-Cretaceous Pacific Plate
Ryukyu Univ.	Takeshi MATSUMOTO	Standardization of marine geophysical data and its application to the ocean floor geodynamics studies
JAMSTEC	Yoshimi KAWAI	Observational research on air-sea interaction in the Kuroshio-Oyashio Extension region
JAMSTEC	Naoyuki KURITA	Rain and seawater sampling for stable isotopes

(4) Cruise period (port call)
11 February 2011 (Sekinehama) – 9 March 2011 (Sekinehama)

(5) Cruise region (geographical boundary)
The western North Pacific (60°N – 30°N, 140°E – 165°W)

(6) Cruise truck and stations

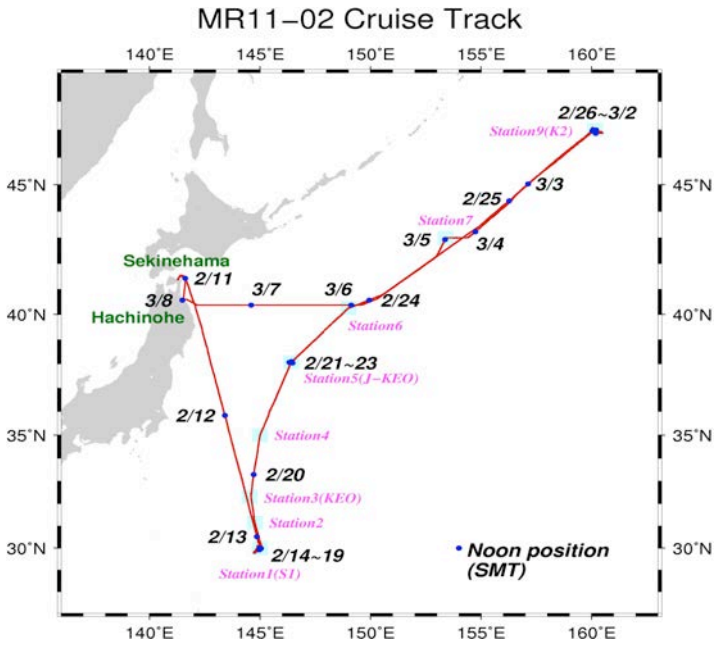

2. Overview of MR11-02

(1) Objective

Objective of this cruise is to collect biological, biogeochemical and physical data in winter at our western Pacific time-series stations K2 (sub-arctic gyre) and S1 (sub-tropical data).

(2) Overview of MR11-02

We originally planned to start our observation at station K2 and end that at station S1. However we left Sekine-hama for station S1 because weather and sea condition was predicted to be bad at station K2. This decision was right and we fortunately conducted various biogeochemical observations including hydrocasting, drifting buoy, in situ pumping and plankton sampling by large plankton net tow system (IONESS). In addition, we successfully exchange the meteorological sensor on NOAA-KEO surface buoy, recovered the stranded part of JAMSTEC-K-TRITON buoy mooring system which was partitioned by longline fishing last October, and we re-deployed K-TRITON buoy at JKEO station.

We were in trouble for bad weather and rough sea condition at station K2. We were forced to cancel several observations. However we was able to conduct minimum observation enough to verify winter oceanography at station K2.

The followings are preliminary results at station S1 and K2.

1) S1

Water temperature upper 200m was approximately 18°C (Fig. 1a) and the lowest among three cruises (MR10-01: January-February 2010, MR10-06: October–November 2010, and this cruise). Surface mixed layer, established based on a difference in water density of 0.125 from the surface layer, of approximately 200 m was the deepest among three cruises (Fig. 1c). Concentrations of nutrients (nitrate and silicate) were almost same as or slightly higher level than that in winter 2010 (Fig. 2a, b). Surface pCO_2 (xCO_2) was 320 – 330 ppm while atmospheric pCO_2 was approximately 390 ppm. This indicated that station S1 was potentially sink of atmospheric CO_2.

It is noteworthy that concentration of chlorophyll *a* (chl-*a*) was quite higher than that in winter 2010 and autumn 2010. Concentration of chl-*a* was observed three times and concentration of chl-a at surface was measured to be approximately 0.8 μg L^{-1} twice and that at subsurface maximum layer around 80 m was measured to be approximately 1 μg L^{-1} once (Fig. 3a). Based on satellite observation during last 10 years (Sasaoaka, personal communication), annual maximum of surface chl-*a* is at most 0.5 μg L^{-1} around station S1 and, therefore, observed chl-*a* this cruise was abnormally high. Integrated chl-*a* (chl-*a*(int)) upper 200 m this cruise was estimated to be 91±19 mg m^{-2}. This was approximately 4 times higher than that in autumn 2010 (24±6 mg m^{-2}) and approximately 2 times higher than that in winter 2010 (48±6 mg m^{-2}). Based on measurement of accessory-pigments by HPLC, diatom was unexpectedly predominant (3b). In addition, primary productivity (PP) was also high. Integrated PP was 1153 - 1354 mg-C m^{-2} day^{-1}. These large values were higher than the maximum integrated PP at station K2 that must be more productive (ca. 700 mg-C m^{-2} day^{-1}).

It was also noted that freshwater and / or coastal zooplankton and phytoplankton were discovered at station S1 (Drs. Kawachi and Kobari, personal communication, Fig. 4). However high salinity did not support exist of freshwater or coastal water (Fig. 1b). In future, it is important to clarify what mechanism enhances ocean productivity and how fresh and or coastal plankton is transported horizontally to station S1.

2) K2

Surface seawater temperature (SST) at station K2 was approximately 1.8°C and lower than that in winter 2010. However SST was higher than that of intermediate cold water of ca. 1°C observed at around 100 in autumn2010 (Fig. 5a). It was suspected that K2 was going to the winter maximum and SST and surface mixed layer would be lower and deeper, respectively. Concentrations of nutrients (nitrate and silicate) were comparable to those in winter 2010 (Fig. 6a, b).

Concentration of chl-*a* at surface was approximately 0.45 μg L^{-1} and constant upper 100 m (Fig. 7a). Chl-*a* was 0 at around 125 m. Chl-*a*(int) was estimated to be 48±6 mg m^{-2}. This was 1.7 times higher than that in autumn 2010 (30±1 mg m^{-2}) and comparable to that in winter 2010 (50±11 mg m^{-2}). Measurement of accessory pigment revealed that diatom was relatively predominant followed by hyptophytes. (Fig. 7b). PP decreased with increased depth (Fig. 7c). Integrated PP was estimated to be approximately 200 mgC m^{-2} day^{-1}. This was two times larger than that in the winter 2010 (~ 90 mgC m^{-2} day^{-1}).

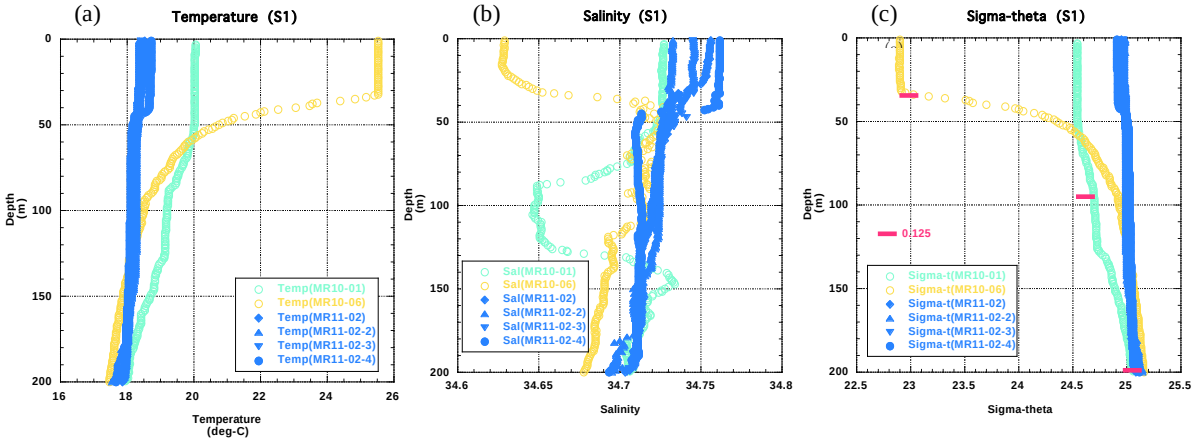

Fig.1 Vertical profiles of (a) temperature (b) salinity (c) density (sigma-theta) upper 200m at station S1.

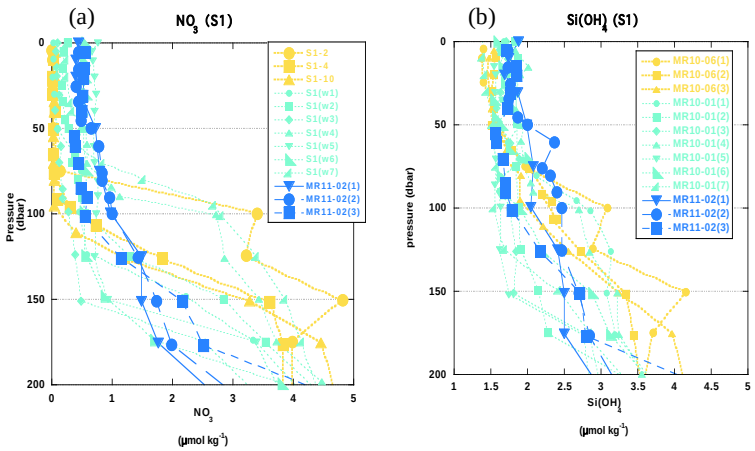

Fig.2 Vertical profiles of (a) nitrate (NO_3) and (b) silicate ($Si(OH)_4$) upper 200 m at station S1

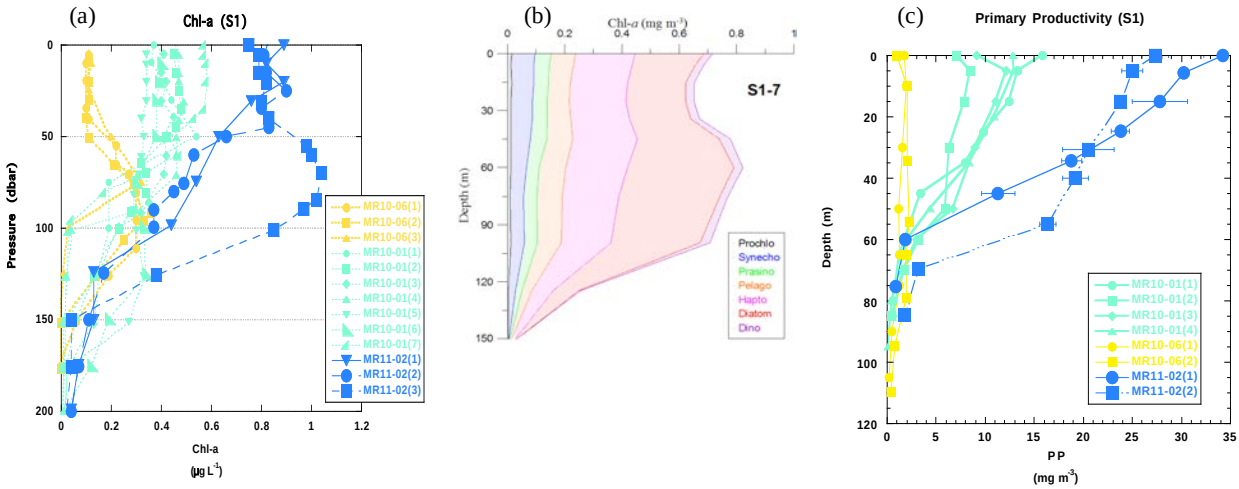

Fig. 3 Vertical profiles of (a) chl-a (b) composition of phytoplankton based on measurement of accessory pigments by HPLC and (c) primary productivity (simulated in situ method) at station S1

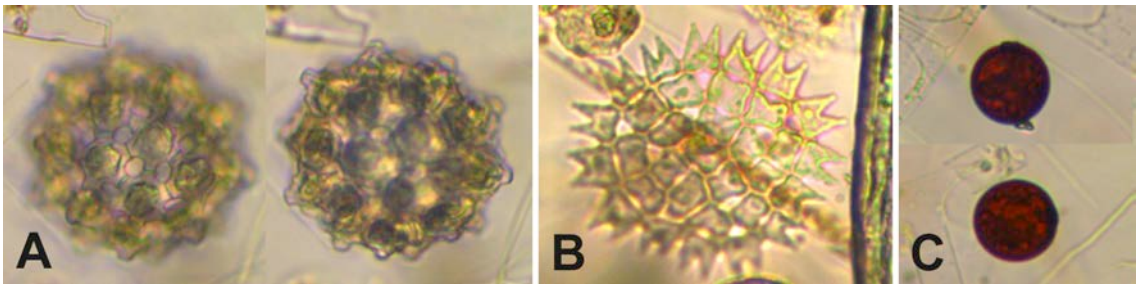

Fig. 4 Freshwater phytoplankton, usually living in pond and / or lake on land, discovered at station S1
A. *Coelastrum sp.*, B. *Pediastrum sp.* , C. *Trachelomonas sp.*（courtesy of Dr. Kawachi of NIES）

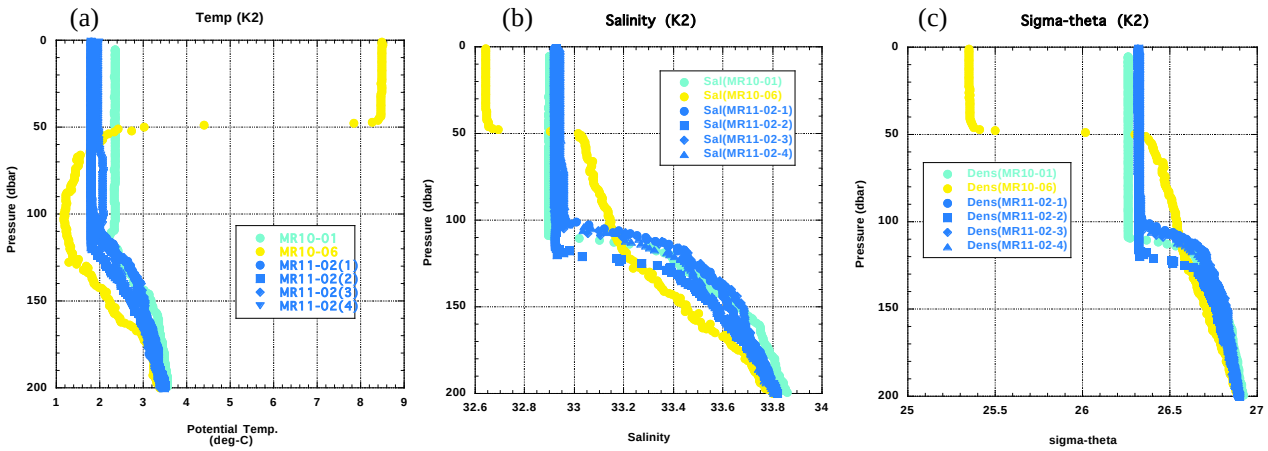

Fig. 5 Vertical profiles of (a) water temperature (b) salinity and (c) density (sigma-theta) upper 200 m at station K2

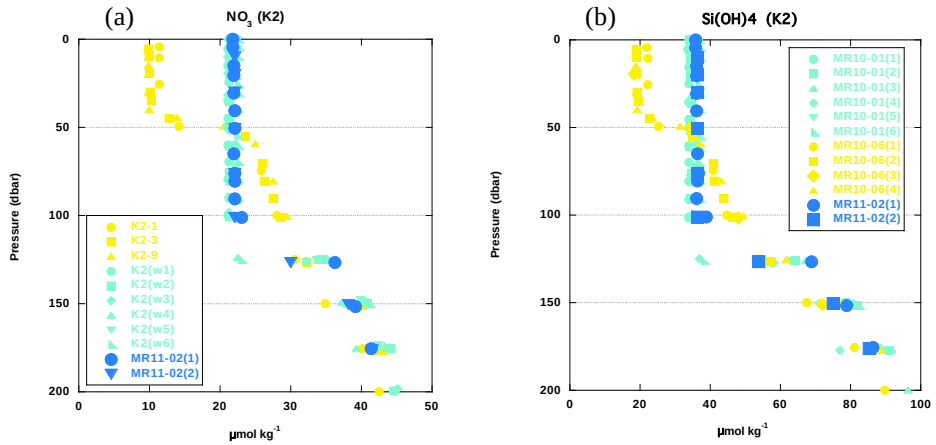

Fig.6 Vertical profiles of (a) nitrate (NO_3) and (b) silicate ($Si(OH)_4$) upper 200 m at station K2

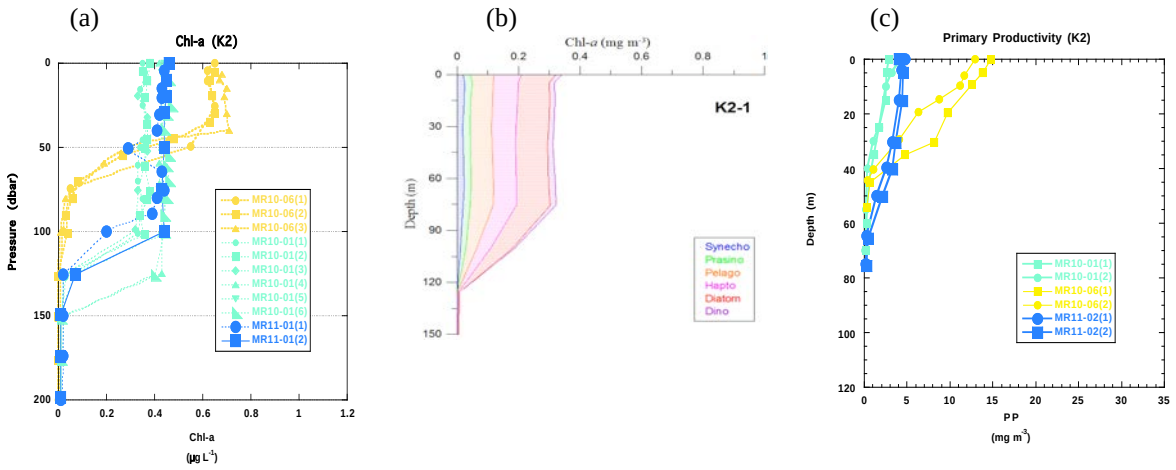

Fig. 7 Vertical profiles of (a) chl-a (b) composition of phytoplankton based on measurement of accessory pigments by HPLC and (c) primary productivity (simulated in situ method) at station K2

B. Text

1. Outline of MR11-02

Makio HONDA (JAMSTEC RIGC)
Principal Investigator of MR11-02

1.1 Cruise summary

(1) Introduction of principal science proposal

Some disturbing effects are progressively coming to the fore in the ocean by climate change, such as rising water temperature, intensification of upper ocean stratification and oceanic acidification. It is supposed that these effects result in serious damage to the ocean ecosystems. Disturbed ocean ecosystems will change a material cycle through the change of biological pump efficiency, and it will be fed back into the climate. We are aimed at clarifying the mechanisms of changes in the oceanic structure in ocean ecosystems derived from the climate change,

We arranged the time-series observation stations in the subarctic gyre (K2: 47°N 160°E) and the subtropical gyre (S1: 30°N, 145°E) in the western North Pacific. In general, biological pump is more efficient in the subarctic gyre than the subtropical gyre because large size phytoplankton (diatom) is abundant in the subarctic gyre by its eutrophic oceanic condition. It is suspected that the responses against climate change are different for respective gyres. To elucidate the oceanic structures in ocean ecosystems and material cycles at both gyres is important to understand the relationship between ecosystem, material cycle and climate change in the global ocean.

There are significant seasonal variations in the ocean environments in both gyres. The seasonal variability of oceanic structures will be estimated by the mooring systems and by the seasonally repetitive ship observations scheduled for next several years.

(2) Objective of this cruise

Objective of this cruise is to collect biogeochemical and physical data in winter at our western Pacific time-series stations K2 (subarctic gyre) and S1 (subtropical data).

(3) Overview of MR11-02

We originally planned to start our observation at station K2 and ended that at station S1. However we left Sekine-hama for station S1 because weather and sea condition was predicted to be bad at station K2. This decision was right and we fortunately conducted various biogeochemical observations including hydrocasting, drifting buoy, in situ pumping and plankton sampling by large plankton net tow system (IONESS). In addition, we successfully exchange the meteorological sensor on NOAA-KEO surface buoy, recovered the stranded part of JAMSTEC-K-TRITON buoy mooring system which was partitioned by longline fishing last October, and we re-deployed K-TRITON buoy at JKEO station.

We were in trouble for bad weather and rough sea condition at station K2. We were forced to cancel several observations. However we was able to conduct minimum observation enough to verify winter oceanography at station K2.

The followings are preliminary results at station S1 and K2.

1) S1

Water temperature upper 200m was approximately 18°C (Fig. 1a) and the lowest among three cruises (MR10-01: January-February 2010, MR10-06: October–November 2010, and this cruise). Surface mixed layer (0.125 criteria) of approximately 200 m was the deepest among three cruises (Fig. 1c). Concentrations of nutrients (nitrate and silicate) were almost same as or slightly higher level than that in winter 2010 (Fig. 2a, b). Surface pCO_2 (xCO_2) was 320 – 330 ppm while atmospheric pCO_2 was approximately 400 ppm. This indicated that station S1 was potentially sink of atmospheric CO_2.

It is noteworthy that concentration of chlorophyll *a* (chl-*a*) was quite higher than that in winter 2010 and autumn 2010. Concentration of chl-*a* a was observed three times and concentration of chl-a at surface was measured to be approximately 0.8 μg L^{-1} twice and that at subsurface maximum layer around 80 m was measured to be approximately 1 μg L^{-1} once (Fig. 3a). Based on satellite observation during last 10 years (Sasaoaka, personal communication), annual maximum of chl-*a* is at most 0.5 μg L^{-1} around station S1 and, therefore, observed chl-*a* this cruise was abnormally high. Integrated chl-a (chl-*a*(int)) upper 200 m this cruise was estimated to be 91±19 mg m^{-2}. This was approximately 4 times higher than that in autumn 2010 (24±6 mg m^{-2}) and approximately 2 times higher than that in winter 2010 (48±6 mg m^{-2}). Based on measurement of accessory-pigments by HPLC, diatom was unexpectedly predominant (3b). In addition, primary productivity (PP) was also high. Integrated PP was 1153 - 1354 mg-C m^{-2} day^{-1}. These large values were higher than the maximum integrated PP at station K2 that must be more productive (ca. 700 mg-C m^{-2} day^{-1}).

It was also noted that freshwater and / or coastal zooplankton and phytoplankton was discovered at station S1 (Kobari, Kawachi, personal communication, Fig. 4). However high salinity did not support exist of freshwater or coastal water (Fig. 1b). In future, it is important to clarify what mechanism enhances ocean productivity and how fresh and or coastal plankton is transported horizontally to station S1.

2) K2

Surface seawater temperature (SST) at station K2 was approximately 1.8°C and lower than that in winter 2010. However SST was higher than that of intermediate cold water of ca. 1°C observed at around 100 in autumn2010 (Fig. 5a). It was suspected that K2 was going to the winter maximum and SST and surface mixed layer would be lower and deeper, respectively. Concentrations of nutrients (nitrate and silicate) were comparable to those in winter 2010 (Fig. 6a, b).

Concentration of chl-a at surface was approximately 0.45 μg L^{-1} and constant upper 100 m (Fig. 7a). Chl-a was 0 at around 125 m. Chl-a(int) was estimated to be 48±6 mg m^{-2}. This was 1.7 times higher than that in autumn 2010 (30±1 mg m^{-2}) and comparable to that in winter 2010 (50±11 mg m^{-2}). Measurement of accessory pigment revealed that diatom was relatively predominant followed by hyptophytes. (Fig. 7b). Primary productivity decreased with increased depth (Fig. 7c). Integrated primary productivity was estimated to be approximately 200 mgC m^{-2} day^{-1}. This was two times larger than that in the winter 2010 (~ 90 mgC m^{-2} day^{-1}).

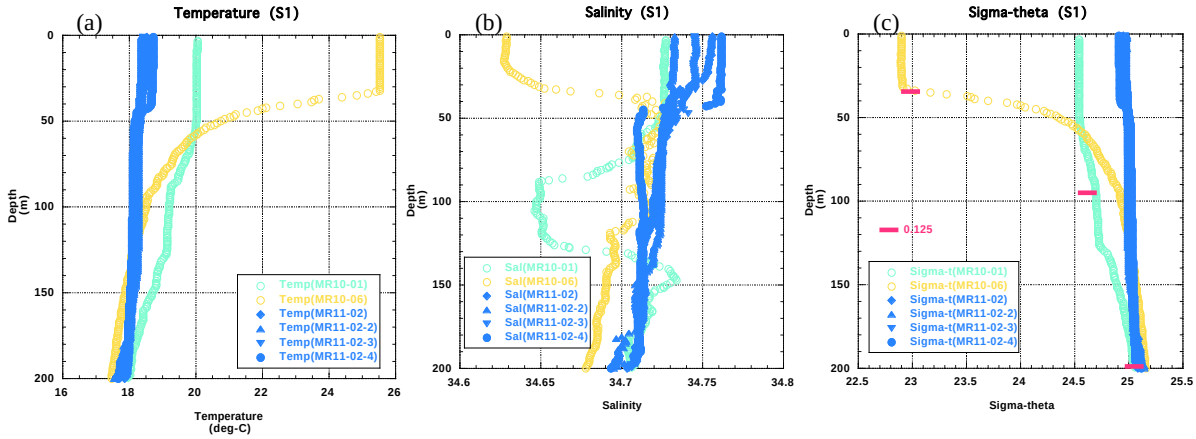

Fig.1 Vertical profiles of (a) temperature (b) salinity (c) density (sigma-theta) upper 200m at station S1.

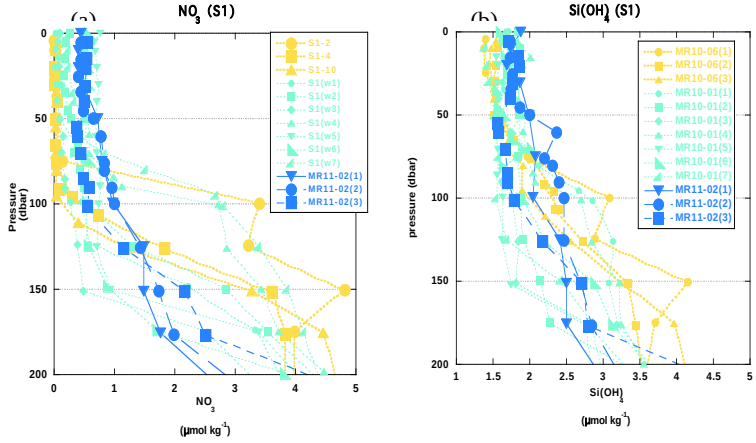

Fig.2 Vertical profiles of (a) nitrate (NO_3) and (b) silicate ($Si(OH)_4$) upper 200 m at station S1

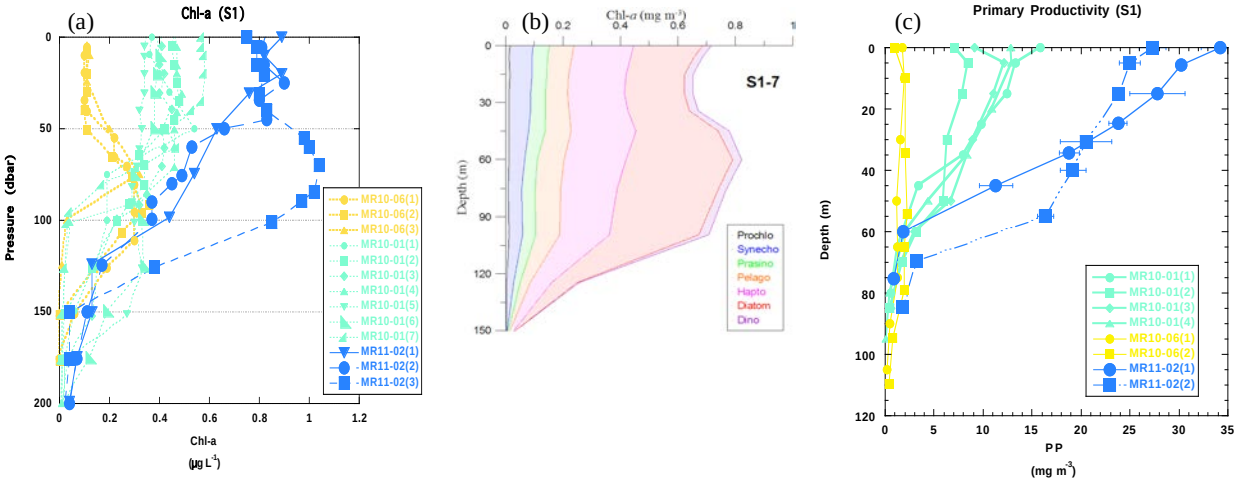

Fig. 3 Vertical profiles of (a) chl-a (b) composition of phytoplankton based on measurement of accessory pigments by HPLC and (c) primary productivity (simulated in situ method) at station S1

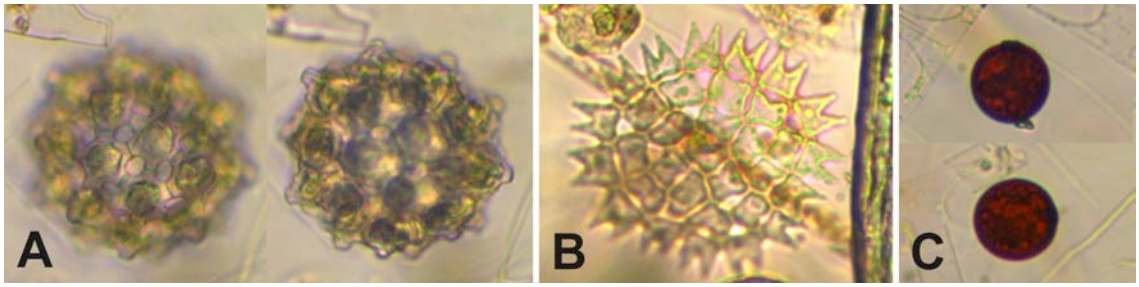

Fig. 4 Freshwater phytoplankton, usually living in pond and / or lake on land, discovered at station S1

A. *Coelastrum sp.*. B. *Pediastrum sp.* . C. *Trachelomonas sp.*（courtesy of Dr. Kawachi of NIES）

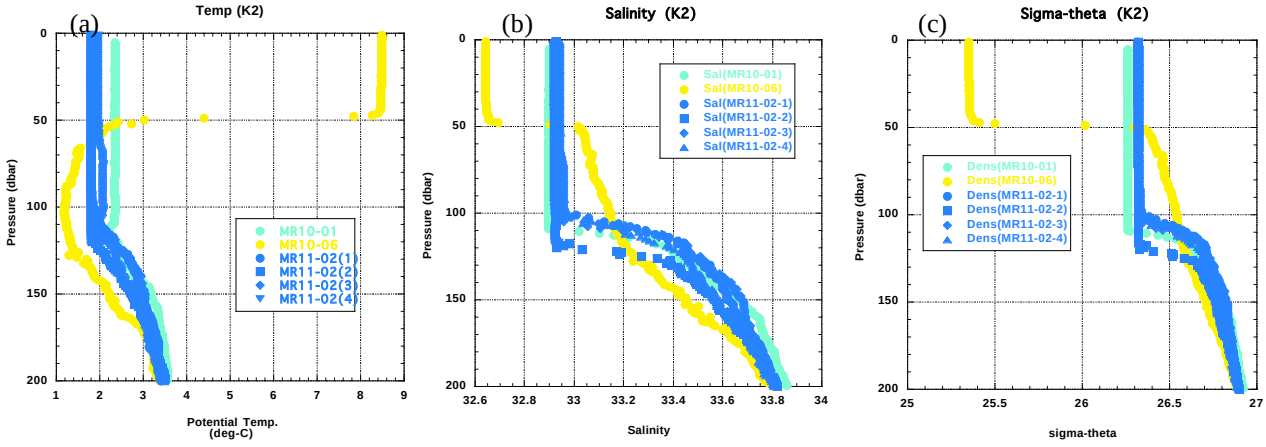

Fig. 5 Vertical profiles of (a) water temperature (b) salinity and (c) density (sigma-theta) upper 200 m at

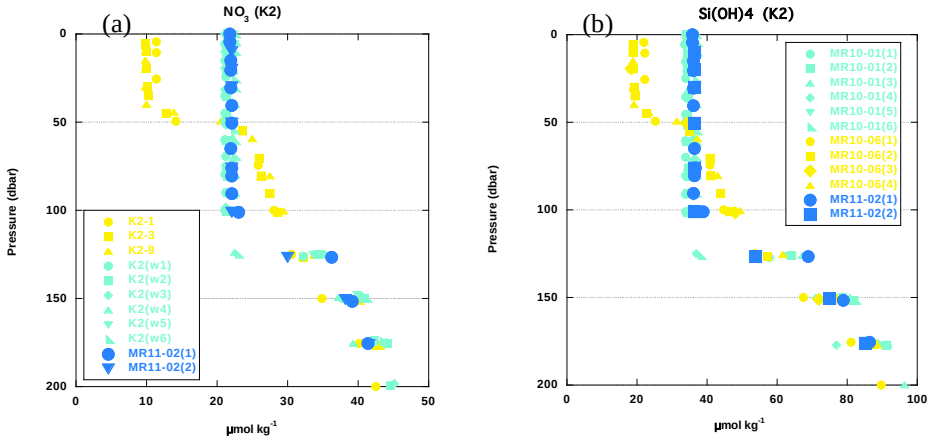

Fig.6 Vertical profiles of (a) nitrate (NO_3) and (b) silicate ($Si(OH)_4$) upper 200 m at station K2

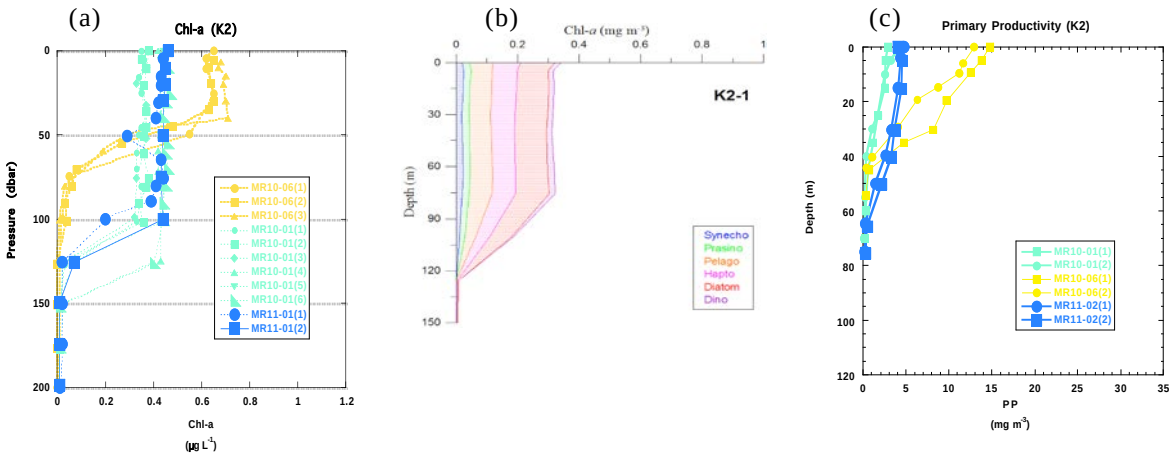

Fig. 7 Vertical profiles of (a) chl-a (b) composition of phytoplankton based on measurement of

(4) Scientific gears

All hydrocasts were conducted using 36-position 12 liter Niskin bottles carousel system with SBE CTD-DO system, fluorescence and transmission sensors. JAMSTEC scientists and MWJ (Marine Work Japan Co. Ltd.) technician group were responsible for analyzing water sample for salinity, dissolved oxygen, nutrients, CFCs, total carbon contents, alkalinity and pH. Cruise participants from JAMSTEC, Nagoya University, Tokyo University, Kagoshima University and National Institution for Environmental Study (NIES) helped to divide seawater from Niskin bottles to sample bottles for analysis. Surface water was collected with bucket.

Optical measurement in air and underwater was conducted with PAR sensor (RAMSES-ACC) and SPMR/SMSR called “Free Fall”.

For collecting suspended particles at station K2 and S1, Large Volume Pump (LVP) was deployed. For observing in situ particles, optical sensor called LISST (Laser In Situ Scattering and Transmissometer) and VPR (Visual Plankton recorder) were deployed by University of Tokyo and JAMSTEC, respectively.

GODI technicians group undertook responsibility for underway current direction and velocity measurements using an Acoustic Current Profiler (ADCP), geological measurements (topography, geo-magnetic field and gravity), and collecting meteorological data.

For collection of zooplankton, NORPAC plankton net, and IONESS were deployed.

For conducting in situ incubation for measurement of primary productivity and collecting sinking particles at station K2, drifter was deployed at station K2 and S1.

For observing vertical profile of primary productivity optically, FRRF was deployed.

In order to conduct time-series observation in biogeochemical cycle, JAMSTEC POPPS mooring was recovered and re-deployed at station S1.

For observation of atmospheric chemistry (aerosol and gas), various instruments including “sky-radiometer” and “MAX-DOAS” were onboard and automatic measurement was conducted.

In addition, we successfully exchange the meteorological sensor on NOAA-KEO surface buoy, recovered the stranded part of JAMSTEC-K-TRITON buoy mooring system which was partitioned by longline fishing last October, and we re-deployed K-TRITON buoy at JKEO station.

Please read text for more detail information and other instruments used for oceanographic and meteorological or atmospheric observation.

1.2 Track and log

1.2.1 Research Area

The western North Pacific (60°N – 30°N, 140°E – 165°W)

1.2.2 Cruise track

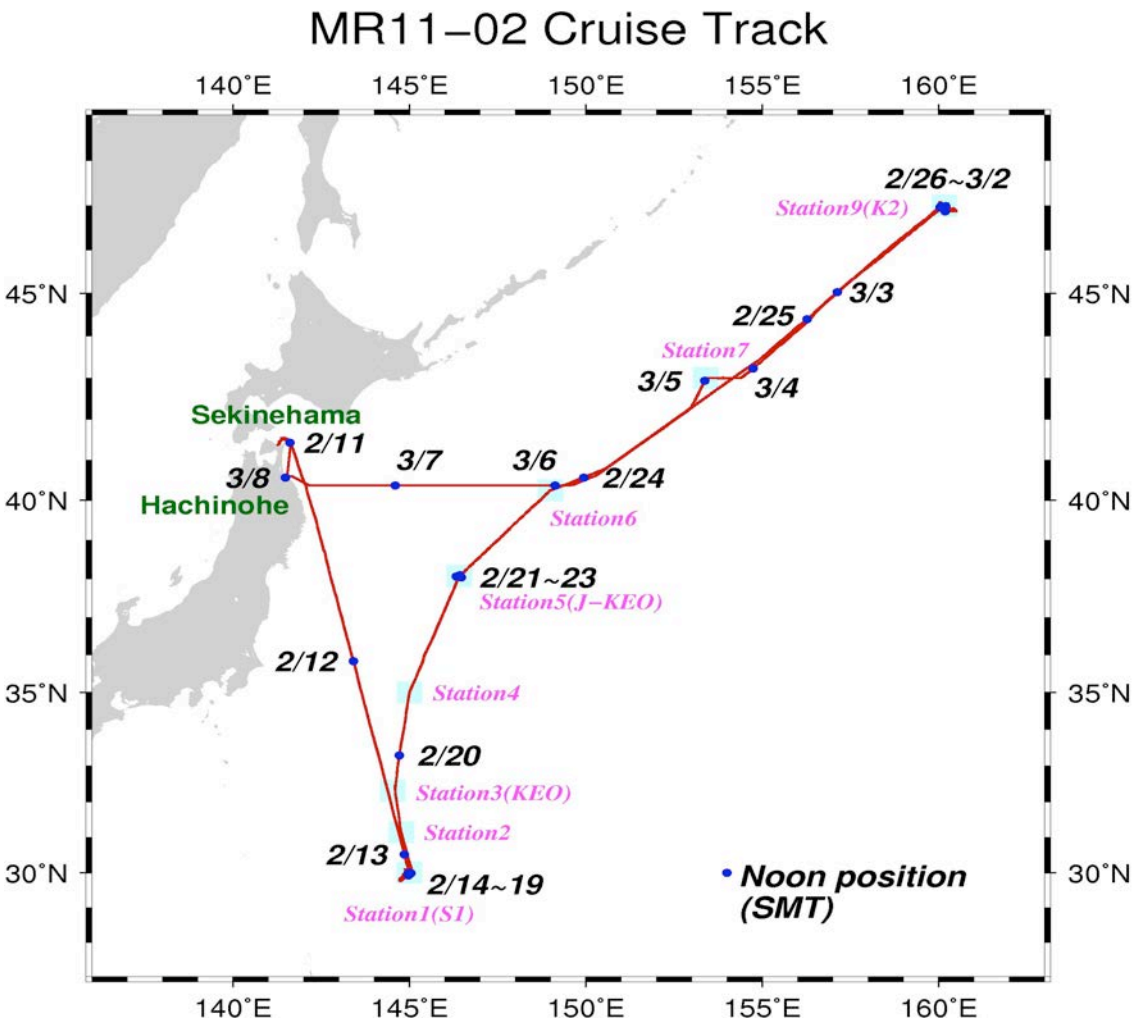

1.2.3 Cruise log

SMT		UTC		Position		Events
Date	Time	Date	Time	Lat.	Lon.	
2.11	1:00	2.11	10:00	41-22N	141-14E	Departure from Sekinehama
	5:30		14:30	-	-	Continuously observations start
2.12	13:00	2.12	22:00	-	-	Time adjustment +1 hour (SMT=UTC+10h)
2.13	4:18	2.13	14:18	30-00N	145-00E	Arrival at Station 01 (S1)
	7:25		17:25	30-00.06N	144-59.96E	CTD cast #01 (5,000 m)
	19:59	2.14	5:59	29-59.94N	144-59.83E	CTD cast #02 (5,947 m)
2.14	0:24		10:24	29-59.66N	144-59.39E	FRRF #01 (200 m)
	1:18		11:18	29-59.94N	144-59.29E	Free fall optical measruements #01
	3:11		13:11	29-56.21N	144-57.30E	BGC mooring recovery
	6:27		16:27	29-57.00N	144-54.91E	Calibration for magnetometer #01
	8:53		18:53	30-00.03N	144-59.95E	Visual Plankton Recorder (VPR) #01 (500 m)
	9:29		19:29	30-00.21N	144-59.75E	Plankton net #01-1 (NORPAC: 50 m)
	9:35		19:35	30-00.26N	144-59.72E	Plankton net #01-2 (NORPAC: 50 m)
	9:41		19:41	30-00.31N	144-59.68E	Plankton net #01-3 (NORPAC: 50 m)
	9:48		19:48	30-00.37N	144-59.65E	Plankton net #01-4 (NORPAC: 50 m)
	17:57	2.15	3:57	30-00.05N	144-54.12E	CTD cast #03 (300 m)
	18:54		4:54	30-00.26N	144-54.12E	FRRF #02 (200 m)
	20:19		6:19	29-59.93N	144-53.81E	Surface drifting float buoy deployment #01
	21:06		7:06	29-59.34N	144-53.91E	FRRF #03 (200 m)
	22:59		8:59	30-00.14N	145-00.00E	CTD cast #04 (1,000 m)
2.15	0:29		10:29	30-00.06N	144-59.88E	FRRF #04 (200 m)
	1:11		11:11	30-00.24N	145-00.15E	Free fall optical measruements #02
	1:57		11:57	30-00.14N	144-59.99E	Plankton net #02 (NORPAC: 200 m)

	2:11		12:11	30-00.28N	145-00.02E	FRRF #05 (200 m)
	3:10		13:10	30-00.21N	145-00.03E	Large Volume Pump (LVP) #01 (1,000 m)
	6:25		16:25	30-00.01N	145-00.00E	Water sampling for buckets #01
	10:05		20:05	29-59.78N	145-00.21E	CTD cast #05 (200 m)
	11:08		21:08	29-59.81N	144-58.90E	IONESS #01 (1,000 m)
	20:15	2.16	6:15	29-57.37N	144-48.59E	Surface drifting float buoy recovery #01
	21:07		7:07	29-57.68N	144-48.59E	Drifting sediment trap buoy deployment #01
2.16	23:27		9:27	29-59.96N	144-59.81E	Plankton net #03 (200 m)
	1:23		11:23	30-00.05N	144-59.47E	CTD cast #06 (1,000 m)
	3:30		13:30	30-00.11N	144-59.78E	Plankton net #04-1 (50 m)
	3:44		13:44	30-00.14N	144-59.68E	Plankton net #04-2 (50 m)
	3:55		13:55	30-00.15N	144-59.59E	Plankton net #04-3 (50 m)
	4:07		14:07	30-00.20N	144-59.47E	Plankton net #04-4 (150 m)
	8:00		18:00	29-59.91N	144-59.92E	LISST #01 (200 m)
	9:14		19:14	30-00.05N	144-59.15E	Plankton net #05-1 (50 m)
	9:25		19:25	30-00.09N	144-59.05E	Plankton net #05-2 (50 m)
	9:36		19:36	30-00.08N	144-58.95E	Plankton net #05-3 (50 m)
	9:47		19:47	30-00.07N	144-58.80E	Plankton net #05-4 (150 m)
	10:07		20:07	30-00.06N	144-58.62E	Plankton net #06 (200 m)
	22:11	2.17	8:11	29-54.70N	144-53.89E	POPPS mooring deployment
				29-56.19N	144-58.01E	POPPS mooring fixed position
2.17	1:23		11:23	29-56.30N	144-58.73E	Free fall optical measruements #03
	3:14		13:14	29-55.78N	144-58.02E	Free fall optical measruements #04
	7:54		17:54	29-59.94N	145-00.07E	Plankton net #07-1 (60m)
	8:02		18:02	29-59.95N	145-00.04E	Plankton net #07-2 (60m)
	8:08		18:08	29-59.96N	145-00.00E	Plankton net #07-3 (60m)
	8:15		18:15	29-59.94N	144-59.97E	Plankton net #07-4 (60m)
	10:55		20:55	30-00.49N	144-57.66E	IONESS #02 (1,000 m)
	18:30	2.18	4:30	30-00.07N	144-59.86E	CTD cast #07 (300 m)

	22:27		8:27	30-00.00N	144-59.87E	LVP #02 (200 m)
2.18	8:57		18:57	30-00.01N	144-59.83E	VPR #02 (500 m)
	9:53		19:53	29-59.84N	144-59.68E	Plankton net #08-1 (200 m)
	10:08		20:08	29-59.73N	144-59.60E	Plankton net #08-2 (50 m)
	10:24		20:24	29-59.50N	144-59.48E	CTD cast #08 (200 m)
	20:48	2.19	6:48	29-58.91N	144-42.64E	Drifting sediment trap buoy recovery #01
	22:54		8:54	29-54.70N	144-50.56E	CTD cast #09 (300 m)
2.19	1:00		11:00	29-58.11N	145-01.00E	IONESS #03 (1,000 m)
	4:06		14:06	-	-	Departure from Station 01 (S1)
	9:12		19:12	31-10N	144-46E	Arrival at Station 02
	9:12		19:12	31-09.47E	144-46.00E	CTD cast #10 (1,000 m)
	10:24		20:24	-	-	Departure from Station 02
	16:24	2.20	2:24	32-28N	144-35E	Arrival at Station 03 (KEO)
	16:25		2:25	32-27.93N	144-35.15E	CTD cast #11 (5,703 m)
	21:57		7:57	32-29.36N	144-36.28E	Replacement sensors of KEO buoy
	22:36		8:36	-	-	Departure from Station 03
2.20	9:00		19:00	35-00N	145-00E	Arrival at Station 04
	9:03		19:03	35-00.04N	145-00.10E	CTD cast #12 (1,000 m)
	10:12		20:12	-	-	Departure from Station 04
2.21	0:13	2.21	10:13	38-03.54N	146-24.45E	XCTD for sound velocity #01
	0:36		10:36	38-05N	146-26E	Arrival at Station 05
	3:00		13:00	38-02.12N	146-29.44E	CTD cast #13 (5,386 m)
	7:40		17:40	38-05.19N	146-25.59E	Calibration for flow meter of Plankton net #01
2.22	3:52	2.22	13:52	38-06.29N	146-26.20E	J-KEO buoy recovery

2.23	3:14	2.23	13:14	38-03.81N	146-18.39E	J-KEO buoy deployment
	14:00			38-05.06N	146-26.87E	J-KEO buoy fixed position
	8:50		18:50	38-05.27N	146-26.52E	Drifting wave buoy deployment #01
	9:58		20:58	22-49.99N	145-01.77E	Departure from Station 05
	17:21	2.24	3:21	39-40.01N	148-18.14E	XCTD for sound velocity #02
	21:48		7:48	40-15N	149-00E	Arrival at Station 06
	21:57		7:57	40-14.93N	149-00.04E	CTD cast #14 (1,000 m)
	23:02		9:02	40-14.94N	149-01.14E	Argo float deployment #01
	22:06		9:06	-	-	Departure from Station 06
2.25	1:27	2.25	11:27	44-23.59N	156-15.49E	Free fall optical measruements #05
	17:42	2.26	3:42	47-00N	160-00E	Arrival at Station 09 (K2)
	17:58		3:58	47-00.21N	160-10.20E	CTD cast #15 (300 m)
	19:55		5:55	47-01.55N	160-09.98E	Drifting sediment trap buoy deployment #02
	20:57		6:57	47-00.72N	160-10.38E	CTD cast #16 (5,230 m)
2.26	1:32		11:32	47-00.37N	160-12.11E	IONESS #04 (1,000 m)
	4:55		14:55	46-54.26N	160-14.94E	CTD cast #17 (1,000 m)
	8:56		18:56	46-58.04N	160-07.90E	Plankton net #09-1 (65 m)
	8:23		18:23	46-58.11N	160-07.90E	Plankton net #09-2 (65 m)
	8:34		18:34	46-58.16N	160-07.90E	Plankton net #09-3 (65 m)
	8:46		18:46	46-58.22N	160-07.87E	Plankton net #09-4 (65 m)
	9:01		19:01	46-58.26N	160-07.96E	Plankton net #09-5 (65 m)
	10:58		20:58	46-59.01N	160-06.70E	IONESS #05 (1,000 m)
	17:59	2.27	3:59	47-00.20N	160-04.52E	CTD cast #18 (5,224 m)
2.27	2:59		12:59	46-57.06N	160-02.01E	Plankton net #10-1 (NORPAC: 65 m)
	3:11		13:11	46-56.86N	160-01.69E	Plankton net #10-2 (Twin-NORPAC: 200 m)
3.1	17:59	3.2	3:59	46-52.60N	160-21.45E	CTD cast #19 (200 m)

	18:40		4:40	46-52.39N	160-21.31E	Plankton net #11 (NORPAC: 65 m)
	20:03		6:03	46-53.43N	160-17.00E	Drifting sediment trap buoy recovery #01
	21:34		7:34	46-54.00N	160-17.23E	LVP #03 (1,000 m)
3.2	2:19		12:19	46-52.85N	160-11.48E	Calibration for magnetometer #02
	3:07		13:07	46-53.17N	160-11.14E	LVP #04 (200 m)
	5:19		15:19	46-52.71N	160-11.84E	CTD cast #20 (1,000 m)
	8:54		18:54	47-00.07N	160-05.12E	Plankton net #12-1 (Twin-NORPAC: 200 m)
	9:08		19:08	47-00.10N	160-05.11E	Plankton net #12-2 (NORPAC: 100 m)
	9:18		19:18	47-00.13N	160-05.10E	Plankton net #12-3 (NORPAC: 100 m)
	9:30		19:30	47-00.15N	160-05.08E	LISST #02 (200 m)
	10:21		20:21	47-00.38N	160-04.97E	VPR #03 (500 m)
	10:54		20:54	-	-	Departure from Station 09 (K2)
3.4	21:00	3.5	7:00	43-00N	153-24E	Arrival at Station 07
				-	-	Station 07 - cancel
3.5	1:30		11:30	-	-	Departure from Station 07
3.6	12:00	3.6	22:00	-	-	Time adjustment -1 hours (SMT=UTC+9h)
	22:48	3.7	7:48	40-22N	144-41E	Arrival at CTD cable test point
	23:02		8:02	40-21.90N	144-40.92E	CTD cable test (6,000 m)
3.7	2:21		11:21	40-21.90N	144-40.66E	Free fall optical measruements #06
	2:36		11:36	-	-	Departure from CTD cable test point
	6:55		15:55	-	-	Continuously observations finish
3.7	23:50	3.8	8:50	40-32N	141-33E	Arrival at Hachinohe
	6:50		15:50	-	-	Departure from Hachinohe
3.9	0:10	3.9	09:10	41-22N	141-14E	Arrival at Sekinehama

1.3 Cruise Participants

	Name	Affiliation	Appointment
1	Makio HONDA (Principal Investigator)	Research Institute for Global Change (RIGC), Japan Agency for Marine-Earth Science and Technology (JAMSTEC)	Senior research scientist (II)
2	Kazuhiko MATSUMOTO (Deputy PI)	RIGC, JAMSTEC	Research scientist
3	Minoru KITAMURA	Institute of Biogeoscience (BIOGEOS) , JAMSTEC	Scientist
4	Hajime KAWAKAMI	Mutsu Institute for Oceanography (MIO), JAMSTEC	Research scientist
5	Masahide WAKITA	Same as above	Scientist
6	Tetsuichi FUJIKI	RIGC, JAMSTEC	Scientist
7	Yoshimi KAWAI	RIGC, JAMSTEC	Senior Scientist
8	Akira NAGANO	RIGC, JAMSTEC	Scientist
9	Ryo KANEKO	Atmosphere and Ocean Research Institute (AORI), The University of Tokyo	Postdoctoral researcher
10	Jaeho Song	Same as above	Graduate student
11	Keigo WATANABE	Same as above	Graduate student
12	Osamu ABE	Graduate school of environmental studies, Nagoya University	Assistant professor
13	Yoshihisa MINO	Hydrospheric Atmospheric Research Center (HyARC), Nagoya University	Same as above
14	Chiho SUKIGARA	Same as above	Postdoctoral fellow
15	Toru KOBARI	Kagoshima University	Associate professor
16	Kei ISAMI	Same as above	Undergraduate student
17	Masanobu KAWACHI	National Institute for Environmental Studies	Senior researcher
18	Naoji YUBUKI	University of British Columbia	Postdoctral fellow
19	Minoru KAMATA （Principal Marine Tech.）	Marine Works Japan Inc. (MWJ)	Marin Technician
20	Hirokatsu UNO	Same as above	Same as above
21	Fujio KOBAYASHI	Same as above	Same as above
22	Toru IDAI	Same as above	Same as above
23	Tomoyuki TAKAMORI	Same as above	Same as above
24	Shinsuke TOYODA	Same as above	Same as above
25	Shungo OSHITANI	Same as above	Same as above
26	Hideki YAMAMOTO	Same as above	Same as above
27	Kenichiro SATO	Same as above	Same as above

28	Yasuhiro ARII	Same as above	Same as above
29	Miyo IKEDA	Same as above	Same as above
30	Ayaka HASTSUYAMA	Same as above	Same as above
31	Shoko TATAMISASHI	Same as above	Same as above
32	Tomonori WATAI	Same as above	Same as above
33	Misato KUWAHARA	Same as above	Same as above
34	Masahiro ORUI	Same as above	Same as above
35	Kanako YOSHIDA	Same as above	Same as above
36	Sayaka KAWAMURA	Same as above	Same as above
37	Kazuho YOSHIDA (Principal Marine Tech.)	Global Ocean Development Inc. (GODI)	Same as above

2. General observation

2.1 Meteorological observations
2.1.1 Surface Meteorological Observation

Kazuho YOSHIDA (Global Ocean Development Inc., GODI)
Wataru TOKUNAGA (Mirai Crew)

(1) Objectives

Surface meteorological parameters are observed as a basic dataset of the meteorology. These parameters bring us the information about the temporal variation of the meteorological condition surrounding the ship.

(2) Methods

Surface meteorological parameters were observed throughout the MR11-02 cruise. During this cruise, we used three systems for the observation.

i. MIRAI Surface Meteorological observation (SMet) system
ii. Shipboard Oceanographic and Atmospheric Radiation (SOAR) system

i. MIRAI Surface Meteorological observation (SMet) system

Instruments of SMet system are listed in Table.2.1.1-1 and measured parameters are listed in Table.2.1.1-2. Data were collected and processed by KOAC-7800 weather data processor made by Koshin-Denki, Japan. The data set consists of 6-second averaged data.

ii. Shipboard Oceanographic and Atmospheric Radiation (SOAR) measurement system

SOAR system designed by BNL (Brookhaven National Laboratory, USA) consists of major three parts.

a) Portable Radiation Package (PRP) designed by BNL – short and long wave downward radiation.
b) Zeno Meteorological (Zeno/Met) system designed by BNL – wind, air temperature, relative humidity, pressure, and rainfall measurement.
c) Scientific Computer System (SCS) developed by NOAA (National Oceanic and Atmospheric Administration, USA) – centralized data acquisition and logging of all data sets.

SCS recorded PRP data every 6 seconds, while Zeno/Met data every 10 seconds. Instruments and their locations are listed in Table.2.1.1-3 and measured parameters are listed in Table.2.1.1-4.

For the quality control as post processing, we checked the following sensors, before and after the cruise.

i. Young Rain gauge (SMet and SOAR)
Inspect of the linearity of output value from the rain gauge sensor to change Input value by adding fixed quantity of test water.
ii. Barometer (SMet and SOAR)
Comparison with the portable barometer value, PTB220CASE, VAISALA.
iii. Thermometer (air temperature and relative humidity) (SMet and SOAR)

Comparison with the portable thermometer value, HMP41/45, VAISALA.

(3) Preliminary results

Figure 2.1.1-1 shows the time series of the following parameters;

Wind (SMet)
Air temperature (SMet)
Relative humidity (SMet)
Precipitation (SOAR, Optical rain gauge)
Short/long wave radiation (SOAR)
Pressure (SMet)
Sea surface temperature (SMet)
Significant wave height (SMet)

(4) Data archives

These meteorological data will be submitted to the Data Management Group (DMG) of JAMSTEC just after the cruise.

(5) Remarks

i. SST (Sea Surface Temperature) data are available in the following period.
05:29UTC 11 Feb. 2011 - 06:55UTC 07 Mar. 2011

ii. In following periods, increasing of SMet capacitive rain gauge data were invalid.
due to test transmitting for MF/HF radio
03:40UTC - 03:50UTC 15 Feb. 2011
09:40UTC - 09:43UTC 20 Feb. 2011

iii. Air temperature and relative humidity of SOAR portside are invalid in the following period
00:48:19UTC - 00:48:49UTC, 06 Mar. 2011

iv. FRSR sensor trouble arose.
1) PRP data acquisition was suspended due to maintenance of FRSR.
00:39UTC - 00:55UTC 13 Feb. 2011 (intermittently)
12:47UTC - 12:48UTC 13 Feb. 2011

2) FRSR Data were invalid due to FRSR sensor trouble.
14:25:33UTC 12 Feb. - 16:09:08UTC 12 Feb. 2011 (intermittently)
16:24:24UTC - 16:26:36UTC 12 Feb. 2011
22:04:33UTC - 22:45:08UTC 12 Feb. 2011
23:47:08UTC 12 Feb. - 01:00:00UTC 13 Feb. 2011

3) Only FRSR data acquisition was suspended
01:00UTC 13 Feb. 2011 to the end of this cruise

v. Sensor cleaning
04:58UTC - 04:59UTC 15 Feb. 2011 (PRP)
04:59UTC 15 Feb. 2011 (SOAR ORG)
22:45UTC 01 Mar. 2011 (SMet ORG)

Table.2.1.1-1 Instruments and installations of MIRAI Surface Meteorological observation system

Sensors	Type	Manufacturer	Location (altitude from surface)
Anemometer	KE-500	Koshin Denki, Japan	foremast (24 m)
Tair/RH	HMP45A	Vaisala, Finland	
with 43408 Gill aspirated radiation shield		R.M. Young, USA	compass deck (21 m)
			starboard side and port side
Thermometer: SST	RFN1-0	Koshin Denki, Japan	4th deck (-1m, inlet -5m)
Barometer	Model-370	Setra System, USA	captain deck (13 m)
			weather observation room
Rain gauge	50202	R. M. Young, USA	compass deck (19 m)
Optical rain gauge	ORG-815DR	Osi, USA	compass deck (19 m)
Radiometer (short wave)	MS-801	Eiko Seiki, Japan	radar mast (28 m)
Radiometer (long wave)	MS-200	Eiko Seiki, Japan	radar mast (28 m)
Wave height meter	MW-2	Tsurumi-seiki, Japan	bow (10 m)

Table.2.1.1-2 Parameters of MIRAI Surface Meteorological observation system

Parameter	Units	Remarks
1 Latitude	degree	
2 Longitude	degree	
3 Ship's speed	knot	Mirai log, DS-30 Furuno
4 Ship's heading	degree	Mirai gyro, TG-6000, Tokimec
5 Relative wind speed	m/s	6sec./10min. averaged
6 Relative wind direction	degree	6sec./10min. averaged
7 True wind speed	m/s	6sec./10min. averaged
8 True wind direction	degree	6sec./10min. averaged
9 Barometric pressure	hPa	adjusted to sea surface level
		6sec. averaged
10 Air temperature (starboard side)	degC	6sec. averaged
11 Air temperature (port side)	degC	6sec. averaged
12 Dewpoint temperature (starboard side)	degC	6sec. averaged
13 Dewpoint temperature (port side)	degC	6sec. averaged
14 Relative humidity (starboard side)	%	6sec. averaged
15 Relative humidity (port side)	%	6sec. averaged
16 Sea surface temperature	degC	6sec. averaged
17 Rain rate (optical rain gauge)	mm/hr	hourly accumulation
18 Rain rate (capacitive rain gauge)	mm/hr	hourly accumulation
19 Down welling shortwave radiation	W/m2	6sec. averaged
20 Down welling infra-red radiation	W/m2	6sec. averaged
21 Significant wave height (bow)	m	hourly
22 Significant wave height (aft)	m	hourly
23 Significant wave period (bow)	second	hourly
24 Significant wave period (aft)	second	hourly

Table.2.1.1-3 Instruments and installation locations of SOAR system

Sensors (Zeno/Met)	Type	Manufacturer	Location (altitude from surface)
Anemometer	05106	R.M. Young, USA	foremast (25 m)
Tair/RH	HMP45A	Vaisala, Finland	
with 43408 Gill aspirated radiation shield		R.M. Young, USA	foremast (23 m)
Barometer	61202V	R.M. Young, USA	
with 61002 Gill pressure port		R.M. Young, USA	foremast (22 m)
Rain gauge	50202	R.M. Young, USA	foremast (24 m)
Optical rain gauge	ORG-815DA	Osi, USA	foremast (24 m)

Sensors (PRP)	Type	Manufacturer	Location (altitude from surface)
Radiometer (short wave)	PSP	Epply Labs, USA	foremast (25 m)
Radiometer (long wave)	PIR	Epply Labs, USA	foremast (25 m)
Fast rotating shadowband radiometer		Yankee, USA	foremast (25 m)

Table.2.1.1-4 Parameters of SOAR system

Parameter	Units	Remarks
1 Latitude	degree	
2 Longitude	degree	
3 SOG	knot	
4 COG	degree	
5 Relative wind speed	m/s	
6 Relative wind direction	degree	
7 Barometric pressure	hPa	
8 Air temperature	degC	
9 Relative humidity	%	
10 Rain rate (optical rain gauge)	mm/hr	
11 Precipitation (capacitive rain gauge)	mm	reset at 50 mm
12 Down welling shortwave radiation	W/m2	
13 Down welling infra-red radiation	W/m2	
14 Defuse irradiance	W/m2	

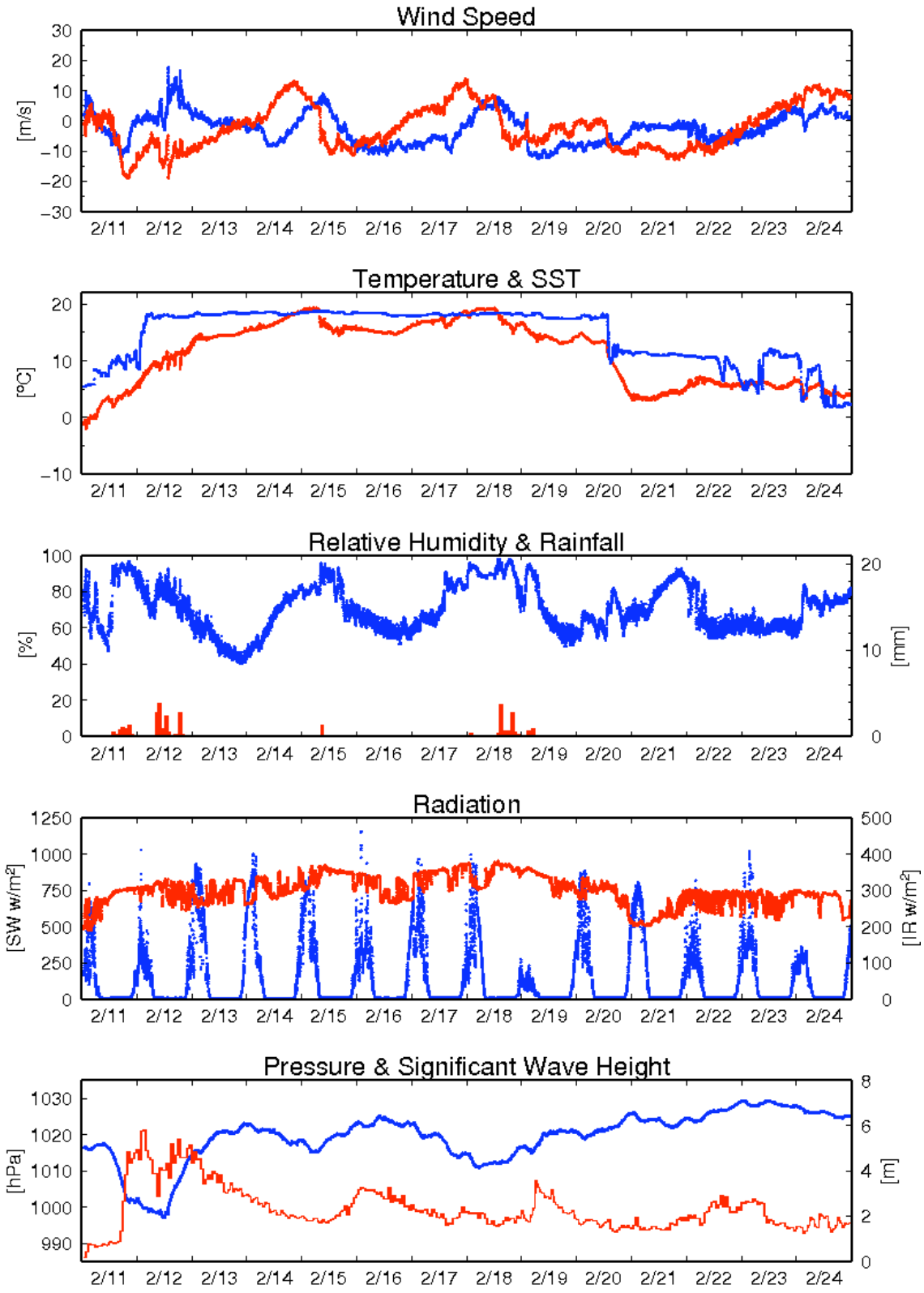

Fig.2.1.1-1 Time series of surface meteorological parameters during the MR11-02 cruise

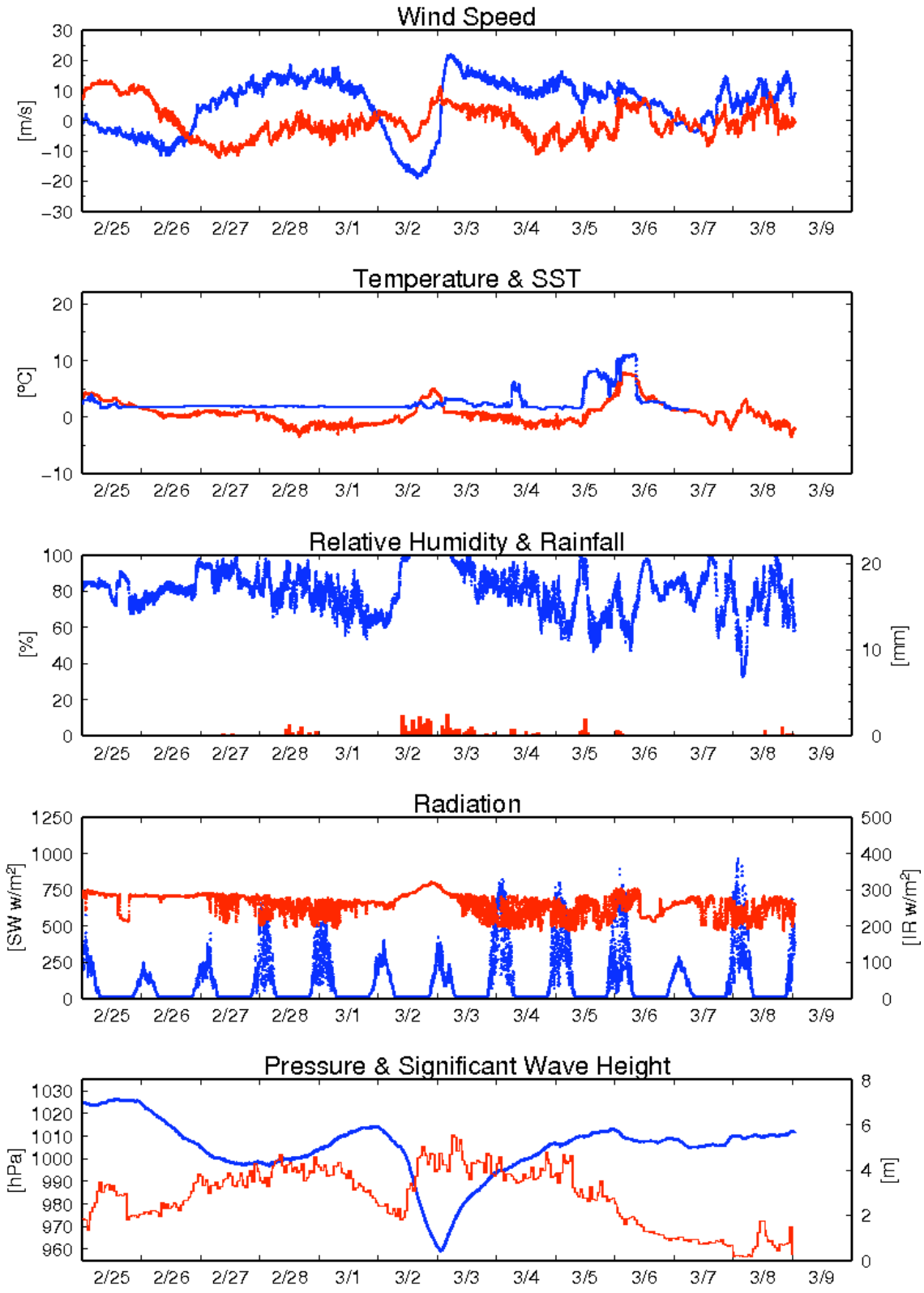

Fig.2.1.1-1 Continued

2.1.2 Ceilometer Observation

Kazuho YOSHIDA (Global Ocean Development Inc., GODI)
Wataru TOKUNAGA (Mirai Crew)

(1) Objectives

The information of cloud base height and the liquid water amount around cloud base is important to understand the process on formation of the cloud. As one of the methods to measure them, the ceilometer observation was carried out.

(2) Parameters

1. Cloud base height [m].
2. Backscatter profile, sensitivity and range normalized at 30 m resolution.
3. Estimated cloud amount [oktas] and height [m]; Sky Condition Algorithm.

(3) Methods

We measured cloud base height and backscatter profile using ceilometer (CT-25K, VAISALA, Finland) throughout the MR11-02 cruise from the departure of Sekinehama on 11 February 2011 to arrival of Sekinehama on 11 February 2011.

Major parameters for the measurement configuration are as follows;

Laser source:	Indium Gallium Arsenide (InGaAs) Diode
Transmitting wavelength:	905±5 mm at 25 degC
Transmitting average power:	8.9 mW
Repetition rate:	5.57 kHz
Detector:	Silicon avalanche photodiode (APD)
	Responsibility at 905 nm: 65 A/W
Measurement range:	0 ~ 7.5 km
Resolution:	50 ft in full range
Sampling rate:	60 sec
Sky Condition	0, 1, 3, 5, 7, 8 oktas (9: Vertical Visibility)
	(0: Sky Clear, 1:Few, 3:Scattered, 5-7: Broken, 8: Overcast)

On the archive dataset, cloud base height and backscatter profile are recorded with the resolution of 30 m (100 ft).

(4) Preliminary results

Figure 2.1.2-1 shows the time series of the lowest, second and third cloud base height.

(5) Data archives

The raw data obtained during this cruise will be submitted to the Data Integration and Analysis Group (DIAG) in JAMSTEC.

(6) Remarks

i.Window cleaning;

00:40UTC 11 Feb. 2011
02:40UTC 15 Feb. 2011
04:39UTC 22 Feb. 2011
22:45UTC 01 Mar. 2011

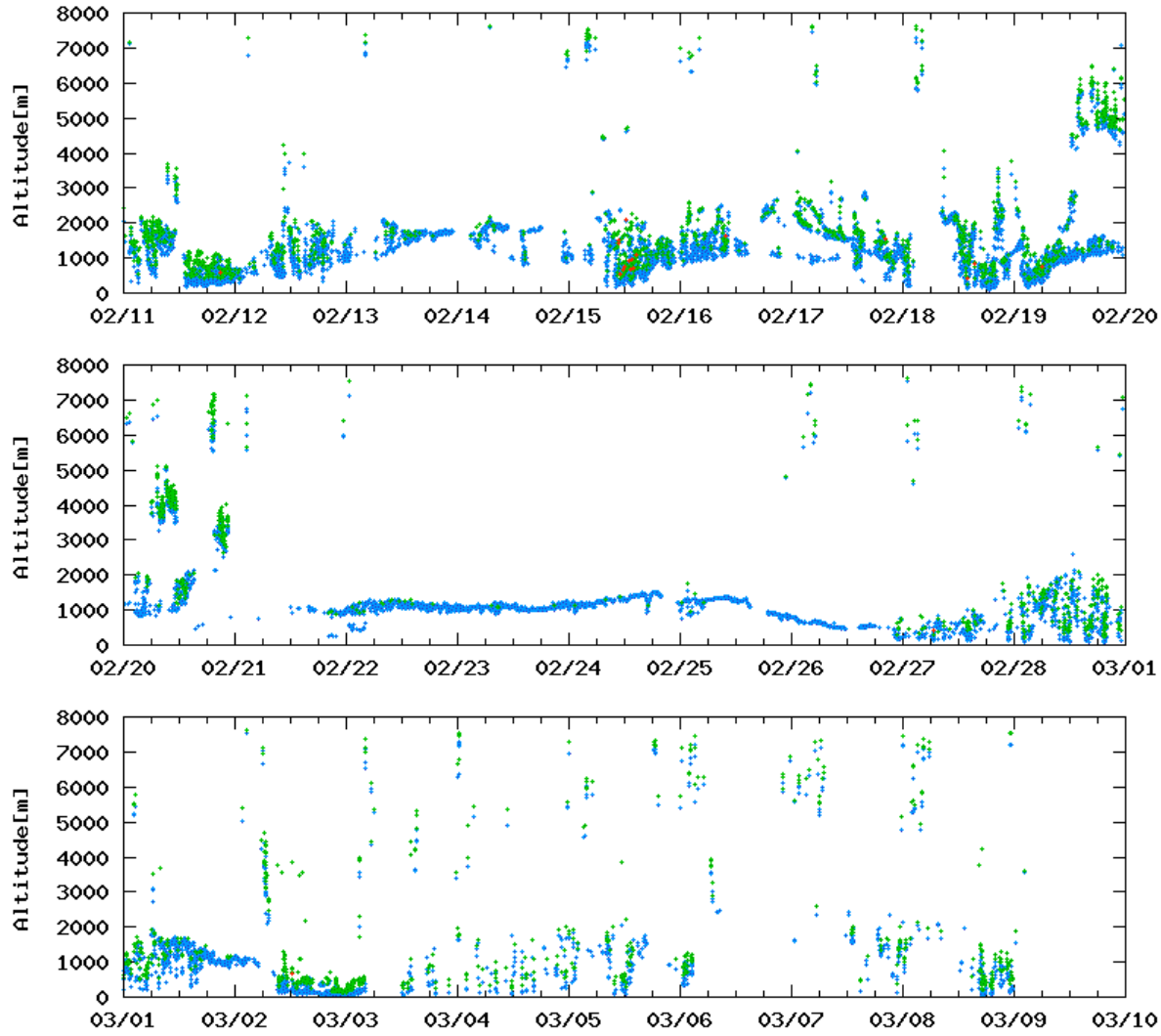

Fig.2.1.2-1 Lowest (blue), 2nd (green) and 3rd(red) cloud base height during the cruise.

2.1.3 Lidar observations of clouds and aerosols

Nobuo SUGIMOTO (National Institute for Environmental Studies: NIES, not on board),
Ichiro MATSUI (NIES)
Atsushi SHIMIZU (NIES)
Tomoaki NISHIZAWA(NIES)
Lidar operation was supported by Global Ocean Development Inc.

(1) Objectives

Objectives of the observations in this cruise is to study distribution and optical characteristics of ice/water clouds and marine aerosols using a two-wavelength lidar.

(2) Measured parameters

- Vertical profiles of backscattering coefficient at 532 nm
- Vertical profiles of backscattering coefficient at 1064 nm
- Depolarization ratio at 532 nm

(3) Method

Vertical profiles of aerosols and clouds were measured with a two-wavelength lidar. The lidar employs a Nd:YAG laser as a light source which generates the fundamental output at 1064 nm and the second harmonic at 532 nm. Transmitted laser energy is typically 30 mJ per pulse at both of 1064 and 532 nm. The pulse repetition rate is 10 Hz. The receiver telescope has a diameter of 20 cm. The receiver has three detection channels to receive the lidar signals at 1064 nm and the parallel and perpendicular polarization components at 532 nm. An analog-mode avalanche photo diode (APD) is used as a detector for 1064 nm, and photomultiplier tubes (PMTs) are used for 532 nm. The detected signals are recorded with a transient recorder and stored on a hard disk with a computer. The lidar system was installed in a container which has a glass window on the roof, and the lidar was operated continuously regardless of weather. Every 10 minutes vertical profiles of four channels (532 parallel, 532 perpendicular, 1064, 532 near range) are recorded.

(4) Results

As obtained data has not been transferred to NIES, observation results are not shown here.

(5) Data archive

- raw data
  - lidar signal at 532 nm
  - lidar signal at 1064 nm
  - depolarization ratio at 532 nm
  - temporal resolution 10min/ vertical resolution 6 m
  - data period (UTC): February 11, 2011 - March 8, 2011
- processed data (plan)
  - cloud base height, apparent cloud top height
  - phase of clouds (ice/water)
  - cloud fraction
  - boundary layer height (aerosol layer upper boundary height)

backscatter coefficient of aerosols
particle depolarization ratio of aerosols

(6) Data policy and Citation

Contact NIES lidar team (nsugimot/i-matsui/shimizua/nisizawa@nies.go.jp) to utilize lidar data for productive use.

2.1.4 Optical characteristics of aerosol measured by Shipborne Sky radiometer

Kazuma AOKI (University of Toyama) Principal Investigator / not onboard
Tadahiro HAYASAKA (Tohoku University) Co-worker / not onboard

(1) Objective

Objective of the observations in this aerosol is to study distribution and optical characteristics of marine aerosols by using a ship-borne sky radiometer (POM-01 MKII: PREDE Co. Ltd., Japan). Furthermore, collections of the data for calibration and validation to the remote sensing data were performed simultaneously.

(2) Methods and Instruments

Sky radiometer is measuring the direct solar irradiance and the solar aureole radiance distribution, has seven interference filters (0.34, 0.4, 0.5, 0.675, 0.87, 0.94, and 1.02 μm). Analysis of these data is performed by SKYRAD.pack version 4.2 developed by Nakajima *et al*. 1996.

@ Measured parameters

- Aerosol optical thickness at five wavelengths (400, 500, 675, 870 and 1020 nm)
- Ångström exponent
- Single scattering albedo at five wavelengths
- Size distribution of volume (0.01 μm – 20 μm)

GPS provides the position with longitude and latitude and heading direction of the vessel, and azimuth and elevation angle of sun. Horizon sensor provides rolling and pitching angles.

(3) Preliminary results

This study is not onboard. Data obtained in this cruise will be analyzed at University of Toyama.

(4) Data archives

Measurements of aerosol optical data are not archived so soon and developed, examined, arranged and finally provided as available data after certain duration. All data will archived at University of Toyama (K.Aoki, SKYNET/SKY: http://skyrad.sci.u-toyama.ac.jp/) after the quality check and submitted to JAMSTEC.

2. 1.5 Tropospheric aerosol and gas profile observations by MAX-DOAS on a research vessel

Hisahiro TAKASHIMA (PI, JAMSTEC/RIGC, not on board)
Hitoshi IRIE (JAMSTEC/RIGC)
Yugo KANAYA (JAMSTEC/RIGC)

(1) Objectives

- To quantify typical background values of atmospheric aerosol and gas over the ocean
- To clarify transport processes from source over Asia to the ocean (and also clarify the gas emission from the ocean (including organic gas))
- To validate satellite measurements (as well as chemical transport model)

(2) Methods

Multi-Axis Differential Optical Absorption Spectroscopy (MAX-DOAS) is a passive remote sensing technique using scattered visible and ultraviolet (UV) solar radiation at several elevation angles. The MAX-DOAS system used in this study records spectra of scattered solar radiation every 0.2-0.4 second. Measurements were made at several elevation angles of 0, 1.5, 3, 5, 10, 20, 30, 70, 110, 150, 160, 170, 175, 177 and 178.5 degrees using a movable mirror, which repeated the same sequence of elevation angles every 30-min. The UV/visible spectra range was changed every min (284-423 nm and 391-528 nm). On the roof top of the anti-rolling system of R/V *Mirai*, the telescope unit was installed on a gimbal mount, which compensates for the pitch and roll of the ship. A sensor measuring pitch and roll of the telescope unit (10Hz) is used together to measure an offset of elevation angle due to incomplete compensation by the gimbal. The line of sight was in directions of the starboard and portside of the ship.

After measurements were made, we first selected spectrum data with an elevation angle offset less than ±0.2 degrees. For those spectra, DOAS spectral fitting was performed to quantify the slant column density (SCD), defined as the concentration integrated along the light path, for each elevation angle. In this analysis, SCDs of NO_2 (and other gases) and O_4 (O_2-O_2, collision complex of oxygen) were obtained together. Next, O_4 SCDs were converted to the aerosol optical depth (AOD) and the vertical profile of aerosol extinction coefficient (AEC) at a wavelength of 476 nm using an optimal estimation inversion method with a radiative transfer model. Using derived aerosol information, another inversion is performed to retrieve the tropospheric vertical column/profile of NO_2 and other gases.

(3) Preliminary results

These data for the whole cruise period will be analyzed.

(4) Data archives

The data will be submitted to the Marine-Earth Data and Information Department (MEDID) of JAMSTEC after the full analysis of the raw spectrum data is completed, which will be <2 years after the end of the cruise.

2.1.6 Rain, water vapor and surface water sampling

Naoyuki KURITA (JAMSTEC) Principal Investigator（not on-board）
Kazuho YOSHIDA (Global Ocean Development Inc.: GODI) Operator

(1) Objective

It is well known that the variability of stable water isotopes (HDO and $H_2{}^{18}O$) is closely related with the moisture origin and hydrological processes during the transportation from the source region to deposition site. Thus, water isotope tracer is recognized as the powerful tool to study of the hydrological cycles in the atmosphere. However, oceanic region is one of sparse region of the isotope data, it is necessary to fill the data to identify the moisture sources by using the isotope tracer. In this study, to fill this sparse observation area, intense water isotopes observation was conducted along the cruise track of MR11-02.

(2) Method

Following observation was carried out throughout this cruise.

- Atmospheric moisture sampling:

  Water vapor was sampled from the height about 20m above the sea level. The air was drawn at rate of 2.0-4.0L/min through a plastic tube attached to top of the compass deck. The flow rate is regulated according to the water vapor content to collect the sample amount 4-20ml. The water vapor was trapped in a glass trap submerged into an ethanol cooled to 100 degree C by radiator, and then they are collected every 12 or 24 hour during the cruise. After collection, water in the trap was subsequently thawed and poured into the 6ml glass bottle.

- Rainwater sampling

  Rainwater samples gathered in rain/snow collector were collected just after precipitation events have ended. The collected sample was then transferred into glass bottle (6ml) immediately after the measurement of precipitation amount.

- Surface seawater sampling

  Seawater sample taken by the pump from 4m depth were collected in glass bottle (6ml) around the noon at the local time.

(3) Results

Sampling of water vapor for isotope analysis is summarized in Table X.XX-1 (26 samples). The detail of rainfall sampling (9 samples) is summarized in Table X.XX-2. Described rainfall amount is calculated from the collected amount of precipitation. Sampling of surface seawater taken by pump from 4m depths is summarized in Table X.XX-3 (24 samples).

(4) Data archive

Isotopes (HDO, $H_2{}^{18}O$) analysis will be done at RIGC/JAMSTEC, and then analyzed isotopes data will be submitted to JAMSTEC Data Integration and Analysis Group (DIAG).

Table X.XX-1 Summary of water vapor sampling for isotope analysis

	Start		End						
Sample	Date	Time (UT)	Date	Time (UT)	Lon	Lat	T.M. (m^3)	Sam. (ml)	H2O ppm
V-1	2.10	23:40	2.11	11:06	142-22.6E	39-24.9N	2.72	6.0	2745
V-2	2.11	11:12	2.11	23:08	143-12.1E	36-34.0N	2.85	11.0	4803
V-3	2.11	23:15	2.12	20:55	144-36.0E	31-29.3N	4.07	22.0	6727
V-4	2.12	22:07	2.13	22:05	145-00.0E	30-00.0N	4.27	24.2	7053
V-5	2.13	22:11	2.14	22:04	144-56.1E	29-59.6N	4.25	32.5	9516
V-6	2.14	22:10	2.15	22:00	144-50.3E	29-58.3N	2.85	29.8	13012
V-7	2.15	22:07	2.16	22:00	144-53.8E	29-54.7N	2.86	18.6	8093
V-8	2.16	22:04	2.17	22:01	144-59.6E	30-00.2N	2.86	25.5	11096
V-9	2.17	22:07	2.18	22:04	144-36.3E	29-51.3N	2.87	34.4	14916
V-10	2.18	22:10	2.19	22:00	144-36.3E	32-26.4N	2.85	20.4	8908
V-11	2.19	22:04	2.20	22:00	146-13.1E	37-39.1N	2.87	15.4	6678
V-12	2.20	22:03	2.21	22:00	146-26.1E	38-05.5N	2.90	9.8	4205
V-13	2.21	22:03	2.22	22:00	146-24.5E	38-05.7N	2.86	10.0	4351
V-14	2.22	22:06	2.23	22:02	149-00.1E	40-14.9N	4.30	14.0	4052
V-15	2.23	22:06	2.24	22:00	155-24.1E	43-47.2N	4.30	15.8	4573
V-16	2.24	22:05	2.25	22:06	160-10.2E	47-00.7N	4.32	16.0	4609
V-17	2.25	22:12	2.26	22:00	160-05.3E	47-00.2N	4.30	12.2	3531
V-18	2.26	22:06	2.27	22:06	160-09.1E	46-57.4N	4.34	14.6	4186
V-19	2.27	22:12	2.28	22:26	160-09.7E	47-00.5N	4.37	11.8	3360
V-20	2.28	22:29	3.1	22:13	160-13.9E	46-53.9N	4.31	9.8	2830
V-21	3.1	22:18	3.2	22:02	157-51.7E	45-32.3N	4.29	14.0	4061
V-22	3.2	22:06	3.3	22:06	155-07.7E	43-30.9N	4.33	16.4	4713
V-23	3.3	22:09	3.4	22:01	153-22.3E	42-59.8N	4.30	11.4	3299
V-24	3.4	22:04	3.5	22:03	149-58.2E	40-30.3N	4.33	10.0	2874
V-25	3.5	22:07	3.6	23:00	149-41.0E	40-22.0N	4.48	21.2	5889
V-26	3.6	23:04	3.7	23:09	141-32.6E	40-32.6N	4.34	13.4	3842

Table X.XX-2 Summary of precipitation sampling for isotope analysis.

	Date	Time (UT)	Lon	Lat	Date	Time (UT)	Lon	Lat	Rain (mm)	R / S
R-1	2.11	00:40	141-14E	41-22N	2.11	23:26	143-13.0E	36-30.6N	3.7	S
R-2	2.11	23:26	143-13.0E	36-30.6N	2.12	20:55	144-31.4E	31-46.8N	15.5	R
R-3	2.12	20:55	144-31.4E	31-46.8N	2.15	20:50	144-48.6E	29-57.6N	0.6	R
R-4	2.15	20:50	144-48.6E	29-57.6N	2.18	04:57	145-00.1E	29-59.8N	0.9	R

R-5	2.18	04:57	145-00.1E	29-59.8N	2.19	00:33	144-59.7E	29-58.2N	9.0	R
R-6	2.19	00:35	145-00.0E	29-58.2N	2.20	08:22	144-58.5E	34-51.3N	2.4	R
R-7	2.20	08:22	144-58.5E	34-51.3N	3.01	22:34	160-13.8E	46-53.6N	10.6	S
R-8	3.01	22:34	160-13.8E	46-53.6N	3.04	04:22	154-37.9E	43-09.1N	16.9	S
R-9	3.04	04:27	154-37.7E	43-09.0N	3.06	04:31	148-36.5E	40-22.1N	9.4	S

Table X.XX-3 Summary of water vapor sampling for isotope analysis

Sampling No.		Date	Time	Position	
			(UTC)	LON	LAT
MR11-02 O-	1	2.12	03:07	143-25.1E	35-49.1N
MR11-02 O-	2	2.13	02:03	144-51.8E	30-30.6N
MR11-02 O-	3	2.14	02:10	144-57.3E	29-56.5N
MR11-02 O-	4	2.15	02:05	145-00.0E	30-00.2N
MR11-02 O-	5	2.16	02:01	144-59.4E	30-00.1N
MR11-02 O-	6	2.17	02:16	144-59.4E	29-55.6N
MR11-02 O-	7	2.18	02:00	144-59.6E	30-00.5N
MR11-02 O-	8	2.19	02:02	145-02.4E	29-59.6N
MR11-02 O-	9	2.20	02:05	144-43.2E	33-19.4N
MR11-02 O-	10	2.21	02:28	146-29.9E	38-02.1N
MR11-02 O-	11	2.22	06:38	146-24.4E	38-07.5N
MR11-02 O-	12	2.23	02:00	146-19.6E	38-04.0N
MR11-02 O-	13	2.24	02:04	149-57.9E	40-34.4N
MR11-02 O-	14	2.25	02:04	156-17.5E	44-24.6N
MR11-02 O-	15	2.26	02:04	160-12.6E	46-59.5N
MR11-02 O-	16	2.27	02:00	160-02.8E	46-57.6N
MR11-02 O-	17	2.28	02:00	160-05.0E	46-59.6N
MR11-02 O-	18	3.1	02:16	160-07.2E	46-59.6N
MR11-02 O-	19	3.2	02:03	160-11.6E	46-52.5N
MR11-02 O-	20	3.3	02:03	157-07.2E	45-01.2N
MR11-02 O-	21	3.4	02:03	154-44.7E	43-13.9N
MR11-02 O-	22	3.5	02:00	153-22.1E	42-56.2N

MR11-02 O-	23	3.6	02:01	149-07.6E	40-21.8N
MR11-02 O-	24	3.7	03:02	144-35.6E	40-21.9N

2.1.7 Air-sea surface eddy flux measurement

Osamu TSUKAMOTO **(Okayama University) Principal Investigator**
*** not on board**
Fumiyoshi KONDO **(University of Tokyo) * not on board**
Hiroshi ISHIDA **(Kobe University) * not on board**
Satoshi OKUMURA **(Global Ocean Development Inc. (GODI))**

(1) Objective

To better understand the air-sea interaction, accurate measurements of surface heat and fresh water budgets are necessary as well as momentum exchange through the sea surface. In addition, the evaluation of surface flux of carbon dioxide is also indispensable for the study of global warming. Sea surface turbulent fluxes of momentum, sensible heat, latent heat, and carbon dioxide were measured by using the eddy correlation method that is thought to be most accurate and free from assumptions. These surface heat flux data are combined with radiation fluxes and water temperature profiles to derive the surface energy budget.

(2) Instruments and Methods

The surface turbulent flux measurement system (Fig. 1) consists of turbulence instruments (Kaijo Co., Ltd.) and ship motion sensors (Kanto Aircraft Instrument Co., Ltd.). The turbulence sensors include a three-dimensional sonic anemometer-thermometer (Kaijo, DA-600) and an infrared hygrometer (LICOR, LI-7500). The sonic anemometer measures three-dimensional wind components relative to the ship. The ship motion sensors include a two-axis inclinometer (Applied Geomechanics, MD-900-T), a three-axis accelerometer (Applied Signal Inc., QA-700-020), and a three-axis rate gyro (Systron Donner, QRS-0050-100). LI7500 is a CO_2/H_2O turbulence sensor that measures turbulent signals of carbon dioxide and water vapor simultaneously. These signals are sampled at 10 Hz by a PC-based data logging system (Labview, National Instruments Co., Ltd.). By obtaining the ship speed and heading information through the Mirai network system it yields the absolute wind components relative to the ground. Combining wind data with the turbulence data, turbulent fluxes and statistics are calculated in a real-time basis. These data are also saved in digital files every 0.1 second for raw data and every 1 minute for statistic data.

(3) Observation log

The observation was carried out throughout this cruise.

(4) Data Policy and citation

All data are archived at Okayama University, and will be open to public after quality checks and corrections. Corrected data will be submitted to JAMSTEC Marine-Earth Data and Information Department.

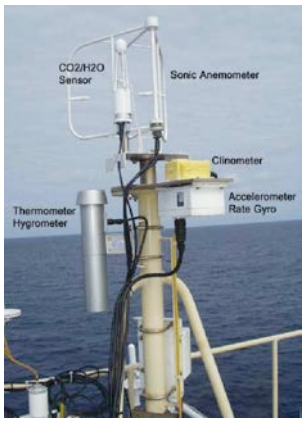

Fig. 1 Turbulent flux measurement system on the top deck of the foremast

2.2 Physical oceanographic observation

2.2.1 CTD cast and water sampling

Masahide WAKITA (JAMSTEC RIGC)
Shinsuke TOYODA (MWJ)
Hirokatsu UNO (MWJ)
Fujio KOBAYASHI (MWJ)
Toru IDAIi (MWJ)
Tomoyuki TAKAMORI (MWJ)
Shungo OSHITANI (MWJ)

(1) Objective

Investigation of oceanic structure and water sampling.

(2) Parameters

Temperature (Primary and Secondary)
Conductivity (Primary and Secondary)
Pressure
Dissolved Oxygen
Fluorescence
Transmission Voltage
Dissolved Oxygen Voltage
Photosynthetically Active Radiation
Altimeter

(3) Instruments and Methods

CTD/Carousel Water Sampling System, which is a 36-position Carousel water sampler (CWS) with Sea-Bird Electronics, Inc. CTD (SBE9plus), was used during this cruise. 12-litter Niskin Bottles, which were washed by alkaline detergent and 1 N HCl, were used for sampling seawater. The sensors attached on the CTD were temperature (Primary and Secondary), conductivity (Primary and Secondary), pressure, fluorescence, transmission voltage, RINKO-III (dissolved oxygen sensor), ARO-CAV (dissolved oxygen sensor), dissolved oxygen, altimeter, PAR sensor and deep ocean standards thermometer. The Practical Salinity was calculated by measured values of pressure, conductivity and temperature. The CTD/CWS was deployed from starboard on working deck.

The CTD raw data were acquired on real time using the Seasave-Win32 (ver.7.20g) provided by Sea-Bird Electronics, Inc. and stored on the hard disk of the personal computer. Seawater was sampled during the up cast by sending fire commands from the personal computer. We usually stop at each layer for 30 seconds to stabilize then fire.

20 casts of CTD measurements were conducted (table 2.2.1-1).

Primary temperature sensor was changed, before the first cast. So we used MR1102B.con configuration file.

In the up cast of Stn.S01cast 1 (filename: S01M01), sift was observed in the dissolved oxygen voltage (SBE43).

Data processing procedures and used utilities of SBE Data Processing-Win32 (ver.7.18d) and

SEASOFT were as follows:

(The process in order)

DATCNV: Convert the binary raw data to engineering unit data. DATCNV also extracts bottle information where scans were marked with the bottle confirm bit during acquisition. The duration was set to 4.4 seconds, and the offset was set to 0.0 seconds.

RINKOCOR (original module): Corrected of the hysteresis of RINK-III voltage and ARO-CAV voltage.

RINKOCORROS (original module): Corrected of the hysteresis of RINKO-III voltage bottle data and ARO-CAV voltage bottle data.

BOTTLESUM: Create a summary of the bottle data. The data were averaged over 4.4 seconds.

ALIGNCTD: Convert the time-sequence of sensor outputs into the pressure sequence to ensure that all calculations were made using measurements from the same parcel of water. Dissolved oxygen data are systematically delayed with respect to depth mainly because of the long time constant of the dissolved oxygen sensor and of an additional delay from the transit time of water in the pumped pluming line. This delay was compensated by 6 seconds advancing dissolved oxygen sensor (SBE43) output (dissolved oxygen voltage) relative to the temperature data. RINKO-III data, ARO-CAV data and transmission voltage data are also delayed by slightly slow response time to the sensor. The delay was compensated by 1 second or 2 seconds advancing.

WILDEDIT: Mark extreme outliers in the data files. The first pass of WILDEDIT obtained an accurate estimate of the true standard deviation of the data. The data were read in blocks of 1000 scans. Data greater than 10 standard deviations were flagged. The second pass computed a standard deviation over the same 1000 scans excluding the flagged values. Values greater than 20 standard deviations were marked bad. This process was applied to pressure, depth, temperature, conductivity and dissolved oxygen voltage (SBE43).

CELLTM: Remove conductivity cell thermal mass effects from the measured conductivity. Typical values used were thermal anomaly amplitude alpha = 0.03 and the time constant 1/beta = 7.0.

FILTER: Perform a low pass filter on pressure with a time constant of 0.15 second. In order to produce zero phase lag (no time shift) the filter runs forward first then backward

WFILTER: Perform a median filter to remove spikes in the fluorescence data and transmission voltage data. A median value was determined by 49 scans of the window.

SECTIONU (original module of SECTION): Select a time span of data based on scan number in order to reduce a file size. The minimum number was set to be the starting time when the CTD package was beneath the sea-surface after activation of the pump. The maximum number of was set to be the end time when the package came up from the surface.

LOOPEDIT: Mark scans where the CTD was moving less than the minimum velocity of 0.0 m/s (traveling backwards due to ship roll).

DESPIKE (original module): Remove spikes of the data. A median and mean absolute deviation was calculated in 1-dbar pressure bins for both down and up cast, excluding the flagged values. Values greater than 4 mean absolute deviations from the median were marked bad for each bin. This process was performed 2 times for temperature, conductivity, dissolved oxygen voltage (SBE43), RINKO-III voltage and ARO-CAV voltage.

DERIVE: Compute dissolved oxygen (SBE43).

BINAVG: Average the data into 1-dbar pressure bins.

DERIVE: Compute the Practical Salinity, potential temperature, and sigma-theta.

SPLIT: Separate the data from an input .cnv file into down cast and up cast files.

Configuration file: MR1102B.con

Specifications of the sensors are listed below.
CTD: SBE911plus CTD system
Under water unit:
SBE9plus (S/N 09P79511-0677, Sea-Bird Electronics, Inc.)
Pressure sensor: Digiquartz pressure sensor (S/N 79511)
Calibrated Date: 07 Jul. 2010
Temperature sensors:
Primary: SBE03Plus (S/N 03P2730, Sea-Bird Electronics, Inc.)
Calibrated Date: 16 Sep. 2010
Secondary: SBE03-04/F (S/N 031359, Sea-Bird Electronics, Inc.)
Calibrated Date: 20 Jul. 2010
Conductivity sensors:
Primary: SBE04-04/0 (S/N 041206, Sea-Bird Electronics, Inc.)
Calibrated Date: 20 Jul. 2010
Secondary: SBE04-04/0 (S/N 041203, Sea-Bird Electronics, Inc.)
Calibrated Date: 20 Jul. 2010
Fluorescence:

Chlorophyll Fluorometer (S/N 3054, Seapoint Sensors, Inc.)

Altimeter:

Benthos PSA-916T (S/N 1100, Teledyne Benthos, Inc.)

Dissolved Oxygen sensor:

SBE43 (S/N 430394, Sea-Bird Electronics, Inc.)

Calibrated Date: 10 Dec. 2010

Dissolved Oxygen sensors:

RINK-III (S/N 006, Alec Electronics Co. Ltd.)

ARO-CAV (S/N 0024, Alec Electronics Co. Ltd.)

Photosynthetically Active Radiation:

PAR sensor (S/N 0049, Satlantic Inc.)

Calibrated Date: 22 Jan. 2009

Deep Ocean Standards Thermometer:

SBE35 (S/N 0053, Sea-Bird Electronics, Inc.)

Calibrated Date: 24 Jun. 2010

Carousel water sampler:

SBE32 (S/N 3227443-0391, Sea-Bird Electronics, Inc.)

Deck unit: SBE11plus (S/N 11P7030-0272, Sea-Bird Electronics, Inc.)

(4) Preliminary Results

During this cruise, 20 casts of CTD observation were carried out. Date, time and locations of the CTD casts are listed in Table 2.2.1-1.

(5) Data archive

All raw and processed data files were copied onto HD provided by Data Integration and Analyses Group (DIAG), JAMSTEC will be opened to public via “R/V MIRAI Data Web Page” in the JAMSTEC home page.

Table 2.2.1-1 MR11-02 CTD Casttable

Stnnbr	Castno	Date(UTC)	Time(UTC)		BottomPosition		Depth	Wire Out	HT Above	Max Depth	Max Pressure	CTD Filename	Remark
		(mmddyy)	Start	End	Latitude	Longitude							
S01	1	021311	07:31	10:34	30-00.06N	144-59.96E	5969.0	5006.0	-	4999.8	5094.5	S01M01	Bacteria
S01	2	021311	20:05	00:08	29-59.93N	144-59.83E	5969.0	5954.8	8.1	5947.1	6072.8	S01M02	Routine
S01	3	021411	18:02	18:41	30-00.05N	144-53.97E	5874.0	299.3	-	301.1	303.0	S01M03	P.P.
S01	4	021411	23:01	23:52	30-00.13N	145-00.05E	5971.0	1006.0	-	1002.0	1011.9	S01M04	P.E.
S01	5	021511	10:11	10:40	29-59.77N	145-00.21E	5962.0	196.6	-	199.5	201.3	S01M05	K.U. & N.U.
S01	6	021611	01:28	02:28	30-00.05N	144-59.47E	5967.0	1022.0	-	1001.7	1011.0	S01M06	RI
S01	7	021711	18:36	19:17	30-00.06N	144-59.86E	5966.0	298.2	-	300.3	303.0	S01M07	P.P.
S01	8	021811	10:30	10:50	29-59.49N	144-59.47E	5953.0	196.6	-	200.1	201.7	S01M08	K.U. & N.U.
S01	9	021811	22:59	23:13	29-54.70N	144-50.56E	5914.0	299.8	-	300.9	303.7	S01M09	TEST
002	1	021911	09:17	10:16	31-09.46N	144-46.00E	5675.0	1006.2	-	1001.8	1011.5	002M01	O.I.
KEO	1	021911	16:32	20:15	32-27.92N	144-35.15E	5685.0	5707.8	7.8	5703.0	5820.2	KEOM01	Routine
004	1	022011	09:09	10:05	35-00.04N	145-00.10E	5800.0	1001.8	-	1001.3	1010.5	004M01	O.I.
JKO	1	022111	03:06	06:38	38-02.12N	146-29.44E	5401.0	5403.9	9.1	5387.3	5497.1	JKOM01	Routine
006	1	022311	22:02	22:50	40-14.93N	149-00.29E	5687.0	1002.0	-	1000.5	1010.8	006M01	O.I.
K02	1	022511	18:04	18:43	47-00.21N	160-10.19E	5260.0	298.0	-	301.2	303.8	K02M01	P.P.
K02	2	022511	21:02	00:26	47-00.71N	160-10.37E	5255.0	5273.4	10.4	5230.0	5338.4	K02M02	Routine
K02	3	022611	05:01	06:01	46-54.26N	160-14.93E	5243.0	995.4	-	1000.4	1010.9	K02M03	RI
K02	4	022611	18:04	21:30	47-00.20N	160-04.52E	5239.0	5248.6	9.4	5225.2	5331.3	K02M04	Bacteria
K02	5	030111	18:02	18:28	46-52.60N	160-21.45E	5257.0	193.5	-	201.2	202.1	K02M05	P.P.
K02	6	030211	05:25	06:21	46-52.71N	160-11.84E	5206.0	1002.2	-	1000.5	1010.8	K02M06	DO^{14}C

Routine: Routine sampling cast
Bacteria: Bacteria sampling cast
P.P.: Primary Production cast
P.E.: P vs. E curve cast
K.U.: Kagoshima Univ. & Nagoya Univ. cast
RI: radioisotope cast
O.I.: Oxygen Isotope cast
DO^{14}C: DO^{14}C sampling cast
TEST: Niskin bottles test cast

2.2.2 Salinity measurement

Masahide WAKITA (JAMSTEC MIO): Principal investigator
Fujio KOBAYASHI (MWJ): Operation leader

(1) Objective

To measure bottle salinity obtained by CTD casts, bucket sampling, and The Continuous Sea Surface Water Monitoring System (TSG).

(2) Methods

a. Salinity Sample Collection

Seawater samples were collected with 12 liter Niskin-X bottles, bucket, and TSG. The salinity sample bottle of the 250ml brown grass bottle with screw cap was used for collecting the sample water. Each bottle was rinsed three times with the sample water, and was filled with sample water to the bottle shoulder. The salinity sample bottles for TSG were sealed with a plastic inner cap and a screw cap because we took into consideration the possibility of storage for about a month. These caps were rinsed three times with the sample water before use. The bottle was stored for more than 12 hours in the laboratory before the salinity measurement.

The number of samples are shown as follows ;

Table 2.2.2-1 The number of samples

Sampling type	Number of Samples
CTD and Bucket	258
TSG	27
Total	285

b. Instruments and Method

The salinity analysis on R/V MIRAI was carried out during the cruise of MR11-02 using the salinometer (Model 8400B “AUTOSAL” ; Guildline Instruments Ltd.: S/N 62827) with an additional peristaltic-type intake pump (Ocean Scientific International, Ltd.). A pair of precision digital thermometers (Model 9540; Guildline Instruments Ltd.:S/N 66528 and 62525) were used. The thermometer monitored the ambient temperature and the bath temperature of the salinometer.

The specifications of AUTOSAL salinometer and thermometer are shown as follows ;

Salinometer (Model 8400B “AUTOSAL” ; Guildline Instruments Ltd.)

Measurement Range	:	0.005 to 42 (PSU)
Accuracy	:	Better than ±0.002 (PSU) over 24 hours without re-standardization
Maximum Resolution	:	Better than ±0.0002 (PSU) at 35 (PSU)

Thermometer (Model 9540 ; Guildline Instruments Ltd.)

Measurement Range	:	-40 to +180 deg C
Resolution	:	0.001
Limits of error ±deg C	:	0.01 (24 hours @ 23 deg C ±1 deg C)
Repeatability	:	±2 least significant digits

The measurement system was almost the same as Aoyama *et al*. (2002). The salinometer was operated in the air-conditioned ship's laboratory at a bath temperature of 24 deg C. The ambient temperature varied from approximately 20 deg C to 25 deg C, while the bath temperature was very stable and varied within +/- 0.001 deg C on rare occasion.

The measurement for each sample was done with the double conductivity ratio and defined as the median of 31 readings of the salinometer. Data collection was started 5 seconds after filling the cell with the sample and it took about 10 seconds to collect 31 readings by a personal computer. Data were taken for the sixth and seventh filling of the cell after rinsing five times. In the case of the difference between the double conductivity ratio of these two fillings being smaller than 0.00002, the average value of the double conductivity ratio was used to calculate the bottle salinity with the algorithm for practical salinity scale, 1978 (UNESCO, 1981). If the difference was greater than or equal to 0.00003, an eighth filling of the cell was done. In the case of the difference between the double conductivity ratio of these two fillings being smaller than 0.00002, the average value of the double conductivity ratio was used to calculate the bottle salinity. In the case of the double conductivity ratio of eighth filling did not satisfy the criteria above, we measured a ninth filling of the cell and calculated the bottle salinity. The measurement was conducted in about 3 - 9 hours per day and the cell was cleaned with soap after the measurement of the day.

(3)Preliminary Result

a. Standard Seawater

Standardization control of the salinometer was set to 467 and all measurements were done at this setting. The value of STANDBY was 24+5396 +/- 0002 and that of ZERO was 0.0+0000 +/- 0001. The conductivity ratio of IAPSO Standard Seawater batch P152 was 0.99981 (the double conductivity ratio was 1.99962) and was used as the standard for salinity. We measured 22 bottles of P152 except for 6 bottles used before standardization.

The specifications of SSW used in this cruise are shown as follows ;

Batch	:	P152
conductivity ratio	:	0.99981
salinity	:	34.993
Use by	:	5th May 2013

Fig.2.2.2-1 shows the history of the double conductivity ratio of the

Standard Seawater batch P152 before correction. The average of the double conductivity ratio was 1.99961 and the standard deviation was 0.00001, which is equivalent to 0.0002 in salinity.

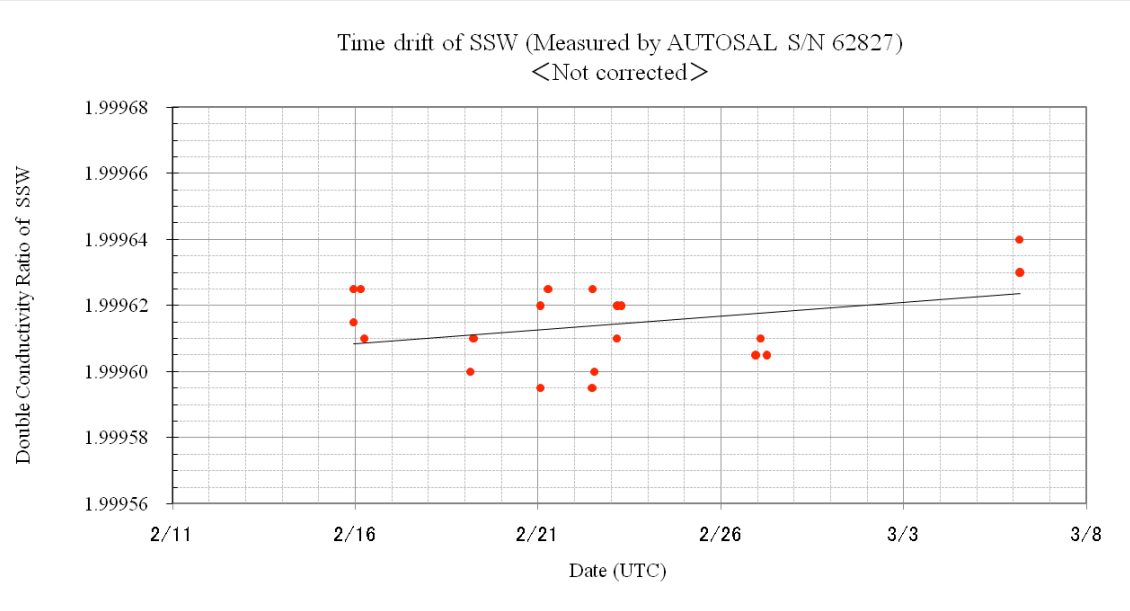

Fig. 2.2.2-1 The history of the double conductivity ratio for the Standard Seawater batch P152 (Before correction)

Fig.2.2.2-2 shows the history of the double conductivity ratio of the Standard Seawater batch P152 after correction. The average of the double conductivity ratio after correction was 1.99962 and the standard deviation was 0.00001, which is equivalent to 0.0002 in salinity.

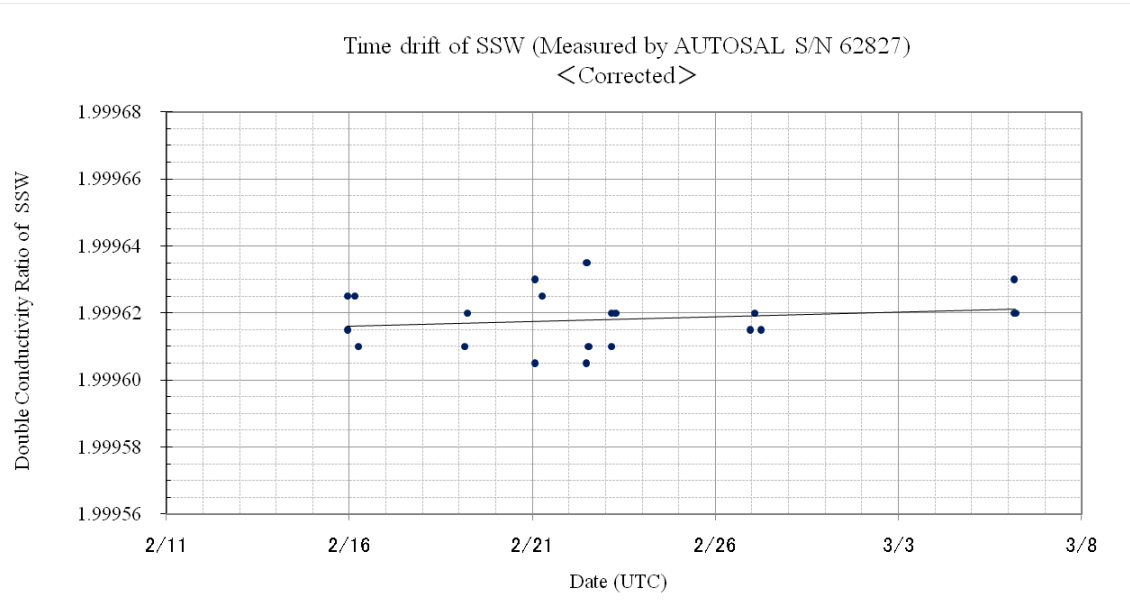

Fig. 2.2.2-2 The history of the double conductivity ratio for the Standard Seawater

batch P152 (After correction)

b. Sub-Standard Seawater

Sub-standard seawater was made from deep-sea water filtered by a pore size of 0.45 micrometer and stored in a 20-liter container made of polyethylene and stirred for at least 24 hours before measuring. It was measured about every 6 samples in order to check for the possible sudden drifts of the salinometer.

c. Replicate Samples

We estimated the precision of this method using 29 pairs of replicate samples taken from the same Niskin bottle. Fig.2.2.2-3 shows the histogram of the absolute difference between each pair of the replicate samples. There was 1 questionable measurement in the replicate samples. The average and the standard deviation of absolute deference among 29 pairs of replicate samples were 0.0002 and 0.0003 in salinity, respectively.

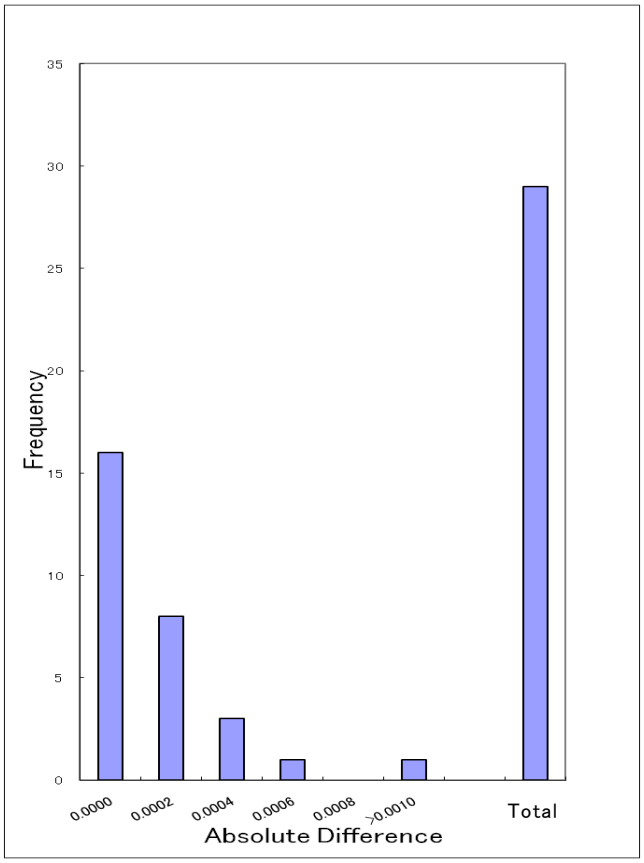

Fig. 2.2.2-3 The histogram of the double conductivity ratio
for the absolute difference of replicate samples

(4) Data archive

These raw datasets will be submitted to JAMSTEC Data Management Office (DMO).

(5) Reference

・Aoyama, M., T. Joyce, T. Kawano and Y. Takatsuki : Standard seawater comparison up to P129. Deep-Sea Research, I, Vol. 49, 1103～1114, 2002

・UNESCO : Tenth report of the Joint Panel on Oceanographic Tables and Standards. UNESCO Tech. Papers in Mar. Sci., 36, 25 pp., 1981

2.2.3 Shipboard ADCP

Kazuho Yoshida **(Global Ocean Development Inc., GODI)**
Wataru Tokunaga **(Mirai Crew)**

(1) Objective

To obtain continuous measurement of the current profile along the ship's track.

(2) Methods

Upper ocean current measurements were made throughout MR11-02 cruise, using the hull-mounted Acoustic Doppler Current Profiler (ADCP) system that is permanently installed on the R/V MIRAI. For most of its operation, the instrument was configured for water-tracking mode recording. Bottom-tracking mode, interleaved bottom-ping with water-ping, was made in shallower water region to get the calibration data for evaluating transducer misalignment angle. The system consists of following components;

i) R/V MIRAI has installed the Ocean Surveyor for vessel-mount (acoustic frequency 75 kHz; Teledyne RD Instruments). It has a phased-array transducer with single ceramic assembly and creates 4 acoustic beams electronically. We mounted the transducer head rotated to a ship-relative angle of 45 degrees azimuth from the keel
ii) For heading source, we use ship's gyro compass (Tokimec, Japan), continuously providing heading to the ADCP system directory. Additionally, we have Inertial Navigation System (INS) which provide high-precision heading, attitude information, pitch and roll, are stored in ".N2R" data files with a time stamp.
iii) DGPS system (Trimble SPS751 & StarFixXP) providing position fixes.
iv) We used VmDas version 1.4.2 (TRD Instruments) for data acquisition.
v) To synchronize time stamp of ping with GPS time, the clock of the logging computer is adjusted to GPS time every 1 minute
vi) We have placed ethylene glycol into the fresh water to prevent freezing in the sea chest.
vii) The sound speed at the transducer does affect the vertical bin mapping and vertical velocity measurement, is calculated from temperature, salinity (constant value; 35.0 psu) and depth (6.5 m; transducer depth) by equation in Medwin (1975).

Data was configured at 8-m intervals starting 23-m below the surface. Every ping was recorded as raw ensemble data (.ENR). Also, 60 seconds and 300 seconds averaged data were recorded as short term average (.STA) and long term average (.LTA) data, respectively. Major parameters for the measurement (Direct Command) are shown Table 2.2.4-1 Major parameters.

(3) Preliminary results

Fig.2.2.3-1 and Fig.2.2.3-2 show an hour averaged surface (100 – 140m) current vector along the ship track.

(4) Data archive

These data obtained in this cruise will be submitted to the Data Management Group (DMG) of JAMSTEC, and will be opened to the public via "R/V MIRAI Data Web Page" in JAMSTEC home page.

(5) Remarks

Table 2.2.3-1 Major parameters

Bottom-Track Commands	
BP = 001	Pings per Ensemble (almost less than 1000m depth) 23:29 UTC, 10 Feb. – 13:03 UTC, 11 Feb. 16:55 UTC, 08 Mar. – 00:13 UTC, 11 Mar.
BP = 000	Disable bottom-track ping (almost over 1000m depth) 13:04 UTC, 11 Feb. – 16:54 UTC, 08 Mar
Environmental Sensor Commands	
EA = +04500	Heading Alignment (1/100 deg)
EB = +00000	Heading Bias (1/100 deg)
ED = 00065	Transducer Depth (0 - 65535 dm)
EF = +001	Pitch/Roll Divisor/Multiplier (pos/neg) [1/99 - 99]
EH = 00000	Heading (1/100 deg)
ES = 35	Salinity (0-40 pp thousand)
EX = 00000	Coord Transform (Xform:Type; Tilts; 3Bm; Map)
EZ = 10200010	Sensor Source (C; D; H; P; R; S; T; U) C (1): Sound velocity calculates using ED, ES, ET (temp.) D (0): Manual ED H (2): External synchro P (0), R (0): Manual EP, ER (0 degree) S (0): Manual ES T (1): Internal transducer sensor U (0): Manual EU
Timing Commands	
TE = 00:00:02.00	Time per Ensemble (hrs:min:sec.sec/100)
TP = 00:02.00	Time per Ping (min:sec.sec/100)
Water-Track Commands	
WA = 255	False Target Threshold (Max) (0-255 count)
WB = 1	Mode 1 Bandwidth Control (0=Wid, 1=Med, 2=Nar)
WC = 120	Low Correlation Threshold (0-255)
WD = 111 110 000	Data Out (V; C; A; PG; St; Vsum; Vsum^2;#G;P0)
WE = 1000	Error Velocity Threshold (0-5000 mm/s)
WF = 0800	Blank After Transmit (cm)
WG = 001	Percent Good Minimum (0-100%)
WI = 0	Clip Data Past Bottom (0 = OFF, 1 = ON)
WJ = 1	Rcvr Gain Select (0 = Low, 1 = High)
WM = 1	Profiling Mode (1-8)
WN = 100	Number of depth cells (1-128)
WP = 00001	Pings per Ensemble (0-16384)
WS = 0800	Depth Cell Size (cm)
WT = 000	Transmit Length (cm) [0 = Bin Length]
WV = 0390	Mode 1 Ambiguity Velocity (cm/s radial)

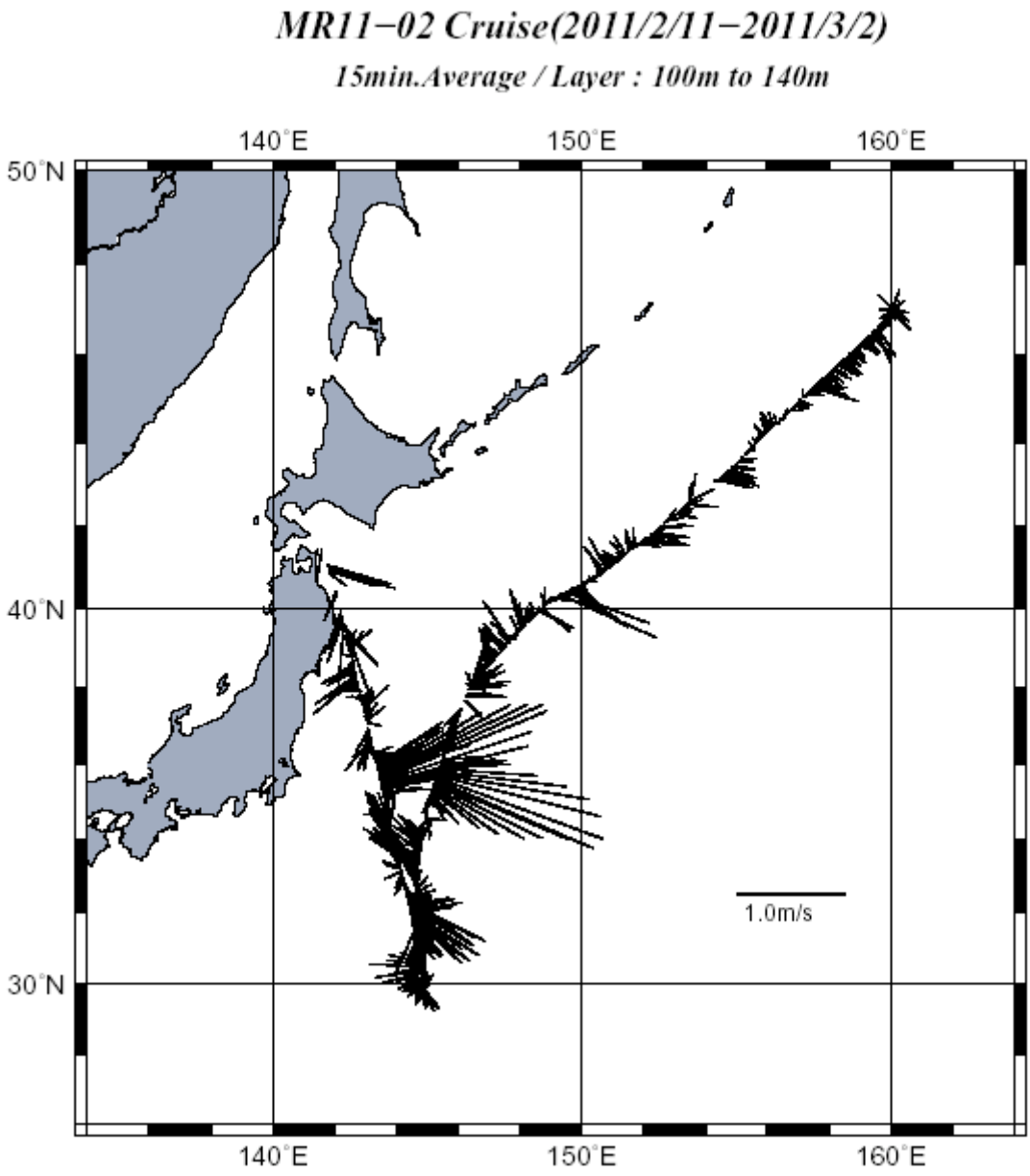

Fig. 2.2.3-1 15 minutes averaged surface (100-140 m) current vector along the ship track

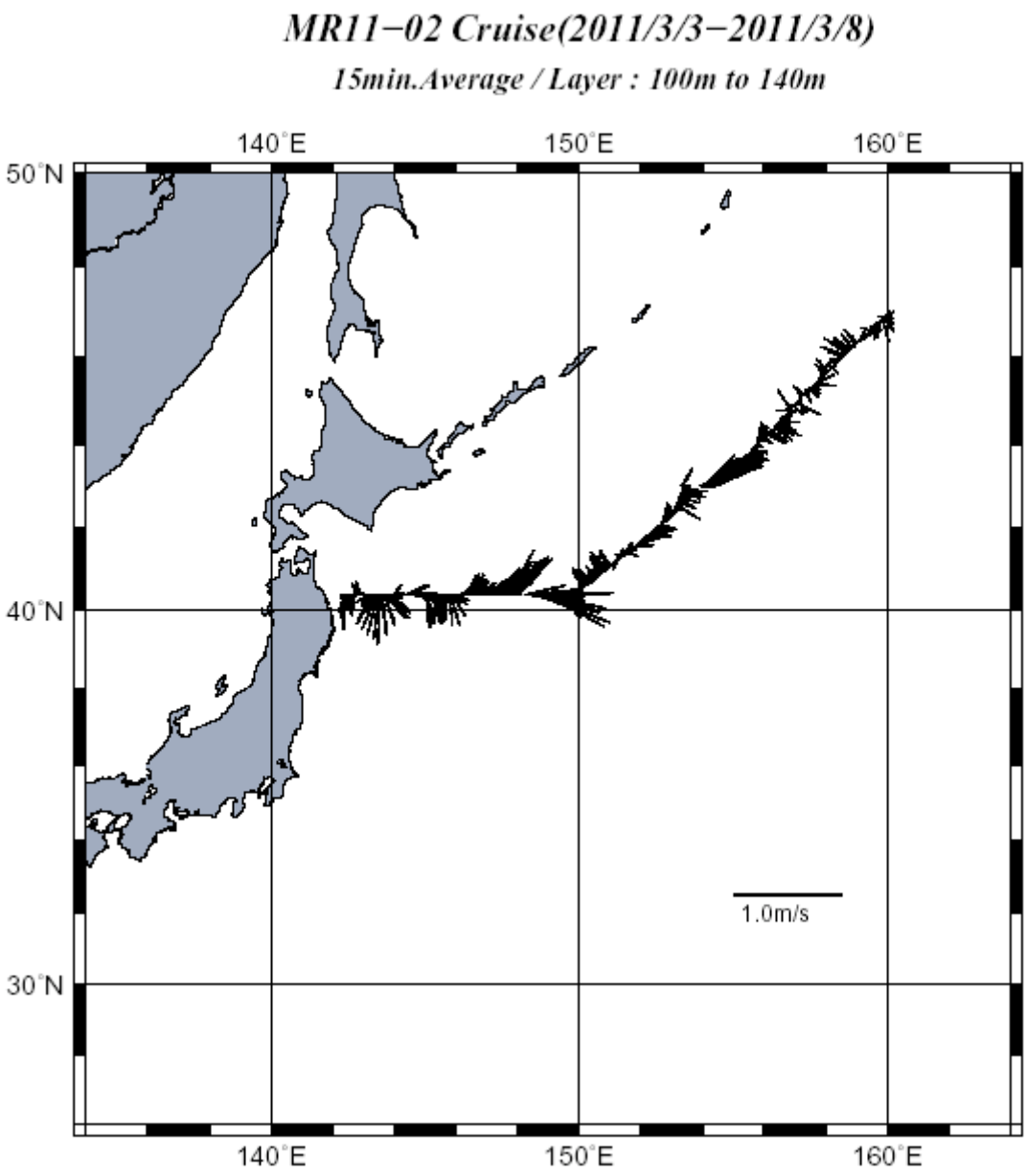

Fig. 2.2.3-2 15 minutes averaged surface (100-140 m) current vector along the ship track

2.3 Sea surface water monitoring

Masahide WAKITA (JAMSTEC): Principal Investigator
Misato KUWAHARA (Marine Works Japan Co. Ltd): Operation Leader
Hideki YAMAMOTO (Marine Works Japan Co. Ltd)

(1) Objective

Our purpose is to obtain temperature, salinity, dissolved oxygen, and fluorescence data continuously in near-sea surface water.

(2) Parameters

Temperature (surface water)
Salinity (surface water)
Dissolved oxygen (surface water)
Fluorescence (surface water)

(3) Instruments and Methods

The Continuous Sea Surface Water Monitoring System (Marine Works Japan Co. Ltd.) has five sensors and automatically measures temperature, salinity, dissolved oxygen and fluorescence in near-sea surface water every one minute. This system is located in the "*sea surface monitoring laboratory*" and connected to shipboard LAN-system. Measured data, time, and location of the ship were stored in a data management PC. The near-surface water was continuously pumped up to the laboratory from about 4.5 m water depth and flowed into the system through a vinyl-chloride pipe. The flow rate of the surface seawater was adjusted to be 5 dm^3 min^{-1}.

a. Instruments

Software

Seamoni-kun Ver.1.10

Sensors

Specifications of the each sensor in this system are listed below.

Temperature and Conductivity sensor

Model:	SBE-45, SEA-BIRD ELECTRONICS, INC.
Serial number:	4552788-0264
Measurement range:	Temperature -5 to +35 ^oC
	Conductivity 0 to 7 S m^{-1}
Initial accuracy:	Temperature 0.002 ^oC
	Conductivity 0.0003 S m^{-1}
Typical stability (per month):	Temperature 0.0002 ^oC
	Conductivity 0.0003 S m^{-1}
Resolution:	Temperatures 0.0001 ^oC
	Conductivity 0.00001 S m^{-1}

Bottom of ship thermometer

Model:	SBE 38, SEA-BIRD ELECTRONICS, INC.

Serial number: 3852788-0457
Measurement range: -5 to +35 ^{o}C
Initial accuracy: ±0.001 ^{o}C
Typical stability (per 6 month): 0.001 ^{o}C
Resolution: 0.00025 ^{o}C

Dissolved oxygen sensor
Model: OPTODE 3835, AANDERAA Instruments.
Serial number: 0985
Measuring range: 0 - 500 μmol dm^{-3}
Resolution: <1 μmol dm^{-3}
Accuracy: <8 μmol dm^{-3} or 5% whichever is greater
Settling time: <25 s

Fluorometer
Model: C3, TURNER DESIGNS
Serial number: 2300123

b. Measurements

Periods of measurement during MR 11-02 are listed in Table 2.3-1.

Table 2.3-1 Events list of the Sea surface water monitoring during MR11-02

System Date [UTC]	System Time [UTC]	Events	Remarks
2011/02/11	06:38	All the measurements were started and data was available.	Cruise start
2011/02/11	21:49	All the measurements were stopped for seawater leak	
2011/02/11	23:12	All the measurements were restarted and data was available.	
2011/02/19	3:28~19:30	C3 primary data shifted.	
2011/02/22	22:34	C3 measurement was stopped for maintenance	
2011/02/22	22:39	C3 measurement was restarted and data was available.	
2011/02/28	03:32	All the measurements were stopped for seawater line maintenance	
2011/02/28	05:26	All the measurements were restarted and data was available.	
2011/03/07	6:48	All the measurements were stopped.	Cruise end

(5) Preliminary Result

Preliminary data of temperature, salinity, dissolved oxygen and fluorescence at sea surface is shown in Fig. 2.3-1.

We took the surface water samples to compare sensor data with bottle data of salinity, dissolved oxygen and fluorescence. The results are shown in Figs. 2.3-2 - 4. All the salinity samples were analyzed by the Guideline 8400B “AUTOSAL” (see 2.2.2), and dissolve oxygen

samples were analyzed by Winkler method (see 2.4), and fluorescence were analyzed by 10-AU (see 3.2.1).

(6) Data archive

All data will be submitted to Chief Scientist.

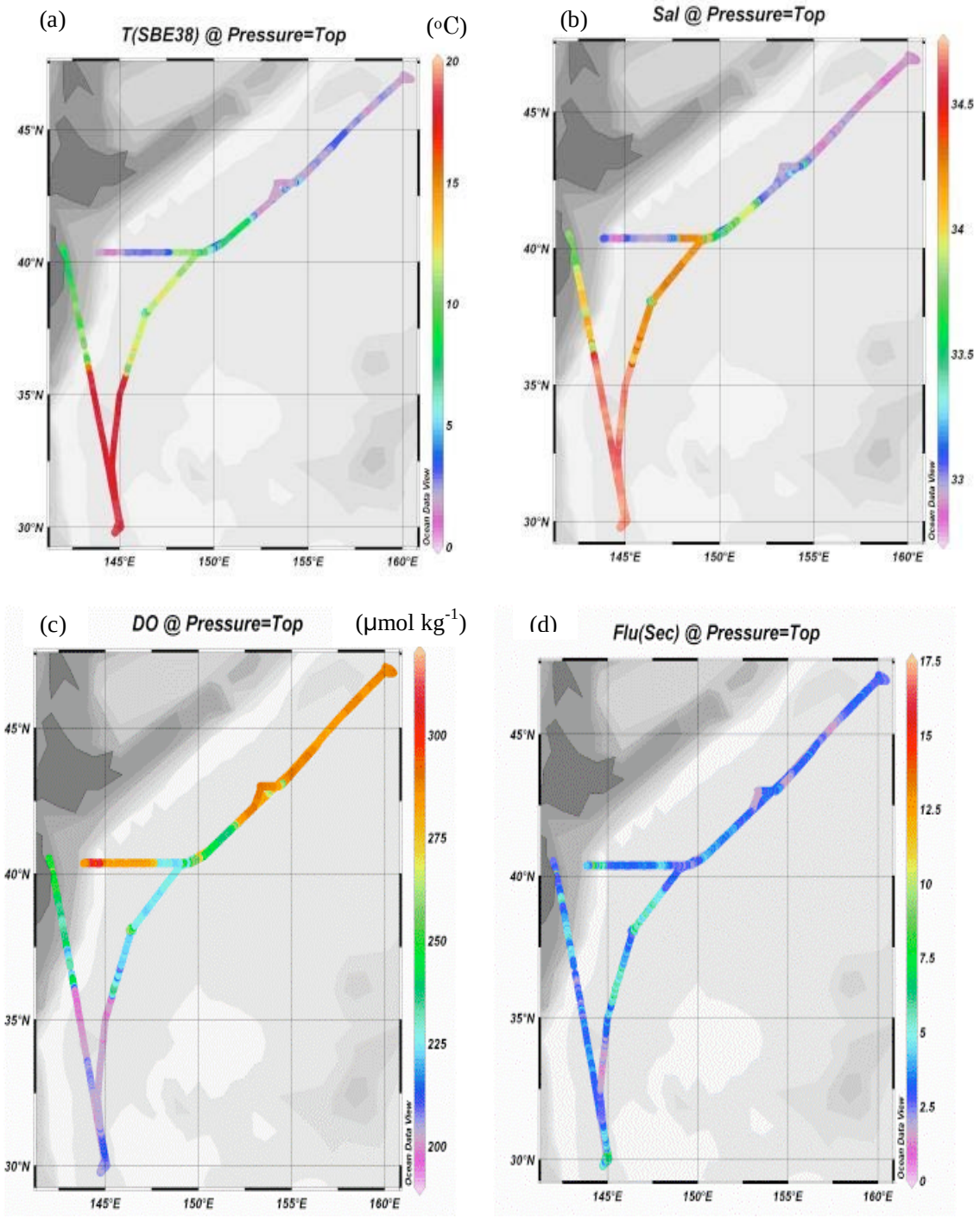

Fig. 2.3-1. Spatial and temporal distribution of (a) temperature, (b) salinity, (c) dissolved oxygen and (d) fluorescence in MR11-02 cruise.

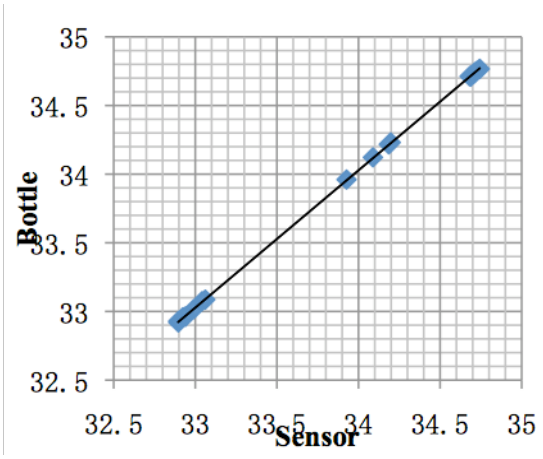

Fig. 2.3-2. Correlation of salinity between sensor and bottle data

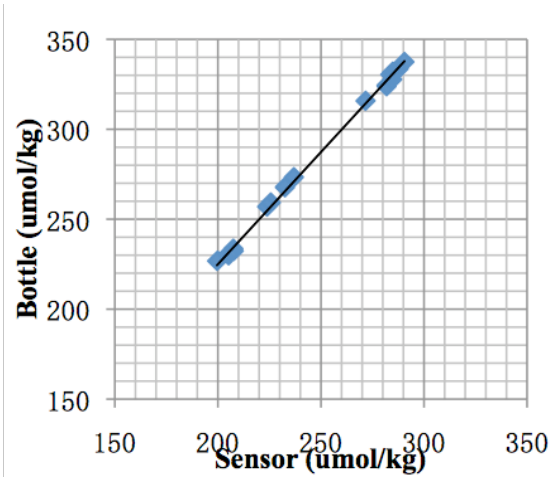

Fig. 2.3-3. Correlation of dissolved oxygen between sensor and bottle data

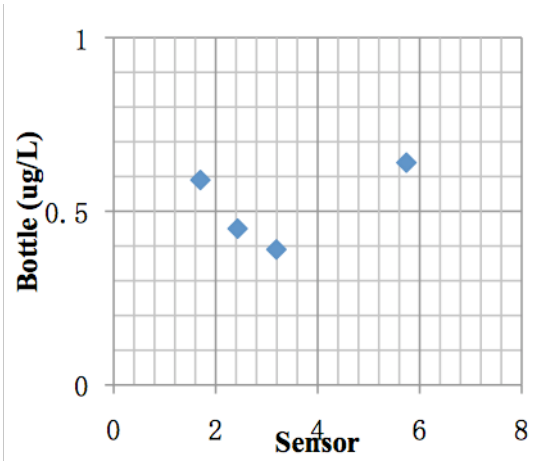

Fig. 2.3-4. Correlation of fluorescence between sensor and bottle data

2.4 Dissolved oxygen

Masahide WAKITA (JAMSTEC): Principal Investigator
Misato KUWAHARA (Marine Works Japan Co. Ltd): Operation Leader
Hideki YAMAMOTO (Marine Works Japan Co. Ltd)

(1) Objectives

Determination of dissolved oxygen in seawater by Winkler titration.

(2) Parameter

Dissolved Oxygen

(3) Instruments and Methods

Following procedure is based on an analytical method, entitled by "Determination of dissolved oxygen in sea water by Winkler titration", in the WHP Operations and Methods (Dickson, 1996).

a. Instruments

Burette for sodium thiosulfate and potassium iodate;

APB-510 manufactured by Kyoto Electronic Co. Ltd. / 10 cm^3 of titration vessel

Detector;

Automatic photometric titrator (DOT-01) manufactured by Kimoto Electronic Co. Ltd.

Software;

DOT controller Ver.2.2.1

b. Reagents

Pickling Reagent I: Manganese chloride solution (3 mol dm^{-3})
Pickling Reagent II: Sodium hydroxide (8 mol dm^{-3}) / sodium iodide solution (4 mol dm^{-3})
Sulfuric acid solution (5 mol dm^{-3})
Sodium thiosulfate (0.025 mol dm^{-3})
Potassium iodide (0.001667 mol dm^{-3})
CSK standard of potassium iodide:
Lot TSK3592, Wako Pure Chemical Industries Ltd., 0.0100N

c. Sampling

Seawater samples were collected with Niskin bottle attached to the CTD-system and surface bucket sampler. Seawater for oxygen measurement was transferred from sampler to a volume calibrated flask (ca. 100 cm^3). Three times volume of the flask of seawater was overflowed. Temperature was measured by digital thermometer during the overflowing. Then two reagent solutions (Reagent I and II) of 0.5 cm^3 each were added immediately into the sample flask and the stopper was inserted carefully into the flask. The sample flask was then shaken vigorously to mix the contents and to disperse the precipitate finely throughout. After the precipitate has settled at least halfway down the flask, the flask was shaken again vigorously to disperse the precipitate. The sample flasks containing pickled samples were stored in a laboratory until they were titrated.

d. Sample measurement

At least two hours after the re-shaking, the pickled samples were measured on board. 1 cm^3 sulfuric acid solution and a magnetic stirrer bar were added into the sample flask and stirring began. Samples were titrated by sodium thiosulfate solution whose morality was determined by potassium iodate solution. Temperature of sodium thiosulfate during titration was recorded by a digital thermometer. During this cruise, we measured dissolved oxygen concentration using 2 sets of the titration apparatus. Dissolved oxygen concentration ($\mu mol\ kg^{-1}$) was calculated by sample temperature during seawater sampling, salinity of the CTD sensor, flask volume, and titrated volume of sodium thiosulfate solution without the blank. When we measured low concentration samples, titration procedure was adjusted manually.

e. Standardization and determination of the blank

Concentration of sodium thiosulfate titrant was determined by potassium iodate solution. Pure potassium iodate was dried in an oven at 130 ^oC. 1.7835 g potassium iodate weighed out accurately was dissolved in deionized water and diluted to final volume of 5 dm^3 in a calibrated volumetric flask (0.001667 mol dm^{-3}). 10 cm^3 of the standard potassium iodate solution was added to a flask using a volume-calibrated dispenser. Then 90 cm^3 of deionized water, 1 cm^3 of sulfuric acid solution, and 0.5 cm^3 of pickling reagent solution II and I were added into the flask in order. Amount of titrated volume of sodium thiosulfate (usually 5 times measurements average) gave the morality of sodium thiosulfate titrant.

The oxygen in the pickling reagents I (0.5 cm^3) and II (0.5 cm^3) was assumed to be 3.8 x 10^{-8} mol (Murray *et al.*, 1968). The blank due to other than oxygen was determined as follows. 1 and 2 cm^3 of the standard potassium iodate solution were added to two flasks respectively using a calibrated dispenser. Then 100 cm^3 of deionized water, 1 cm^3 of sulfuric acid solution, and 0.5 cm^3 of pickling reagent solution II and I each were added into the flask in order. The blank was determined by difference between the first (1 cm^3 of KIO_3) titrated volume of the sodium thiosulfate and the second (2 cm^3 of KIO_3) one. The results of 3 times blank determinations were averaged.

Table 2.4.-1 shows results of the standardization and the blank determination during this cruise.

f. Repeatability of sample measurement

Replicate samples were taken at every CTD casts. Total amount of the replicate sample pairs of good measurement was 28. The standard deviation of the replicate measurement was 0.15 $\mu mol\ kg^{-1}$ that was calculated by a procedure in Guide to best practices for ocean CO_2 measurements Chapter4 SOP23 Ver.3.0 (2007). The diagram of replicate samples is shown in Fig. 2.4-1 and 2.

Table 2.4-1 Results of the standardization and the blank determinations during this cruise.

Date	KIO_3 ID	$Na_2S_2O_3$	DOT-01(No.1)		DOT-01(No.2)		Stations
			E.P.	Blank	E.P.	Blank	
2011/2/12	20100630-02-01	20100702-05	3.944	0.000	3.944	-0.002	Stn.S01 cast2,cast3
2011/2/13	CSK	20100702-05	3.937	0.000	3.937	-0.002	
2011/2/17	20091215-05-09	20100702-05	3.936	0.000	3.937	0.000	
2011/2/17	20100630-02-02	20100702-05	3.945	0.000	3.944	0.000	Stn.S01 cast7,002,KEO,004,JKO
2011/2/23	20100630-02-03	20100702-05	3.945	0.000	3.945	-0.002	
2011/2/23	20100630-02-03	20100702-06	3.937	0.000	3.939	-0.001	Stn.006,K02 cast1,cast2
2011/2/27	20100630-02-04	20100702-06	3.934	0.000	3.933	0.000	Stn.K02 cast5
2011/3/4	20100630-02-05	20100702-06	3.933	0.000	3.932	-0.001	
2011/3/6	20100630-02-06	20100702-06	3.935	0.000	3.934	-0.001	
2011/3/6	CSK	20100702-06	3.931	0.000	3.931	-0.001	

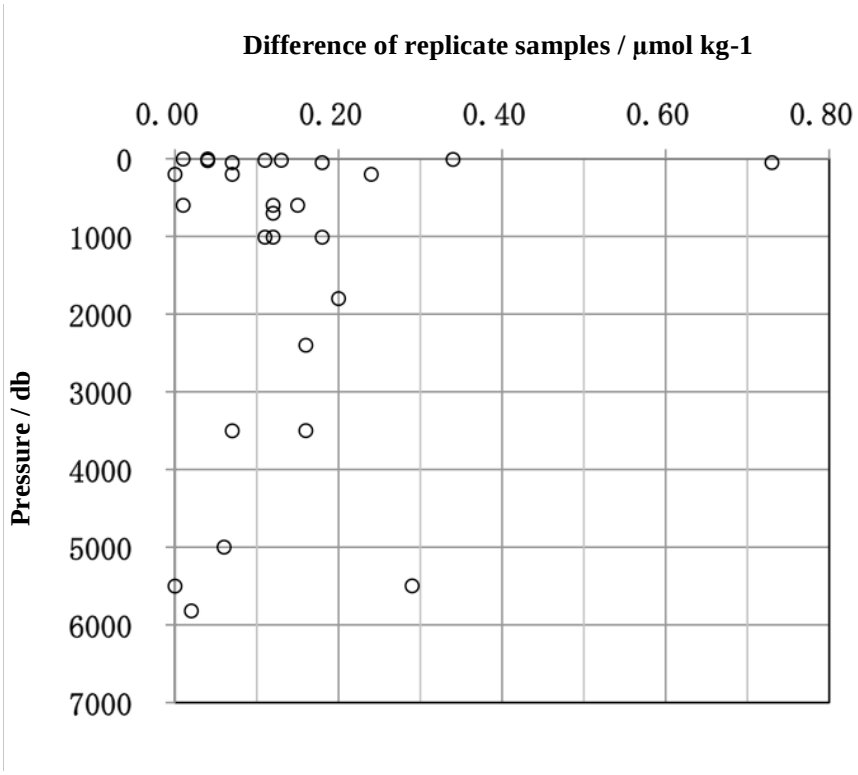

Fig. 2.4-1 Difference of replicate samples against pressure

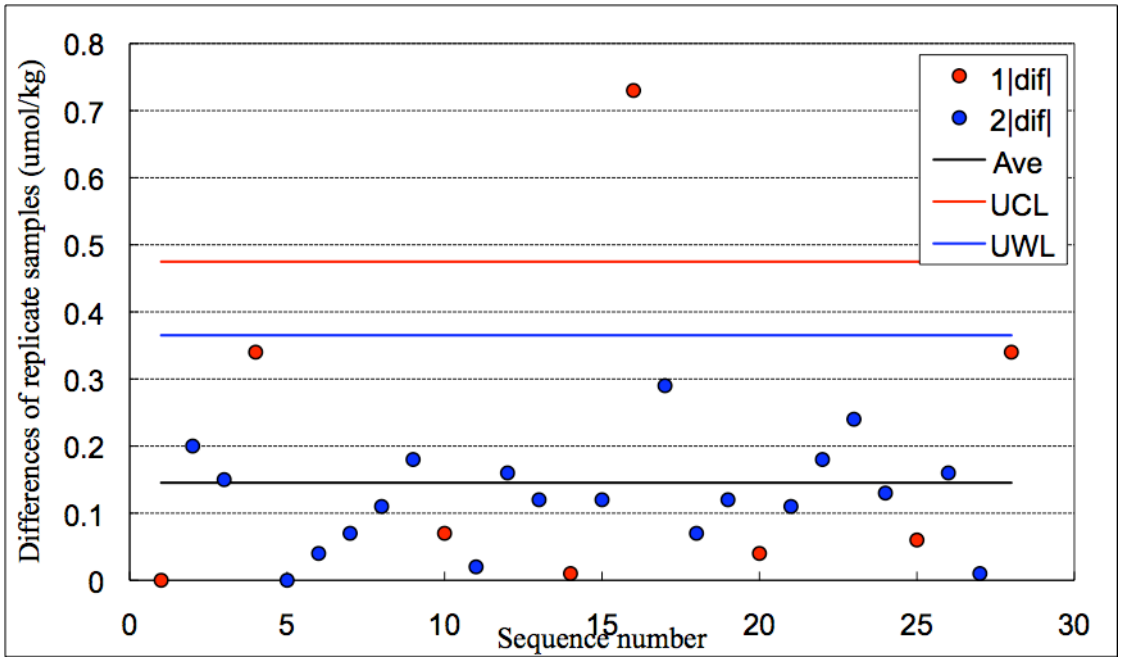

Fig. 2.4-2 Difference of replicate samples against sequence number

(4) Data archive

All data will be submitted to Chief Scientist.

(5) References

Dickson, A.G., Determination of dissolved oxygen in sea water by Winkler titration. (1996)

Dickson, A.G., Sabine, C.L. and Christian, J.R. (Eds.), Guide to best practices for ocean CO2 measurements. (2007)

Culberson, C.H., WHP Operations and Methods July-1991 “Dissolved Oxygen”, (1991)

Japan Meteorological Agency, Oceanographic research guidelines（Part 1）. (1999)

KIMOTO electric CO. LTD., Automatic photometric titrator DOT-01 Instruction manual

2.5 Nutrients

Michio AOYAMA (Meteorological Research Institute) Principal investigator
Masahide WAKITA (JAMSTEC MIO)
Kenichiro SATO (Department of Marine Science, Marine Works Japan Ltd.)
Yasuhiro ARII (Department of Marine Science, Marine Works Japan Ltd.)

(1) Objectives

The objectives of nutrients analyses during the R/V Mirai MR11-02 cruise in the North Pacific Ocean are as follows:

- Describe the present status of nutrients concentration with excellent comparability.
- Provide excellent nutrients data to biologist onboard MR11-02 to help their study.

(2) Parameters

The determinants are nitrate, nitrite, phosphate, silicate and ammonia in the western North Pacific Ocean.

(3) Summary of nutrients analysis

We made 10 QuAAtro runs for the samples at 7 stations (13 casts) in MR11-02. The total amount of layers of the seawater sample reached up to 229 for MR11-02. We made duplicate measurement at all layers.

(4) Instrument and Method

a). Analytical detail using QuAAtro system

The phosphate analysis was a modification of the procedure of Murphy and Riley (1962). Molybdic acid was added to the seawater sample to form phosphomolybdic acid which was in turn reduced to phosphomolybdous acid using L-ascorbic acid as the reductant.

Nitrate + nitrite and nitrite were analyzed according to the modification method of Grasshoff (1970). The sample nitrate was reduced to nitrite in a cadmium tube inside of which was coated with metallic copper. The sample streamed with its equivalent nitrite was treated with an acidic, sulfanilamide reagent and the nitrite forms nitrous acid which reacted with the sulfanilamide to produce a diazonium ion. N-1-Naphthylethylene-diamine added to the sample stream then coupled with the diazonium ion to produce a red, azo dye. With reduction of the nitrate to nitrite, both nitrate and nitrite reacted and were measured; without reduction, only nitrite reacted. Thus, for the nitrite analysis, no reduction was performed and the alkaline buffer was not necessary. Nitrate was computed by difference.

The silicate method was analogous to that described for phosphate. The method used was essentially that of Grasshoff et al. (1983), wherein silicomolybdic acid was first formed from the silicate in the sample and added molybdic acid; then the silicomolybdic acid was reduced to silicomolybdous acid, or "molybdenum blue" using ascorbic acid as the reductant. The analytical methods of the nutrients, nitrate, nitrite, silicate and phosphate, during this cruise were same as the methods used in (Kawano et al. 2009).

The ammonia in seawater was mixed with an alkaline containing EDTA, ammonia as gas state was formed from seawater. The ammonia (gas) was absorbed in sulfuric acid by way of 0.5 μm pore size membrane filter (ADVANTEC PTFE) at the dialyzer attached to analytical system. The ammonia absorbed in sulfuric acid was determined by coupling with phenol and hypochlorite to form indophenols blue. Wavelength using ammonia analysis was 630 nm, which

was absorbance of indophenols blue.

The flow diagrams and reagents for each parameter are shown in Figures 2.5.2 to 2.5.6.

b). Nitrate + Nitrite Reagents

Imidazole (buffer), 0.06 M (0.4 % w/v)

Dissolved 4 g imidazole, $C_3H_4N_2$, in ca. 1000 ml DIW; added 2 ml concentrated HCl. After mixing, 1 ml Triton®X-100 (50 % solution in ethanol) was added.

Sulfanilamide, 0.06 M (1 % w/v) in 1.2M HCl

Dissolved 10 g sulfanilamide, 4-$NH_2C_6H_4SO_3H$, in 900 ml of DIW, added 100 ml concentrated HCl. After mixing, 2 ml Triton®X-100 (50 % solution in ethanol) was added.

N-1-Napthylethylene-diamine dihydrochloride, 0.004 M (0.1 %f w/v)

Dissolved 1 g NED, $C_{10}H_7NHCH_2CH_2NH_2$•2HCl, in 1000 ml of DIW and added 10 ml concentrated HCl. After mixing, 1 ml Triton®X-100 (50 % solution in ethanol) was added. This reagent was stored in a dark bottle.

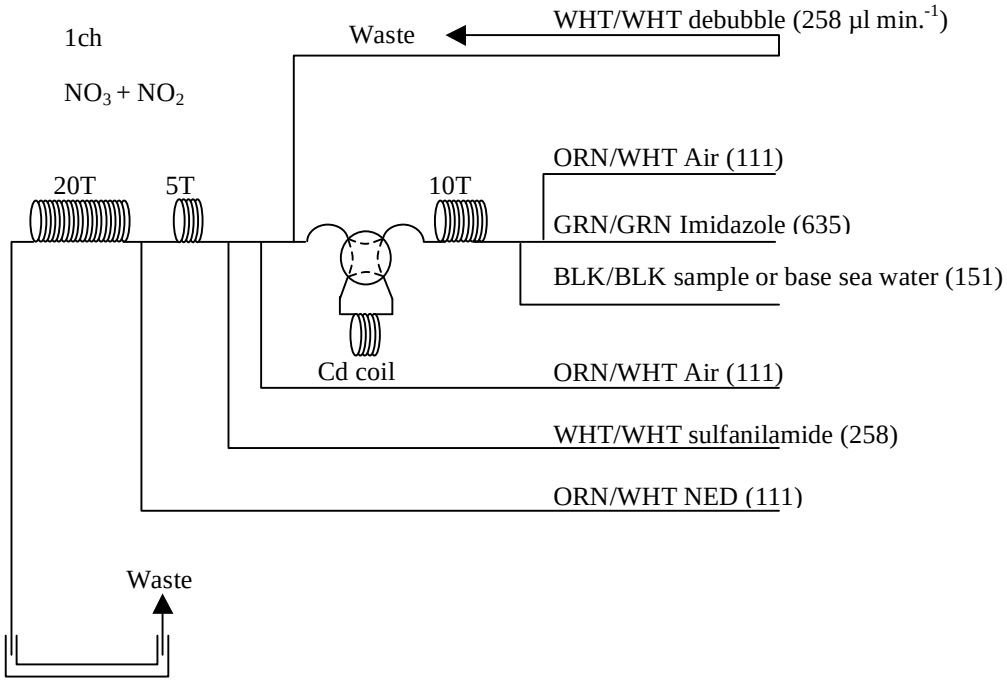

Figure 2.5.2 NO_3+NO_2 (1ch.) Flow diagram.

c). Nitrite Reagents

Sulfanilamide, 0.06 M (1 % w/v) in 1.2 M HCl

Dissolved 10g sulfanilamide, 4-$NH_2C_6H_4SO_3H$, in 900 ml of DIW, added 100 ml concentrated HCl. After mixing, 2 ml Triton®X-100 (50 % solution in ethanol) was added.

N-1-Napthylethylene-diamine dihydrochloride, 0.004 M (0.1 % w/v)

Dissolved 1 g NED, $C_{10}H_7NHCH_2CH_2NH_2$•2HCl, in 1000 ml of DIW and added 10 ml concentrated HCl. After mixing, 1 ml Triton®X-100 (50 % solution in ethanol) was added. This reagent was stored in a dark bottle.

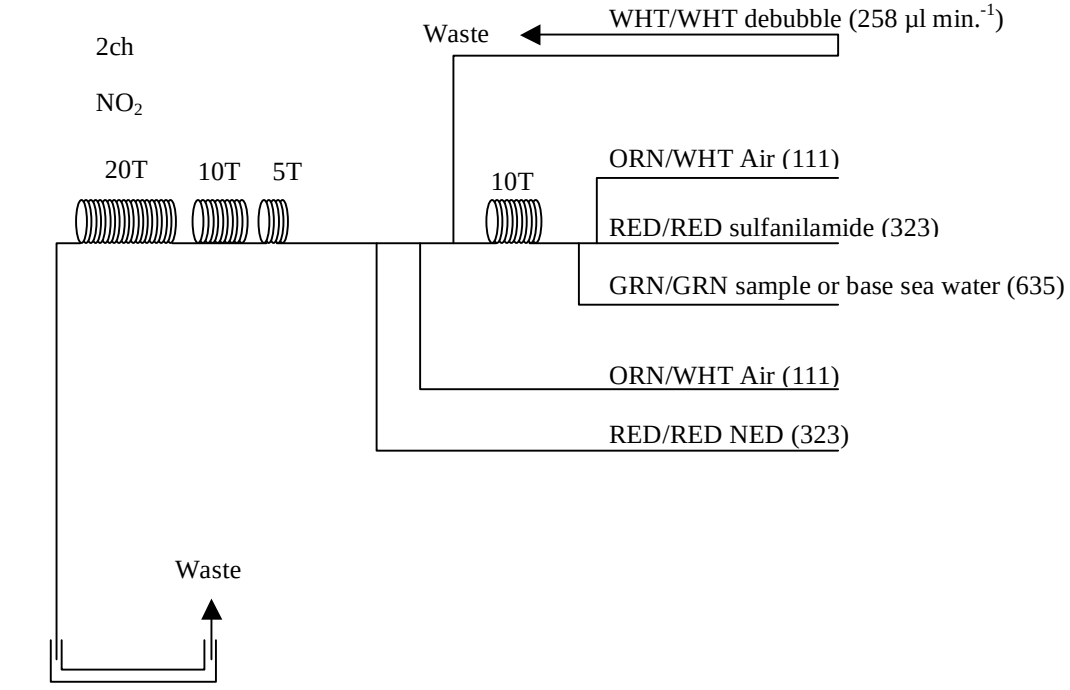

Figure 2.5.3 NO_2 (2ch.) Flow diagram.

d. Silicate Reagents

Molybdic acid, 0.06 M (2 % w/v)

Dissolved 15 g disodium molybdate (VI) dihydrate, $Na_2M_oO_4 \cdot 2H_2O$, in 980 ml DIW, added 8 ml concentrated H_2SO_4. After mixing, 20 ml sodium dodecyl sulphate (15 % solution in water) was added.

Oxalic acid, 0.6 M (5 % w/v)

Dissolved 50 g oxalic acid anhydrous, HOOC:COOH, in 950 ml of DIW.

Ascorbic acid, 0.01M (3 % w/v)

Dissolved 2.5g L (+)-ascorbic acid, $C_6H_8O_6$, in 100 ml of DIW. This reagent was freshly prepared before every measurement.

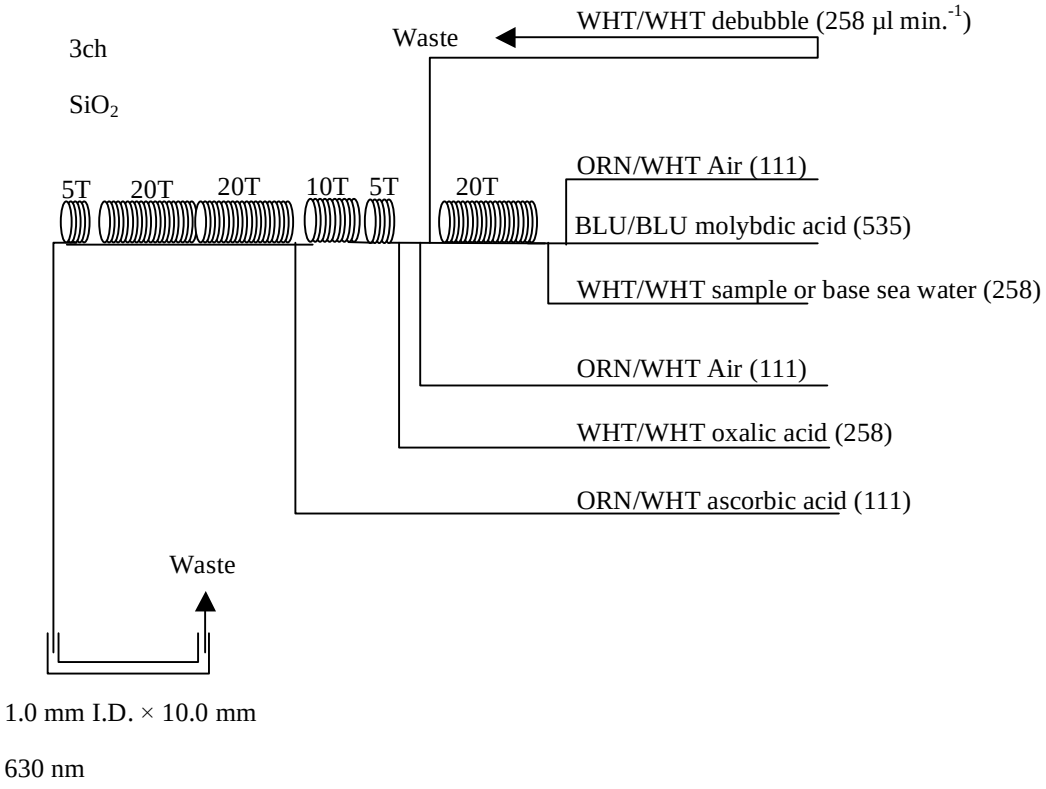

Figure 2.5.4 SiO_2 (3ch.) Flow diagram.

e). Phosphate Reagents

Stock molybdate solution, 0.03M (0.8 % w/v)

Dissolved 8 g disodium molybdate (VI) dihydrate, $Na_2M_oO_4 \cdot 2H_2O$, and 0.17 g antimony potassium tartrate, $C_8H_4K_2O_{12}Sb_2 \cdot 3H_2O$, in 950 ml of DIW and added 50 ml concentrated H_2SO_4.

Mixed Reagent

Dissolved 2.5 g L (+)-ascorbic acid, $C_6H_8O_6$, in 150 ml of stock molybdate solution. After mixing, 3 ml sodium dodecyl sulphate (15 % solution in water) was added. This reagent was freshly prepared before every measurement.

Reagent for sample dilution

Dissolved sodium chloride, NaCl, 10 g in ca. 950 ml of DIW, added 50 ml acetone and 4 ml concentrated H_2SO_4. After mixing, 5 ml sodium dodecyl sulphate (15 % solution in water) was added.

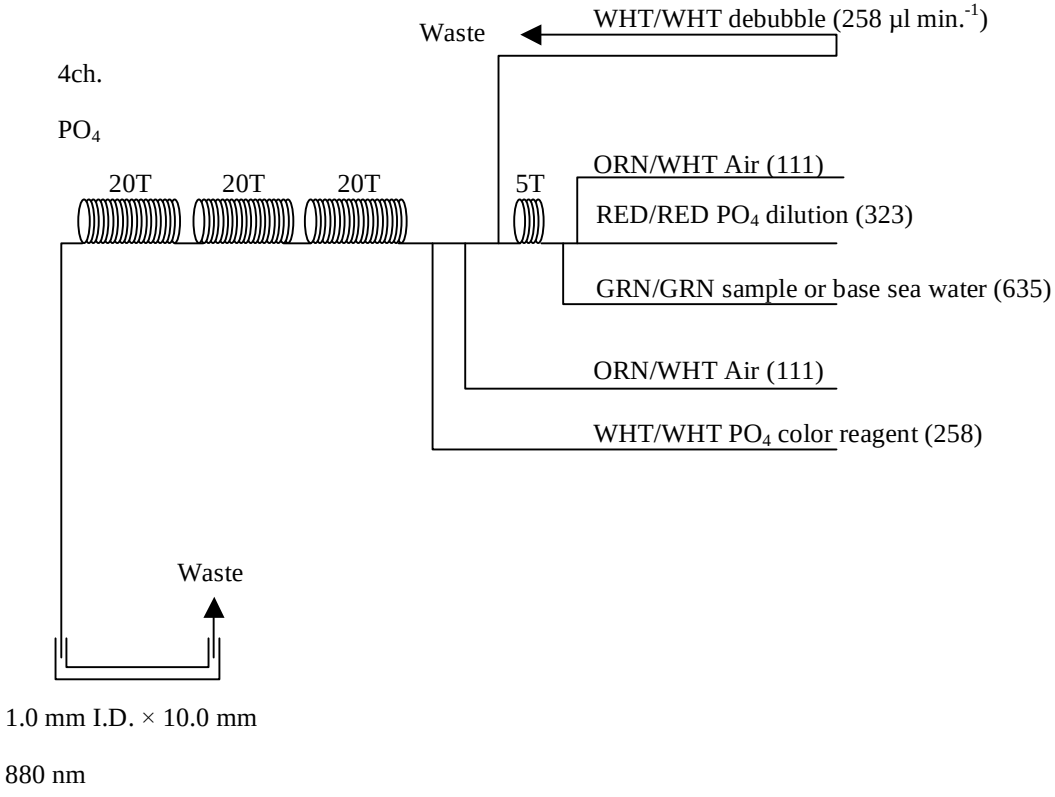

Figure 2.5.5 PO_4 (4ch.) Flow diagram.

f). Ammonia Reagents

EDTA

Dissolved 41 g EDTA (ethylenediaminetetraacetatic acid tetrasodium salt), $C_{10}H_{12}N_2O_8Na_4 \cdot 4H_2O$, and 2 g boric acid, H_3BO_3, in 200 ml of DIW. After mixing, 1 ml Triton®X-100 (30 % solution in DIW) was added. This reagent was prepared at a week about.

NaOH

Dissolved 5 g sodium hydroxide, NaOH, and 16 g EDTA in 100 ml of DIW. This reagent was prepared at a week about.

Stock Nitroprusside

Dissolved 0.25 g sodium pentacyanonitrosylferrate (II), $Na_2[Fe(CN)_5NO]$, in 100 ml of DIW and added 0.2 ml 1N H_2SO_4. Stored in a dark bottle and prepared at a month about.

Nitroprusside solution

Mixed 4 ml stock nitroprusside and 5 ml 1N H_2SO_4 in 500 ml of DIW. After mixing, 1 ml Triton®X-100 (30 % solution in DIW) was added. This reagent was stored in a dark bottle and prepared at every 2 or 3 days.

Alkaline phenol

Dissolved 10 g phenol, C_6H_5OH, 5 g sodium hydroxide and citric acid, $C_6H_8O_7$, in 200 ml DIW. Stored in a dark bottle and prepared at a week about.

NaClO solution

Mixed 3 ml sodium hypochlorite solution, NaClO, in 47 ml DIW. Stored in a dark bottle and fleshly prepared before every measurement. This reagent was prepared 0.3% available chlorine.

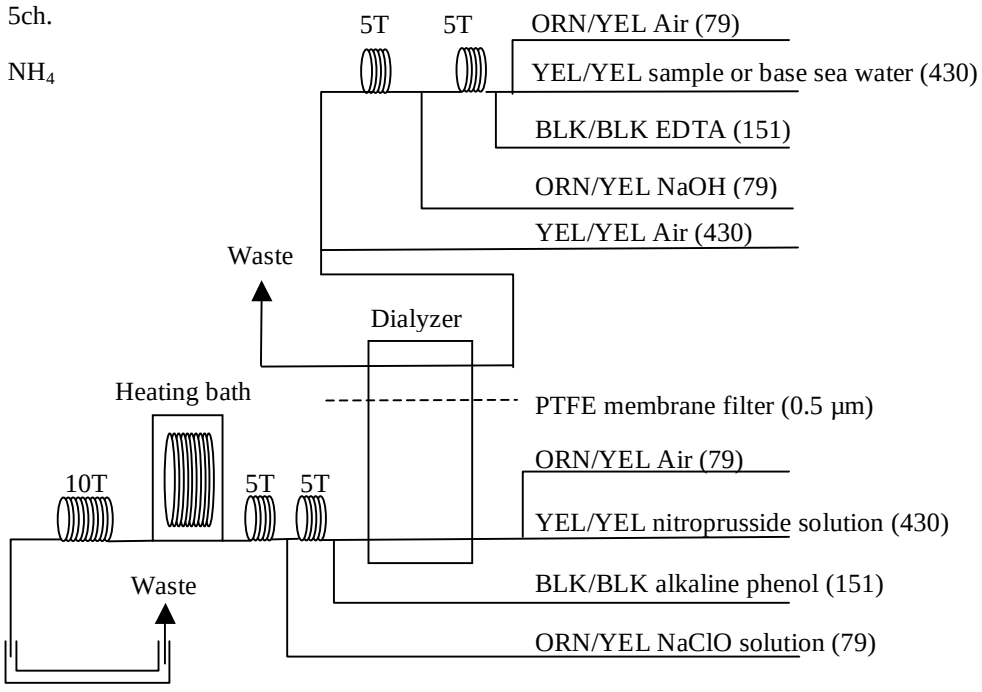

Figure 2.5.6 NH_4 (5ch.) Flow diagram.

g). Sampling procedures

Sampling of nutrients followed that oxygen, salinity and trace gases. Samples were drawn into two of virgin 10 ml polyacrylates vials without sample drawing tubes. These were rinsed three times before filling and vials were capped immediately after the drawing. The vials were put into water bath adjusted to ambient temperature, 26 ± 2 deg. C, in about 30 minutes before use to stabilize the temperature of samples in MR11-02.

No transfer was made and the vials were set an auto sampler tray directly. Samples were analyzed after collection basically within 24 hours in MR11-02.

h). Data processing

Raw data from QuAAtro was treated as follows:

- Checked baseline shift.
- Checked the shape of each peak and positions of peak values taken, and then changed the positions of peak values taken if necessary.
- Carry-over correction and baseline drift correction were applied to peak heights of each samples followed by sensitivity correction.
- Baseline correction and sensitivity correction were done basically using liner regression.
- Loaded pressure and salinity from CTD data to calculate density of seawater.
- Calibration curves to get nutrients concentration were assumed second order equations.

(5) Nutrients standards

a). Volumetric laboratory ware of in-house standards

All volumetric glass ware and polymethylpentene (PMP) ware used were gravimetrically calibrated. Plastic volumetric flasks were gravimetrically calibrated at the temperature of use within 0 to 4 K.

Volumetric flasks

Volumetric flasks of Class quality (Class A) were used because their nominal tolerances are 0.05 % or less over the size ranges likely to be used in this work. Class A flasks were made of borosilicate glass, and the standard solutions were transferred to plastic bottles as quickly as possible after they were made up to volume and well mixed in order to prevent excessive dissolution of silicate from the glass. PMP volumetric flasks were gravimetrically calibrated and used only within 0 to 4 K of the calibration temperature.

The computation of volume contained by glass flasks at various temperatures other than the calibration temperatures were done by using the coefficient of linear expansion of borosilicate crown glass.

Because of their larger temperature coefficients of cubical expansion and lack of tables constructed for these materials, the plastic volumetric flasks were gravimetrically calibrated over the temperature range of intended use and used at the temperature of calibration within 0 to 4 K. The weights obtained in the calibration weightings were corrected for the density of water and air buoyancy.

Pipettes and pipettors

All pipettes had nominal calibration tolerances of 0.1 % or better. These were gravimetrically calibrated in order to verify and improve upon this nominal tolerance.

b). Reagents, general considerations

Specifications

For nitrate standard, “potassium nitrate 99.995 suprapur®” provided by Merck, CAS No.: 7757-91-1, was used.

For phosphate standard, “potassium dihydrogen phosphate anhydrous 99.995 suprapur®” provided by Merck, CAS No.: 7778-77-0, was used.

For nitrite standard, “sodium nitrate” provided by Wako, CAS No.: 7632-00-0, was used. And assay of nitrite was determined according JIS K8019 and assays of nitrite salts were 98.04 %. We used that value to adjust the weights taken.

For the silicate standard, we use “Silicon standard solution SiO_2 in NaOH 0.5 mol/l CertiPUR®” provided by Merck, CAS No.: 1310-73-2, of which lot number HC074650 was used. The silicate concentration was certified by NIST-SRM3150 with the uncertainty of 0.5 %. Factor of HC074650 was signed 1.000, however we reassigned the factor as 0.975 from the result of comparison among HC814662, HC074650 and RMNS in MR10-05 cruise.

For ammonia standard, “ammonia sulfate” provided by Wako, CAS No.: 7783-20-2, was used.

Ultra pure water

Ultra pure water (Milli-Q) freshly drawn was used for preparation of reagent, standard solutions and for measurement of reagent and system blanks.

Low-nutrients seawater (LNSW)

Surface water having low nutrient concentration was taken and filtered using 0.45 μm pore size membrane filter. This water was stored in 20 liter cubitainer with paper box. The concentrations of nutrient of this water were measured carefully in Jul 2008.

c). Concentrations of nutrients for A, B and C standards

Concentrations of nutrients for A, B and C standards (working standards) were set as shown in Table 2.5.1. The working standard was prepared according recipes as shown in Table 2.5.2. All volumetric laboratory tools were calibrated prior the cruise as stated in chapter (5). Then the actual concentration of nutrients in each fresh standard was calculated based on the ambient, solution temperature and determined factors of volumetric laboratory wares.

The calibration curves for each run were obtained using 5 levels working standards, C-1, C-2, C-3, C-4 and C-5.

Table 2.5.1 Nominal concentrations of nutrients for A, B and C standards.

	A	B	C-1	C-2	C-3	C-4	C-5
NO_3 (μM)	22000	900	0.03	9.2	18.3	36.6	55.0
NO_2 (μM)	4000	20	0.00	0.2	0.4	0.8	1.2
SiO_2 (μM)	36000	2800	0.80	28	56	111	167
PO_4 (μM)	3000	60	0.04	0.6	1.2	2.4	3.6
NH_4 (μM)	4000	200	0.00	0.0	2.0	4.0	6.0

Table 2.5.2 Working standard recipes.

C Std.	B-1 Std.	B-2 Std.	B-3 Std.	DIW
C-1	0 ml	0 ml	0 ml	75 ml
C-2	5 ml	5 ml	0 ml	65 ml
C-3	10 ml	10 ml	5 ml	40 ml
C-4	20 ml	20 ml	10 ml	25 ml
C-5	30 ml	30 ml	15 ml	0 ml

B-1 Std.: Mixture of nitrate, silicate and phosphate.
B-2 Std.: Nitrite.
B-3 Std.: Ammonia.

d). Renewal of in-house standard solutions

In-house standard solutions as stated in paragraph c) were renewed as shown in Table 2.5.3(a) to (c).

Table 2.5.3(a) Timing of renewal of in-house standards.

NO_3, NO_2, SiO_2, PO_4, NH_4	Renewal
A-1 Std. (NO_3)	maximum 1 month
A-2 Std. (NO_2)	maximum 1 month
A-3 Std. (SiO_2)	commercial prepared solution
A-4 Std. (PO_4)	maximum 1 month
A-5 Std. (NH_4)	maximum 1 month
B-1 Std. (mixture of NO_3, SiO_2, PO_4)	8 days
B-2 Std. (NO_2)	8 days
B-3 Std. (NH_4)	8 days

Table 2.5.3(b) Timing of renewal of working calibration standards.

Working standards	Renewal
C Std. (mixture of B-1 , B-2 and B-3 Std.)	24 hours

Table 2.5.3(c) Timing of renewal of in-house standards for reduction estimation.

Reduction estimation	Renewal
D-1 Std. (3600 μM NO_3)	8 days
43 μM NO_3	when C Std. renewed
47 μM NO_2	when C Std. renewed

(6) Reference material of nutrients in seawater

To get the more accurate and high quality nutrients data to achieve the objectives stated above, huge numbers of the bottles of the reference material of nutrients in seawater (hereafter RMNS) are prepared (Aoyama et al., 2006, 2007, 2008, 2009). In the previous worldwide expeditions, such as CLIVAR cruises, the higher reproducibility and precision of nutrients measurements were required (Joyce and Corry, 1994). Since no standards were available for the measurement of nutrients in seawater at that time, the requirements were described in term of reproducibility. The required reproducibility was 1 %, 1 to 2 %, 1 to 3 % for nitrate, phosphate and silicate, respectively. Although nutrient data from the WOCE one-time survey was of unprecedented quality and coverage due to much care in sampling and measurements, the differences of nutrients concentration at crossover points are still found among the expeditions (Aoyama and Joyce, 1996, Mordy et al., 2000, Gouretski and Jancke, 2001). For instance, the mean offset of nitrate concentration at deep waters was 0.5 μmol kg^{-1} for 345 crossovers at world oceans, though the maximum was 1.7 μmol kg^{-1} (Gouretski and Jancke, 2001). At the 31 crossover points in the Pacific WHP one-time lines, the WOCE standard of reproducibility for nitrate of 1 % was fulfilled at about half of the crossover points and the maximum difference was 7 % at deeper layers below 1.6 deg. C in potential temperature (Aoyama and Joyce, 1996).

a). RMNS for this cruise

RMNS lots BA, AS, AY, AX, BD, BE, AZ and BF, which cover full range of nutrients concentrations in the North Pacific Ocean are prepared. These RMNS assignment were completely done based on random number. The RMNS bottles were stored at a room in the ship, REAGENT STORE, where the temperature was maintained 10 - 22 deg. C.

b). Assigned concentration for RMNSs

We assigned nutrients concentrations for RMNS lots BA, AS, AY, AX, BD, BE, AZ and BF as shown in Table 2.5.4.

Table 2.5.4 Assigned concentration of RMNSs.

unit: μmol kg^{-1}

	Nitrate	Phosphate	Silicate	Nitrite	Ammonia
BA	0.07	0.068	1.60	0.02	0.97
AS	0.11	0.077	1.58	0.02	-

AY	5.60	0.516	29.42	0.62	0.81
AX	21.42	1.619	58.06	0.35	-
BD	29.83	2.182	64.41	0.04	2.93
BE	36.70	2.662	99.20	0.03	-
AZ	42.36	3.017	133.93	0.03	-
BF	41.39	2.809	150.23	0.02	-

(7) Quality control

a). Precision of nutrients analyses during the cruise

Precision of nutrients analyses during the cruise was evaluated based on the 5 to 7 measurements, which are measured every 6 to 14 samples, during a run at the concentration of C-5 std. Summary of precisions are shown as shown in Table 2.5.5. Analytical precisions previously evaluated were 0.08 % for nitrate, 0.10 % for phosphate and 0.07 % for silicate in CLIVAR P21 revisited cruise of MR09-01 cruise in 2009, respectively. During this cruise, analytical precisions were 0.08 % for nitrate, 0.18 % for phosphate, 0.11 % for silicate, 0.19 % for nitrite and 0.24 % for ammonia in terms of median of precision, respectively. Then we can conclude that the analytical precisions for nitrate, phosphate and silicate were maintained throughout this cruise.

Table 2.5.5 Summary of precision based on the replicate analyses.

	Nitrate CV %	Nitrite CV %	Phosphate CV %	Silicate CV %	Ammonia CV%
Median	0.08	0.19	0.18	0.11	0.24
Mean	0.10	0.19	0.20	0.11	0.32
Maximum	0.19	0.23	0.32	0.18	0.60
Minimum	0.05	0.08	0.10	0.07	0.19
N	10	10	10	10	4

b). Carry over

We can also summarize the magnitudes of carry over throughout the cruise. These are small enough within acceptable levels as shown in Table 2.5.6.

Table 2.5.6 Summary of carry over throughout MR11-02.

	Nitrate %	Nitrite %	Phosphate %	Silicate %	Ammonia %
Median	0.15	0.09	0.09	0.23	0.52
Mean	0.13	0.10	0.11	0.21	0.52
Maximum	0.20	0.29	0.45	0.29	0.95
Minimum	0.00	0.00	0.00	0.03	0.09
N	10	10	10	10	4

(8) Problems/improvements occurred and solutions.

a). Deterioration of pump tubes of QuAAtro

In MR10-05 and MR10-06 cruises, standard pump tubes by BL TEC were deteriorated at 40 to 80 hours. Therefore, we used a long life pump tube for QuAAtro in this cruise. The long

life pump tube could be used over 100 hours.

b). Precipitation at ammonia line

In MR10-05 and MR10-06 cruises, there was a precipitation at the point of mixed seawater sample, EDTA and NaOH in ammonia line. We changed the recipe of EDTA 25g to 41g in EDTA reagent.

c). Sample to wash ratio

Sample to wash ratio was set up 2.0 (sample time; 60 s, wash time; 30 s) in past cruises. We changed sample time 75 s and wash time 15 s in this cruise because ISAC was larger than past cruise.

(9) Station list

Table 2.5.7 List of stations

Cruise	Station	Cast	Year	Month	Date	Latitude		Longitude	
MR1102	S01	02	2011	2	13	29.999	N	144.997	E
MR1102	S01	03	2011	2	14	30.001	N	144.900	E
MR1102	S01	04	2011	2	14	30.002	N	145.001	E
MR1102	S01	07	2011	2	17	30.001	N	144.998	E
MR1102	002	01	2011	2	19	31.158	N	144.767	E
MR1102	KEO	01	2011	2	19	32.465	N	144.586	E
MR1102	004	01	2011	2	20	35.001	N	145.002	E
MR1102	JKO	01	2011	2	21	38.035	N	146.491	E
MR1102	006	01	2011	2	23	40.249	N	149.005	E
MR1102	K02	01	2011	2	25	47.004	N	160.170	E
MR1102	K02	02	2011	2	25	47.012	N	160.173	E
MR1102	K02	05	2011	3	1	46.877	N	160.358	E
MR1102	K02	06	2011	3	2	46.879	N	160.197	E

(10) Data archive

All data will be submitted to JAMSTEC Data Integration and Analyses Group (DIAG) and is currently under its control.

References

Aminot, A. and Kerouel, R. 1991. Autoclaved seawater as a reference material for the determination of nitrate and phosphate in seawater. Anal. Chim. Acta, 248: 277-283.

Aminot, A. and Kirkwood, D.S. 1995. Report on the results of the fifth ICES intercomparison exercise for nutrients in sea water, ICES coop. Res. Rep. Ser., 213.

Aminot, A. and Kerouel, R. 1995. Reference material for nutrients in seawater: stability of nitrate, nitrite, ammonia and phosphate in autoclaved samples. Mar. Chem., 49: 221-232.

Aoyama M., and Joyce T.M. 1996, WHP property comparisons from crossing lines in North Pacific. In Abstracts, 1996 WOCE Pacific Workshop, Newport Beach, California.

Aoyama, M., 2006: 2003 Intercomparison Exercise for Reference Material for Nutrients in Seawater in a Seawater Matrix, Technical Reports of the Meteorological Research Institute No.50, 91pp, Tsukuba, Japan.

Aoyama, M., Susan B., Minhan, D., Hideshi, D., Louis, I. G., Kasai, H., Roger, K., Nurit, K., Doug, M., Murata, A., Nagai, N., Ogawa, H., Ota, H., Saito, H., Saito, K., Shimizu, T.,

Takano, H., Tsuda, A., Yokouchi, K., and Agnes, Y. 2007. Recent Comparability of Oceanographic Nutrients Data: Results of a 2003 Intercomparison Exercise Using Reference Materials. Analytical Sciences, 23: 1151-1154.

Aoyama M., J. Barwell-Clarke, S. Becker, M. Blum, Braga E. S., S. C. Coverly,E. Czobik, I. Dahllof, M. H. Dai, G. O. Donnell, C. Engelke, G. C. Gong, Gi-Hoon Hong, D. J. Hydes, M. M. Jin, H. Kasai, R. Kerouel, Y. Kiyomono, M. Knockaert, N. Kress, K. A. Krogslund, M. Kumagai, S. Leterme, Yarong Li, S. Masuda, T. Miyao, T. Moutin, A. Murata, N. Nagai, G.Nausch, M. K. Ngirchechol, A. Nybakk, H. Ogawa, J. van Ooijen, H. Ota, J. M. Pan, C. Payne, O. Pierre-Duplessix, M. Pujo-Pay, T. Raabe, K. Saito, K. Sato, C. Schmidt, M. Schuett, T. M. Shammon, J. Sun, T. Tanhua, L. White, E.M.S. Woodward, P. Worsfold, P. Yeats, T. Yoshimura, A.Youenou, J. Z. Zhang, 2008: 2006 Intercomparison Exercise for Reference Material for Nutrients in Seawater in a Seawater Matrix, Technical Reports of the Meteorological Research Institute No. 58, 104pp.

Gouretski, V.V. and Jancke, K. 2001. Systematic errors as the cause for an apparent deep water property variability: global analysis of the WOCE and historical hydrographic data・REVIEW ARTICLE, Progress In Oceanography, 48: Issue 4, 337-402.

Grasshoff, K., Ehrhardt, M., Kremling K. et al. 1983. Methods of seawater anylysis. 2nd rev. Weinheim: Verlag Chemie, Germany, West.

Joyce, T. and Corry, C. 1994. Requirements for WOCE hydrographic programmed data reporting. WHPO Publication, 90-1, Revision 2, WOCE Report No. 67/91.

Kawano, T., Uchida, H. and Doi, T. WHP P01, P14 REVISIT DATA BOOK, (Ryoin Co., Ltd., Yokohama, 2009).

Kirkwood, D.S. 1992. Stability of solutions of nutrient salts during storage. Mar. Chem., 38 : 151-164.

Kirkwood, D.S. Aminot, A. and Perttila, M. 1991. Report on the results of the ICES fourth intercomparison exercise for nutrients in sea water. ICES coop. Res. Rep. Ser., 174.

Mordy, C.W., Aoyama, M., Gordon, L.I., Johnson, G.C., Key, R.M., Ross, A.A., Jennings, J.C. and Wilson. J. 2000. Deep water comparison studies of the Pacific WOCE nutrient data set. Eos Trans-American Geophysical Union. 80 (supplement), OS43.

Murphy, J., and Riley, J.P. 1962. Analytica chim. Acta 27, 31-36.

Uchida, H. & Fukasawa, M. WHP P6, A10, I3/I4 REVISIT DATA BOOK Blue Earth Global Expedition 2003 1, 2, (Aiwa Printing Co., Ltd., Tokyo, 2005).

2.6 pH measurement

Masahide WAKITA (JAMSTEC MIO): Principal Investigator
Minoru KAMATA (MWJ)

(1) Objective

Since the global warming is becoming an issue world-widely, studies on the greenhouse gases such as CO_2 are drawing high attention. The ocean plays an important role in buffering the increase of atmospheric CO_2, and studies on the exchange of CO_2 between the atmosphere and the sea becomes highly important. Oceanic biosphere, especially primary production, has an important role concerned to oceanic CO_2 cycle through its photosynthesis and respiration. However, the diverseness and variability of the biological system make difficult to reveal their mechanism and quantitative understanding of CO_2 cycle. Dissolved CO_2 in water alters its appearance into several species, but the concentrations of the individual species of CO_2 system in solution cannot be measured directly. However, two of the four measurable parameters (alkalinity, total dissolved inorganic carbon, pH and pCO_2) can estimate each concentration of CO_2 system (Dickson et al., 2007). Seawater acidification associated with CO_2 uptake into the ocean possibly changes oceanic ecosystem and CO_2 garners in Ocean recently. We here report on board measurements of pH during MR11-02 cruise.

(2) Methods, Apparatus and Performance

(2)-1 Seawater sampling

Seawater samples were collected with CTD system mounted 12 liter Niskin bottles and a bucket at 4 stations. Seawater was sampled in a 100 ml glass bottle that was previously soaked in 5 % non-phosphoric acid detergent (pH13) solution at least 3 hours and was cleaned by fresh water for 5 times and Milli-Q ultrapure water for 3 times. A sampling silicone rubber tube with PFA tip was connected to the Niskin bottle when the sampling was carried out. The glass bottles were filled from the bottom smoothly, without rinsing, and were overflowed for 2 times bottle volume (about 10 seconds) with care not to leave any bubbles in the bottle. The water in the bottle was sealed by a glass made cap gravimetrically fitted to the bottle mouth without additional force. After collecting the samples on the deck, the bottles were carried into the lab and put in the water bath kept about 25 deg C before the measurement.

(2)-2 Seawater analyses

pH (-log[H+]) of the seawater was measured potentiometrically in the glass bottles. The pH / Ion meter (Radiometer PHM240) is used to measure the electromotive force (e.m.f.) between the glass electrode cell (Radiometer pHG201) and the reference electrode cell (Radiometer REF201) in the sample with its temperature controlled to 25 +/- 0.05 deg C.

Ag, AgCl reference electrode | solution of KCl || test solution | H+ -glass electrode.

To calibrate the electrodes, the TRIS buffer (Lot=100715-1: pH=8.0906 pH units at 25 deg C, Delvalls and Dickson, 1998) and AMP buffer (Lot=100720-1: pH=6.7838 pH units at 25 deg C, DOE, 1994) in the synthetic seawater (Total hydrogen ion concentration scale) were applied. pH_T of seawater sample (pH_{spl}) is calculated from the expression:

$$pH_{spl} = pH_{TRIS} + (E_{TRIS} - E_{spl}) / ER$$

where electrode response ER is calculated as follows:

$$ER = (E_{AMP} - E_{TRIS}) / (pH_{TRIS} - pH_{AMP})$$

ER value should be equal to the ideal Nernst value as follows:

ER = RT LN(10) / F = 59.16 mV / pH units at 25 deg C

(3) Preliminary results

A replicate analysis of seawater sample was made at 4 layers (ex. 50, 300, 1600, and 3500 dbar depth) of deep cast or 2 layers (ex. 10 % irradiance depth, and 125 m depth) of shallow cast. The difference between each pair of analyses was plotted on a range control chart (see Figure 2.6-1). The average of the difference was 0.001 pH units (n = 19 pairs) with its standard deviation of 0.001 pH units. These values were lower than the value recommended by Guide (Dickson et al., 2007).

(4) Data Archive

All data will be submitted to JAMSTEC and is currently under its control.

(5) Reference

DOE (1994), Handbook of methods for the analysis of the various parameters of the carbon dioxide system in sea water; version 2, A. G. Dickson & C. Goyet, Eds., ORNS/CDIAC-74

DelValls, T. A. and Dickson, A. G., 1998. The pH of buffers based on 2-amino-2-hydroxymethyl-1,3-propanediol (‘tris’) in synthetic sea water. Deep-Sea Research Ⅰ 45, 1541-1554.

Dickson, A. G., C. L. Sabine and J. R. Christian, Eds. (2007): Guide to best practices for ocean CO_2 measurements, PICES Special Publication 3, 199pp.

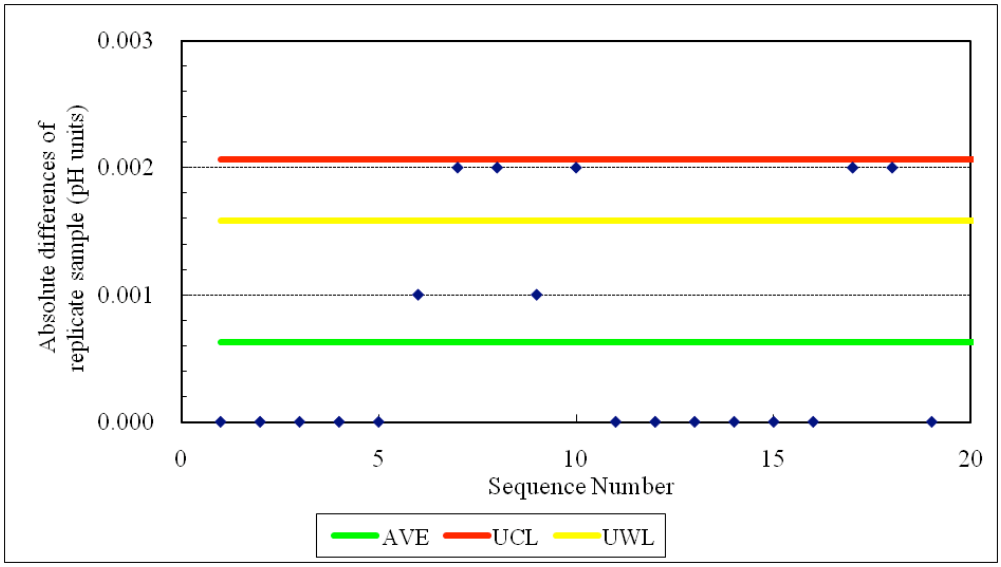

Figure 2.6-1 Range control chart of the absolute differences of replicate measurements of pH carried out during the cruise. AVE represents the average value, UCL upper control limit (UCL = AVE * 3.267), and UWL upper warning limit (UWL = AVE * 2.512) (Dickson et al., 2007).

2.7 Dissolved inorganic carbon-DIC

Masahide WAKITA (JAMSTEC MIO): Principal Investigator
Ayaka HATSUYAMA (MWJ)
Tomonori WATAI (MWJ)

(1) Objective

Concentration of CO_2 in the atmosphere is now increasing at a rate of 1.5 ppmv yr^{-1} owing to human activities such as burning of fossil fuels, deforestation, and cement production. The ocean plays an important role in buffering the increase of atmospheric CO_2, therefore the urgent tasks are to clarify the mechanism of the oceanic CO_2 absorption and to estimate of CO_2 absorption capacity of the oceans. Oceanic biosphere, especially primary production, has an important role concerned to oceanic CO_2 cycle through its photosynthesis and respiration. However, the diverseness and variability of the biological system make difficult to reveal their mechanism and quantitative understanding of the CO_2 cycle. When CO_2 dissolves in water, chemical reaction takes place and CO_2 alters its appearance into several species. Concentrations of the individual species of the CO_2 system in solution cannot be measured directly, but calculated from two of four parameters: total alkalinity, total dissolved inorganic carbon, pH and pCO_2 (Dickson et al., 2007). We here report on-board measurements of DIC performed during the MR11-02 cruise.

(2) Methods, Apparatus and Performance

(2)-1 Seawater sampling

Seawater samples were collected by 12 liter Niskin bottles mounted on the CTD/Carousel system at 4 stations. Among these stations, deep and shallow casts were carried out for 2 stations. When shallow casts were performed, surface seawater samples were also collected by a bucket. Seawater was sampled in a 300 ml glass bottle (SCHOTT DURAN) that was previously soaked in 5 % non-phosphoric acid detergent (pH = 13) solution at least 3 hours and was cleaned by fresh water for 5 times and Milli-Q deionized water for 3 times. A sampling silicone rubber tube with PFA tip was connected to the Niskin bottle when the sampling was carried out. The glass bottles were filled from the bottom, without rinsing, and were overflowed for 20 seconds. They were sealed using the polyethylene inner lids with its diameter of 29 mm with care not to leave any bubbles in the bottle. After collecting the samples on the deck, the glass bottles were carried to the laboratory to be measured. Within one hour after the sampling, 3 ml of the sample (1 % of the bottle volume) was removed from the glass bottle and poisoned with 100 µl of over saturated solution of mercury chloride. Then the samples were sealed by the polyethylene inner lids with its diameter of 31.9 mm and stored in a refrigerator at approximately 5 deg C until analyzed. Before the analysis, the samples were put in the water bath kept about 20 deg C for one hour.

(2)-2 Seawater analysis

Measurements of DIC were made with total CO_2 measuring system (Nippon ANS, Inc.). The system comprise of seawater dispensing unit, a CO_2 extraction unit and a coulometer (Model seacat2000, Nippon ANS, Inc.)

The seawater dispensing unit has an auto-sampler (6 ports), which dispenses the seawater from a glass bottle to a pipette of nominal 21 ml volume. The pipette was kept at 20 ± 0.05 deg C by a water jacket, in which water circulated through a thermostatic water bath (RTE

10, Thermo) set at 20 deg C.

The CO_2 dissolved in a seawater sample is extracted in a stripping chamber of the CO_2 extraction unit by adding phosphoric acid (10 % v/v). The stripping chamber is made approx. 25 cm long and has a fine frit at the bottom. First, the certain amount of acid is taken to the constant volume tube and added to the stripping chamber from its bottom by pressurizing an acid bottle with nitrogen gas (99.9999 %). Second, a seawater sample kept in a pipette is introduced to the stripping chamber by the same method as that for an acid. The seawater and phosphoric acid are stirred by the nitrogen bubbles through a fine frit at the bottom of the stripping chamber. The CO_2 stripped in the chamber is carried by the nitrogen gas (flow rates of 140 ml min^{-1}) to the coulometer through two electric dehumidifiers (kept at 0.5 deg C) and a chemical desiccant ($Mg(ClO_4)_2$).

Measurements of 1.5 % CO_2 standard gas in a nitrogen base, system blank (phosphoric acid blank), and seawater samples (6 samples) were programmed to repeat. The variation of 1.5 % CO_2 standard gas signal was used to correct the signal drift results from chemical alternation of coulometer solutions.

(3) Preliminary results

During the cruise, 217 samples were analyzed for DIC. A replicate analysis was performed at the interval decided beforehand and the difference between each pair of analyses was plotted on a range control chart (Figure 2.7-1). The average of the differences was 0.7 μmol kg^{-1} (n = 19). The standard deviation was 0.6 μmol kg^{-1}, which indicates that the analysis was accurate enough according to the Guide to best practices for ocean CO_2 measurements (Dickson et al., 2007).

(4) Data Archive

These data obtained in this cruise will be submitted to the Data Management Office (DMO) of JAMSTEC, and will opened to the public via “R/V Mirai Data Web Page” in JAMSTEC home page.

(5) Reference

Dickson, A. G., Sabine, C. L. & Christian, J. R. (2007), Guide to best practices for ocean CO_2 measurements; PICES Special Publication 3, 199pp.

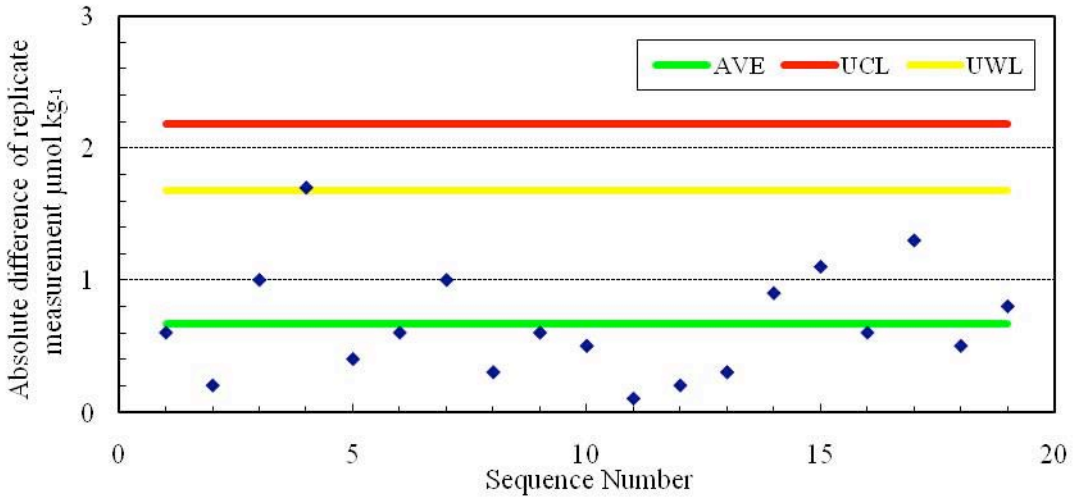

Figure 2.7-1 Range control chart of the absolute differences of replicate measurements of DIC carried out during this cruise. UCL and UWL represents the upper control limit (UCL=AVE*3.267) and upper warning limit (UWL=AVE*2.512), respectively.

2.8 Total Alkalinity

Masahide WAKITA (JAMSTEC MIO): Principal Investigator
Tomonori WATAI (MWJ)
Ayaka HATSUYAMA (MWJ)

(1) Objective

Global warming is becoming an issue world-widely, therefore studies on green house gases, especially carbon dioxide (CO_2), are indispensable. The ocean currently absorbs one third of the 6 Gt of carbon emitted into the atmosphere each year by human activities, such as burning of fossil fuels, deforestation, and cement production. When CO_2 dissolves in sea water, chemical reaction takes place and CO_2 alters its appearance into several species and make the oceanic CO_2 cycle complicated. Furthermore, oceanic biological activity, especially oceanic primary production, plays an important role concerned to the CO_2 cycle through its photosynthesis and respiration. The concentrations of the individual CO_2 species cannot be measured directly, however, two of four measurable parameters: total alkalinity, total dissolved inorganic carbon, pH, and pCO_2, can clarify the whole distribution of the CO_2 species (Dickson et al., 2007). We here report on-board measurements of total alkalinity performed during the MR11-02 cruise.

(2) Methods, Apparatus and Performance

(2)-1 Seawater sampling

Seawater samples were collected by 12 liter Niskin bottles mounted on the CTD/Carousel Water Sampling System at 4 stations. Among these stations, deep and shallow casts were carried out for 2 stations. Surface seawater samples were also collected by a bucket when shallow casts were performed. A sampling silicone rubber tube with PFA tip was used to sample the seawater from the Niskin bottle. The 125 ml borosilicate glass bottles (SHOTT DURAN) were filled from the bottom smoothly, without rinsing, and were overflowed for 2 times bottle volume (10 seconds) with care not to leave any bubbles in the bottle. These bottles were pre-washed by soaking in 5 % non-phosphoric acid detergent (pH = 13) for more than 3 hours and then rinsed 5 times with tap water and 3 times with Milli-Q deionized water. After collecting the samples on the deck, the bottles were carried into the laboratory to be measured. The samples were stored in a refrigerator at approximately 5 deg C until being analyzed. Before the analysis, the samples were put in the water bath kept about 25 deg C for one hour.

(2)-2 Seawater analyses

The TA was measured using a spectrophotometric system (Nippon ANS, Inc.) using a scheme of Yao and Byrne (1998). The constant volume of sample seawater, with its value of 42.1517 ml, was transferred from a sample bottle into the titration cell kept at 25 deg C in a thermostated compartment. Then, the sample seawater was circulated through the tube connecting the titration cell and the pH cell in the spectrophotometer (Carry 50 Scan, Varian) by a peristaltic pump. The length and volume of the pH cell are 8 cm and 13 ml, respectively, and its temperature is also kept at 25 deg C in a thermostated compartment. The TA is calculated by measuring two sets of absorbance at three wavelengths (750, 616 and 444 nm). One is the absorbance of seawater sample before injecting an acid with indicator solution (bromocresol green sodium) and another is the one after the injection. For mixing the acid with indicator solution and the seawater, and for degassing CO_2 from the mixed solution sufficiently, they are

circulated between the titration and pH cell by a peristaltic pump for 7 and half minutes before the measurement.

The TA is calculated based on the following equation:

$$pH_T = 4.2699 + 0.002578 * (35 - S) + \log((R(25) - 0.00131) / (2.3148 - 0.1299 * R(25))) - \log(1 - 0.001005 * S), \quad (1)$$

$$A_T = (N_A * V_A - 10 \wedge pH_T * DensSW(T, S) * (V_S + V_A)) * (DensSW(T, S) * V_S)^{-1}, \quad (2)$$

where R(25) represents the difference of absorbance at 616 and 444 nm between before and after the injection. The absorbance of wavelength at 750 nm is used to subtract the variation of absorbance caused by the system. DensSW (T, S) is the density of seawater at temperature (T) and salinity (S), N_A the concentration of the added acid, V_A and V_S the volume of added acid and seawater, respectively.

To keep the high analysis precision, some treatments were carried out during the cruise. The acid with indicator solution stored in 1 L DURAN bottle is kept in a bath with its temperature of 25 deg C, and about 10 ml of it is discarded at first before the batch of measurement. For mixing the seawater and the acid with indicator solution sufficiently, TYGON tube used on the peristaltic pump was periodically renewed. Absorbance measurements were done 10 times during each analysis, and the stable last five and three values are averaged and used for above listed calculation for before and after the injection, respectively.

(3) Preliminary results

A few replicate samples were taken at most of stations and the difference between each pair of analyses was plotted on a range control chart (see Figure 2.8-1). The average of the difference was 0.7 μmol kg^{-1} (n = 18) with its standard deviation of 0.6 μmol kg^{-1}, which indicates that the analysis was accurate enough according to the Guide to best practices for ocean CO_2 measurements (Dickson et al., 2007).

(4) Data Archive

These data obtained in this cruise will be submitted to the Data Management Office (DMO) of JAMSTEC, and will opened to the public via “R/V Mirai Data Web Page” in JAMSTEC home page.

(5) References

Yao, W. and Byrne, R. H. (1998), Simplified seawater alkalinity analysis: Use of linear array spectrometers. Deep-Sea Research Part I, Vol. 45, 1383-1392.

Dickson, A. G., Sabine, C. L. & Christian, J. R. (2007), Guide to best practices for ocean CO_2 measurements; PICES Special Publication 3, 199pp.

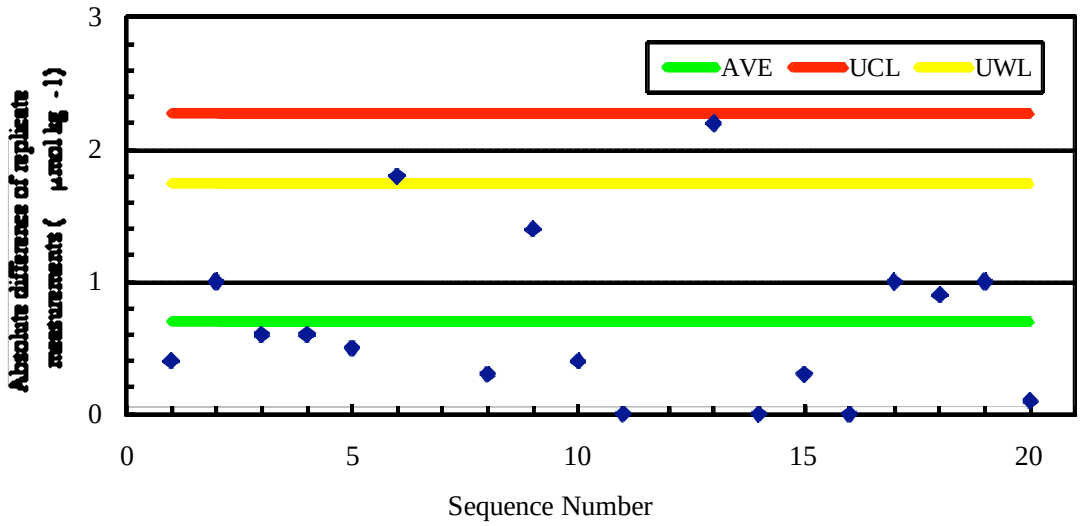

Figure 2.8-1 Range control chart of the absolute differences of replicate measurements carried out in the analysis of TA during the MR11-02 cruise. UCL and UWL represents the upper control limit (UCL=AVE*3.267) and upper warning limit (UWL=AVE*2.512), respectively.

2.9 Underway pCO_2

Masahide WAKITA (JAMSTEC MIO): Principal Investigator
Tomonori WATAI (MWJ)
Ayaka HATSUYAMA (MWJ)

(1) Objectives

Concentrations of CO_2 in the atmosphere are increasing at a rate of 1.5 ppmv yr^{-1} owing to human activities such as burning of fossil fuels, deforestation, and cement production. Oceanic CO_2 concentration is also considered to be increased with the atmospheric CO_2 increase, however, its variation is widely different by time and locations. Underway pCO_2 observation is indispensable to know the pCO_2 distribution, and it leads to elucidate the mechanism of oceanic pCO_2 variation. We here report the underway pCO_2 measurements performed during MR11-02 cruise.

(2) Methods, Apparatus and Performance

Oceanic and atmospheric CO_2 concentrations were measured during the cruise using an automated system equipped with a non-dispersive infrared gas analyzer (NDIR; LI-7000, Li-Cor). Measurements were done every about one and a half hour, and 4 standard gasses, atmospheric air, and the CO_2 equilibrated air with sea surface water were analyzed subsequently in this hour. The concentrations of the CO_2 standard gases were 299.834, 350.002, 400.099 and 450.374 ppmv. Atmospheric air taken from the bow of the ship (approx.30 m above the sea level) was introduced into the NDIR by passing through a electrical cooling unit, a mass flow controller which controls the air flow rate of 0.5 L min^{-1}, a membrane dryer (MD-110-72P, perma pure llc.) and chemical desiccant ($Mg(ClO_4)_2$). The CO_2 equilibrated air was the air with its CO_2 concentration was equivalent to the sea surface water. Seawater was taken from an intake placed at the approximately 4.5 m below the sea surface and introduced into the equilibrator at the flow rate of 4 - 5 L min^{-1} by a pump. The equilibrated air was circulated in a closed loop by a pump at flow rate of 0.7 - 0.8 L min^{-1} through two cooling units, a membrane dryer, the chemical desiccant, and the NDIR.

(3) Preliminary results

Cruise track during pCO_2 observation is shown in Figure 2.9-1. Temporal variations of both oceanic and atmospheric CO_2 concentration (xCO_2) are shown in Fig. 2.9-2.

(4) Data Archive

Data obtained in this cruise will be submitted to the Data Management Office (DMO) of JAMSTEC, and will opened to the public via “R/V Mirai Data Web Page” in JAMSTEC home page.

(5) Reference

Dickson, A. G., Sabine, C. L. & Christian, J. R. (2007), Guide to best practices for ocean CO_2 measurements; PICES Special Publication 3, 199pp.

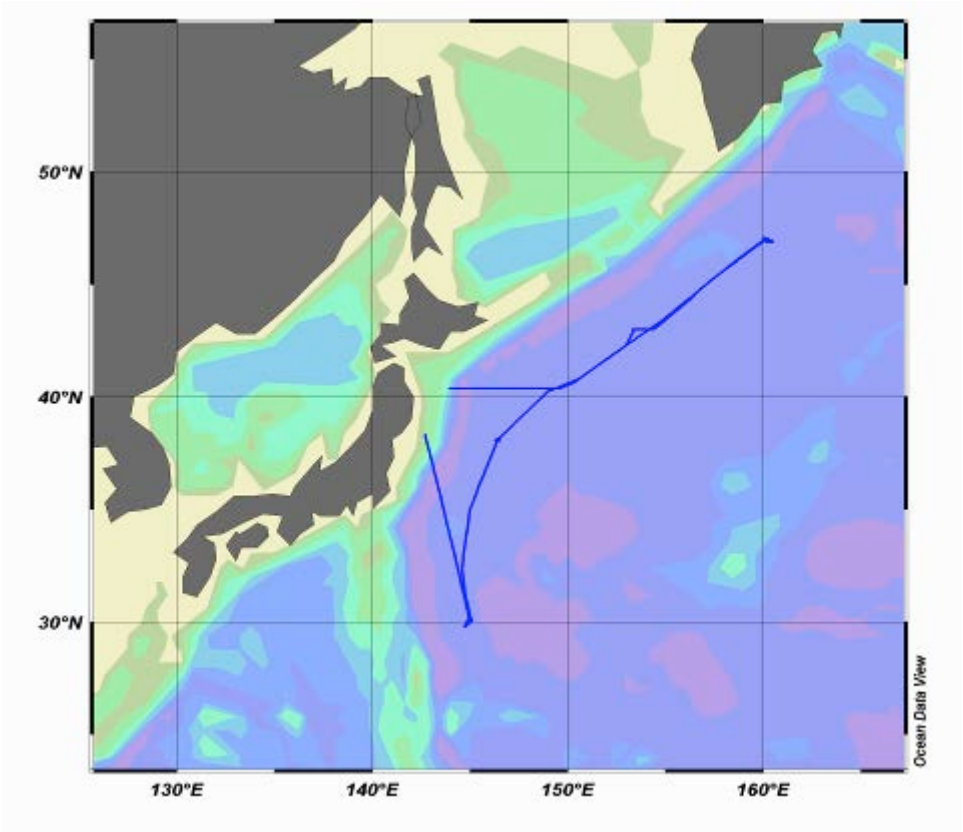

Figure 2.9-1 Observation map

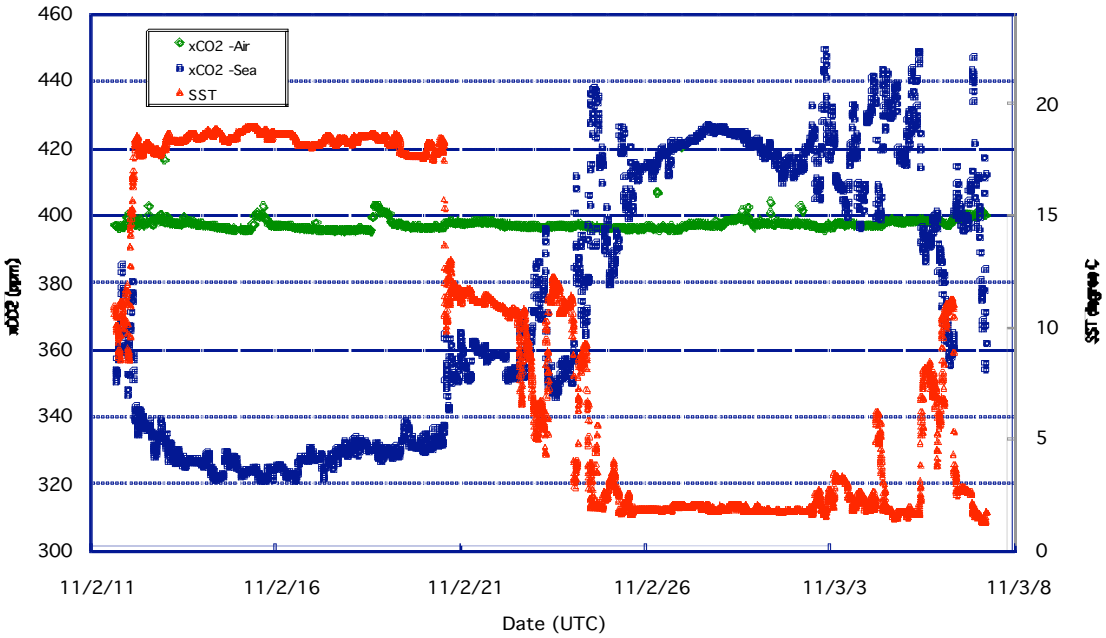

Figure 2.9-2 Temporal variations of oceanic and atmospheric CO_2 concentration (xCO_2). Blue dots represent oceanic xCO_2 variation and green atmospheric xCO_2. SST variation (red) is also shown.

3. Special observation

3.1 Underwater profiling buoy system (Primary productivity profiler)

Tetsuichi FUJIKI (JAMSTEC)
Toru IDAI (MWJ)
Tetsuya NAKAMURA (Nichiyu Giken Kogyo)

(1) Objective

An understanding of the variability in phytoplankton productivity provides a basic knowledge of how aquatic ecosystems are structured and functioning. The primary productivity of the world oceans has been measured mostly by the radiocarbon tracer method or the oxygen evolution method. As these traditional methods use the uptake of radiocarbon into particulate matter or changes in oxygen concentration in the bulk fluid, measurements require bottle incubations for periods ranging from hours to a day. This methodological limitation has hindered our understanding of the variability of oceanic primary productivity. To overcome these problems, algorithms for estimating primary productivity by using satellite ocean color imagery have been developed and improved. However, one of the major obstacles to the development and improvement of these algorithms is a lack of *in situ* primary productivity data to verify the satellite estimates.

During the past decade, the utilization of active fluorescence techniques in biological oceanography has brought marked progress in our understanding of phytoplankton photosynthesis in the oceans. Above all, fast repetition rate (FRR) fluorometry reduces the primary electron acceptor (Q_a) in photosystem (PS) II by a series of subsaturating flashlets and can measure a single turnover fluorescence induction curve in PSII. The PSII parameters derived from the fluorescence induction curve provide information on the physiological state related to photosynthesis and can be used to estimate gross primary productivity. FRR fluorometry has several advantages over the above-mentioned traditional methods. Most importantly, because measurements made by FRR fluorometry can be carried out without the need for time-consuming bottle incubations, this method enables real-time high-frequency measurements of primary productivity. In addition, the FRR fluorometer can be used in platform systems such as moorings, drifters, and floats.

The current study aimed to assess the vertical and temporal variations in PSII parameters and primary productivity in the western Pacific, by using an underwater profiling buoy system that uses the FRR fluorometer (system name: Primary productivity profiler)

(2) Methods

a) Primary productivity profiler

The primary productivity profiler (original design by Nichiyu Giken Kogyo) consisted mainly of an observation buoy equipped with a submersible FRR fluorometer (Diving Flash, Kimoto Electric), a scalar irradiance sensor (QSP-2200, Biospherical Instruments), a CTD sensor (MCTD, Falmouth Scientific) and a dissolved oxygen sensor (Compact Optode, Alec Electronics), an underwater winch, an acoustic Doppler current profiler (Workhorse Long Ranger, Teledyne RD Instruments) and an acoustic releaser (Fig. 1). The observation buoy moved between the winch depth and the surface at a rate of 0.2 m s^{-1} and measured the vertical profiles of phytoplankton fluorescence, irradiance, temperature, salinity and dissolved oxygen. The profiling rate of the observation buoy was set to 0.2 m s^{-1} to detect small-scale variations

(approx. 0.5 m) in the vertical profile. To minimize biofouling of instruments, the underwater winch was placed below the euphotic layer so that the observation buoy was exposed to light only during the measurement period. In addition, the vertical migration of observation buoy reduced biofouling of instruments.

b) Measurement principle of FRR fluorometer

The FRR fluorometer consists of closed dark and open light chambers that measure the fluorescence induction curves of phytoplankton samples in darkness and under actinic illumination. To allow relaxation of photochemical quenching of fluorescence, the FRR fluorometer allows samples in the dark chamber to dark adapt for about 1 s before measurements. To achieve cumulative saturation of PSII within 150 μs — i.e., a single photochemical turnover — the instrument generates a series of subsaturating blue flashes at a light intensity of 25 mmol quanta m^{-2} s^{-1} and a repetition rate of about 250 kHz s^{-1}. The PSII parameters are derived from the single-turnover-type fluorescence induction curve by using the numerical fitting procedure described by Kolber et al. (1998). Analysis of fluorescence induction curves measured in the dark and light chambers provides PSII parameters such as fluorescence yields, photochemical efficiency and effective absorption cross section of PSII, which are indicators of the physiological state related to photosynthesis. Using the PSII parameters, the rate of photosynthetic electron transport and the gross primary productivity can be estimated.

c) Site description and observations

The primary productivity profiler deployed at station S1 in MR10-06 was recovered on 14 February 2011 (UTC). In addition, the primary productivity profiler was newly-deployed on 17 February 2011 (UTC) (Fig. 2, target position: 29° 56.268 N, 144° 58.513 E, 5915 m; actual position: 29° 56.187 N, 144° 58.007 E, 5913 m). The measurements began on 19 February 2011 and will continue until 27 June 2011.

Measurement schedule at station S1 (Japan time)

1. 11/02/19 02:00	2. 11/02/19 11:00	3. 11/02/21 02:00	4. 11/02/21 11:00
5. 11/02/23 11:00	6. 11/02/25 02:00	7. 11/02/25 11:00	8. 11/02/27 11:00
9. 11/03/01 02:00	10. 11/03/01 11:00	11. 11/03/03 11:00	12. 11/03/05 02:00
13. 11/03/05 11:00	14. 11/03/07 11:00	15. 11/03/09 02:00	16. 11/03/09 11:00
17. 11/03/11 11:00	18. 11/03/13 02:00	19. 11/03/13 11:00	20. 11/03/15 11:00
21. 11/03/17 02:00	22. 11/03/17 11:00	23. 11/03/19 11:00	24. 11/03/21 02:00
25. 11/03/21 11:00	26. 11/03/23 11:00	27. 11/03/25 02:00	28. 11/03/25 11:00
29. 11/03/27 11:00	30. 11/03/29 02:00	31. 11/03/29 11:00	32. 11/03/31 11:00
33. 11/04/02 02:00	34. 11/04/02 11:00	35. 11/04/04 11:00	36. 11/04/06 02:00
37. 11/04/06 11:00	38. 11/04/08 11:00	39. 11/04/10 02:00	40. 11/04/10 11:00
41. 11/04/12 11:00	42. 11/04/14 02:00	43. 11/04/14 11:00	44. 11/04/16 11:00
45. 11/04/18 02:00	46. 11/04/18 11:00	47. 11/04/20 11:00	48. 11/04/22 02:00
49. 11/04/22 11:00	50. 11/04/24 11:00	51. 11/04/26 02:00	52. 11/04/26 11:00
53. 11/04/28 11:00	54. 11/04/30 02:00	55. 11/04/30 11:00	56. 11/05/02 11:00
57. 11/05/04 02:00	58. 11/05/04 11:00	59. 11/05/06 11:00	60. 11/05/08 02:00
61. 11/05/08 11:00	62. 11/05/10 11:00	63. 11/05/12 02:00	64. 11/05/12 11:00
65. 11/05/14 11:00	66. 11/05/16 02:00	67. 11/05/16 11:00	68. 11/05/18 11:00
69. 11/05/20 02:00	70. 11/05/20 11:00	71. 11/05/22 11:00	72. 11/05/24 02:00

73. 11/05/24 11:00	74. 11/05/26 11:00	75. 11/05/28 02:00	76. 11/05/28 11:00
77. 11/05/30 11:00	78. 11/06/01 02:00	79. 11/06/01 11:00	80. 11/06/03 11:00
81. 11/06/05 02:00	82. 11/06/05 11:00	83. 11/06/07 11:00	84. 11/06/09 02:00
85. 11/06/09 11:00	86. 11/06/11 11:00	87. 11/06/13 02:00	88. 11/06/13 11:00
89. 11/06/15 11:00	90. 11/06/17 02:00	91. 11/06/17 11:00	92. 11/06/19 11:00
93. 11/06/21 02:00	94. 11/06/21 11:00	95. 11/06/23 11:00	96. 11/06/25 02:00
97. 11/06/25 11:00	98. 11/06/27 02:00		

To gain a better understanding of observational data from primary productivity profiler, separately from the primary productivity profiler, we moved up and down a submersible FRR fluorometer between surface and ~200 m at the station S1 using a ship winch, and measured the vertical and spatial variation in PSII parameters. In addition, the potential photosynthetic activity of phytoplankton assemblage was measured using a desktop type FRR fluorometer.

(3) Preliminary results

The operating condition of observation buoy in the primary productivity profiler recovered from station S1 was shown in figure 3. Unfortunately, the fluorescence data were not collected because of a problem (submergence) with the FRR fluorometer.

(4) Data archives

The data will be submitted to JAMSTEC Data Management Office.

(5) References

Kolber, Z. S., O. Prášil and P. G. Falkowski. 1998. Measurements of variable chlorophyll fluorescence using fast repetition rate techniques: defining methodology and experimental protocols. *Biochim. Biophys. Acta*. 1367: 88-106.

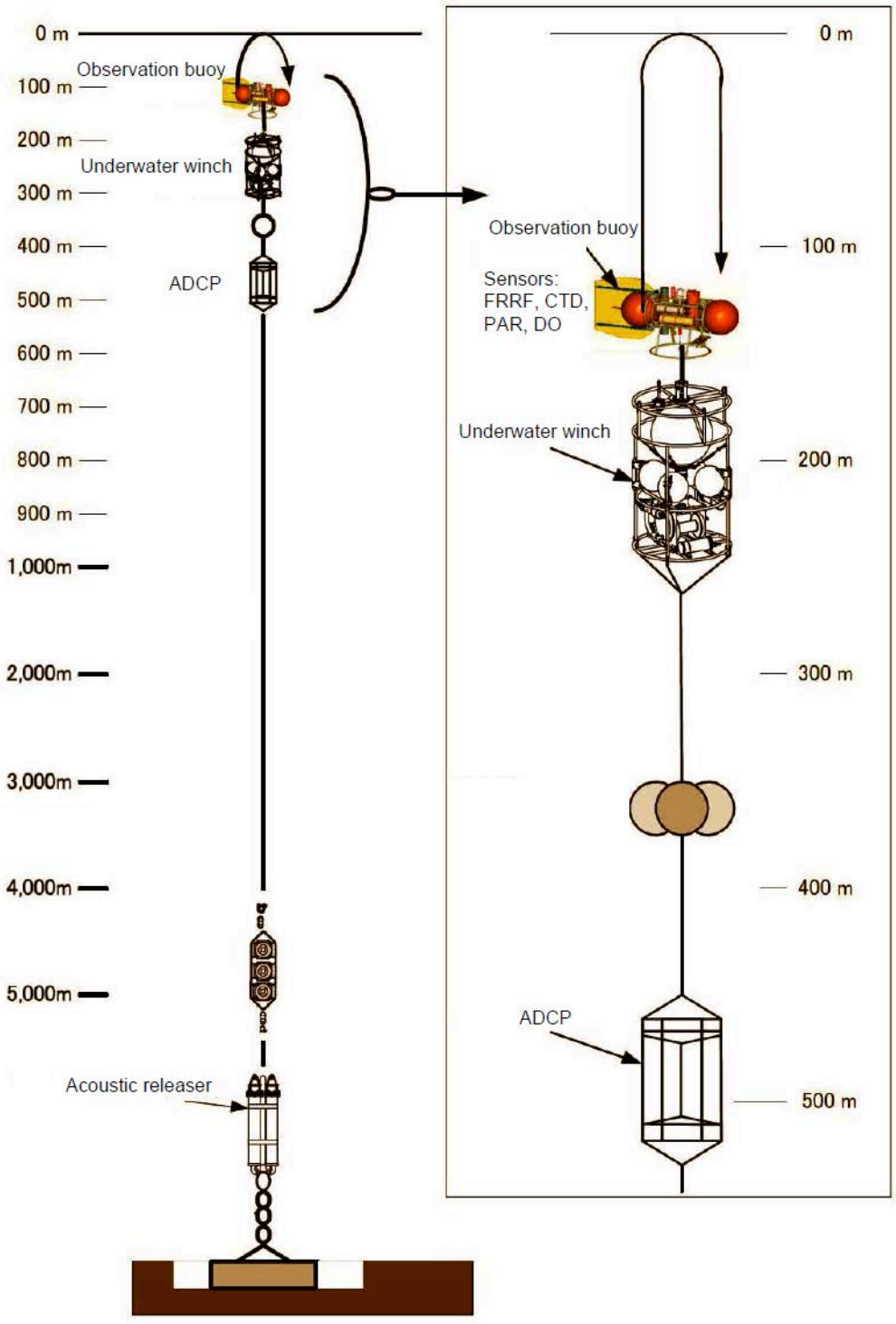

Figure 1. Schematic diagram of the primary productivity profiler.

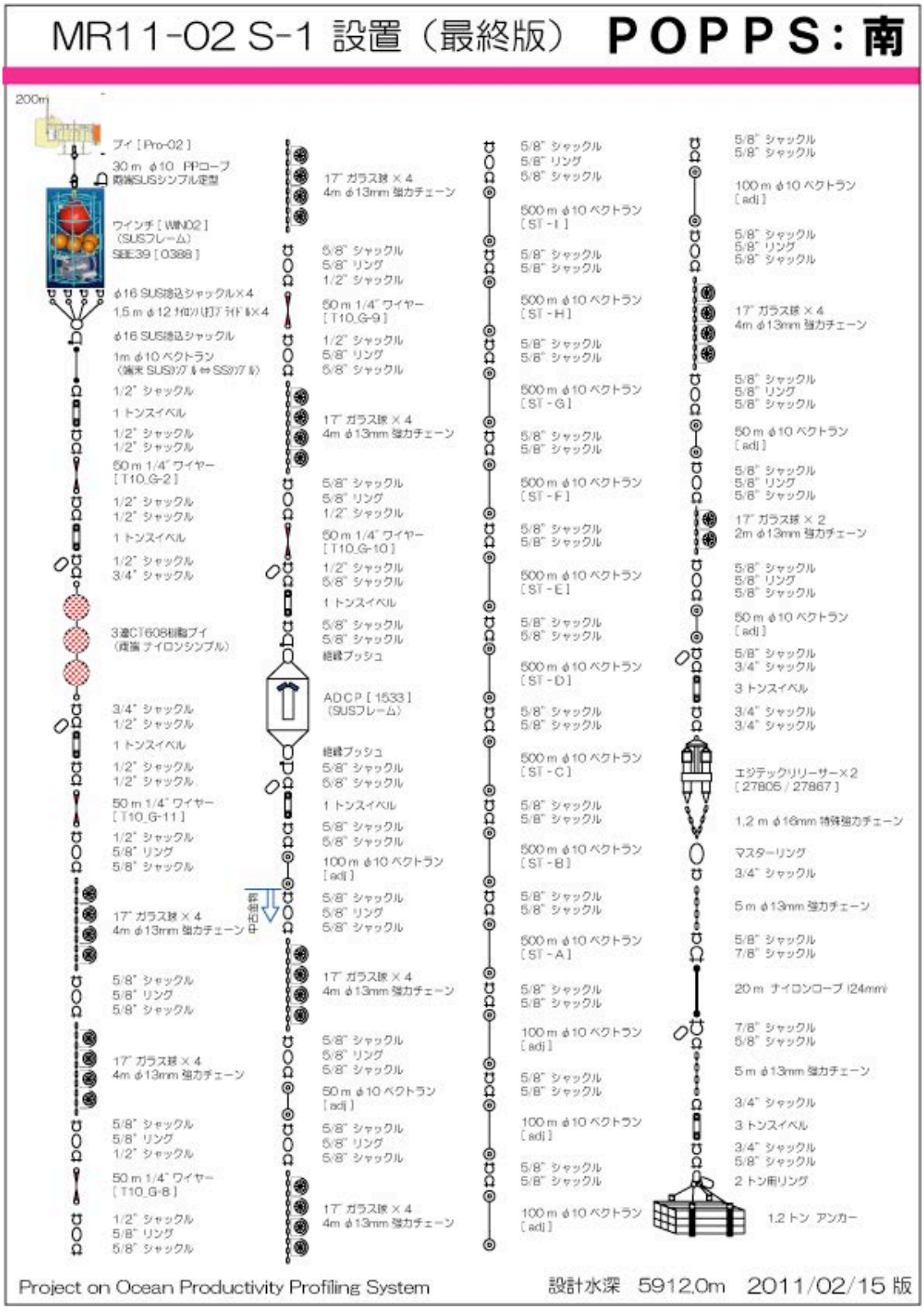

Figure 2. Detailed design of the primary productivity profiler deployed at station S1 in MR11-02.

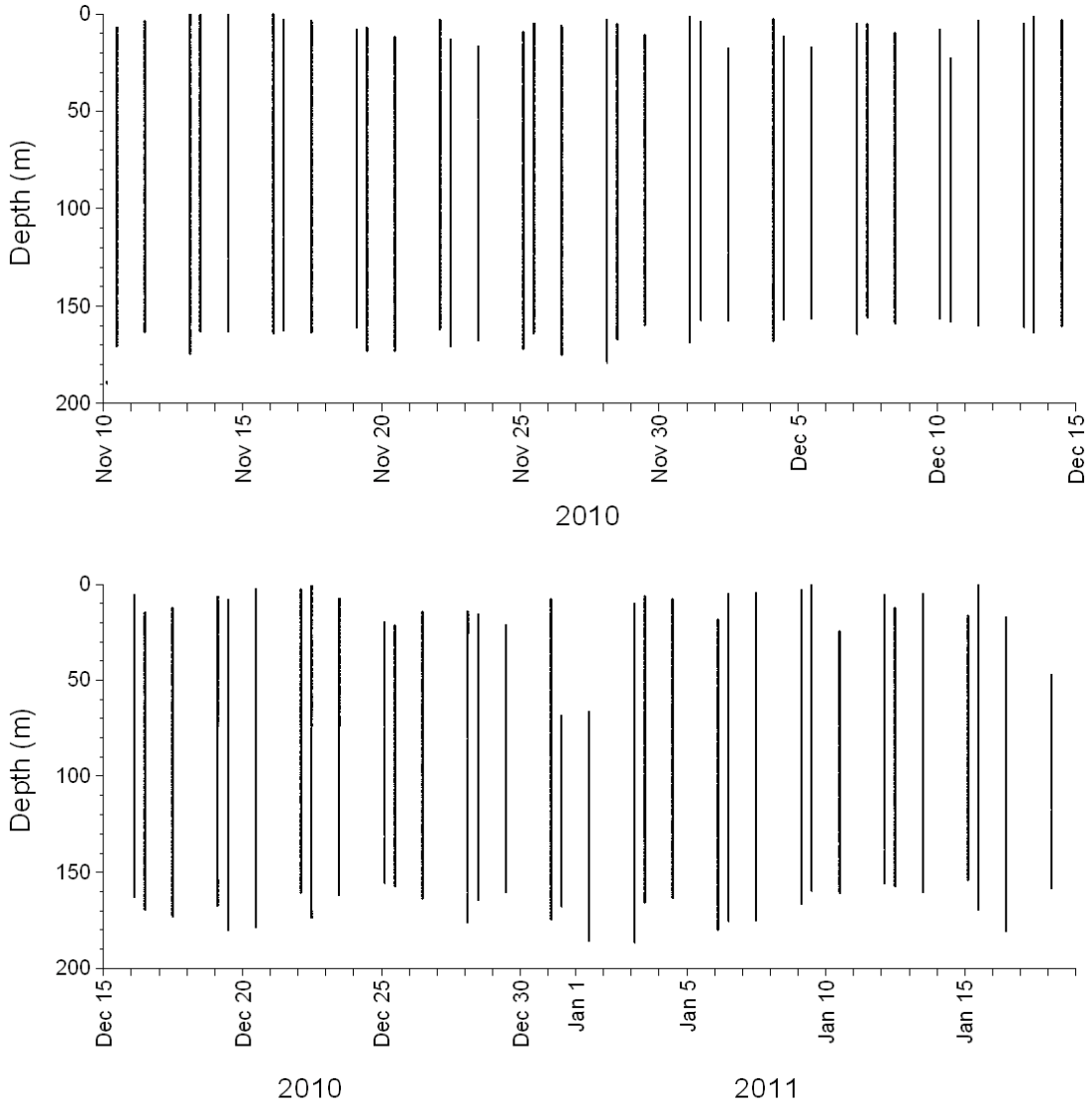

Figure 3. The operating condition of observation buoy in the primary productivity profiler recovered from station S1.

3.2.1 Chlorophyll *a* measurements by fluorometric determination

Kazuhiko MATSUMOTO (JAMSTEC)
Masahiro ORUI (MWJ)

1. Objective

Phytoplankton biomass can estimate as the concentration of chlorophyll *a* (chl-*a*), because all oxygenic photosynthetic plankton contain chl-*a*. Phytoplankton exist various species in the ocean, but the species are roughly characterized by their cell size. The objective of this study is to investigate the vertical distribution of phytoplankton and their size fractionations as chl-*a* by using the fluorometric determination.

2. Sampling

Samplings of total chl-*a* were conducted from 11 depths between the surface and 200 m at all observational stations. At the cast for primary production, water samples were collected at eight depths from among the surface, 0.5%, 1%, 2.5%, 5%, 10%, 25%, 50% light depths relative to the surface and at three other depths between the surface and 200 m at the station of S1 and K2.

3. Instruments and Methods

Water samples (0.5L) for total chl-*a* were filtered (<0.02 MPa) through 25mm-diameter Whatman GF/F filter. Size-fractionated chl-*a* were obtained by sequential filtration (<0.02 MPa) of 1-L water sample through 10-µm, 3-µm and 1-µm polycarbonate filters (47-mm diameter) and Whatman GF/F filter (25-mm diameter). Phytoplankton pigments retained on the filters were immediately extracted in a polypropylene tube with 7 ml of N,N-dimethylformamide (Suzuki and Ishimaru, 1990). Those tubes were stored at –20°C under the dark condition to extract chl-*a* for 24 hours or more.

Fluorescences of each sample were measured by Turner Design fluorometer (10-AU-005), which was calibrated against a pure chl-*a* (Sigma-Aldrich Co.). We applied two kind of fluorometric determination for the samples of total chl-*a*: “Non-acidification method” (Welschmeyer, 1994) and “Acidification method” (Holm-Hansen *et al*., 1965). Size-fractionated samples were applied only “Non-acidification method”. Analytical conditions of each method were listed in table 1.

4. Preliminary Results

The results of total chl-*a* at station S1 and K2 were shown in Figure 1 and 2. The results of size fractionated chl-*a* were shown in Figure3.

6. Data archives

The processed data file of pigments will be submitted to the JAMSTEC Data Integration and Analysis Group (DIAG) within a restricted period. Please ask PI for the latest information.

7. Reference

Suzuki, R., and T. Ishimaru (1990), An improved method for the determination of phytoplankton chlorophyll using N, N-dimethylformamide, *J. Oceanogr. Soc. Japan*, 46, 190-194.

Holm-Hansen, O., Lorenzen, C. J., Holmes, R.W. and J. D. H. Strickland (1965), Fluorometric determination of chlorophyll. *J. Cons. Cons. Int. Explor. Mer.* 30, 3-15.

Welschmeyer, N. A. (1994), Fluorometric analysis of chlrophyll *a* in the presence of chlorophyll *b* and pheopigments. *Limnol. Oceanogr.* 39, 1985-1992.

Table 1. Analytical conditions of "Non-acidification method" and "Acidification method" for chlorophyll *a* with Turner Designs fluorometer (10-AU-005).

	Non-acidification method	Acidification method
Excitation filter (nm)	436	340-500
Emission filter (nm)	680	>665
Lamp	Blue Mercury Vapor	Daylight White

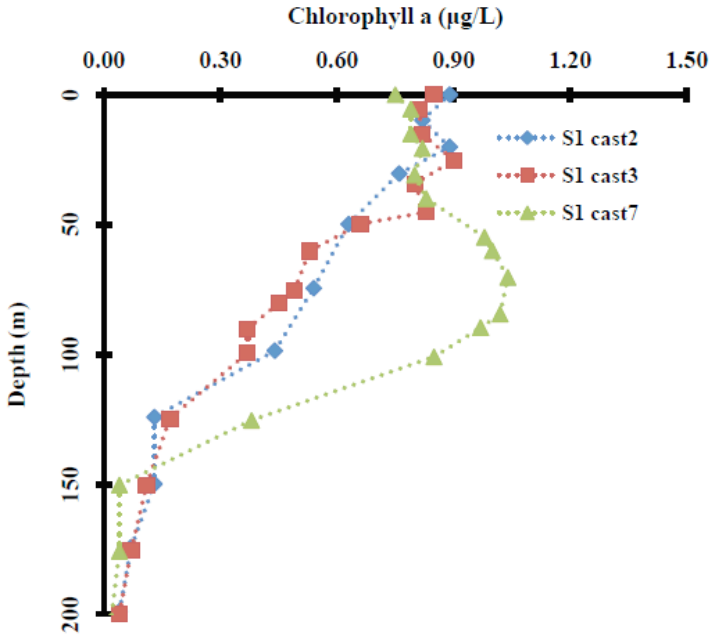

Figure1. Vertical distribution of chlorophyll *a* at Stn.S1

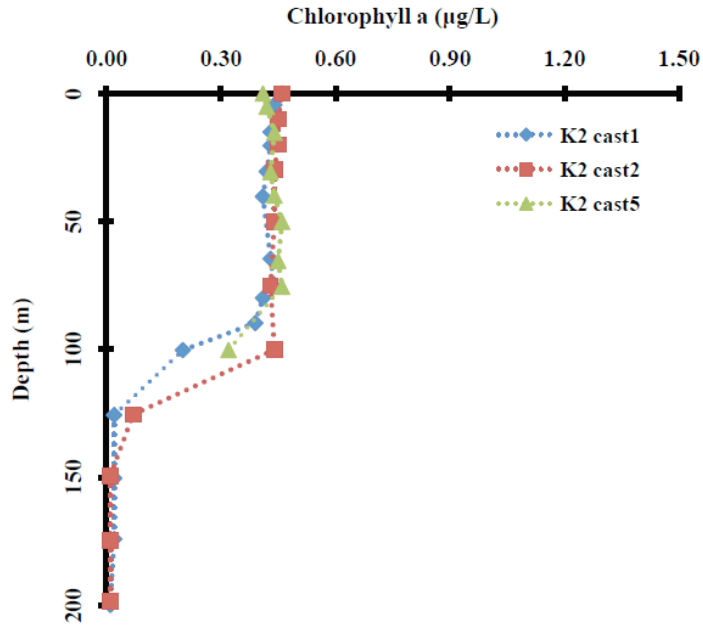

Figure2. Vertical distribution of chlorophyll *a* at Stn.K2

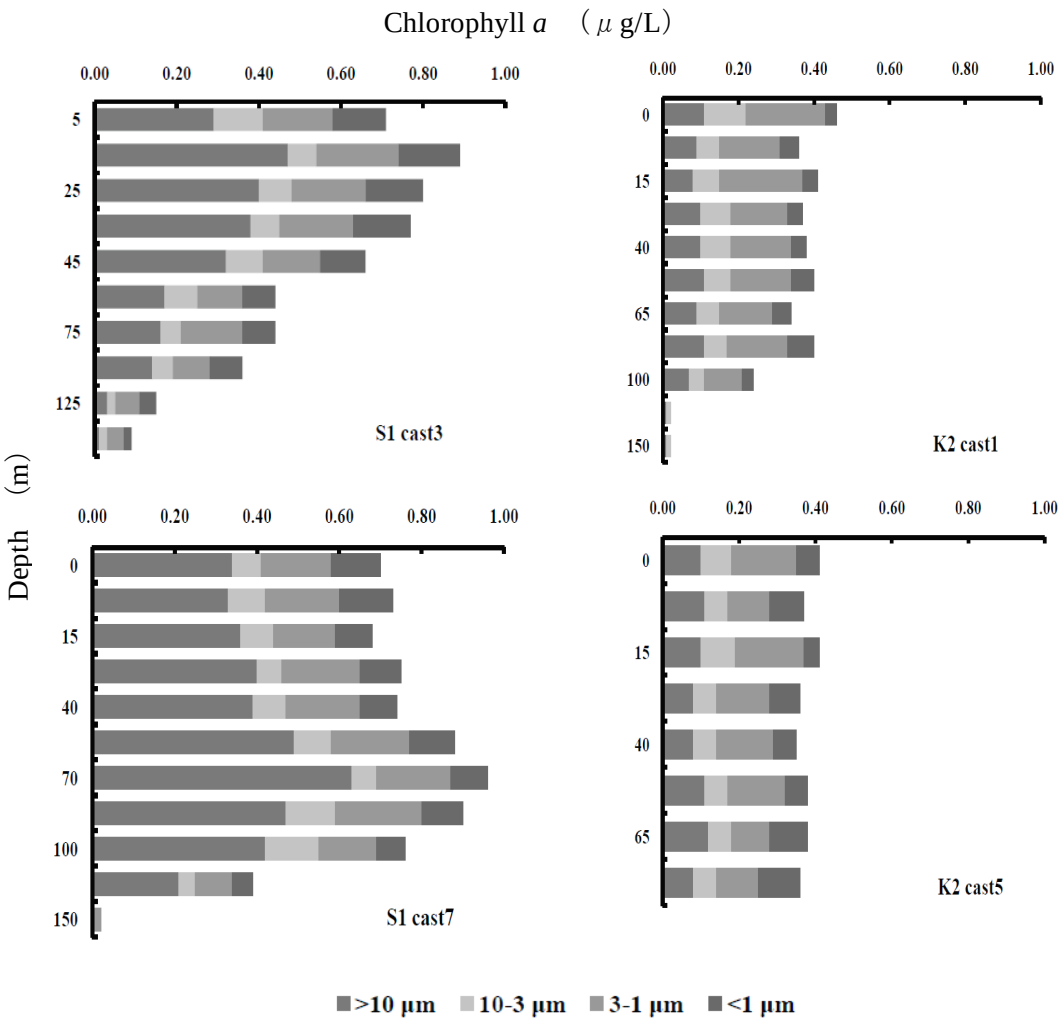

Figure3. Vertical distribution of size-fractionated chlorophyll *a*

3.2.2. HPLC measurements of marine phytoplankton pigments

Kazuhiko MATSUMOTO (JAMSTEC RIGC)
Shoko TATAMISASHI (MWJ)

(1) Objective

The chemotaxonomic assessment of phytoplankton populations present in natural seawater requires taxon-specific algal pigments as good biochemical markers. A high-performance liquid chromatography (HPLC) measurement is an optimum method for separating and quantifying phytoplankton pigments in natural seawater. In this cruise, we measured the marine phytoplankton pigments by HPLC to investigate the marine phytoplankton community structure in the western North Pacific.

(2) Methods, Apparatus and Performance

Seawater samples were collected from 11 depths between the surface and 200 m at the cast for the primary production. Sampling depths were determined by the light intensity at eight depths from among the surface, 0.5%, 1%, 2.5%, 5%, 10%, 25%, 50% light depths relative to the surface and at three other depths between the surface and 200 m. Seawater samples were collected using Niskin bottles, except for the surface water, which was taken by a bucket. Seawater samples (5L) were filtered (<0.02 MPa) through the 47-mm diameter Whatman GF/F filter. To remove retaining seawater in the sample filters, GF/F filters were vacuum-dried in a freezer (0 °C) within 6 hours. Subsequently, phytoplankton pigments retained on a filter were extracted in a glass tube with 4 ml of N,N-dimethylformamide (HPLC-grade) for at least 24 hours in a freezer (-20 °C), and analyzed by HPLC within a few days.

Residua cells and filter debris were removed through polypropylene syringe filter (pore size: 0.2 μm) before the analysis. The samples injection of 500 μl was conducted by auto-sampler with the mixture of extracted pigments (350 μl), pure water (150 μl) and internal standard (10 μl). Phytoplankton pigments were quantified based on C_8 column method containing pyridine in the mobile phase (Zapata *et al*., 2000).

(i) HPLC System

HPLC System was composed by Agilent 1200 modular system, G1311A Quaternary pump (low-pressure mixing system), G1329A auto-sampler and G1315D photodiode array detector.

(ii) Stationary phase

Analytical separation was performed using a YMC C_8 column (150×4.6 mm). The column was thermostatted at 35 °C in the column heater box.

(iii) Mobile phases

The eluant A was a mixture of methanol: acetonitrile: aqueous pyridine solution (0.25M pyridine), (50:25:25, v:v:v). The eluant B was a mixture of methanol: acetonitrile: acetone (20:60:20, v:v:v). Organic solvents for mobile phases were used reagents of HPLC-grade.

(iv) Calibrations

HPLC was calibrated using the standard pigments (Table 1). The solvents of pigment

standards were displaced to N,N-dimethylformamide, but the concentrations were determined with spectrophotometer by using its extinction coefficient in ethanol or acetone.

(v) Internal standard

Ethyl-apo-8'-carotenoate was added into the samples prior to the injection as the internal standard. The mean chromatogram area and its coefficient of variation (CV) of internal standard were estimated as the following two samples:

Standard samples (Figure 1): 162.5 ± 1.7 (n = 32), CV=1.1%

Seawater samples: 169.5 ± 2.7 (n = 90), CV=1.7%

(vi) Pigment detection and identification

Chlorophylls and carotenoids were detected by photodiode array spectroscopy (350~800 nm). Pigment concentrations were calculated from the chromatogram area at different five channels (Table 1). First channel was allocated at 409 nm of wavelength for the absorption maximum of Pheophorbide a and Pheophytin a. Second channel was allocated at 431 nm for the absorption maximum of chlorophyll *a*. Third channel was allocated at 440 nm for the absorption maximum of [3,8-divinyl]-protochlorophyllide. Fourth channel was allocated at 450 nm for other pigments. Fifth channel was allocated at 462 nm for chlorophyll *b*.

(3) Preliminary results

Vertical profiles of major pigments (Chlorophyll *a*,Chlorophyll *b*, Fucoxanthin 19'-hexanoyloxyfucoxanthin, 19'-butanoyloxyfucoxanthin ,and zeaxanthin) at the station K2 and S1 were shown in Figure 2 and 3.

(4) Data archives

The processed data file of pigments will be submitted to the JAMSTEC Data Integration and Analyses Group (DIAG) within a restricted period. Please ask PI for the latest information.

(5) Reference

Zapata M, Rodriguez F, Garrido JL (2000), Separation of chlorophylls and carotenoids from marine phytoplankton: a new HPLC method using a reversed phase C_8 column and pyridine-containing mobile phases, *Mar. Ecol. Prog. Ser.*, 195, 29-45.

Table 1. Retention time and wavelength of identification for pigment standards.

No.	Pigment	Productions	Retention Time (minute)	Wavelength of identification (nm)
1	Chlorophyll *c3*	DHI Co.	8.119	462
2	Chlorophyllide *a*	DHI Co.	10.370	431
3	[3,8-Divinyl]-Protochlorophyllide	DHI Co.	10.871	440
4	Chlorophyll *c2*	DHI Co.	11.417	450
5	Peridinin	DHI Co.	14.382	450
6	Pheophorbide *a*	DHI Co.	16.716	409
7	19'-butanoyloxyfucoxanthin	DHI Co.	18.124	450
8	Fucoxanthin	DHI Co.	19.141	450
9	Neoxanthin	DHI Co.	19.570	440
10	Prasinoxanthin	DHI Co.	20.805	450
11	19'-hexanoyloxyfucoxanthin	DHI Co.	21.658	450
12	Violaxanthin	DHI Co.	21.613	440
13	Diadinoxanthin	DHI Co.	24.236	450
14	Antheraxanthin	DHI Co.	26.005	450
15	Alloxanthin	DHI Co.	26.953	450
16	Diatoxanthin	DHI Co.	27.951	450
17	Zeaxanthin	DHI Co.	28.715	450
18	Lutein	DHI Co.	28.916	450
19	Ethyl-apo-8’-carotenoate	Sigma-Aldrich Co.	30.890	462
20	Crocoxanthin	DHI Co.	32.933	450
21	Chlorophyll *b*	Sigma-Aldrich Co.	33.369	462
22	Divinyl Chlorophyll *a*	DHI Co.	34.655	440
23	Chlorophyll *a*	Sigma-Aldrich Co.	34.920	431
24	Pheophytin a	DHI Co.	37.204	409
25	Alpha-carotene	DHI Co.	37.850	450
26	Beta-carotene	WAKO Ltd.	37.676	450

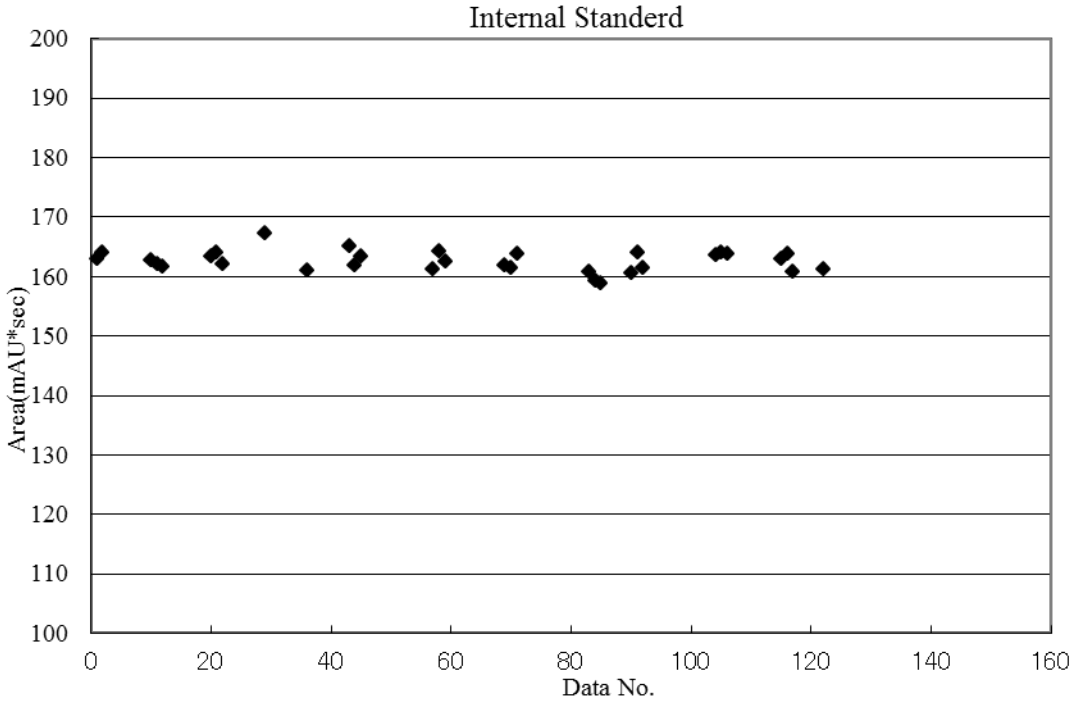

Figure 1. Variability of chromatogram areas for the internal standard.

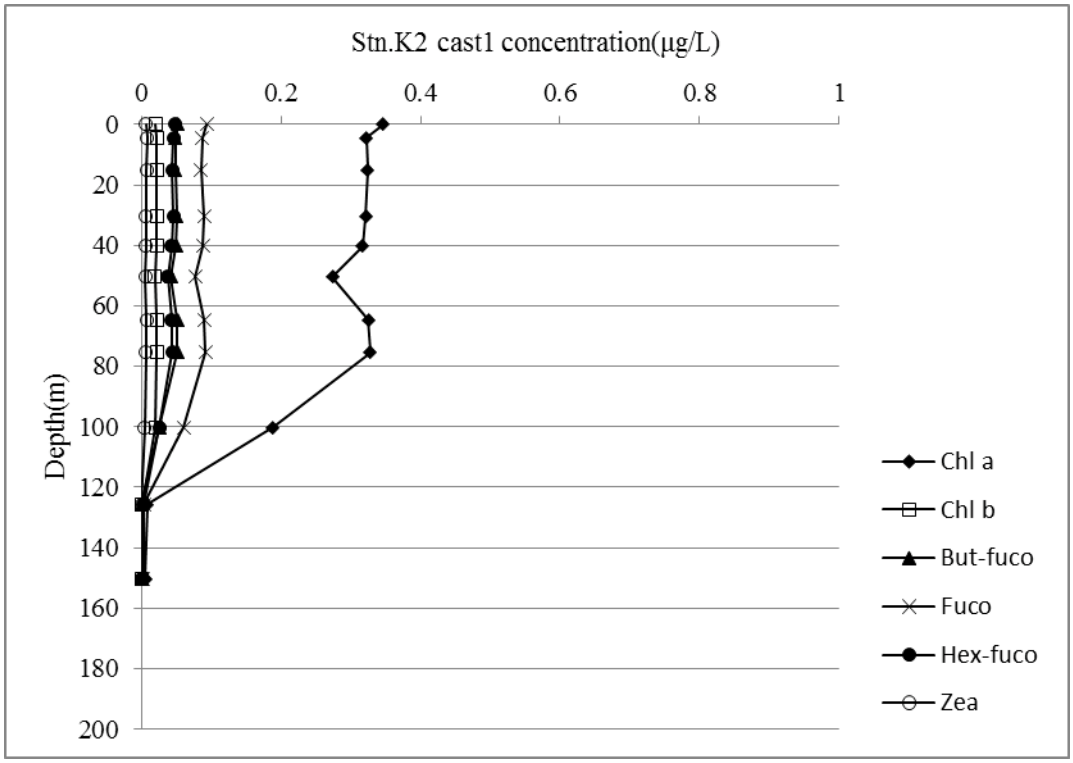

Figure 2. Vertical distributions of major phytoplankton pigments Chlorophyll *a*, Chlorophyll *b*, Fucoxanthin, 19’-hexanoyloxyfucoxanthin, 19'-butanoyloxyfucoxanthin and zeaxanthin) at Stn.K2.

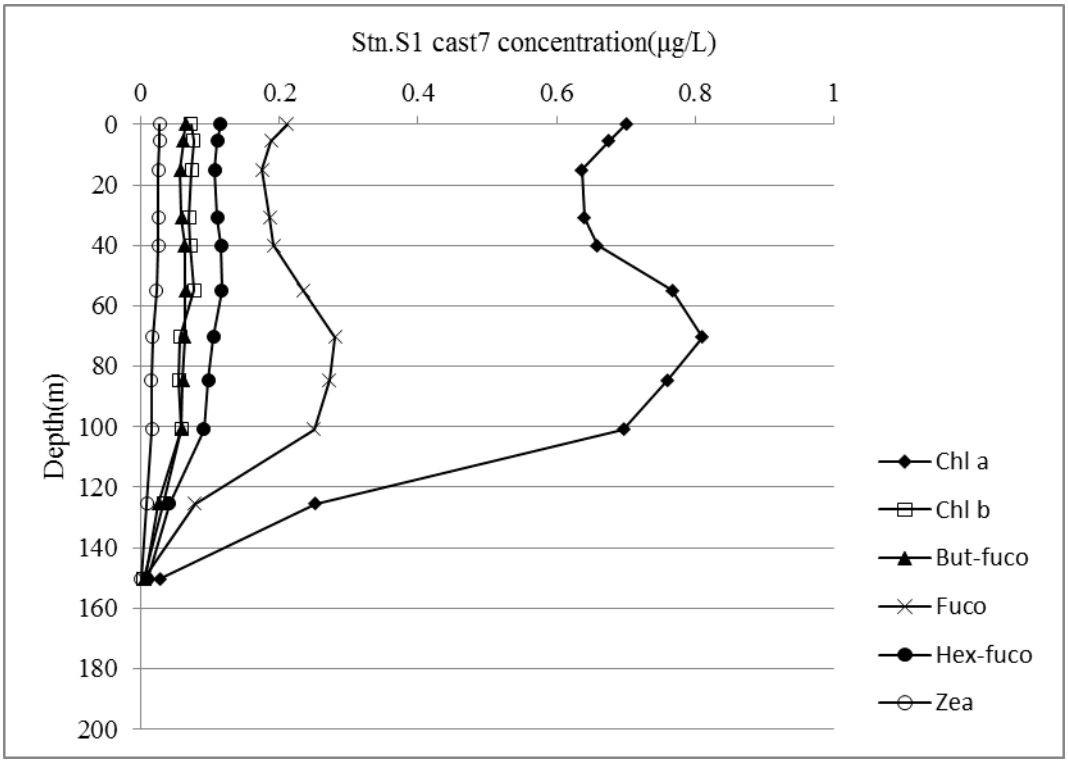

Figure 3. Vertical distributions of major phytoplankton pigments (Chlorophyll *a*, Chlorophyll *b*, Fucoxanthin, 19'-hexanoyloxyfucoxanthin, 19'-butanoyloxyfucoxanthin and zeaxanthin) at Stn.S1.

3.2.3. Phytoplankton abundance

Kazuhiko MATSUMOTO (JAMSTEC)

(1) Objectives

The main objective of this study is to estimate phytoplankton abundances and their taxonomy in the subarctic gyre and the subtropical gyre in the western North Pacific. Phytoplankton abundances were measured with two kinds of methods: microscopy for large size phytoplankton and flowcytometry for small size phytoplankton.

(2) Sampling

Samplings were conducted using Niskin bottles, except for the surface water, which was taken by a bucket. Samplings were carried out at the two observational stations of K2 and S1.

(3) Methods

1) Microscopy

Water samples were placed in 500 ml plastic bottle at station K2 and in 1000 ml plastic bottle at station S1. Samples were fixed with neutral-buffered formalin solution (1% final concentration). The microscopic measurements are scheduled after the cruise.

2) Flowcytometry

2)-1 Equipment

The flowcytometry system used in this research was BRYTE HS system (Bio-Rad Laboratories Inc). System specifications are follows:

Light source: 75W Xenon arc lamp
Excitation wavelength: 350-650 nm
Detector: high-performance PMT
Analyzed volume: 75 µl
Flow rate: 10 µl min^{-1}
Sheath fluid: Milli-Q water
Filter block: B2 as excitation filter block, OR1 as fluorescence separator block
B2 and OR1 have ability as follows:

B2:	Excitation filter	390-490 nm
	Beam-splitter	510 nm
	Emission filter	515-720 nm
OR1:	Emission filter 1	565-605 nm
	Beam-splitter	600 nm
	Emission filter 2	>615 nm

2)-2 Measurements

The water samples were fixed immediately with glutaraldehyde (1% final concentration) and stored in the dark at 4°C. The analysis by the flow cytometer was acquired on board within 24 hours after the sample fixation. Calibration was achieved with standard beads of 0.356 – 9.146 µm (Polysciences, Inc.). Standard beads of 2.764 µm were added into each sample prior to the injection of flow cytometer as internal standard. Phytoplankton cell populations were estimated from the forward light scatter signal. Acquired data were

stored in list mode file and analyzed with WinBryte software. Phytoplankton are classified with prokaryotic cyanobacteria (*Prochlorococcus* and *Synechococcus*) and other eukaryotes on the basis of scatter and fluorescence signals. *Synechococcus* is discriminated by phycoerythrin as the orange fluorescence, while other phytoplankton are recognized by chlorophylls as the red fluorescence without the orange fluorescence. *Prochlorococcus* and picoeukaryotes were distinguished with their cell size, but it was difficult to identify the abundance of *Prochlorococcus* accurately in the surface mixed layer due to its decreased chlorophyll fluorescence. The cell size was estimated using the empirically-determined relationship between cell diameter (d_{cell}) and bead diameter (d_{bead}) with the forward light scatter signal (FS) by Blanchot *et al*., (2001) as follows.

$$d_{cell} = d_{bead} (FS)^{1/5}$$

(4) Preliminary result

The vertical profile of phytoplankton group identified by flow cytometer at station K2 and station S1 are shown in Figure 1 and Figure 2, respectively.

K2:

Prochlorococcus was not observed in this station. The mean cell size of *Synechococcus* (SYN) was estimated to 0.9 – 1.0 μm. The mean cell size of eukaryotic phytoplankton of EUK-1 and EUK-2 were estimated to 1.5 – 1.8 μm and 2.3 – 2.6 μm, respectively. The population of EUK-3 was isolated in cell size of >4.0 μm.

S1:

The mean cell size of *Prochlorococcus* (PRO) and *Synechococcus* (SYN) were estimated to 0.6 – 0.7 μm and 0.9 – 1.0 μm, respectively. The mean cell size of eukaryotic phytoplankton of EUK-1 and EUK-2 were estimated to 1.2 – 1.3 μm and 1.7 – 1.9 μm, respectively. The population of EUK-3 was isolated in cell size of >3.0 μm.

(6) Data Archive

All data will be submitted to Data Integration and Analysis Group (DIAG), JAMSTEC. Please ask PI for the latest information.

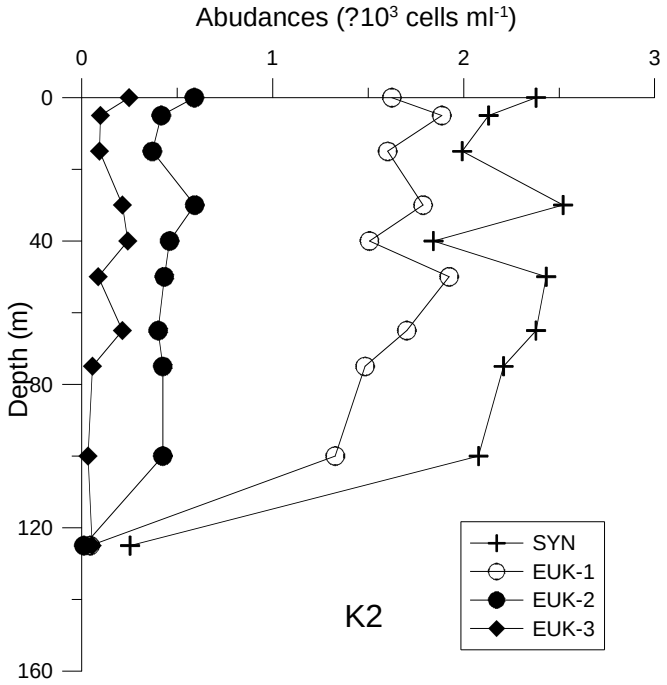

Figure 1. Vertical profile of phytoplankton abundances at K2

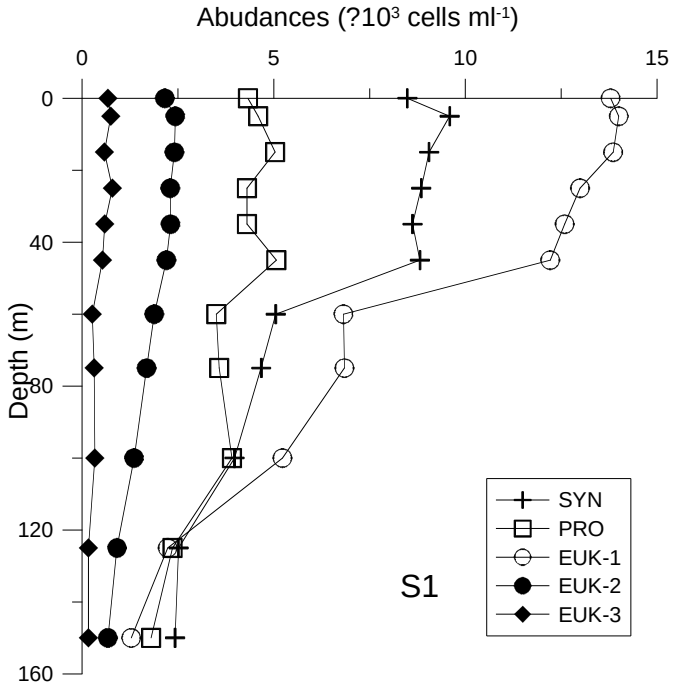

Figure 2. Vertical profile of phytoplankton abundances at S1

3.2.4 Primary production and new production

Kazuhiko MATSUMOTO (JAMSTEC IRGC)
Miyo IKEDA (MWJ)
Kanako YOSHIDA (MWJ)
Sayaka KAWAMURA (MWJ)

(1) Objective

Quantitative assessment of temporal and spatial variation in carbon and nitrate uptake in the surface euphotic layer should be an essential part of biogeochemical studies in the western North Pacific. Primary production (PP) was measured as incorporation of inorganic C^{13}, and new production (NP), measurement of nitrate uptake rate was conducted with ^{15}N stable isotope tracer at K2 and S1 stations.

(2) Methods

1) Sampling, incubation bottle and filter

Seawater samples were collected using Teflon-coated and acid-cleaned Niskin bottles, except for the surface water, which was taken by a bucket. Sampling depths were determined by the light intensity at eight depths from among the surface, 0.5%, 1%, 2.5%, 5%, 10%, 25%, 50% light depths relative to the surface obtained by SPMR sensor. Seawater samples were placed into acid-cleaned clear polycarbonate bottles in duplicate for PP and NP, and in a single for the dark and the time-zero samples. The time-zero sample was filtered immediately after the addition of ^{13}C and ^{15}N solution. Filtration of seawater sample was conducted with pre-combusted glass fiber filters (Whatman GF/F 25 mm) with temperature of 450 degree C for at least 4 hours.

2) Incubation

Each bottle was spiked with sufficient $NaH^{13}CO_3$ just before incubation so that ^{13}C enrichment was about 10% of ambient dissolved inorganic carbon as final concentration of 0.2 mmol dm^{-3} (Table 3.2.4-1). The ^{15}N-enriched NO_3, $K^{15}NO_3$ solution, was injected to the incubation bottles (except PP bottles), resulting that the final concentration of ^{15}N enrichment was about 10% of ambient nitrate (Table 3.2.4-2). Incubation was begun at predawn and continued for 24 h, generally by the simulated *in situ* method. The simulated *in situ* method was conducted in the on-deck bath cooled by running surface seawater for the samples within the mixed layer or by immersion cooler for the samples below the mixed layer. The light environment of each bottle in the simulated *in situ* method was adjusted using blue film corresponding to the light levels at the sampling depths. The incubation by the *in situ* method was conducted for PP at the station of S1. In the *in situ* method, bottles were placed appropriate depths on a line attached to a drifting mooring system (see the chapter 3.4.1).

3) Measurement

After 24 hours incubation, samples were filtered though GF/F filter, and the filters were kept in a freezer (-20 degree C) on board until analysis. Before analysis, the filters were dried in the oven (45 degree C) for at least 20 hours, and inorganic carbon was removed by acid treatment in a HCl vapor bath for 30 minutes. During the cruise, all samples were measured by a mass spectrometer ANCA-SL system at MIRAI.

Instruments: preprocessing equipment ROBOPLEP-SL (Europa Scientific Ltd.; now SerCon Ltd.) stable isotope ratio mass spectrometer EUROPA20-20 (Europa Scientific Ltd.; now SerCon Ltd.)
Methods: Dumas method, Mass spectrometry
Precision: All specifications are for n=5 samples.
It is a natural amount and five time standard deviation of the analysis as for amount 100 μg of the sample. We measured repeatability 8 times in this cruise. ^{13}C (0.1 – 0.2 ‰), ^{15}N (0.1 – 0.5 ‰)
Reference Material: The third-order reference materials L-aspartic acid (SHOKO Co., Ltd.)

4) Calculation

(a) Primary Production

Based on the balance of ^{13}C, assimilated organic carbon (DPOC) is expressed as follows (Hama *et al*., 1983):

$$^{13}C_{(POC)} * POC = {}^{13}C_{(sw)} * DPOC + (POC - DPOC) * {}^{13}C_{(0)}$$

This equation is converted to the following equation;

$$DPOC = POC * ({}^{13}C_{(POC)} - {}^{13}C_{(0)}) / ({}^{13}C_{(sw)} - {}^{13}C_{(0)})$$

where $^{13}C_{(POC)}$ is concentration of ^{13}C of particulate organic carbon after incubation, *i.e.*, measured value(%). $^{13}C_{(0)}$ is that of particulate organic carbon before incubation, *i.e.*, that for samples as a blank.
$^{13}C_{(sw)}$ is concentration of 13C of ambient seawater with a tracer. This value for this study was determined based on the following calculation;

$$^{13}C_{(sw)} (\%) = [(TDIC * 0.011) + 0.0002] / (TDIC + 0.0002) * 100$$

where TDIC is concentration of total dissolved inorganic carbon at respective bottle depth(mol dm^{-3}) and 0.011 is concentration of ^{13}C of natural seawater (1.1%). 0.0002 is added ^{13}C (mol) as a tracer. Taking into account for the discrimination factor between ^{13}C and ^{12}C (1.025), primary production (PP) was, finally, estimated by

$$PP = 1.025 * DPOC$$

(b) New production

NO_3 uptake rate or new production (NP) was estimated with following equation:

$$NP (mg\ dm^{-3}\ day^{-1}) = ({}^{15}N_{excess} * PON) / ({}^{15}N_{enrich}) / day$$

where $^{15}N_{excess}$, PON and $^{15}N_{enrich}$ are excess ^{15}N (measured ^{15}N minus ^{15}N natural abundance, 0.366 atom%) in the post-incubation particulate sample (%), particulate nitrogen content of the sample after incubation (mg dm^{-3}) and ^{15}N enrichment in the dissolved fraction (%), respectively.

(3) Preliminary results

Fig. 3.2.4.1 and 3.2.4.2 show the vertical profile of primary production (PP) and the

diurnal change of photosynthetically available radiation (PAR) observed by PUV-510B (Biospherical Instruments Inc.).

(4) Data archives

All data will be submitted to JAMSTEC Data Integration and Analyses Group (DIAG).

Table 3.2.4-1 Sampling cast table and spike ^{13}C concentration

Incubation type	Station	CTD cast No.	$NaH^{13}CO_3$ (μmol dm^{-3})
SIS	S1	3	200
IS	S1	3	200
SIS	S1	7	200
SIS	K2	1	200
SIS	K2	5	200

Table 3.2.4-2 Sampling cast table and spike ^{15}N concentration

Incubation type	Station	CTD cast No.	Light Intensity	$K^{15}NO_3$ (μmol dm^{-3})
SIS	S1	3	100 % -5 % 2.5 % - 0.5 %	0.04 0.07
SIS	S1	7	100 % -5 % 2.5 % - 0.5 %	0.04 0.07
SIS	K2	1	100 % - 0.5 %	2
SIS	K2	5	100 % - 0.5 %	2

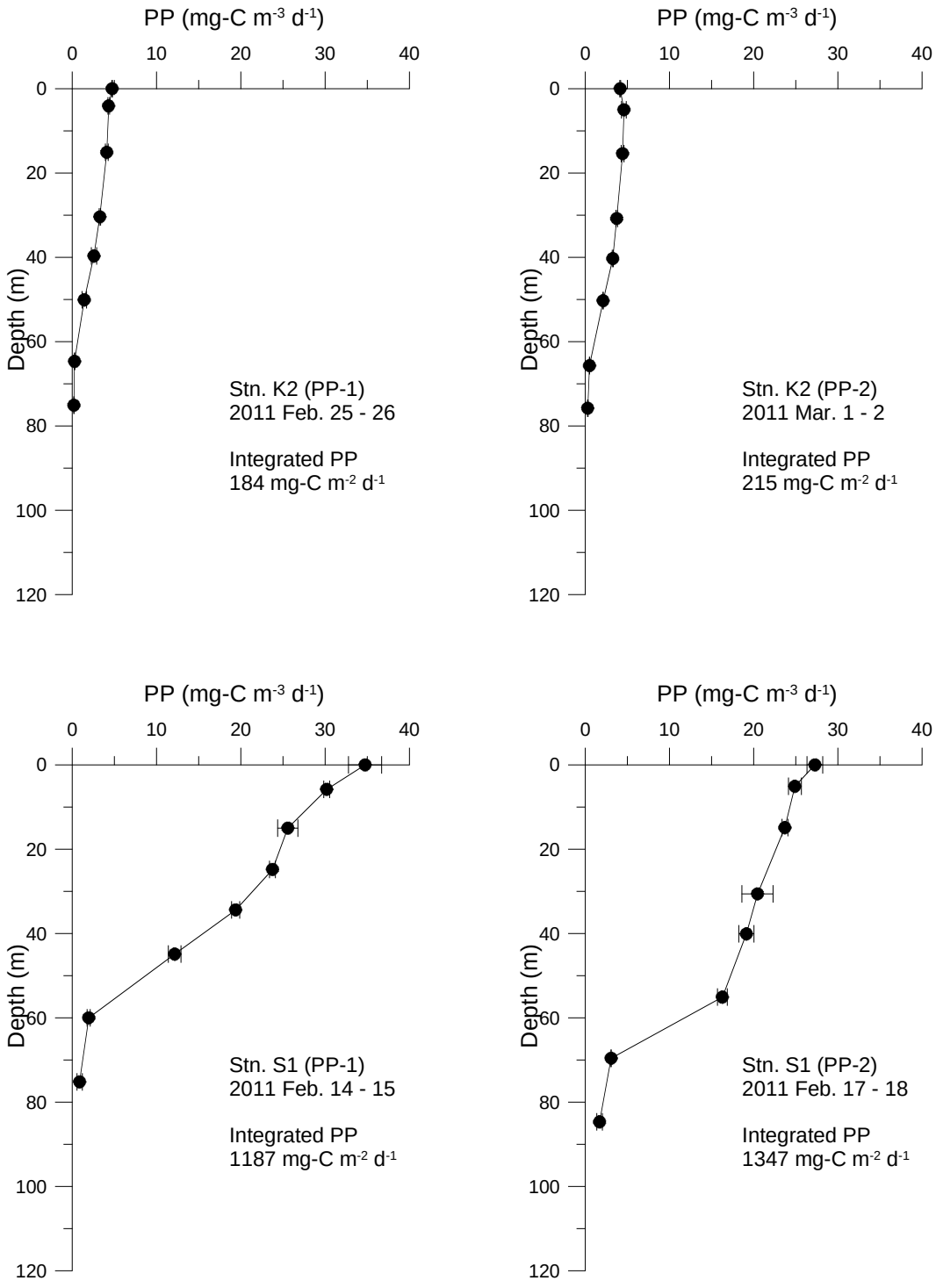

Figure 3.2.4.1 Vertical profile of primary production

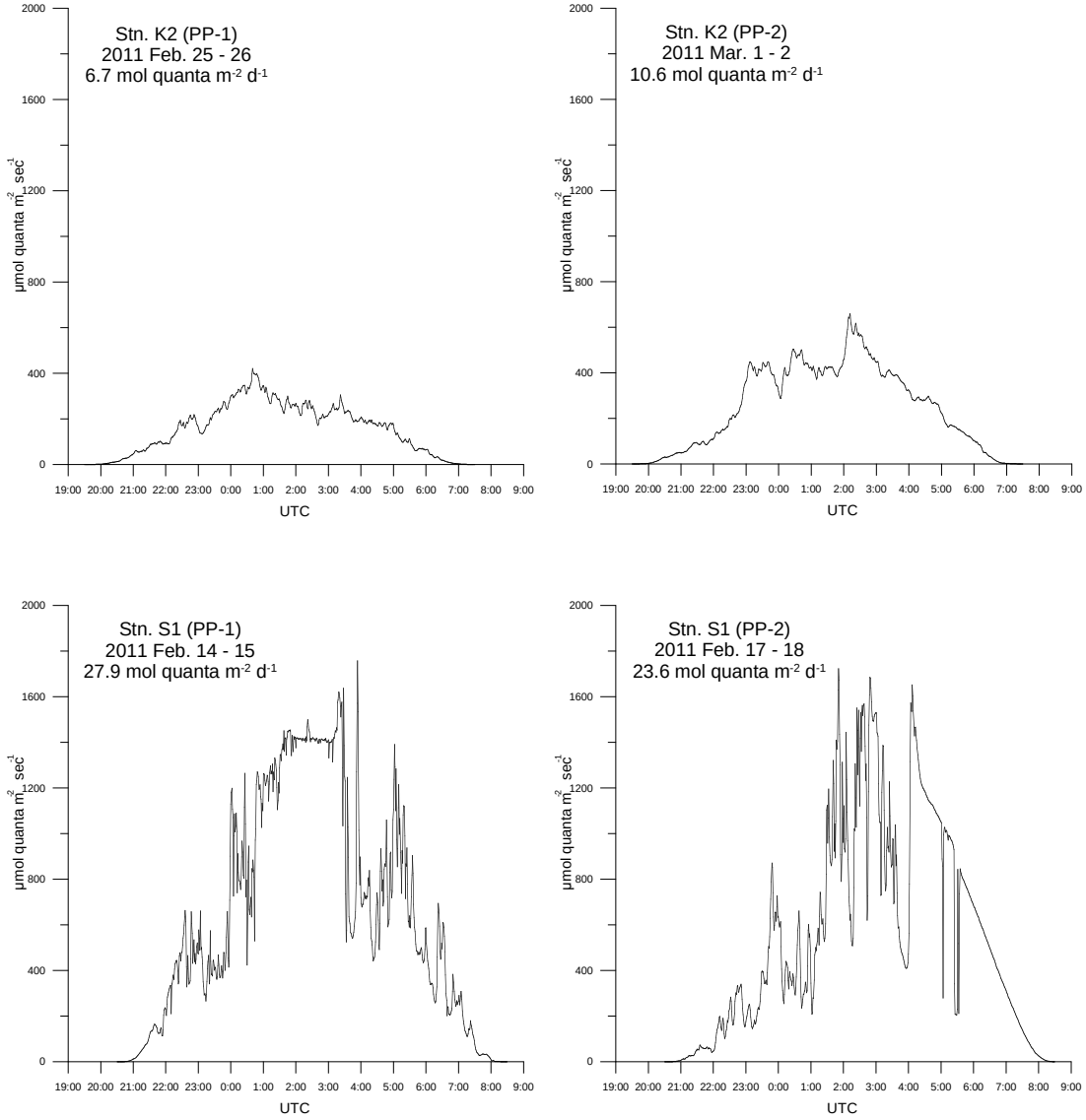

Figure 3.2.4.2 Photosynthetically available radiation (PAR) during incubation experiment

.3.2.5 P vs. E curve

Kazuhiko MATSUMOTO (JAMSTEC RIGC)
Miyo IKEDA (MWJ)
Kanako YOSHIDA (MWJ)
Sayaka KAWAMURA (MWJ)

(1) Objectives

The objective of this study is to estimate the relationship between phytoplankton photosynthetic rate (P) and scalar irradiance (E) in the western North Pacific.

(2)Methods

1) Sampling

Samplings were carried out at two observational stations of K2 and S1. Sample water was collected at the surface at the station of K2, and at three depths of different irradiance level at the station of S1, using Teflon-coated and acid-cleaned Niskin bottles.

2) Incubation

Three incubators filled in water were used, illuminated at one end by a 500W halogen lamp. Water temperature was controlled by circulating water cooler (Fig. 3.2.5-1). Water samples were poured into acid-cleaned clear nine flasks (approx. 1 liter) and arranged in the incubator linearly against the lamp after adding the isotope solutions. The isotope solutions of 0.2 mmol dm^{-3} (final concentration) of $NaH^{13}CO_3$ solution were spiked. All flasks were controlled light intensity by shielding with a neutral density filter on lamp side. The light intensities inside the flasks were shown in Table 3.2.5. The incubations were begun at about local noon and continued for 3 h. Filtration of seawater sample was conducted with glass fiber filters (Whatman GF/F 25 mm) which precombusted with temperature of 450 degree C for at least 4 hours.

3) Measurement

After the incubation, samples were treated as same as the primary production experiment. During the cruise, all samples were measured by a mass spectrometer ANCA-SL system at MIRAI. The analytical function and parameter values used to describe the relationship between the photosynthetic rate (P) and scalar irradiance (E) are best determined using a least-squares procedure from the following equation.

$P = P_{max}(1-e^{-\alpha E/Pmax})e^{-b\alpha E/Pmax}$: (Platt et al., 1980)

where, P_{max} is the light-saturated photosynthetic rate, α is the initial slope of the P vs. E curve, b is a dimensionless photoinhibition parameter.

(3) Preliminary results

The *P – E* curves obtained at the stations of K2 and S1 are shown in Fig. 3.2.5-2 and 3.2.5-3.

(4) Data archives

All data will be submitted to JAMSTEC Data Integration and Analyses Group

(DIAG) .

(5) Reference

Platt, T., Gallegos, C.L. and Harrison, W.G., 1980. Photoinhibition of photosynthesis in natural assemblages of marine phytoplankton. *Journal of Marine Research*, 38, 687-701.

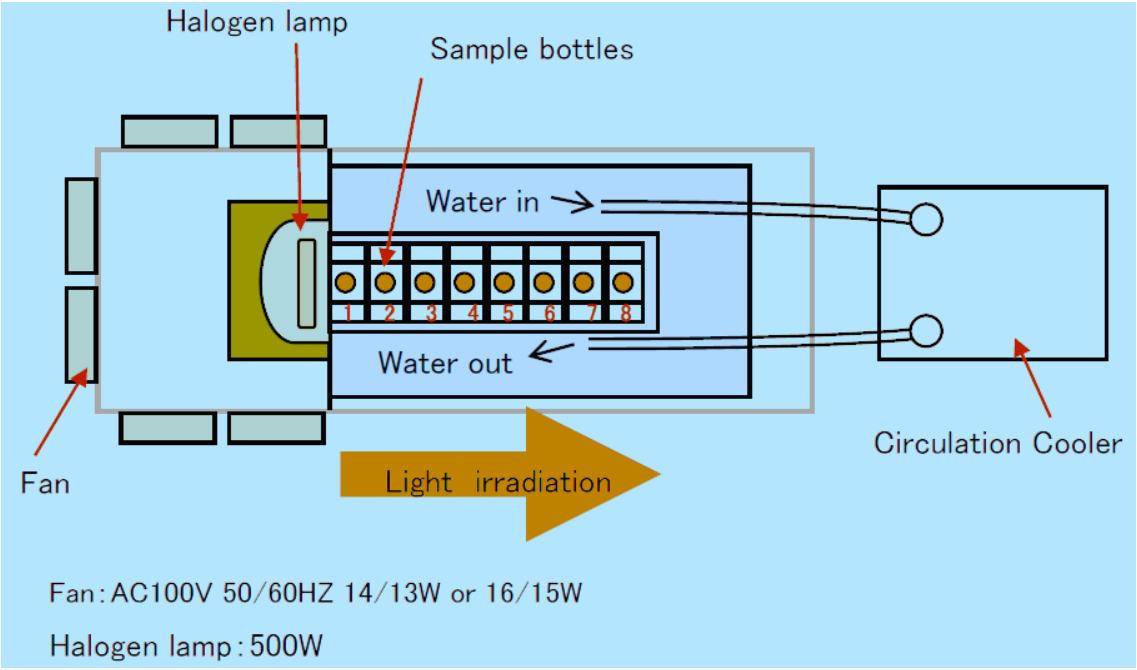

Fig. 3.2.5-1 Look down view of Incubator for Photosynthesis and irradiation curve

Table 3.2.5 Light Intensity of P vs. E measurements

	Bath A	Bath B	Bath C
Bottle No.	Light intensity (µE m^{-2} sec^{-1})		
1	2100	2000	2100
2	1060	1000	1050
3	475	470	480
4	200	230	235
5	95	105	100
6	44	50	46
7	19	23.5	20
8	8.1	11	7.8
9	0	0	0

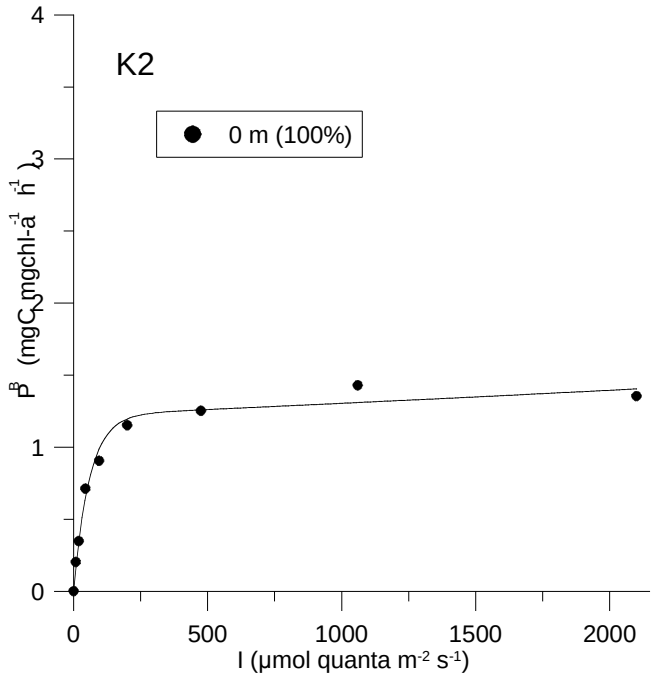

Fig. 3.2.5-2

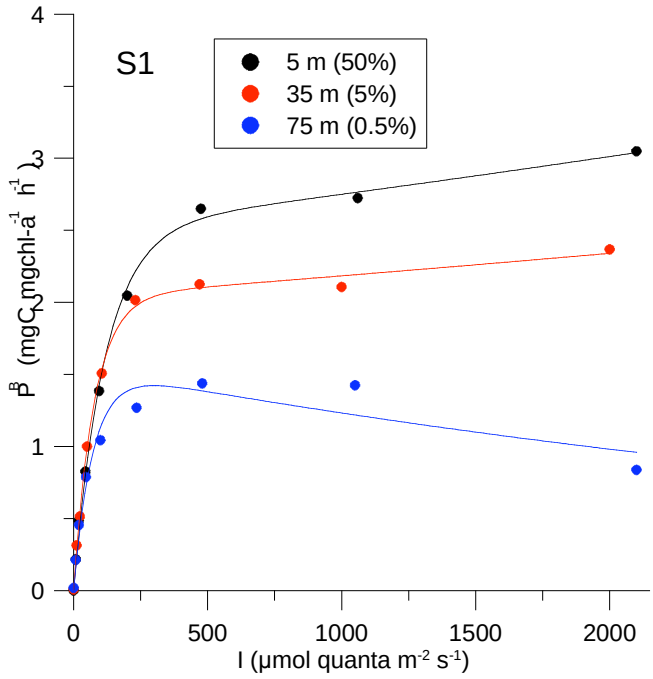

Fig. 3.2.5-3

3.2.6. Oxygen evolution (gross primary productivity)

Tetsuichi FUJIKI (JAMSTEC)
Osamu ABE (Nagoya University)
Misato KUWAHARA (MWJ)
Hideki YAMAMOTO (MWJ)

(1) Objective

Primary productivity in the world's oceans has been measured mostly by the carbon tracer or oxygen evolution methods. In incubations of 24 hours, the former method provides the values closest to net primary productivity (NPP), while the latter comes closest to gross primary productivity (GPP). The GPP is defined as total amount of oxygen released by phytoplankton photosynthesis. The NPP/GPP ratio provides fundamental information on the metabolic balance and carbon cycle in the ocean. In the MR11-02, the GPP were measured using the light–dark bottle and ^{18}O spike methods at the stations S1 and K2.

(2) Methods

Seawater samples were collected from eight depths corresponding to light levels of approximately 100, 50, 25, 10, 5, 2.5, 1 and 0.5% of surface light intensity, using a bucket (surface only). Seawater samples were carefully transferred from Niskin bottle into volume calibrated flasks (ca. 100 cm^3).

Light-dark bottle method

At each light depth, three light and three dark bottles were incubated under light condition that simulated those of the original sampling depth. The dark bottles were wrapped with aluminum foil. After 24 h incubation, the light and dark bottles were fixed immediately. Fixing, storage, reagent preparation, measurement and standardization were followed the dissolve oxygen section. The GPP was estimated by adding the dark respiration in dark bottles to the net oxygen evolution in light bottles.

^{18}O spike method

The samples were spiked with enriched ^{18}O-labeled water (Cambridge Isotope Laboratories) and incubated for 24 h under light condition that simulated those of the original sampling depth as the light-dark bottle method. After incubation, ~100 mL of subsample were drawn into preevacuated gas extraction vessels and capped.

After measurements of the isotopic composition of O_2 in the laboratory on land, the GPP is calculated from the isotopic composition of dissolved oxygen in initial and incubated samples using the following equation (Bender et al. 2000).

$$GPP = \{[\delta^{18}O(O_2)_f - \delta^{18}O(O_2)_i]/[\delta^{18}O_{water} - \delta^{18}O(O_2)_i]\} \times (O_2)_i$$

where the subscripts i and f are the isotopic composition of O_2 in initial and final samples, $(O_2)_i$ is the oxygen concentration of the initial water sample, and $\delta^{18}O_{water}$ is the isotopic composition of the enriched water.

(3) Preliminary results

At stations S1 and K2, the vertical profiles of GPP measured with the light-dark bottle method were shown in figure 3.3.6.1.

(4) Data archives

The data will be submitted to Data Integration and Analyses Group (DIAG), JAMSTEC.

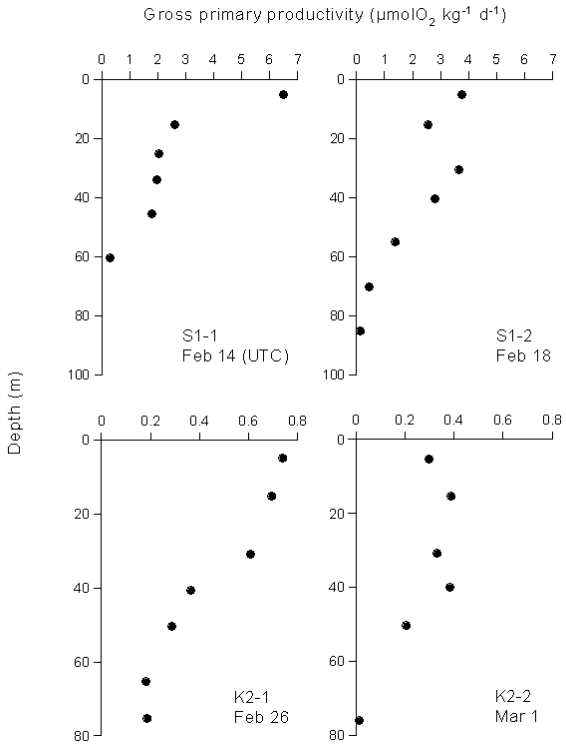

Figure 3.3.6.1. Vertical profiles of gross primary productivity (GPP) measured with the light-dark bottle method at stations S1 and K2.

3.3 Optical measurement

Makio HONDA (JAMSTEC RIGC)
Kazuhiko MATSUMOTO (JAMSTEC RIGC)

(1) Objective

The objective of this measurement is to investigate the air and underwater light conditions at respective stations and to determine depths for *in situ* or simulated *in situ* measurement of primary production by using carbon stable isotope (C-13) during late autumn. In addition, optical data can be used for the validation of satellite data.

(2) Description of instruments deployed

The instrument consisted of the SeaWiFS Profiling Multichannel Radiometer (SPMR) and SeaWiFS Multichannel Surface Reference (SMSR). The SPMR was deployed in a free fall mode through the water column (see right picture). The SPMR profiler called "Free Fall" has a 13 channel irradiance sensors (Ed), a 13 channel radiance sensors (Lu), tilt sensor, and fluorometer. The SMSR has a 13 channel irradiance sensors (Es) and tilt meter (Table 1). These instruments observed the vertical profiles of visible and ultra violet light and chlorophyll concentration.

Table 1. Center wavelength (nm) of the SPMR/SMSR

Es	379.5	399.6	412.2	442.8	456.1	490.9	519.0	554.3	564.5	619.5	665.6	683.0	705.9
Ed	380.0	399.7	412.4	442.9	455.2	489.4	519.8	554.9	565.1	619.3	665.5	682.8	705.2
Lu	380.3	399.8	412.4	442.8	455.8	489.6	519.3	554.5	564.6	619.2	665.6	682.6	704.5

Optical measurements by Free Fall were conducted at our time-series station K2 and S1. Measurements should be ideally conducted at median time. However observations were conducted irregularly because of limited ship-time and other observation's convenience (Table 2). The profiler was dropped twice a each deployment to a depth of 200 m. The SMSR was mounted on the anti-rolling system's deck and was never shadowed by any ship structure. The profiler descended at an average rate of 1.0 m/s with tilts of less than 3 degrees except near surface.

Observed data was analyzed by using software "Satlantic PPROSOFT 6" and extinction rate and photosynthetically available radiation (PAR) were computed.

Table 2 Locations of optical observation and principle characteristics
(Date and Time in LST: UTC+10hr at station K2 and S1)

Date and Time	Station	Lat./Long.	Surface PAR (quanta cm^{-2} sec^{-1})	Euphotic layer* (m)	Memo
2011.2.14 11:25	S1	30N/145E	8.7×10^{16}	74m	1 day before S1-PP incubation #1
2011.2.15 11:22	S1	30N/145E	7.8×10^{16}	74m	during S1-PP incubation #1
2011.2.17 12:30	S1	30N/145E	5.3×10^{16}	84m	1 day before S1-PP incubation #2
2011.2.25 11:34	K2BF	44-23N / 156-15E	3.8×10^{16}	75m	1 day before K2-PP incubation #1

* Euphotic layer: 0.5% of surface PAR

(3) Preliminary result

We deployed “Free Fall sensor” three times at station S1. Surface PAR ranged from approximately 5.3×10^{16} to 8.7×10^{16} quanta cm^{-2} sec^{-1}. The euphotic layers, that is defined as water depth with 0.5 % of surface PAR, were 75 – 85 m. This was shallower than that in autumn 2010 (~ 100 m). This might be attributed to that abundance of phytoplankton was larger during this cruise than that in autumn 2010. Because of schedule and malfunction of “Free Fall sensor”, we deployed “Free Fall sensor” once near K2 (not at K2). Surface PAR was approximately 3.8×10^{16} and the euphotic layers was 75 m.

(4) Data archive

Optical data were filed on two types of file.

(BIN file) digital data of upwelling radiance and downwelling irradiance each 1 m from near surface to approximately 100 m for respective wave-lengths with surface PAR data during “Free Fall” deployment

(PAR file) in situ PAR each 1 m from near surface to approximately 100 m with extinction coefficient with surface PAR data during “Free Fall” deployment

These data files will be submitted to JAMSTEC Data Integration and Analyses Group (DIAG).

3.4 Drifting sediment trap

3.4.1 Drifting mooring system

Hajime KAWAKAMI (JAMSTEC MIO)
Makio C. HONDA (JAMSTEC RIGC)
Yoshihisa MINO (Nagoya University)
Chiho SUKIGARA (Nagoya University)
Ryo KANEKO (University of Tokyo)
Jaeho SONG (University of Tokyo)
Keigo WATANABE (University of Tokyo)
Miyo IKEDA (MWJ)
Kanako YOSHIDA (MWJ)
Sayaka KAWAMURA (MWJ)
Toru IDAI (MWJ)
Fujio KOBAYASHI (MWJ)

In order to conduct drifting sediment trap experiment at stations S1 and K2, drifting mooring system (drifter) was deployed. This drifter consists of radar reflector, GPS radio buoy (Taiyo TGB-100), flush light, surface buoy, ropes and sinker. On this system, "Knauer" type sediment trap at 12 layers were installed together (Traps of JAMSTEC: 60, 100, 150, and 200 m; traps of Nagoya University: 85, 90, 95, 170, 180, and 190 m; traps of University of Tokyo: 105 and 210 m). Thanks to the effort by MWJ technicians, drifting mooring system was upgraded on board. The configuration is shown in Fig. 3.4.1-1.

The drifter was deployed at 21:40 on 15 February (UTC) at station S1 and at 20:30 on 25 February (UTC) at station K2. The drifter was recovered after 3 and 4 days at stations S1 and K2, respectively. The drifter's position was monitored by using GPS radio buoy (Taiyo TGB-100). Fig. 3.4.1-2 shows tracks of the drifter. In general, the drifter tended to drift southwestward and southeastward at stations S1 and K2, respectively.

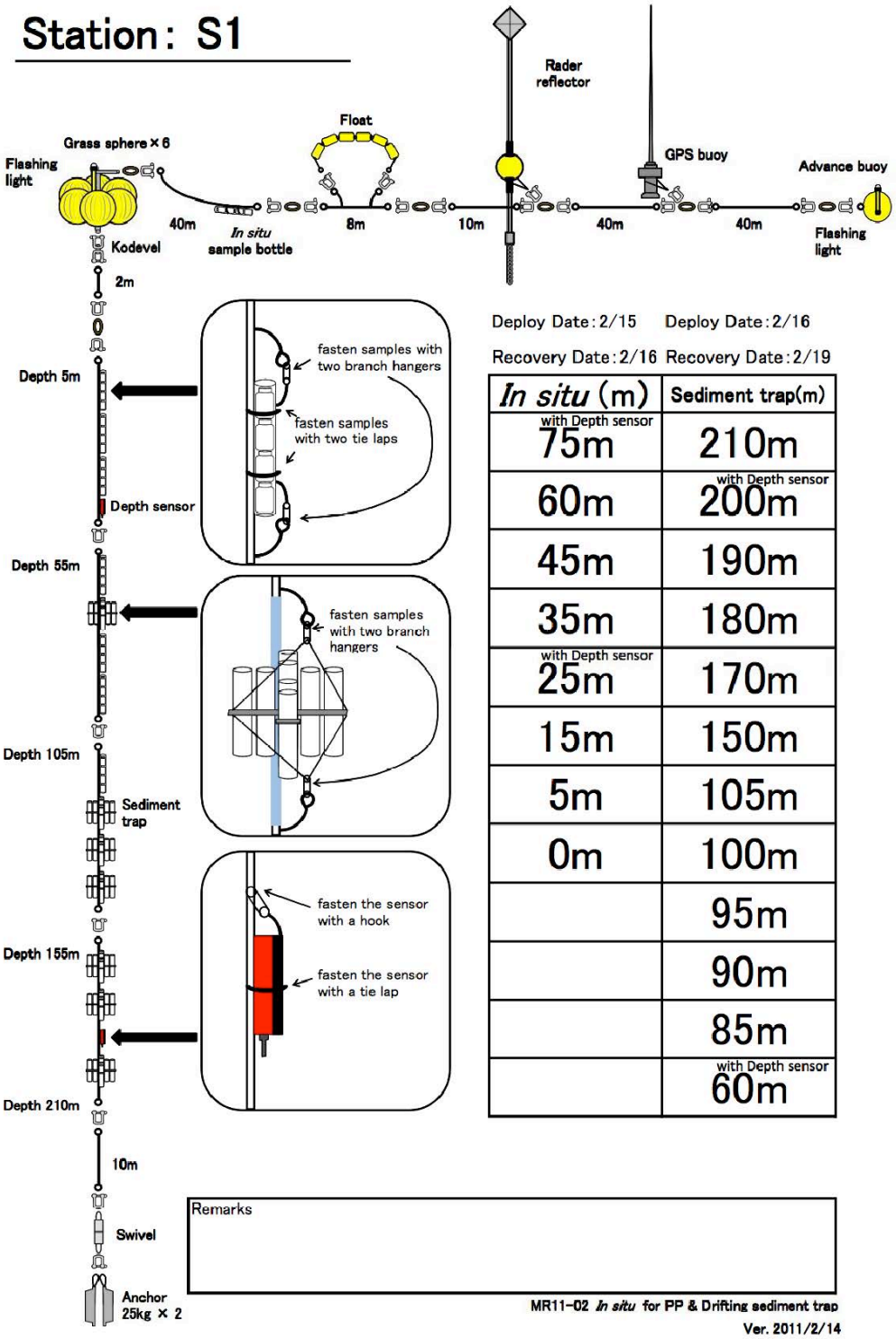

Fig. 3.4.1-1 Drifting mooring system at stations S1 and K2.

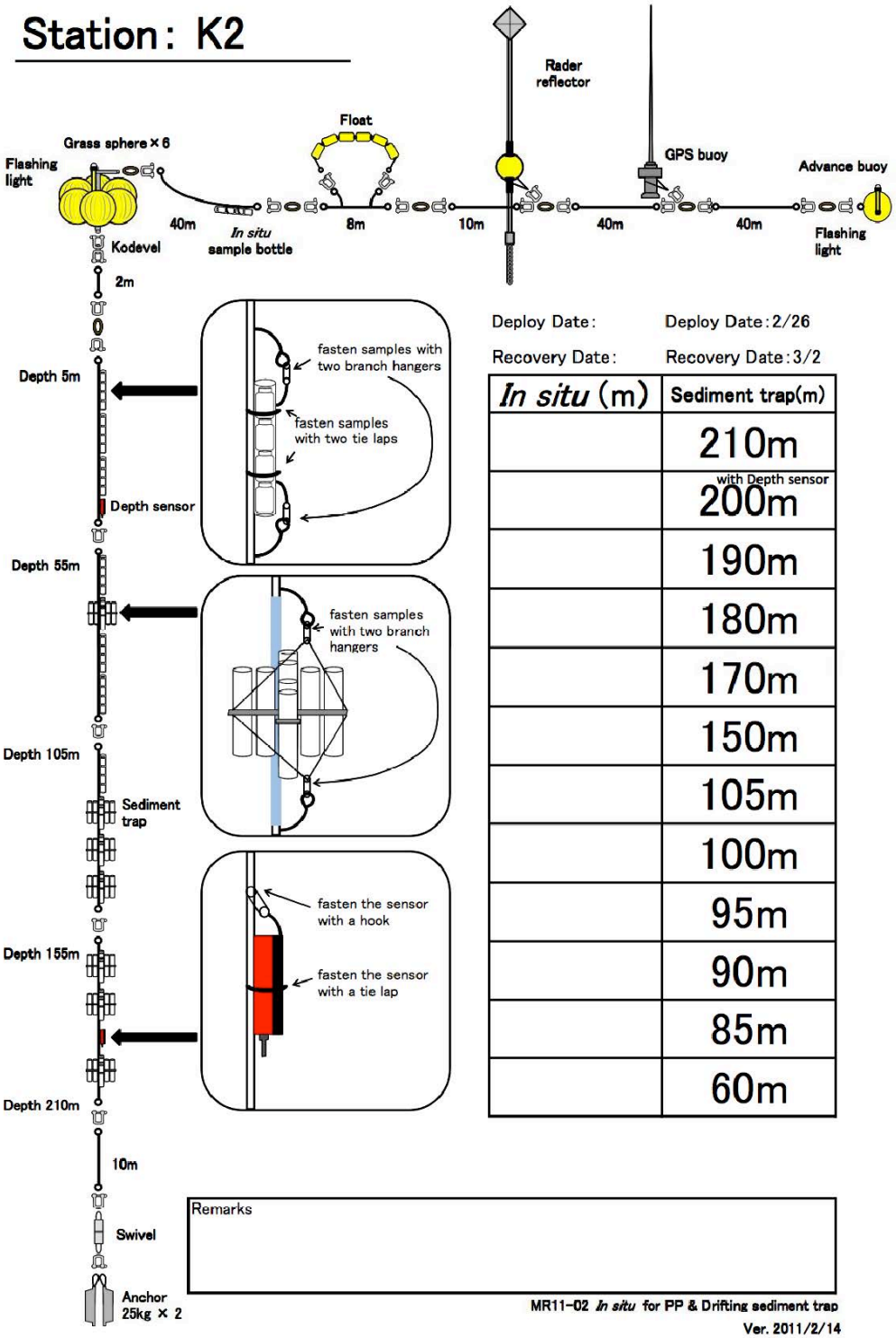

Fig. 3.4.1-1 Continued.

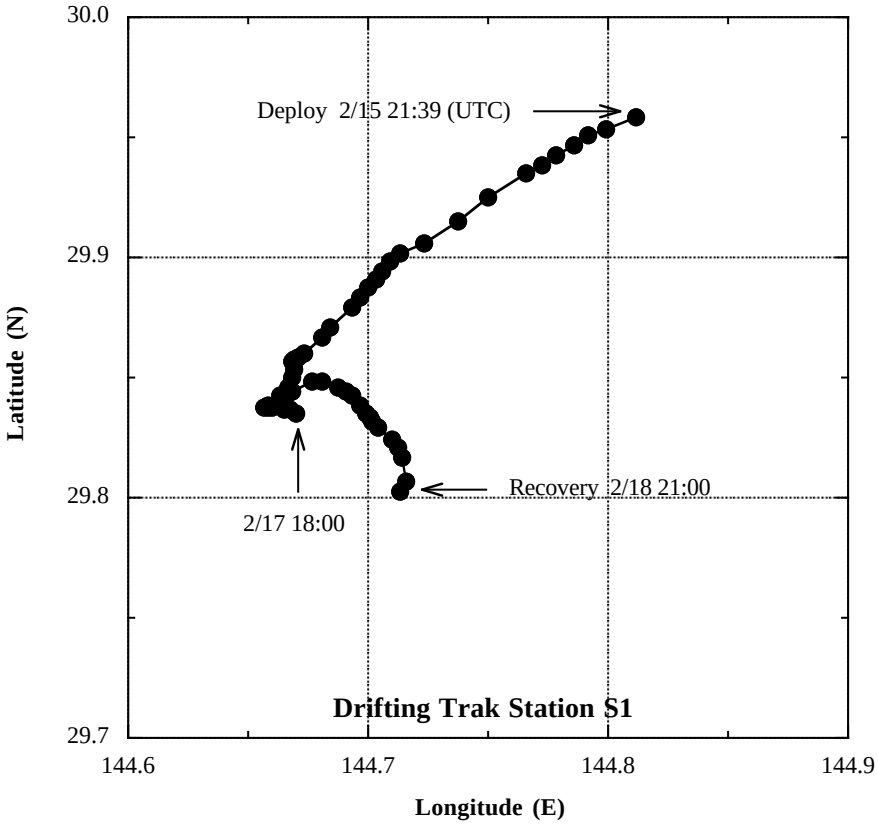

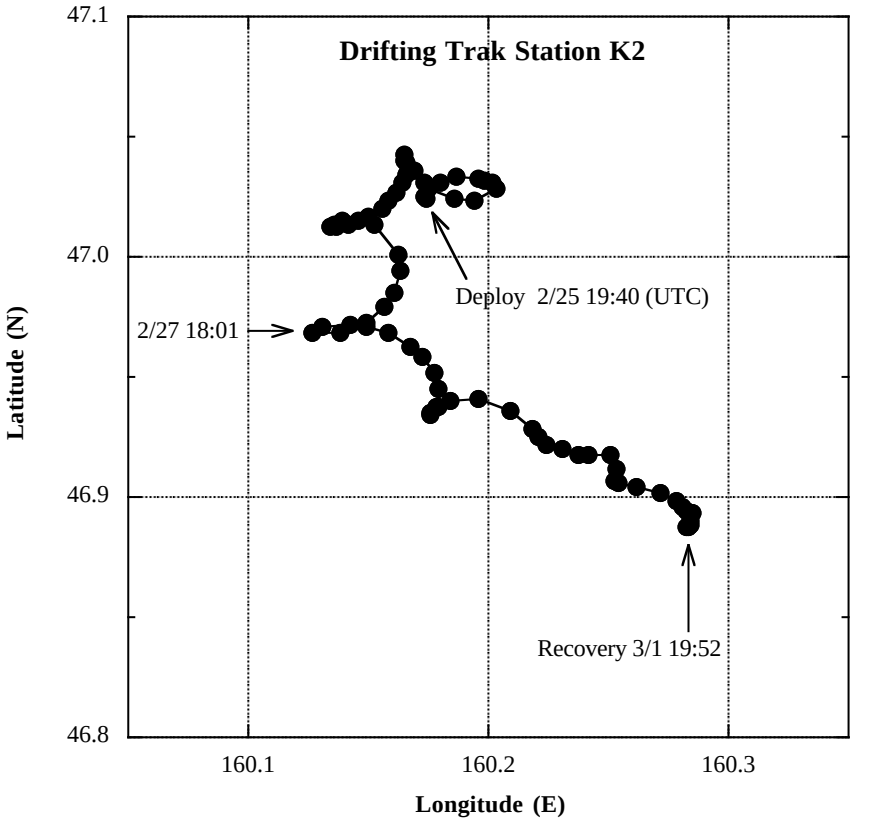

Fig. 3.4.1-2 Track of drifter (GPS buoy) at stations S1 and K2.

3.4.2 Drifting sediment trap of JAMSTEC

Hajime KAWAKAMI (JAMSTEC MIO)
Makio C. HONDA (JAMSTEC RIGC)

In order to collect sinking particles and measure carbon flux, and zooplankton, “Knauer type” cylindrical sediment trap (Photo 3.4.2-1) was deployed at stations S1 and K2 where measurement of primary productivity was conducted. This trap consists of 8 individual transparent policarbonate cylinders with baffle (collection area: ca. 0.0038 m^2, aspect ratio: 620 mm length / 75 mm width = 8.27), which was modified from Knauer (1979). Before deployment, each trap was filled with filtrated surface seawater, which salinity is adjusted to ~ 39 PSU by addition of NaCl (addition of 100 mg NaCl to 20 L seawater) were placed in tubes. These were located at approximately 60, 100, 150, and 200 m. After recovery, sediment traps were left for half hour to make collected particles settle down to the bottle. After seawater in acrylic tube was dumped using siphonic tube, collecting cups were took off. Two cups of samples at each layer were given to the team of Kagoshima University to determine fecal pellets. Four cups of samples at each layer were filtered thorough Nuclepore filter with a nominal pore size of 0.4μm and GF/F filter by two cups, for respective purposes (total mass flux, trace elements, total particulate carbon, and particulate organic carbon). The other samples were added buffered formalin for archive. The filter and archive samples were kept in freezer and refrigerator by the day when these were analyzed, respectively.

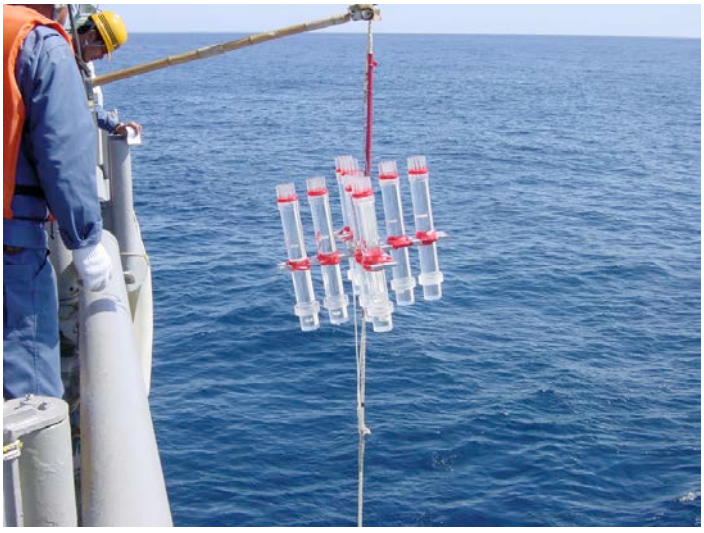

Photo 3.4.2-1 Drifting Sediment Trap.

3.4.3 Vertical changes of fecal pellets

Toru KOBARI (Kagoshima University)
Hiroshi ISAMI (Kagoshima University)

(1) Objective

Sinking particles includes phytoplankton aggregates, zooplankton fecal pellets, feeding mucus, carcass and crustacean molts (e.g. Flower and Knauer, 1986). Especially, fecal pellets significantly contribute to downward flux of particulate organic carbon (POC) and are a key component of the biological pump mediated by zooplankton community (Bishop et al., 1977; Lampitt et al., 1990; Silver and Gowing, 1991; Carroll et al., 1998; Turner, 2002). Fecal pellets are changed by zooplankton ingestion (coprophagy), fragmentation via sloppy feeding or swimming activity (coprorhexy) and loosening of membrane (coprochaly) during sinking (Paffenhöfer and Strickland, 1970; Lampitt et al., 1990; Noji et al., 1991). These processes largely affect transfer efficiency of POC flux (Wilson et al., 2008). It has been believed that fecal pellets are declined by bacterial decomposition (Honjo and Roman, 1978; Arístegui et al., 2002) and/or coprophagy/coprorhexy of small copepods such as cyclopoids and poecilostomatoids for last two decades (González and Smetacek, 1994; Suzuki et al., 2003; Svensen and Nejstgraard, 2003; Huskin et al., 2004; Poulsen and Kiørboe, 2006). In recent years, however, these copepods showed minor contributions to coprophagy/coprorhexy from the field observations (Iversen and Poulsen, 2007) and laboratory experiments (Reigstad et al., 2005). Alternatively, heterotrophic microbes consumed fecal pellets (Poulsen and Iversen, 2008). Thus, we should re-consider how fecal pellets are declined or changed during sinking from surface to mesopelagic depths.

In the present study, we investigated vertical changes in flux, shape and volume of fecal pellets from drifting sediment trap experiments to evaluate how fecal pellets were changed or declined.

(2) Methods

Knauer-type sediment traps were deployed at 60, 100, 150 and 200 m at K2 and S1 in the Northwestern Pacific Ocean for 48 hours during the Mirai cruise (MR11-02) from 9 February to 9 March 2011. The sediment traps were constructed from 8 cylinders (collection area: ca. 0.0038 m^2, aspect ratio: 620 mm length / 75 mm width = 8.27) with a baffle to reduce turbulence, mounted on a polyvinylchloride frame. Approximately 250-mL polycarbonate sample cup was attached to the bottom of each cylinder via screw threads. The sample cup was filled with a brine solution.
Once traps were recovered, samples for particle organic carbon (POC) flux were preserved at 4^oC until filtration. To avoid pellet breakage during processing, samples for POC flux were not screened; i.e. swimmers were picked out under a stereo-dissecting microscope. These samples were filtered through a pre-combusted and pre-weighed Whatman GF/F filter under vacuum pressure less than 10kPa and rinsed with Milli-Q water. Samples for fecal pellet (FP) flux were fixed with 5% buffered formaldehyde solution.

(3) Preliminary results

During the cruise, we collected 8 samples for POC flux and 8 samples for FP flux (Table 1 and 2). In the land laboratory, carbon and nitrogen contents will be measured from these filter samples. For fixed samples, number, shape and volume will be measured under a stereo dissecting microscope.

Table 1. Summary list of oceanographic observations, plankton samplings and experiments at K2 during MR11-02.

Samplings/Observations	Analyses	Stat Date	Stat Time	End Date	End Time	Depth (m)	No. of samples	Reference
Drifting Sediment Trap	FPD	26 Feb	06:30	06:30	07:00	60/100/150/200	4	
	CFlux						4	
Bucket	TC	02 Mar	12:00	03 Mar	12:00	60	45	
	CHL						20	
	FPD		22:15		22:30		24	
Bucket	DE	26 Feb	05:30	27 Feb	05:30		48	
	DE	02 Mar	05:30	03 Mar	05:30		36	
	DE	02 Mar	11:30	03 Mar	11:30		48	
CTD-CMS	Pico	26 Feb	04:00	26 Feb	04:30	0/5/15/25/35/45/60/75	24	
	Nano						8	
	Micro						8	
Single NORPAC	FPD	02 Mar	04:42	02 Mar	04:52	0-65	-	Live poecilostmatoids were sorted
Twin NORPAC	Macro + GP	27 Feb	13:12	27 Feb	13:22	0-200	1	GP sample was frozen
	Macro + GP	02 Mar	18:58	02 Mar	19:08	0-200	1	GP sample was frozen
IONESS	Macro+DM	26 Feb	21:00	27 Feb	00:00	0-1000	16	1/4 sample for Macro and 1/8 sample for DM
		26 Feb	11:00	26 Feb	14:02		16	1/4 sample for Macro and 1/8 sample for DM

Abbreviations		
	FPD	Fecal pellet analyses
	DE	Dilution experiments
	Pico	Microscopic analyses for picoplankton
	Nano	Microscopic analyses for nanozooplankton
	Micro	Microscopic analyses for microplankton
	Macro	Microscopic analyses for macrozooplankton
	GP	Gut pigment analyses
	FPD	Fecal pellet decomposition
	TC	Trophic cascading
	DM	Dry mass measurement
	CHL	Chlorophyll measurement

Table 2. Summary list of oceanographic observations, plankton samplings and experiments at S1 during MR11-02.

Samplings/Observations	Analyses	Stat Date	Stat Time	End Date	End Time	Depth (m)	No. of samples	Reference
Drifting Sediment Trap	FPD	16 Feb	07:00	19 Feb	07:00	60/100/150/200	4	
	CFlux						4	
CTD-CMS	TC	15 Feb	21:40	16 Feb	21:30	60	45	
	CHL						20	
	FPD		22:15		22:30		18	
	TC	18 Feb	21:50	19 Feb	21:50	70	45	
	CHL						20	
	FPD		22:15		22:30		18	
	DE		22:30		22:00		57	
Bucket	DE	15 Feb	05:30	16 Feb	05:30		57	
	DE	15 Feb	17:40	16 Feb	17:40		42	
	DE	18 Feb	05:50	19 Feb	05:50		57	
CTD-CMS	Pico	15 Feb	04:00	15 Feb	04:30	0/5/15/25/35/45/60/75	24	
	Nano						8	
	Micro						8	
Single NORPAC	FPD	14 Feb	19:30	14 Feb	20:00	0-50	-	Live poecilostmatoids were sorted
	FPD	17 Feb	18:00	17 Feb	18:30	0-60	-	Live poecilostmatoids were sorted
Twin NORPAC	Macro + GP	15 Feb	11:58	15 Feb	12:08	0-200	2	GP sample was frozen
	Macro + GP	16 Feb	09:28	16 Feb	09:38	0-200	2	GP sample was frozen
	Macro	16 Feb	13:33	16 Feb	14:05	0-50	3	For IONESS sample missed in 0-50 m
	Macro	16 Feb	19:16	16 Feb	19:58	0-50	3	For IONESS sample missed in 0-50 m
	Macro + GP	16 Feb	20:08	16 Feb	20:18	0-200	2	GP sample was frozen
	Macro + GP	18 Feb	19:55	18 Feb	20:15	0-200	2	GP sample was frozen
IONESS	Macro+DM	15 Feb	21:00	16 Feb	00:00	0-1000	14	1/4 sample for Macro and 1/8 sample for DM
		17 Feb	21:00	18 Feb	00:00		14	1/4 sample for Macro and 1/8 sample for DM
		19 Feb	11:00	19 Feb	14:00		16	1/4 sample for Macro and 1/8 sample for DM

Abbreviations are same to Table 1

(4) Reference

Aristegui, J., Duarte, C.M., Agusti, S., Doval, M., Alvarez-Salgado, X.A., Hansell, D.A. (2002). Dissolved organic carbon support of respiration in the dark ocean. Science, 298, 1967-1967.

Bishop, J.K., Edmond, J.M., Ketten, D.R., Bacon, M.P., Silker, W.B. (1977). Thechemistry, biology, and vertical flux of particulate matter from the upper 400m of the equatorial Atlantic Ocean. Deep-Sea Research, 24, 511-548.

Carroll, M.L., Miquel, J.-C., Fowler, S.W. (1998). Seasonal patterns and depth-specific trends of zooplankton fecal pellet fluxes in the Northwestern Mediterranean Sea. Deep-Sea Research I, 45, 1303–1318.

González, H. E., Smetacek, V. (1994). The possible role of the cyclopoid copepod Oithona in retarding vertical flux of zooplankton fecal material. Marine Ecology Progress Series, 113, 233-246.

Flower, S.W., Knauer, G.A. (1986). Role of large particles in the transport of elements and organic compounds through the oceanic water column. Progress in Oceanography. 16, 147-194.

Honjo, S., Roman, M. R. (1978). Marine copepod fecal pellets: production, preservation and sedimentation. Journal of Marine Research, 36, 45-57.

Huskin, I., Viesca, L., Anado´ n, R. (2004). Particle flux in the Subtropical Atlantic near the Azores: influence of mesozooplankton. Journal of Plankton Research, 26, 403-415.

Iversen, M. H., Poulsen, M. R. (2007). Coprorhexy, coprophagy, and coprochaly in the copepods Calanus helgolandicus, Pseudocalanus elongates, and Oithona similis. Marine Ecology Progress Series, 350, 79-89.

Lampitt, R.S., Noji, T.T., von Bodungen, B. (1990). What happens to zooplankton faecal pellets? Implications for material flux. Marine Biology, 104, 15-23.

Noji, T. T., Estep, K. W., MacIntyre, F., Norrbin, F. (1991). Image analysis of faecal material grazed upon by three species of copepods: evidence for coprohexy, coprophagy, and coprochaly. Journal of the Marine Biological Association of the United Kingdom, 71, 465-480.

Paffenhöfer, G.-A ., Strickland, J. D. H. (1970). A note on the feeding of Calanus helgolandicus on detritus. Marine Biology, 5, 97-99.

Poulsen, L. K., Kiørboe, T. (2006). Vertical flux and degradation rates of copepod fecal pellets in a zooplankton community dominated by small copepods. Marine Ecology Progress Series, 323, 195-204.

Poulsen, M. R., Iversen, M. H. (2008). Degradation of copepod fecal pellets: key role of protozooplankton. Marine Ecology Progress Series, 367, 1-13.

Reigstad, M., Riser, C. W., Svensen, C. (2005). Fate of copepod faecal pellets and the role of Oithona spp. Marine Ecology Progress Series, 304, 265-270.

Silver, M.W., Gowing, M.M. (1991). The “particle” flux: origins and biological components. Oceanography, 26, 75-113.

Suzuki, H., Sasaki, H., Fukuchi, M. (2003). Loss processes of sinking fecal pellets of zooplankton in the mesopelagic layers of the Antarctic marginal ice zone. Journal of Oceanography, 59, 809-818.

Svensen, C., Nejstgaard, J. C. (2003). Is sedimentation of copepod faecal pellets determined by cyclopoids? Evidence from enclosed ecosystems. Journal of Plankton Research, 25, 917-926.

Turner, J.T. (2002). Zooplankton fecal pellets, marine snow and sinking phytoplankton blooms.

Aquatic Microbial Ecology, 27, 57-102.
Wilson, S. E., Steinberg, D. K., Buesseler, K. O. (2008). Changes in fecal pellet characteristics with depth as indicators of zooplankton repackaging of particles in the mesopelagic zone of the subtropical and subarctic North Pacific Ocean. Deep-Sea Research II, 55, 1636-1647.

3.5 Po-210 and export flux

Hajime KAWAKAMI (JAMSTEC MIO)
Makio C. HONDA (JAMSTEC RIGC)

(1) Purpose of the study

The fluxes of POC were estimated from Particle-reactive radionuclide (^{210}Po) and their relationship with POC in the western North Pacific Ocean.

(2) Sampling

Seawater and suspended particulate sampling for ^{210}Po, ^{210}Pb, and POC: 2 stations (stations S1 and K2) and 16 depths (10, 20, 30, 50, 75, 100, 150, 200, 300, 400, 500, 600, 700, 800, 900, and 1000 m) at each station.

Seawater samples (10 L for ^{210}Po and ^{210}Pb) were taken from Hydrocast at each depth. The seawater samples for ^{210}Po were filtered through polypropylene cartridge filters with a nominal pore size of 0.8 μm on board immediately after water sampling.

In situ filtering (suspended particulate) samples were taken from large volume pump sampler (Large Volume Pump WTS-6-1-142V, McLane Inc.). Approximately 200 and 1000 L seawater was filtered through glass-fiber filter with a nominal pore size of 0.7 μm at each station at 10–200m depths and 300–1000m depths, respectively. The filter samples were divided for ^{210}Po and POC.

(3) Chemical analyses

Dissolved and particulate ^{210}Po was absorbed on 25 mm silver disks electrically, and were measured by α-ray counter (Octéte, Seiko EG&G Co. Ltd.). For total (dissolved + particulate) ^{210}Pb measurement, the same procedure was applied to the seawater samples 18 months later, when ^{210}Po come to radioactive equilibrium with ^{210}Pb.

POC was measured with an elemental analyzer (Perkin-Elmer model 2400II) in land-based laboratory.

(4) Preliminary result

The distributions of ^{210}Po and POC will be determined as soon as possible after this cruise. This work will help further understanding of particle dynamics at the euphotic layer and twilight zone.

3.6 Settling velocity of particles in the twilight zone

Yoshihisa MINO (NAGOYA UNIV. HyARC)
Chiho SUKIGARA (NAGOYA UNIV. HyARC)

(1) Objective

Sinking particles have been considered as the most important vehicle, by which the biological pump sequesters carbon in the ocean interior (Buesseler et al., 2007). As the particles sink they undergo the remineralization processes (fragmented into non-sinking ones and consumed by bacteria etc.) in the twilight zone, which leads to POC flux attenuation with depth. A large number of sediment trap studies have revealed that POC flux attenuation varied seasonally and regionally (Berelson, 2001), so it is required to understand this variability in order to better quantify the magnitude of biological pump. Recent studies pointed out the significance of particle settling velocity, varying three orders of magnitude, as a parameter affecting the flux attenuation (Armstrong et al., 2002, 2009; Trull et al., 2008).

This study aim to determine the settling velocity (SV) of particles collected by sediment trap at ~100 and 200 m depth for the subarctic (station K2) and subtropical (S1) North Pacific Ocean, for further understanding the carbon transfer in the twilight zone.

(2) Materials and methods

Particulate samples were collected in the drifting sediment trap experiments conducted during this cruise (see the chapter 3.4 for details on the sediment trap experiments). The depth of sample collection is 85-95, 170-190m at both stations (K2 and S1).

Here we applied the elutriation method (Peterson et al. 2005) to fractionate particles into SV classes using countercurrents of varying speeds. A portion of the sediment trap samples was introduced into the custom-built polycarbonate elutriator and separated into 5 fractions with SVs of >500, 150-500, 50-150, 15-50, <15 m d^{-1}. After the swimmers are removed using the tweezers under microscope, each SV-fraction sample was filtrated onto pre-combusted GF/F filter and stored frozen. The organic carbon content in samples will be determined on shore, which derive the settling velocity spectra of the trapped particles. The carbon and nitrogen isotope abundances are also determined for each SV-fraction.

(3) Data archive

The experimental data sets from this study will be submitted to JAMSTEC Data Integration and Analyses Group (DIAG).

(4) References

Armstrong et al. (2002), Deep-Sea Res. II, 49, 219-236.
Armstrong et al. (2009), Deep-Sea Res. II, 56, 1470-1478.
Berelson, (2001), Oceanography, 14, 59-67.
Buesseler et al. (2007), Science, 316, 567-570.
Peterson et al. (2005), Limnol. Oceanogr.: Methods, 3, 520-532.
Trull et al. (2008), Deep-Sea Res. II, 55, 1684-1695.

3.7 Zooplankton
3.7.1 Community structure and ecological roles

Minoru KITAMURA (JAMSTEC, BioGeos)
Toru KOBARI (Kagoshima Univ.)
Kei ISAMI (Kagoshima Univ.)

(1) Objective

Subarctic western North Pacific is known to be a region with high biological draw down of atmospheric CO_2. And time-series biogeochemical observations conducted at the station K2 have revealed high annual material transportation efficiency to the deep compared to the other time-series sites set in the subtropical regions. Importance of not only sinking particle but also 'active transport' by zooplankton on vertical material transport is recently suggested in several area such as Oyashio region, the station BATS or Antarctic Ocean. However, biogeochemical role of zooplankton is not fully estimated in western subarctic gyre, North Pacific. With these backgrounds, goal of the research is to investigate roles of mesozooplankton and micronekton in vertical material transport in the station K2, western subarctic North Pacific. We deployed two types of plankton nets to investigate species and size composition of zooplankton from the surface to the greater deep.

Material transport through microbial food web is one of the pathways which is little understood. To estimate ecological roles of the nano- and microzooplankton we will also analyze abundance, vertical distribution and grazing pressure of them.

For comparison to K2 ecosystem, we also conducted same samplings at a new time-series station, S1

(2) Materials and methods

Mesozooplankton and micronekton samplings (IONESS Sampling)

For collection of stratified sample sets, multiple opening/closing plankton net system, IONESS, was used. This is a rectangular frame trawl with nine nets. Area of the net mouth is 1.5 m^2 when the net frame is towed at 45° in angle, and mesh pore size is 0.33-mm. Volume of filtering water of each net is estimated using area of net mouth, towing distance, and filtering efficiency. The area of net mouth is calibrated from frame angle during tow, the towing distance is calculated from revolutions of flow-meter, and the filtering efficiency is 96% which was directory measured. The net system is towed obliquely. Ship speed during net tow was about 2 knot, speeds of wire out and reeling were 0.1-0.7 m/s and 0.1-0.3 m/s, respectively.

Total five tows (two at K2, three at S1) of IONESS were done. The stratified sampling layers at stations K2 and S1 were as follows; 0-50, 50-100, 100-150, 150-200, 200-300, 300-500, 500-750, and 750-1000m. To understand diel vertical migration of mesozooplankton and micronekton, the samplings were conducted during both day and night. Towing data such as date, time, position, filtering volume are summarized in Table 3.7.1-1.

NORPAC net sampling

A twin-type NORPAC net with fine mesh (100 mm) and flow meters was used. The net was vertically towed 0-50 m and 0-150 m at the Station S1 (Table 3.7.1-2). Unfortunately, the NORPAC sampling was not conducted in the station K2 due to bad sea state. Zooplankton collected were preserved in the 5% buffered formalin seawater for the later analysis.

Nano- and microzooplankton sampling

Seawater samples were collected at eight depths within the euphotic and three depths

within the aphotic zones in both the stations K2 and S1. The former eight depths corresponded to nominal specific optical depths approximately 100, 50, 25, 10, 5, 2.5, 1 and 0.5% light intensity relative to the surface irradiance as determined from the optical profiles obtained by ‘‘Free-Fall Sensor’’. And the latter thee depths were 200, 400 and 800 m.

Seawater samples were immediately treated with the final concentration of 1% glutaraldehyde and were kept at 4°C until filtering. Each seawater sample were filtered through 1μm pore size Nuclepore fitter, pre-stained by irgalan black, at the low vacuum of 15 cmHg, and were double-stained using DAPI (4’6-diamidino-2-phenylindole dihydrochloride) and proflavine (3-6-diamidino-acridine hemisulfate). Just before the finish of filtering, DAPI was added to sample in filtering funnel for the staining DNA. After the DAPI staining, proflavine was also added for the staining of flagella. Both the staining time is five minute. The working solution of DAPI (10 μg/ml) and proflavine (0.033%) were pre-filtered through 0.45 μm pore size of non-pyrogenic Durapore membrane filter (Millipore, Millex-GX). After the filtering, sample filters put on a slide-glass with one drop of immersion oil, and covered with micro cover glass. All preparations were stored in the deep freezer (-80°C) until the observation.

Sampling data such as depths or filtering volume are summarized in Table 3.7.1-3.

Table 3.7.1-1. Summary of IONESS samplings.

Stn.	Tow ID	Local Time		Position	Sampling layer (upper, m) and filtering vol. (lower, m³)									Remarks
			in out	in out	Net No. 0	1	2	3	4	5	6	7	8	
S1	I110215A	2011.2.15	21:00 23:51	29° 59.81' N 144° 58.90' E	0~1041~1000 3666.7	- -	1000~750 3181.6	750~500 2314.6	500~300 1753.3	300~200 1353.9	200~150 583.8	150~100 617.2	100~50 689.7	trable in release machinery
S1	I110217A	2011.2.17	20:45 0:05	30° 00.04' N 144° 57.66' E 29° 58.91' N 145° 04.15' E	0~1050~1000 2661.9	1000~750 3674.4	750~500 3584.3	- -	500~300 2504.4	300~200 1474.7	200~100 1354.8	100~50 646.0	50~0 361.0	trable in release machinery
S1	I110218A	2011.2.18	10:30 11:02	29° 59.82' N 145° 00.19' E	0–150–0									trable in tow wire
S1	I110219A	2011.2.19	11:02 13:58	30° 02.39' N 145° 05.23' E	0~1050~1000 2079.6	1000~750 3523.7	750~500 3015.8	500~300 2142.8	300~200 1116.2	200~150 594.5	150~100 929.7	100~50 676.1	50~0 510.0	
K2	I110226A	2011.2.26	11:36 14:41	46° 54.26' N 160° 14.80' E	0~1068~1000 2765.5	1000~750 3276.8	750~500 2883.8	500~300 2289.2	300~200 957.9	200~150 372.3	150~100 481.6	100~50 388.3	50~0 197.3	
K2	I110226B	2011.2.26	21:03 23:40	46° 56.57' N 160° 13.10' E	0~1068~1000 2004.8	1000~750 2086.8	750~500 2306.7	500~300 1222.9	300~200 356.8	200~150 311.6	150~100 576.5	100~50 479.7	50~0 160.2	

Table 3.7.1-2. Summary of NORPAC samplings

Stn.	Date	Time	Position		Sampling Layer	Wire out	Wire angle	Flow-meter revolution		Filtering vol. (m³)		Sample archive
			Lat.	Long.	(m)	(m)	(°)	ID3331	ID3332	ID3331	ID3332	
S1	2011 Feb. 16	13:33	30° 00.08' N	144° 59.78' E	50-0	50+1	9	719 (1)	913 (2)	10.7	13.5	(1) Kagoshima Univ., formalin fix., (2) JAMSTEC, formalin fix.
		13:45	30° 00.13' N	144° 59.70' E	50-0	50	0	608 (3)	632 (4)	9.1	9.4	(3) Kagoshima Univ., taxa composition, (4) JAMSTEC, bulk biomass
		13:55	30° 00.14' N	144° 59.60' E	50-0	50	0	576 (5)	641 (6)	8.6	9.5	(5) Kagoshima Univ., formalin fix., (6) JAMSTEC, formalin fix.
		14:09	30° 00.17' N	144° 59.51' E	150-0	150	0	1881	1899	28.0	28.1	JAMSTEC, formalin fix.
	2011 Feb. 16	19:16	30° 00.04' N	144° 59.17' E	50-0	50	0	647 (7)	693 (8)	9.6	10.3	(7) Kagoshima Univ., taxa composition., (8) JAMSTEC, bulk biomass
		19:28	30° 00.08' N	144° 59.06' E	50-0	50	8	643 (9)	660 (10)	9.6	9.8	(9) Kagoshima Univ., formalin fix., (10) JAMSTEC, formalin fix.
		19:38	30° 00.08' N	144° 58.97' E	50-0	50+1	10	707 (11)	682 (12)	10.5	10.1	(11) Kagoshima Univ., formalin fix., (12) JAMSTEC, formalin fix.
		19:48	30° 00.06' N	144° 58.86' E	150-0	150+1	8	2041	2630	30.4	38.9	JAMSTEC

Table 3.7.1-3. Summary of water samplings for nano- and microzooplankton abundance

* Local ship time # Kitamura, ## Kagoshima Univ.

Stn.	Date*	CTD		Depth	Irradiance	Nanozooplankton samplings #			Microzoo ##
		Time*	Cast ID	(m)	(%)	Sample No.	Filtering vol. (ml)	Funnel No.	Sample vol. (ml)
S1	2011 Feb. 15	4:00	001(S1) Cast 3 PP	75	0.5	S1-1	315	1	1000
				60	1	S1-2	350	2	1000
				45	2.5	S1-3	285	3	1000
				35	5	S1-4	295	4	1000
				25	10	S1-5	310	1	1000
				15	25	S1-6	345	2	1000
				5	50	S1-7	250	3	1000
				0	100	S1-S	340	4	1000
	2011 Feb. 15	9:00	001(S1) Cast 4 PE	200		S1-200	255	1	-
				400		S1-400	310	2	-
				800		S1-800	500	4	-
K2	2011 Feb. 26	4:00	009(K2) Cast 1 PP	75	0.5	K2-8	500	1	1000
				65	1	K2-9	500	2	1000
				50	2.5	K2-10	465	3	1000
				40	5	K2-11	500	4	1000
				30	10	K2-12	340	1	1000
				15	25	K2-13	500	2	1000
				5	50	K2-14	500	3	1000
				0	100	K2-S	500	4	1000
	2011 Mar. 3	15:30	009(K2) Cast 6	200		K2-200	500	1	-
				400		K2-400	500	2	-
				800		K2-800	500	3	-

(3) Future plans and sample archives

Community structure and ecological role of mesozooplankton

Subsamples are stored at JAMSTEC or Kagoshima Univ. We will analyze as follows; (1) vertical distribution of zooplankton carbon mass, (2) vertical distribution of biomass in higher taxa revel (copepods, euphausiids, etc.) and taxa composition based on the carbon weight, (3) vertical distribution, composition, biomass, and diel vertical migration for each species of dominant taxa such as copepods, euphausiids and chaetognaths, (4) estimation of carbon transport through diel or ontogenetic migration.

Environmental (T, S) and net status (net number, towing distance, etc.) data were recorded during each IONESS tow. All data is under Kitamura and Kobari.

Vertical distribution of microzooplankton

Sample analysis is consigned to Marine Biological Research Institute of Japan Co. LTD., Shinagawa, Tokyo.

3.7.2 Grazing pressure of microzooplankton

Minoru KITAMURA and Kazuhiko MATSUMOTO (JAMSTEC)
Toru KOBARI (Kagoshima Univ.)
K. ISAMI (Kagoshima Univ.)

(1) Objective

To understand material export from surface to deep ocean, not only estimations of primary productivity or vertical flux but also evaluation of grazing impacts at surface is needed. Grazing by larger organisms might bring about efficient vertical carbon transport through repacking phytoplankton into fecal pellets or active carbon transport by diel and ontogenetic migrator. On the other hand, grazing by smaller organisms might have small or negative impact to vertical export. Identification of influential grazers and quantitative estimation of their grazing rates are essential to discuss the carbon cycle in the ocean. Recently, large grazing pressure of not only the crustacean plankton but also microzooplankton has been recognized in the several area. The grazing pressure by the micro organisms maybe important in the northwestern north Pacific in winter because large calanoid copepods migrate to midwater. Based on this background, we estimated grazing rate of them.

(2) Materials and methods

Six dilution incubation experiments were done through the cruise (Table 3.7.2-1). For each experiment 40 l of water were collected from Niskin bottle or bucket. Water was pre-screened through 200 μm mesh to exclude larger zooplankton. Dilution series were prepared with 25, 50, 75, and 100% of natural seawater. Filtered water was obtained by direct gravity flow through a compact cartridge filter (ADVANTEC, MCS-020-D10SR). Incubation of the dilute water was done in transparent polycarbonate bottle. Duplicate or triplicate bottle were prepared. Incubation lasted for 24 h in a tank with continuous flow of surface seawater under natural light conditions. All the water samplings, filtering, and incubate items were soaked in 10% HCl and rinsed Milli-Q water between each use on board. Nutrient was added in the incubation bottles. To measure initial and final chl. *a* concentration, experiment water were filtered onto GF/F filter and extracted 6 ml DMF at –20°C until measurement. Chl. *a* was measured fluorometrically (Welshmeyer method) with a Turner Design fluorometer. Phytoplankton cell numbers were also counted using flowcytometry.

Apparent phytoplankton growth rate (d^{-1}) were calculated using following equation:

$$\text{Apparent growth rate} = (1/t)\ln(P_t/P_0)$$

where t is incubation time (day), P_t and P_0 are final and initial Chl. *a* concentration or cell number, respectively. When the apparent phytoplankton growth rate is plotted as a function of dilution factor, the y-intercept and negative slope of the approximate line means true phytoplankton growth (k; d^{-1}) and grazing coefficient of microzooplankton (g: d^{-1}), respectively. According to Verity et al. (1993) and Zhang et al. (2006), microzooplankton grazing pressure on primary production (P_p; %) is calculated as the following equation:

$$P_p = (e^{kt} - e^{(k-g)t}) / (e^{kt}-1)*100$$

Through the three incubation experiments, we tried to estimate true growth rate of phytoplankton, grazing rate of microzooplankton and grazing pressure of microzooplankton on primary production. Incubation states are summarized in Table 3.8.2-1.

References

Verity, P.G., D.K. Stoecker, M.E. Sieracki & J.R. Nelson. 1996. Grazing, growth and mortality of microzooplankton during the 1989 North Atlantic spring bloom at 47°N, 18°W. Deep-Sea Res., 40: 1793-1814.

Zhang, W., H. Li, T. Xiao, J. Zhang, C. Li & S. Sun. 2006. Impact of microzooplankton and

copepods on the growth of phytoplankton in the Yellow Sea and East China Sea. Hydrobiologia, 553: 357-366.

Table 3.7.2-1. Dilution experiments, sampling and incubation conditions.

Station	Date*	Exp. ID.	Water sampling								Incubation						Remarks
			Time*	Position	Depth m	Irradiance %	Temp. °C	Chl.*a* µg/l	CTD cast No.	Sampler	Time* start	Time* end	Incubation bottle	Temp. °C	Irradiance %	Nutrients addition	
S1	2011 Feb. 15-16	1	4:00	30° 00.15'N, 144° 53.69'E	0	100	18.3	0.76	001(S1) Cast 3	Bucket	5:30	5:30	1L bottle	18.4-18.9	100	+	FCM Matsumoto, FCM Kobari
S1	2011 Feb. 15-16	2	16:30	30° 00.00'N, 145° 00.00'E	0	100	18.9	0.55	-	Bucket	17:40	17:40	2L bottle	18.4-18.9	100	+	FCM Kobari
S1	2011 Feb. 18-19	3	4:30	30° 00.01'N, 144° 59.92'E	0	100	18.2	0.74	001(S1) Cast 7	Bucket	5:30	5:30	1L bottle	18.1-18.6	100	+	FCM Matsumoto, FCM Kobari
S1	2011 Feb. 18-19	4	20:30	29° 59.78'N, 144° 59.63'E	70	1	18.1	0.56	001(S1) Cast 8	Clean Niskin	22:30	22:30	1L bottle	17.7-18.6	2.5	+	FCM Kobari
K2	2011 Feb. 26-27	5	4:00	47° 00.04'N, 160° 10.00'E	0	100	1.8	0.42	009(K2) Cast 1	Bucket	5:30	5:30	1L bottle	1.7-2.0	100	-	FCM Matsumoto, FCM Kobari
K2	2011 Mar. 2-3	6	4:00	46° 52.78'N, 160° 21.76'E	0	100	1.6	0.41	009(K2) Cast 5	Bucket	5:30	5:45	1L bottle	1.6-2.5	100	-	FCM Matsumoto, FCM Kobari
K2	2011 Mar. 2-3	7	10:00	46° 53.86'N, 160° 13.86'E	0	100	1.8	0.41	-	Bucket	11:25	11:30	2L bottle	1.5-2.8	100	-	FCM Kobari
K2	2011 Mar. 2-4	8	15:30	46° 52.82'N, 160° 12.14'E	5	50	1.8	0.40	009(K2) Cast 6	Clean Niskin	18:20	18:30	1L bottle	1.5-6.2	100	-	no FCM sample, 48h incubation

* Local ship time

(3) Preliminary results

All measurements of Chl. *a* and phytoplankton cell numbers were finished on board. Preliminary results of the experiments in the station S1 and K2 are shown in the Figures 3.7.2-1 and 3.7.2-2.

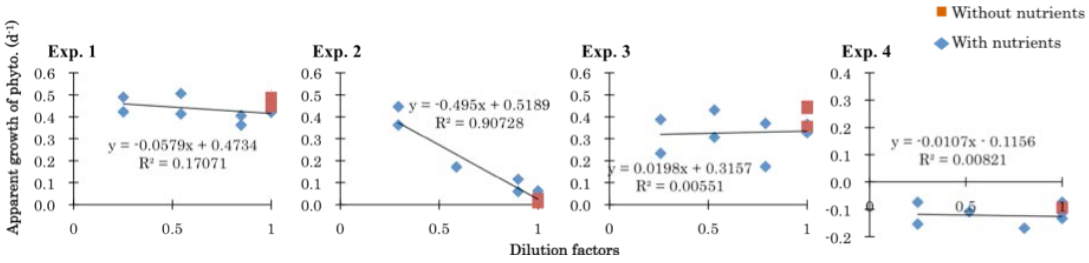

Fig.3.7.2-1. Correlation between apparent growth rates of phytoplankton community and dilution factors estimated from Chl. *a* measurements in the dilution experiments in S1. Slope of the regression equation means grazing rate (d^{-1}) of the microzooplakton community.

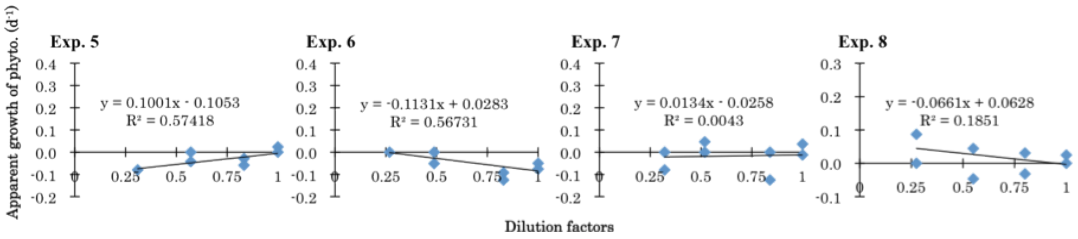

Fig. 3.7.2-2. Correlation between apparent growth rates of phytoplankton community and dilution factors estimated from Chl. *a* measurements in the dilution experiments in S1. Slope of the regression equation means grazing rate (d^{-1}) of the microzooplakton community.

3.8 Effects of zooplankton on sinking carbon flux

Toru KOBARI (Kagoshima University)
Hiroshi ISAMI (Kagoshima University)

3.8.1 Active carbon flux

(1) Objective

It has been long accepted that sinking particles are major pathway of vertical carbon flux into the ocean interior and support mesopelagic carbon demand (Fowler and Knauer, 1986; Zhang and Dam, 1997; Aristegui et al., 2002). In the past decade, a number of studies have also shown that diurnally vertical migrants significantly contribute to carbon flux by consuming POC in surface waters and respiring and excreting the metabolized POC at depth. This "actively transported carbon flux" is equivalent to 3 to 127%, of the sinking POC flux in tropical to subarctic waters (Al-Mutairi and Landry, 2001; Dam et al., 1995; Longhurst et al., 1990; Le Borgne and Rodier, 1997; Steinberg et al., 2000, 2008; Zhang and Dam, 1997). Thus, we should evaluate how mesozooplankton community transports carbon to mesopelagic depth as active carbon flux.
In the present study, we compare abundance, biomass and taxonomic composition of mesozooplankton community between day and night at K2 and S1 in Northwestern Pacific Ocean to estimate active carbon flux.

(2) Methods

Samplings were carried out during the RV Mirai cruise (MR11-02) from 9 February to 9 March 2011 at K2 and S1 in the Northwestern Pacific Ocean. Mesozooplankton were collected from 200 m to sea surface using Twin North Pacific Standard net (Motoda 1957: diameter 45 cm, mesh size 0.1 mm) at a speed of 1 m sec-1. One sample was preserved in borax-buffered 5% formaldehyde for microscopic identification. Another sample was immediately anesthetized with soda water. Sample was frozen in liquid nitrogen after blotting adhering seawater on paper towels and stored at -80oC for measurement of gut pigments.

(3) Preliminary results

During the cruise, 6 samples for microscopic identification and 6 samples for gut pigments were collected (Table). In the land laboratory, major taxa and predominant copepods will be identified under a stereo dissecting microscope from fixed samples. For frozen samples, gut pigments of the predominant copepods will be measured by fluorometer.

(4) Reference

Al-Mutairi, H., Landry, M.R. (2001). Active export of carbon and nitrogen at Station ALOHA by diel migrant zooplankton. Deep-Sea Research II, 48, 2083–2103.

Arıstegui, J., Duarte, C.M., Agustı, S., Doval, M., A´ lvarez-Salgado, X.A., Hansell, D.A. (2002). Dissolved organic carbon support of respiration in the dark ocean. Science, 298, 1967.

Dam, H.G., Roman, M.R., Youngbluth, M.J. (1995). Downward export of respiratory carbon and

dissolved inorganic nitrogen by diel-migrant mesozooplankton at the JGOFS Bermuda time-series station. Deep-Sea Research I, 42, 1187–1197.

Fowler, S.W. Knauer, G.A. (1986). Role of large particles in the transport of elements and organic compounds through the oceanic water column. Progress in Oceanography. 16, 147–194.

Le Borgne, R., Rodier, M. (1997). Net zooplankton and the biological pump: a comparison between oligotrophic and mesotrophic equatorial Pacific. Deep-Sea Research II, 44, 2003–2023.

Longhurst, A.R., Bedo, A.W., Harrison, W.G., Head, E.J.H., Sameoto, D.D. (1990). Vertical flux of respiratory carbon by oceanic diel migrant biota. Deep-Sea Research, 37, 685–694.

Motoda, S., (1957). North Pacific standard net. Information Bulletin of Planktology in Japan, 4, 13-15.

Steinberg, D.K., Carlson, C.A., Bates, N.R., Goldthwait, S.A., Madin, L.P., Michaels, A.F. (2000). Zooplankton vertical migration and the active transport of dissolved organic and inorganic carbon in the Sargasso Sea. Deep-Sea Research I, 47, 137–158.

Steinberg, D.K., Cope, J.S., Wilson, S.E., Kobari, T. (2008). A comparison of mesopelagic mesozooplankton community structure in the subtropical and subarctic North Pacific Ocean. Deep-Sea Research II, 55, 1615– 1635.

Zhang, X., Dam, H.G. (1997). Downward export of carbon by diel migrant mesozooplankton in the central equatorial Pacific. Deep-Sea Research II, 44, 2191–2202.

3.8.2 Production and consumption of fecal pellets

(1) Objective

Fecal pellets are changed by zooplankton ingestion (coprophagy), fragmentation via sloppy feeding or swimming activity (coprorhexy) and loosening of membrane (coprochaly) during sinking (Paffenhöfer and Strickland, 1970; Lampitt et al., 1990; Noji et al., 1991). These processes largely affect transfer efficiency of POC flux (Wilson et al., 2008). It has been believed that fecal pellets are declined by bacterial decomposition (Honjo and Roman, 1978; Arístegui et al., 2002) and/or coprophagy/coprorhexy of small copepods such as cyclopoids and poecilostomatoids for last two decades (González and Smetacek, 1994; Suzuki et al., 2003; Svensen and Nejstgraard, 2003; Huskin et al., 2004; Poulsen and Kiørboe, 2006). In recent years, however, these copepods showed minor contributions to coprophagy/coprorhexy from the field observations (Iversen and Poulsen, 2007) and laboratory experiments (Reigstad et al., 2005), and heterotrophic microbes consume fecal pellets (Poulsen and Iversen, 2008). Thus, we should re-consider how fecal pellets are declined or changed during sinking from surface to mesopelagic depths.

In the present study, we carried out on-board experiments to evaluate how heterotrophic microbes and copepods affect fecal pellets at K2 and S1 in Northwestern Pacific Ocean.

(2) Methods

Samplings were carried out during the RV Mirai cruise from 9 February to 9 March at K2 and S1 in the Northwestern Pacific Ocean. Live copepods were collected from the depth at 1% light intensity to sea surface using North Pacific Standard net (Motoda 1957: diameter 45 cm, mesh size 0.1 mm) at a speed of 0.5 m sec^{-1}.

We carried out on-board experiments to evaluate effects of heterotrophic microbes and copepods on fecal pellets at both stations. Live copepods were identified under stereomicroscope and transferred into chambers (9-mL glass bottle with GF/F filtered seawater) and placed at ambient temperature under dark condition. Fecal pellets were gently collected from incubation bottle from *Artemia salina*. Following the methods of Poulsen and Iversen (2008), bottle incubations were done.

(3) Preliminary results

During the cruise, on-board experiments were carried out twice at S1 and once at K2. Each sample will be brought back to the land laboratory for microscopic analysis on number, shape and volume for fecal pellets.

(4) Reference

Aristegui, J., Duarte, C.M., Agusti, S., Doval, M., Alvarez-Salgado, X.A., Hansell, D.A. (2002). Dissolved organic carbon support of respiration in the dark ocean. Science, 298, 1967-1967.

González, H. E., Smetacek, V. (1994). The possible role of the cyclopoid copepod Oithona in retarding vertical flux of zooplankton fecal material. Marine Ecology Progress Series, 113, 233-246.

Honjo, S., Roman, M. R. (1978). Marine copepod fecal pellets: production, preservation and sedimentation. Journal of Marine Research, 36, 45-57.

Huskin, I., Viesca, L., Anado´ n, R. (2004). Particle flux in the Subtropical Atlantic near the Azores: influence of mesozooplankton. Journal of Plankton Research, 26, 403-415.

Iversen, M. H., Poulsen, M. R. (2007). Coprorhexy, coprophagy, and coprochaly in the copepods Calanus helgolandicus, Pseudocalanus elongates, and Oithona similis. Marine Ecology Progress Series, 350, 79-89.

Lampitt, R.S., Noji, T.T., von Bodungen, B. (1990). What happens to zooplankton faecal pellets? Implications for material flux. Marine Biology, 104, 15-23.

Motoda, S., (1957). North Pacific standard net. Information Bulletin of Planktology in Japan, 4, 13-15.

Noji, T. T., Estep, K. W., MacIntyre, F., Norrbin, F. (1991). Image analysis of faecal material grazed upon by three species of copepods: evidence for coprohexy, coprophagy, and coprochaly. Journal of the Marine Biological Association of the United Kingdom, 71, 465-480.

Paffenhöfer, G.-A ., Strickland, J. D. H. (1970). A note on the feeding of Calanus helgolandicus on detritus. Marine Biology, 5, 97-99.

Poulsen, L. K., Kiørboe, T. (2006). Vertical flux and degradation rates of copepod fecal pellets in a zooplankton community dominated by small copepods. Marine Ecology Progress Series, 323, 195-204.

Poulsen, M. R., Iversen, M. H. (2008). Degradation of copepod fecal pellets: key role of protozooplankton. Marine Ecology Progress Series, 367, 1-13.

Reigstad, M., Riser, C. W., Svensen, C. (2005). Fate of copepod faecal pellets and the role of Oithona spp. Marine Ecology Progress Series, 304, 265-270.

Suzuki, H., Sasaki, H., Fukuchi, M. (2003). Loss processes of sinking fecal pellets of zooplankton in the mesopelagic layers of the Antarctic marginal ice zone. Journal of Oceanography, 59, 809-818.

Svensen, C., Nejstgaard, J. C. (2003). Is sedimentation of copepod faecal pellets determined by cyclopoids? Evidence from enclosed ecosystems. Journal of Plankton Research, 25, 917-926.

Wilson, S. E., Steinberg, D. K., Buesseler, K. O. (2008). Changes in fecal pellet characteristics with depth as indicators of zooplankton repackaging of particles in the mesopelagic zone of the subtropical and subarctic North Pacific Ocean. Deep-Sea Research II, 55, 1636-1647.

3.9 Community structures and metabolic activities of microbes

Ryo KANEKO (Atmosphere and Ocean Research Institute, The University of Tokyo: AORI)
Jeho SONG (AORI)
Keigo WATANABE (AORI)
Mario UCHIMIYA (AORI)
Hideki FUKUDA (AORI)
Hiroshi OGAWA (AORI)
Toshi NAGATA (AORI)
Kazuhiro KOGURE (AORI)
Koji HAMASAKI (AORI)

(1) Objective

A significant fraction of dissolved and particulate organic matter produced in the euphotic layer of oceanic environments is delivered to meso- and bathypelatic layers, where substantial transformation and decomposition of organic matter proceeds due to the actions of diverse microbes thriving in these layers. Statio-temporal variations in organic matter transformation and decomposition in the ocean's interior largely affect patterns in carbon cycling in the global ocean. Thus elucidating diversity, activities and distribution patterns of microbes in deep oceanic waters is fundamentally important in order to better understand major controls of oceanic material cycling in the ocean.

The objective of this study is to determine seasonal variability of microbial diversity and activities during the time-series observation of vertical fluxes at the two distinctive oceanic stations located in the subarctic and subtropical western North Pacific. We investigated i) full-depth profiles of prokaryotic abundance and related biogeochemical parameters including dissolved organic carbon and nitrogen concentrations (potential resources of prokaryotes), and the abundances of viruses (potential predators of prokaryotes), ii) community structures of Bacteria and Archaea and their metabolic activities, iii) sinking velocity and physic-chemical properties of suspended particles in the mixing layer.

(2) Method

Seawater samples were collected from predetermined depths of two CTD casts, i.e. the Atmosphere and Ocean Research Institute (AORI) cast and the Routine cast, conducted at Stations K2 and S1 (see the meta-data sheet for details). Sinking particles were collected by drifting traps to determine fluxes of sinking POC/PON and their weight (see the meta-data sheet for details).

i) Full-depth profiles of prokaryotic activity and abundance and related biogeochemical parameters

a) Prokaryotic abundance: Flow cytometry
b) Virus abundance: Flow cytometry
c) DOC/DON: Concentrations of dissolved organic carbon and total dissolved nitrogen were determined by the high temperature catalytic oxidation (HTCO) method. The concentration of dissolved organic nitrogen was calculated by subtracting the concentration of dissolved inorganic nitrogen (determined by Auto-analyzer) from that of total dissolved nitrogen.

ii) Relationship between community structures of Bacteria and Archaea and their metabolic activities

a) Bacterial community structures: PCR-DGGE method after extracting DNA from particles collected on 0.22 μm-pore-size filters (Sterivex).

b) Activities of bacteria: Bromodeoxyuridine-incorporating methods and exoenzymatic activity measurements.

c) Isolation of bacteria: The high-through-put dilution culture method as well as conventional agar plating.

iii) Sinking velocity and physic-chemical properties of suspended particles

a) Concentrations of particulate organic carbon and nitrogen: Determined using an elemental analyzer for samples collected on GF/F filters.

b) Weight of suspended solid: Determined by weighing samples collected on pre-weighted GF/F filter.

c) Particle size distribution of suspended particles in upper layer (0-200 m): Determined by an *in situ* particle sizing instrument, LISST-100 (Sequoia Scientific Inc., USA).

(3) All results will be submitted to Data Management Office, JAMSTEC after analysis and validation and be opened to public via the web site.

3.10 Dissolved Organic Carbon

Masahide WAKITA (Mutsu Institute for Oceanography, JAMSTEC)

(1) Purpose of the study

Fluctuations in the concentration of dissolved organic carbon (DOC) in seawater have a potentially great impact on the carbon cycle in the marine system, because DOC is a major global carbon reservoir. A change by < 10% in the size of the oceanic DOC pool, estimated to be ~ 700 GtC, would be comparable to the annual primary productivity in the whole ocean. In fact, it was generally concluded that the bulk DOC in oceanic water, especially in the deep ocean, is quite inert based upon ^{14}C-age measurements. Nevertheless, it is widely observed that in the ocean DOC accumulates in surface waters at levels above the more constant concentration in deep water, suggesting the presence of DOC associated with biological production in the surface ocean. This study presents the distribution of DOC during autumn in the northwestern North Pacific Ocean.

(2) Sampling

Seawater samples were collected at stations K2 (Cast 2, 4 and 6) and S1 (Cast 2, and 7) and brought the total to ~130. $\Delta^{14}C$ of DOC and DIC are also sampled to estimate the ^{14}C-age of DOC at station K2 (Cast 4 and 6). Seawater from each Niskin bottle was transferred into 60 ml High Density Polyethylene bottle (HDPE) (for DOC) or 1000 ml Duran glass bottle (for$\Delta^{14}C$ of DOC) rinsed with same water three times. Water taken from the surface to 250 m is filtered using precombusted (450°C) GF/F inline filters as they are being collected from the Niskin bottle. At depths > 250 m, the samples are collected without filtration. After collection, samples are frozen upright and preserved at ~ -20 ℃ cold until analysis in our land laboratory. Before use, all glassware was muffled at 550 ℃ for 5 hrs.

(3) Analysis

Prior to analysis, samples are returned to room temperature and acidified to pH < 2 with concentrated hydrochloric acid. DOC analysis was basically made with a high-temperature catalytic oxidation (HTCO) system improved a commercial unit, the Shimadzu TOC-V (Shimadzu Co.). In this system, the non-dispersive infrared was used for carbon dioxide produced from DOC during the HTCO process (temperature: 680 ℃, catalyst: 0.5% Pt-Al_2O_3).

(4) Preliminary result

The distributions of DOC will be determined as soon as possible after this cruise.

(5) Data Archive

All data will be submitted to JAMSTEC Data Management Office (DMO) within 2 years.

3.11 Chlorofluorocarbons

Masahide WAKITA (JAMSTEC MIO)
Ken-ichi SASAKI (JAMSTEC MIO)

(1) Objective

Chlorofluorocarbons (CFCs) and sulfur hexafluoride (SF_6) are chemically and biologically stable gases that have been synthesized at 1930's and 1960's, respectively. The atmospheric CFCs and SF_6 can slightly dissolve in sea surface water by air-sea gas exchange and then are spread into the ocean interior. The chemical species of CFCs (CFC-11 (CCl_3F), CFC-12 (CCl_2F_2), CFC-113 ($C_2Cl_3F_3$)) and SF_6 can be used as transient chemical tracers for the ocean circulation on timescale of several decades. We measured concentrations of CFCs in seawater and perform the tentative analysis of SF_6 in the seawater.

(2) Apparatus

Dissolved CFCs are measured by an electron capture detector (ECD) – gas chromatograph attached with a purging & trapping system.

Table 3-11-1 Instruments

Gas Chromatograph:	GC-14B (Shimadzu Ltd.)
Detector:	ECD-14 (Shimadzu Ltd)
Analytical Column:	
Pre-column:	Silica Plot capillary column [i.d.: 0.53mm, length: 8 m, film thickness: 0.25μm]
Main column:	Connected two capillary columns (Pola Bond-Q [i.d.: 0.53mm, length: 9 m, film thickness: 6.0μm] followed by Silica Plot [i. d.: 0.53mm, length: 14 m, film thickness: 0.25μm])
Purging & trapping:	Developed in JAMSTEC. Cold trap columns are 1/16" SUS tubing packed with Porapak T.

(3) Procedures

3-1 Sampling

Seawater sub-samples for CFC measurements were collected from 12 litter Niskin bottles to 300 ml glass bottles at stations K2 (Cast 2) and S1 (Cast 2) and brought the total to ~80. The test samples of SF_6 were collected to 400ml glass bottles at station K2 (Cast 2 and 6). The bottles were filled by nitrogen gas before sampling. Three times of the bottle volumes of

seawater sample were overflowed. The bottles filled by seawater sample were kept in water bathes controlled at 5°C until analysis in our land-based laboratory. The CFCs concentrations were determined as soon as possible after this cruise.

In order to confirm CFC concentrations of standard gases and their stabilities, CFC mixing ratios in air were also analyzed. Air samples were collected into a 200ml glass cylinder at outside of our laboratory.

3-2 Analysis

The analytical system is modified from the original design of Bullister and Weiss (1988). Constant volume of sample water (50ml) is taken into a sample loop. The sample is send into stripping chamber and dissolved CFCs are de-gassed by N_2 gas purging for 8 minutes. The gas sample is dried by magnesium perchlorate desiccant and concentrated on a trap column cooled down to -50 °C. Stripping efficiencies of CFCs are confirmed by re-stripping of surface layer samples and more than 99.5 % of dissolved CFCs are extracted on the first purge. Following purging & trapping, the trap column is isolated and electrically heated to 140 °C. CFCs are desorbing by electrically heating the trap column, and lead into the pre-column. CFCs are roughly separated from other compounds in the pre-column and are sent to main analytical column. And then the pre-column is switched to another line and flushed by counter flow of pure nitrogen gas. CFCs sent into main column are separated further and detected by an electron capture detector (ECD). Nitrogen gases used in this system was filtered by gas purifier tube packed Molecular Sieve 13X (MS-13X).

Table 3-11-2 Analytical conditions of dissolved CFCs in seawater.

Temperature	
Analytical Column:	95 °C
Detector (ECD):	240°C
Trap column:	-50 °C (at adsorbing) & 140 °C (at desorbing)
Mass flow rate of nitrogen gas (99.99995%)	
Carrier gas:	15 ml/min
Detector make-up gas:	22 ml/min
Back flush gas:	20 ml/min
Sample purge gas:	130 ml/min
Standard gas (Japan Fine Products co. ltd.)	
Base gas:	Nitrogen

CFC-11:	300 ppt (v/v)
CFC-12:	160 ppt (v/v)
CFC-113:	30 ppt (v/v)

(4) Preliminary result

The distributions of CFCs will be determined as soon as possible after this cruise. The standard gases used in this analysis will be calibrated with respect to SIO scale standard gases and then the data will be corrected.

(5) Data archive

All data will be submitted to JAMSTEC Data Management office (DMO) and under its control.

(6) Reference

Bullister, J.L and Weiss R.F. 1988. Determination of CCl_3F and CCl_2F_2 in seawater and air. Deep Sea Research, 35, 839-853.

3.12 Estimation of primary productivity by measurements of oxygen isotopes, N_2 and noble gases

Osamu ABE (Nagoya University)

(1) Introduction

$\Delta^{17}O$ of dissolved O_2, which is defined approximately as $\delta^{17}O - 0.5\delta^{18}O$ and controlled by primary productivity and gas transfer between atmosphere and water, can be regarded as a conservative component at the subsurface (hypolimnion) water. This means that it may be used to reconstruct past changes of productivity when the water was at the surface. In this study, I aim to clarify inter-annual variation of primary productivity at the subduction area of north Pacific intermediate water (NPIW) by measuring $\Delta^{17}O$ of subsurface water of NPIW. In order to achieve this purpose, vertical water sampling was conducted between Station K2 and S1, dissolved O_2 concentration and isotopic composition will be determined along with measurements for N_2 and noble gases concentrations.

(2) Sampling and on-board preparation procedures

For MR11-02 cruise, vertical water sampling was conducted from 7 stations including Station K2, S1, KEO, JKEO and another two stations between Station K2 and S1. As a result, 206 samples were collected from total 103 sampling points. At Station S1, JKEO and K2, water samples were collected from surface to bottom, whereas collected until 1000m for another locations. At every sampling point, two samples were collected for triple oxygen isotope and gas ratio analyses.

Vacuum sampling flasks, each of which has a volume of 300mL, were used for sampling. Each 100 to 150mL of water was introduced to it directly from CTD water bottles. Then most of dissolved gases (O_2, N_2, Ar, and another lower solubility gases) became both in chemical and isotopic equilibrium with headspace at room temperature. Most of these low solubility gases transferred to headspace in this process. After reaching equilibration, water was sucked out by vacuum pump. Finally, remaining headspace gases were transferred and sealed to 1mL pyrex glass tube with molecular sieve using liquid nitrogen in the vacuum line. These glass ampules were brought back to laboratory on land.

During MR11-02 cruise, 200 samples (30 of MR10-06 and 170 of this cruise) were prepared and approximately 110L of liquid nitrogen were consumed.

(3) Measurements

Most of all dissolved gas components in sampling flasks will be collected using a vacuum line. Then O_2 gas will be purified using molecular sieve packed column and measured by isotope ratio mass spectrometer (IRMS) for $\Delta^{17}O$. For the determination of N_2 and noble gases concentrations, collected gases from flasks will be directly injected to IRMS, and N_2/O_2 or Ar/O_2 ratios will be determined. These gas concentrations will be calculated by these results of gas ratios and dissolved O_2 concentrations those were measured on board.

(4) Expected results

Previous investigations for $\Delta^{17}O$ has been limited to surface mixed layer and used for “present” primary productivity at the surface water. This study will first investigate whether this

parameter would be really conserved the surface condition. On that basis, $\Delta^{17}O$ values for NPIW water masses from each location can be regarded as those surface values when water masses were at the surface. Compare to surface $\Delta^{17}O$, subsurface $\Delta^{17}O$ values would be controlled not only by primary productivity and gas transfer between atmosphere and water, but also by the amount of isopycnal and diapycnal mixing. With regard to gas exchanges between air-water, and stratified water masses could be quantified by measuring degrees of super-saturation for nitrogen and/or noble gases.

(5) Additional Experiments for estimating oxygen productivity by bottle incubation with $H_2{}^{18}O$ tracer

In addition to study on vertical distribution of oxygen triple isotopic composition, bottle incubation experiments to determine oxygen productivity were conducted at Stations S1 and K2 of this cruise. We used $H_2{}^{18}O$ tracer for each of incubation. Photosynthetically generated oxygen has an identical isotopic composition to oxygen of source water, and oxygen productivity could be determined by measuring concentration and isotopic composition of oxygen both for initial and final, without any assumption.

We conducted each of two incubations at Station S1 and K2. At time zero, oxygen sample was collected from Niskin bottle as described above. For each incubation, we added 1.5 mL of 10% diluted $H_2{}^{18}O$ water by nutrient-free seawater to 100 mL incubation flask filled with collected seawater, which makes isotopic composition of incubating water ~1000 permil. Then, 24-hour incubation was conducted along with conventional light-dark bottle experiments. After that, water sample of approximately 70~80 mL was collected to vacuum sampling flask as same as $\Delta^{17}O$ experiment. Finally, residual water of 5 mL was collected for oxygen isotopic composition of incubating water, which would be determined by conventional CO_2-H_2O equilibrium method. On-board and subsequent laboratory procedures were identical to those of $\Delta^{17}O$ analysis.

Compare to conventional light-dark bottle incubation, $H_2{}^{18}O$-based incubation method are not constrained by the assumption that rate of respiration should be ever equal under light or dark condition. Moreover, it could detect oxygen generated by photosynthesis with high sensitivity. Therefore, it could be expected to evaluate rate of respiration under light condition and/or exact determination of oxygen productivity under weak light. Additionally, direct determination of oxygen production enables us to compare it directly with electron transfer velocity observed by FRRF.

3.13 Argo Float

Toshio SUGA (JAMSTEC/RIGC, not on board): Principal Investigator
Shigeki HOSODA (JAMSTEC/RIGC, not on board)
Kanako SATO (JAMSTEC/RIGC, not on board)
Mizue HIRANO (JAMSTEC/RIGC, not on board)
Toru IDAI (MWJ)

(1) Objective

The objective of deployment is to clarify the structure and temporal/spatial variability of water masses in the North Pacific such as Transition Region Mode Water and North Pacific Intermediate Water and their formation mechanism. To achieve the objective, profiling floats are launched to measure vertical profiles of temperature and salinity automatically every ten days. As the vertical resolution of the profiles is very fine, the structure and variability of the water mass can be displayed well. Therefore, the profile data from the floats will enable us to understand the variability and the formation mechanism of the water mass.

(2) Methods (Description of instruments deployed)

We launched one Provor float manufactured by Nke. The float equips one SBE41cp CTD sensor manufactured by Sea-Bird Electronics Inc to measure temperature, salinity and pressure from surface to 2000 dbar. The float usually drifts at a depth of 1000 dbar (called the parking depth), then it dives to a depth of 2000 dbar. During the ascent to the sea surface with increasing its volume in order to change its buoyancy, the float measures sea water temperature, salinity, and pressure. To send the measured data to the Argo data center via the ARGOS transmitting system in real time, the float stays at the sea surface for enough time, approximately 9 hours. Finally the float returns to the parking depth with decreasing volume. The cycle of the float moving repeats each 10 days for 3 or 4 years. The status of the float and the launch is shown in Table 3.13-1.

Table 3.13-1 Specification of launched float

Float Type	Provor float manufactured by Nke.
CTD sensor	SBE41cp manufactured by Sea-Bird Electronics Inc.
Cycle	10 days (approximately 9 hours at the sea surface)
ARGOS transmit interval	30 sec
Target Parking Pressure	1000 dbar
Sampling layers	115
	(2000,1950,1900,1850,1800,1750,1700,1650,1600,1550,1500,1450,1400,1350,1300,1250,1200,1150,1100,1050,1000,980,960,940,920,900,880,860,840,820,800,780,760,740,720,700,680,660,640,620, 00,580,560,540,520,500,490,480,470,460,450,440,430,420,410,400,390,380,370,360,350,340,330,320,310,300,290,280,270,260,250,240,230,220,210,200,195,190,185,180,175,170,165,160,155,150,145,140,135,130,125,120,115,110,105,100,95,90,85,80,75,70,65,60,55,50,45,40,35,30,25,20,15,10,4 or surf, dbar)

(3) Preliminary result

The Float S/N, ARGOS ID, launched date/ time, launched position observation cycle of the float is summarized in Table. 3.13-2. The data will be measured automatically each observation cycle and can be obtained via internet promptly and freely.

Table 3.13-2 Launching area and date/time

Float S/N	ARGOS ID	Date and Time of Reset (UTC)	Date and Time of Launch(UTC)	Location of Launch	Observation Cycle
10015	34865	2011/02/23 22: 08	2011/02/23 23:02	40-14.94 [N] 149-01.14[E]	10days

(4) Data archive

The real-time data are provided to meteorological organizations, research institutes, and universities via Global Data Assembly Center (GDAC: http://www.usgodae.org/argo/argo.html, http://www.coriolis.eu.org/) and Global Telecommunication System (GTS), and utilized for analysis and forecasts of the ocean conditions and the climates.

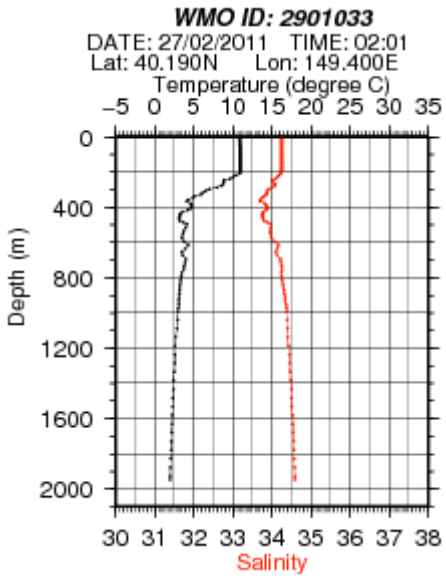

Figure 3.13-1 The first profile of each float launched during MR11-02.

3.14 Optical measurement of marine snow: Visual Plankton Recorder (VPR)

Makio HONDA (JAMSTEC RIGC)

(1) Objective

Aggregated sinking particles, namely “marine show”, play an important role in transporting atmospheric CO_2 to the ocean interior. The study of marine snow has been traditionally conducted by collecting these with “sediment trap” and by chemical and biological analysis in laboratory. On the other hand, in situ qualitative observations of marine snow such as measurement of turbidity and light attenuation have also been conducted. Bishop et al. (2009) tried to estimate abundance and flux of particulate organic carbon (POC) by using the “carbon explorer”, that is “ARGO float” type optical method. Recently application of visual plankton recorder (VPR) to marine snow observation (Lindsay et al., 2008) has been examined. In addition, in situ laser raman spectrometry (LR) has been also examined (Brewer et al., 2004) in order to know chemical composition of seawater and sea-floor sediment (see appendix). In order to conduct the research and development of optical measurement of marine snow, I have started to evaluate VPR and LR.

(2) Method

In this cruise, Visual Plankton Recorder (VPR) (picture 1) was deployed twice at stations S1 and K2, respectively.

VPR takes approximately 12 dark-field images per second. Field of view is approximately 5 cm x 5 cm. In order to take pictures under same light condition, VPR was deployed at night. Deployment record is shown in Table 1. During this cruise, VPR descended to 500 m with downward velocity of 0.5 m/sec. Depth of VPR and vertical profiles in water temperature and salinity was monitored with CTD with sampling time of 0.5 seconds.

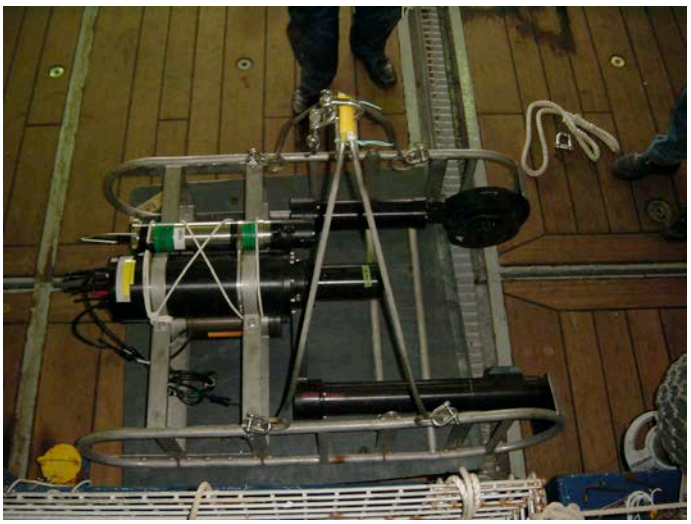

Station	S1 30-0.05N/ 144-59.9E Wave Hight : 2.8 m,	S1 29-59.99N 144-59.83E Wave height: 1.9m	K2
Date	14 February 2011	18 February 2011	2 March 2011
Time (LST)			
Battery connect	18:19	18:09	19:17
CTD connect	18:20	18:11	19:17
Switch ON(Test)	18:20	18:12	19:18
Switch ON	18:52	18:55	20:21
Water In	18:55	18:58	20:23
Start Descend (0.5m/sec ↓)	18:56	19:00	20:24
Bottom (500m)		19:19	20:43
Start Ascend (1.0m/sec ↑)	19:16	19:19	20:44
Water out		19:28	20:54
On deck	19:26	19:28	20:54
Switch OFF	19:26	19:29	20:55

LST= JST + 1 hr = UTC + 10 hr

(3) Data analysis

Data stored in hard disk will be analyzed with image-analysis software (Image pro) on land.

Visual Plankton Recorder

Image analysis of marine snow

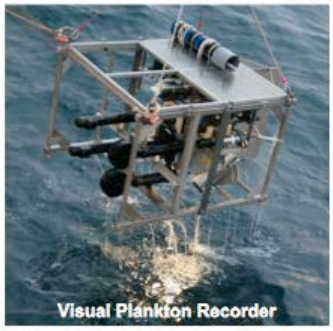

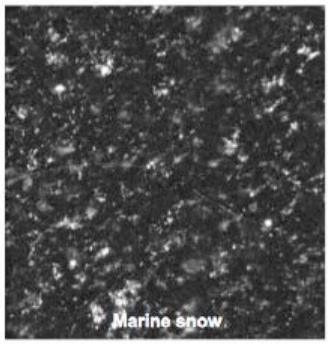

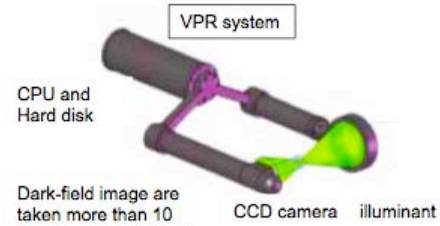

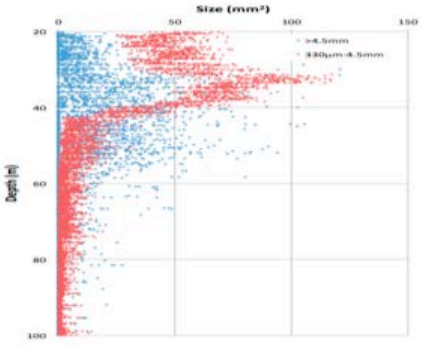

Vertical distribution of particulate materials

Laser Raman Spectrometry

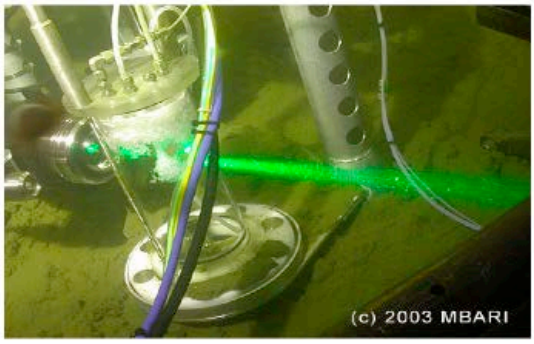

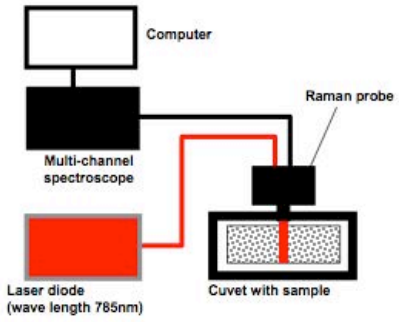

Conceptual diagram of PLRS

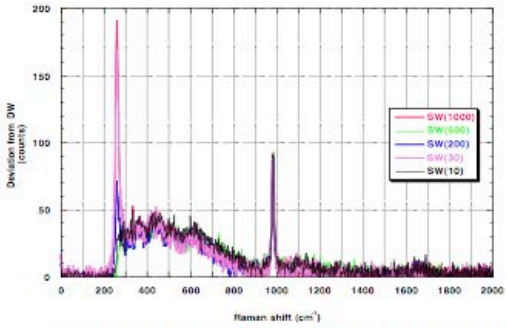

Raman shift of seawater collected from 10 m to 1000m

3.15 K-TRITON and KEO buoy operations

Yoshimi KAWAI (JAMSTEC RIGC) Principal Investigator
Akira NAGANO (JAMSTEC RIGC)
Hirokatsu UNO (MWJ)
Toru IDAI (MWJ)
Takuji WASEDA (JAMSTEC RIGC / University of Tokyo) not on board
Yoshiyuki NAKANO (JAMSTEC) not on board
Meghan CRONIN (NOAA PMEL) not on board
Keith RONNHOLM (NOAA PMEL) not on board

(1) Objective

The objective of the moored-buoy observations is to investigate the air-sea interaction around the Kuroshio Extension, where a large amount of heat is released from the ocean. Surface water pCO_2 is also measured at these two buoys to examine the air-sea CO_2 flux. In addition, wave gauges are attached on the K-TRITON buoy and the drifting buoy released at the JKEO site for freak wave research and wave prediction.

(2) Description of instruments deployed

Each of the K-TRITON and KEO buoys has an anemometer, a thermometer for atmospheric temperature, a hygrometer, a longwave radiometer, a shortwave radiometer, pCO_2 sensors, a rain gauge, a barometer, current meters, CTs (water temperature and salinity) and CTDs (water temperature, salinity, and pressure). A weather transmitter (Vaisala WXT520), which can measure wind speed, wind direction, air temperature, humidity, rain rate, and air pressure, is installed on each buoy as spare. The K-TRITON buoy also has a wave gauge.

The drifting buoy of the University of Tokyo has a function of measuring wave height, atmospheric pressure, air temperature and water temperature.

Furthermore, we observed vertical current profiles with LADCP at the KEO and JKEO sites.

(3) Operations and preliminary result

I. Exchange of sensors on the KEO buoy at the KEO site

The present KEO buoy was deployed at 32°25.59'N, 144°34.63'E (anchor position) in September 2010. Because the weather transmitter and rain gauge on this buoy stopped working, two technicians went to the buoy by a small boat and replaced these sensors with new ones in this cruise (Fig.3.15-1). This operation on the buoy took about 15 minutes and finished at 08:22 LST on 20 Feb. Good rain data have been sent via satellites since this operation, while weather transmitter data are still bad. We observed vertical current profile at the KEO site before the replacement operation (Fig. 3.15-2).

II. Recovery and deployment of the K-TRITON buoy at the JKEO site

The K-TRITON buoy, which was moored in the north of the Kuroshio Extension on 29 Aug. 2009, drifted in the beginning of Oct. 2010 due to the breakage of its mooring wire. The wire was cut at about 4-m depth. Although the buoy hull was already recovered on 12 Oct., all of

its underwater part was left in the ocean. Before the recovery operation, we measured vertical current profile with LADCP (Fig. 3.15-3), and examined if the glass ball floats could reach the sea surface by using the current data and a catenary simulation software on 21 Feb. Because the simulation result showed that the glass ball floats could barely reach the sea surface, we decided to start the recovery operation. In the early morning on 22 Feb., we sent the release command to one of the acoustic releasers by using a deck unit. The glass ball floats were found at the sea surface at 13:45 LST. It took about eight and a half hours for the glass ball floats to reach the sea surface (3.15-4). The recovery operation finished at about 17:35 LST. We successfully recovered all the instruments (two acoustic releasers, one transponder, and nine underwater sensors), the broken wire and rope. As we expected, fishing gear got tangled around the wire, which was the reason for the breakage of the wire. The process of the operations and the conditions of the recovered instruments are summarized in Tables 3.15-1 and 2.

In the afternoon on 23 Feb., we deployed the K-TRITON buoy (Fig.3.15-5). The anchor position is 38°05.0590'N, 146°26.8701'E, and the depth at this point is 5398 m. This time, we first installed two current meters, rain gauge, barometer, and cheap underwater thermometers (trial) on the buoy and wire. We also changed the depths of underwater sensors. To protect the mooring wire from fishing gear, we wound firm fiber sheet and tape around the upper 50 m of the wire, and fixed fairings on the wire with cable ties (see Fig.3.15-5).

Just before leaving the JKEO site, the drifting buoy to measure wave height (Fig. 3.15-6) was released from the stern by using the A frame at 18:50 LST at 38°05.25'N, 146°26.53'E.

(4) Data archive

The meteorological and oceanic data obtained at the K-TRITON buoy, except for pCO_2 and wave data, are released through the Internet (http://www.jamstec.go.jp/iorgc/ocorp/ktsfg/data/jkeo/index.html). The data of the KEO buoy are also released through the Internet (http://www.pmel.noaa.gov/keo/).

The LADCP data will be submitted to the Data Integration and Analysis Group (DIAG) of JAMSTEC just after the cruise.

Table 3.15-1. Process of the operations at the JKEO site

Date and time (LST)	
	Recovery operation
10:40, 21 Feb.	Send the enable command to the transponder, start SSBL, the anchor position is 38°04.8248’N, 146°25.7739’E.
11:08	Lower the transducer at the stern, send the enable command to the lower acoustic releaser, ranging
12:30	Start CTD/LADCP observation
17:23	Finish CTD/LADCP observation
18:30	Examine if we should do the recovery operation, and decide to do it
5:07, 22 Feb.	Send the enable command to the transponder, start SSBL
5:17	Send the release command
13:45	Find the glass ball floats at 38°06.31’N, 146°26.22’E
14:00	A boat went to the glass ball floats
14:40	All the glass ball floats on deck
14:43	Start to recover the rope
17:35	All the wire on deck
	Deployment operation
Morning, 23 Feb.	Prepare the deployment of the buoy
13:10	Start the deployment operation (zero-sai)
13:24	The top buoy on the sea surface
17:23	Release the anchor
17:52	The anchor on the sea floor, the anchor position is 38°05.0590’N, 146°26.8701’E, 5398-m depth.
18:29	Lower the transducer at the stern, ranging (lower releaser good, upper releaser bad)
18:50	Release the drifting buoy from the stern, leave the JKEO site

Table 3.15-2. Conditions of the recovered instruments of the K-TRITON buoy

Instrument	Serial number	Condition
CT SBE-37IM45745 (7.5m)	5043	Failure in communication
CTD SBE-37SM30900 (15m)	2733	Good, but the sensor cover and one of the clamps disappeared
CT SBE-37IM53090 (20m)	6681	Good
CTD SBE-37SM30900 (50m)	2734	Good, but the sensor cover disappeared
CTD SBE-37SM30900 (100m)	2738	Good
CTD SBE-37SM30900 (150m)	2739	Good, but a connector disappeared
TD SBE-39IM46013 (200m)	3652	Measurement stopped at 9:30 on 28 Dec. 2009 since the battery was dead
CTD SBE-37SM30900 (300m)	2748	Good
CTD SBE-37SM30900 (600m)	2758	Broken, seawater got inside
Transponder Benthos XT6001-13	47654	Good
Acoustic releaser Benthos 865A (upper)	1141	Good
Acoustic releaser Benthos 865A (lower)	1208	Good

Figure 3.15-1. (top) Replacement of the weather transmitter and rain gauge on the KEO buoy on 20 Feb. (bottom) Recovered weather transmitter (left) and recovered rain gauge (right).

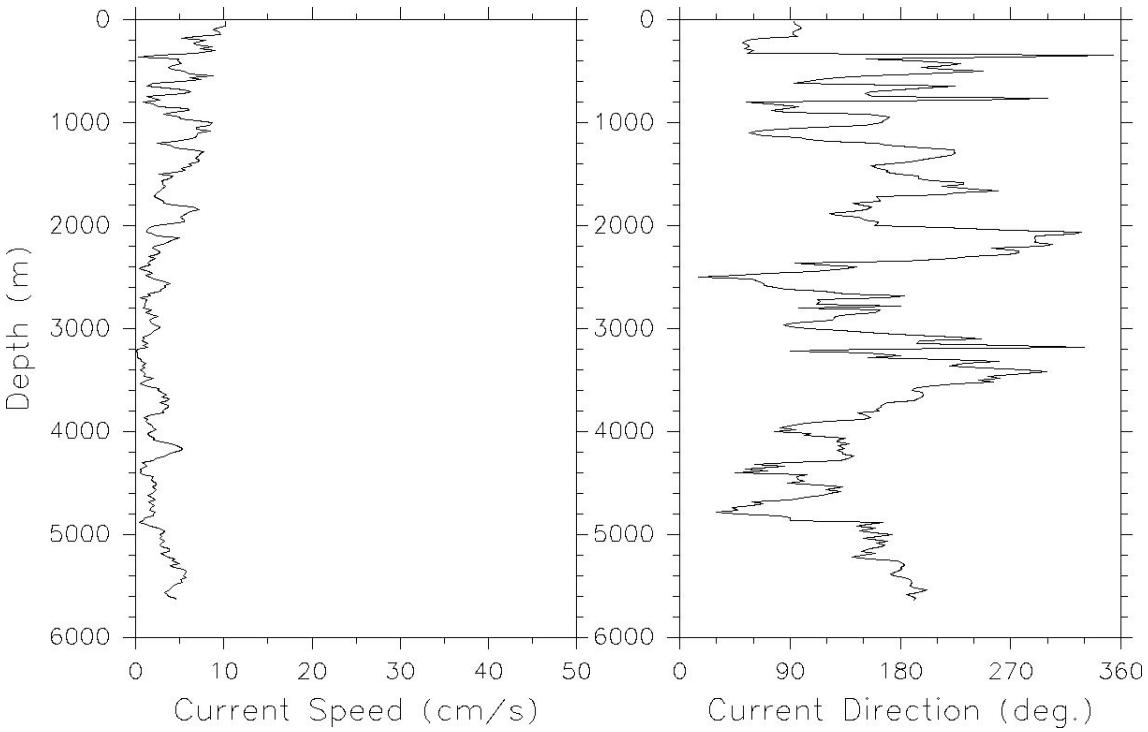

Figure 3.15-2. Vertical current speed (left) and direction (right) profiles at the KEO site measured by LADCP on 20 Feb (01:40-06:55 LST). 0°, 90°, and 180° of the direction represent eastward, northward, and westward, respectively.

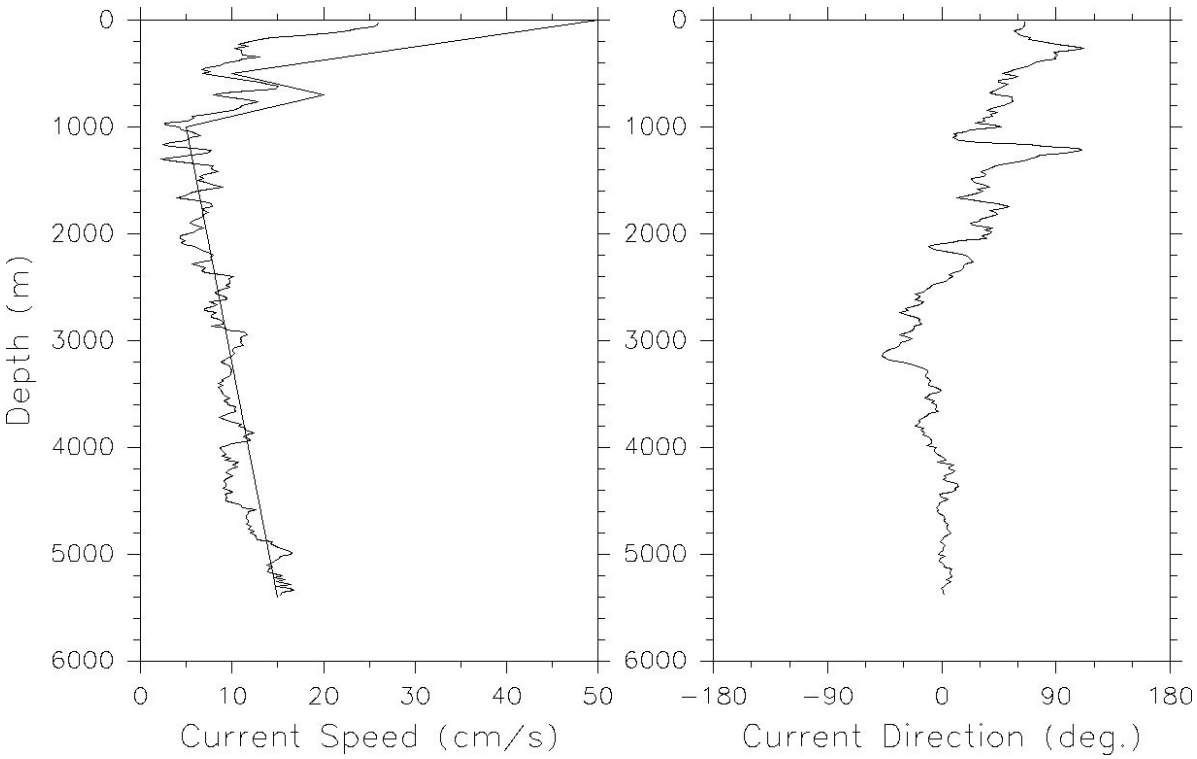

Figure 3.15-3. Vertical current speed (left) and direction (right) profiles at the JKEO site measured by LADCP on 21 Feb (12:30-17:23 LST). Straight lines represent the profile given in the catenary simulation. 0°, 90°, and -90° of the direction represent eastward, northward, and southward, respectively.

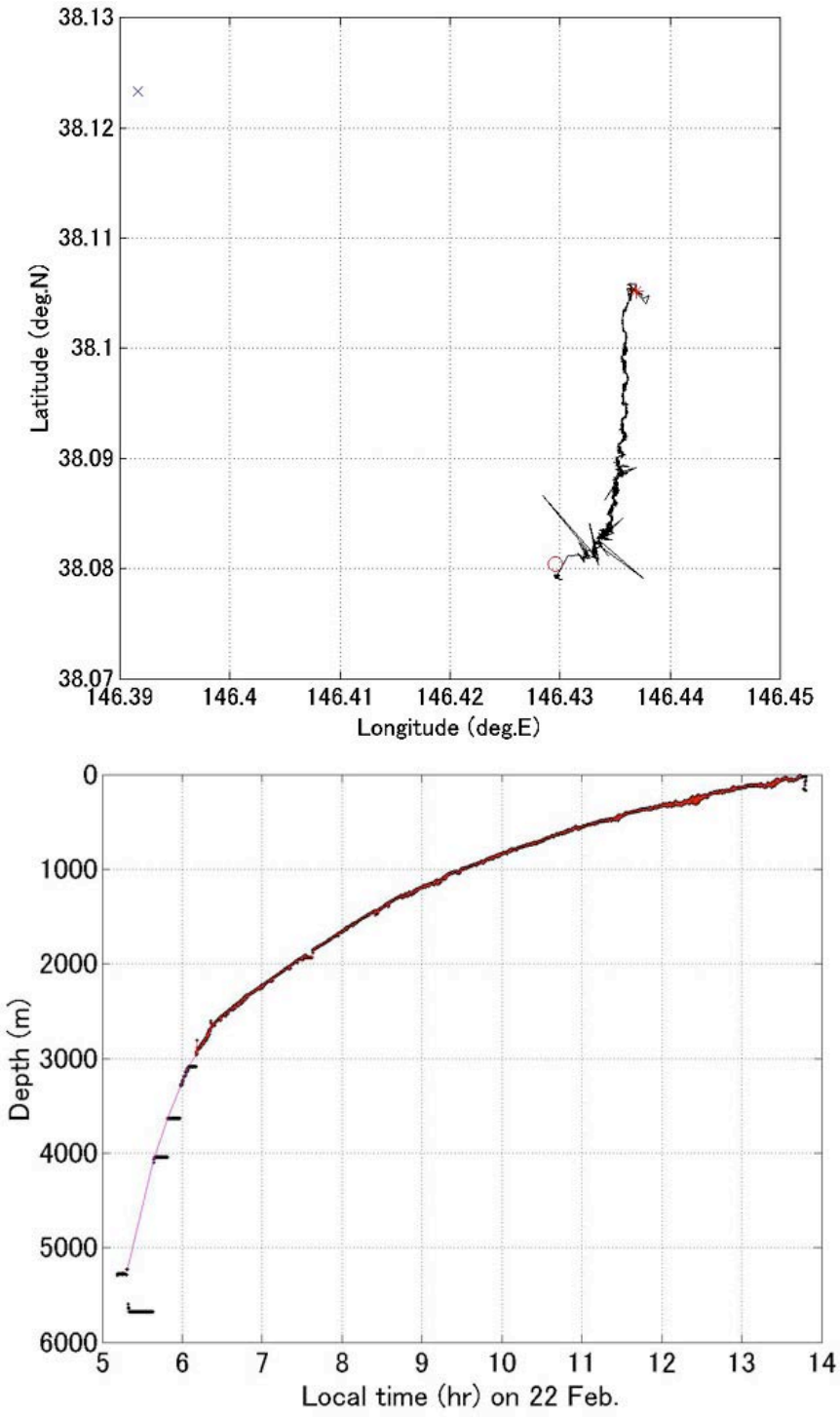

Figure 3.15-4. Tracks of the recovered transponder at the JKEO site measured by SSBL. (top) horizontal position. Black cross, red circle, and red asterisk represent the estimated starting point of top-buoy drifting, the anchor position, and the recovery point of the glass ball floats, respectively. (bottom) depth of the transponder.

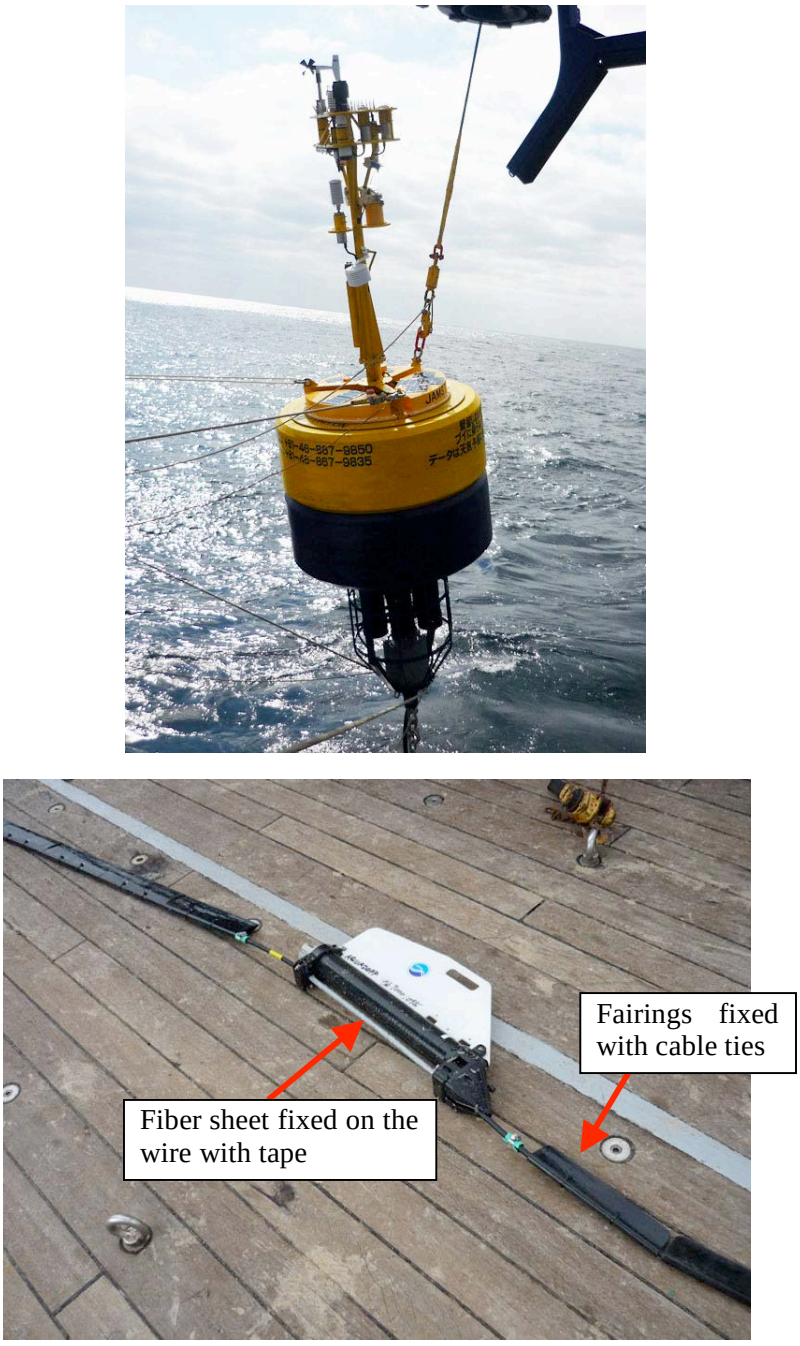

Figure 3.15-5. (top) Deployment of the K-TRITON buoy. (bottom) Protection of the wire.

Figure 3.15-6. Drifting buoy released at the JKEO site.

3.16 Taxonomy and genome analysis of eukaryotic picophytoplankton originated from cryopreserved marine environmental specimens

Masanobu KAWACHI (NIES)
Naoji YUBUKI (University of British Columbia)
Daniel VAULOT (CNRS)

(1) Objective and research outline

Our objective is to obtain morphological, phylogenetic and genomic data for pico-size fraction of marine eukaryotic picophytoplankton that have escaped from culturing until now. Our approach is to use flow cytometry for physically separating the targeted cells. Cell morphology will be examined by electron microscopy. As we will aim to sort as few cells as possible, we will perform Whole Genome Amplification (WGA) a fast developing technique, in order to obtain phylogenetic and genomic data on the sorted cells. During the MR11-02 cruise, we applied cryopreservation method to preserve environmental specimens containing targeted picophytoplankton. This approach will allow long term preservation of natural biodiversity and also repeated analysis on the morphological, phylogenetic and genomic data in laboratory. In addition to the sample treatment during cruise, we also described here results on preliminary observations of phytoplankton diversity at S1 and K2 sites as a background data for further studies.

(2) Sample treatments and preliminary observations of phytoplankton

Sea water samples were collected from both pumping line for continuous seawater monitoring system and Niskin water sampler system. The seawater sample was initially concentrated from 100 fold by tangential flow filtration system and then used for the several treatments; sub-culturing, cryopreservation, DNA analysis, light microscope and scanning electron microscope observation. As for the cryopreservation, samples were cooled with cryoprotectant (5% DMSO) with a rate of -1°C /min to -35°C by using a programmable freezer and then frozen rapidly to –196 °C into liquid nitrogen.

During MR11-02 cruise, we continuously observed both concentrated samples and sub-cultured samples with inverted light microscope. The phytoplankton diversity of both S1 and K2 was partly recorded by taking digital images. Although this is a preliminary observation with low magnification images and also not quantitative analysis, dominant phytoplankton group and remarkable species in each site have been recorded. The species list with additional information (dominancy, habitat, growth ability) was summarized in Table 1.

(3) Phytoplankton diversity at S1 site

Sea water samples at S1 site were collected from 5, 20,75m in depth during 14 to 18 Feb. 2011. The observations of both concentrated and sub-cultured samples revealed dominant species as well as species showing active growing, which were indicated in remark column of Table 1. Almost same phytoplankton species were observed in the investigated depths. Among the phytoplankton species at S1 site, not only absolute pelagic species but also many cosmopolitan species distributing also coastal region were recognized. Interestingly, three freshwater species were observed from several concentrated samples (Fig. 1A-C). The cells of *Coelastrum* sp. and *Pediastrum* sp. almost lost those green color, suggesting loss of viability, while *Trachelomonas* sp. kept cell content, and

probably survived in marine environments. Cells of *Trachelomonas* are usually covered with tight mineralized cell wall (iron and manganic compounds with dark red color), and such tough structure may protect cell from different environmental condition. Existence of both coastal and freshwater species suggests that this area probably has been affected by coastal water. The meander phenomenon of Kuroshio current may related with transportation of coastal water to S1 site (Fig. 1D).

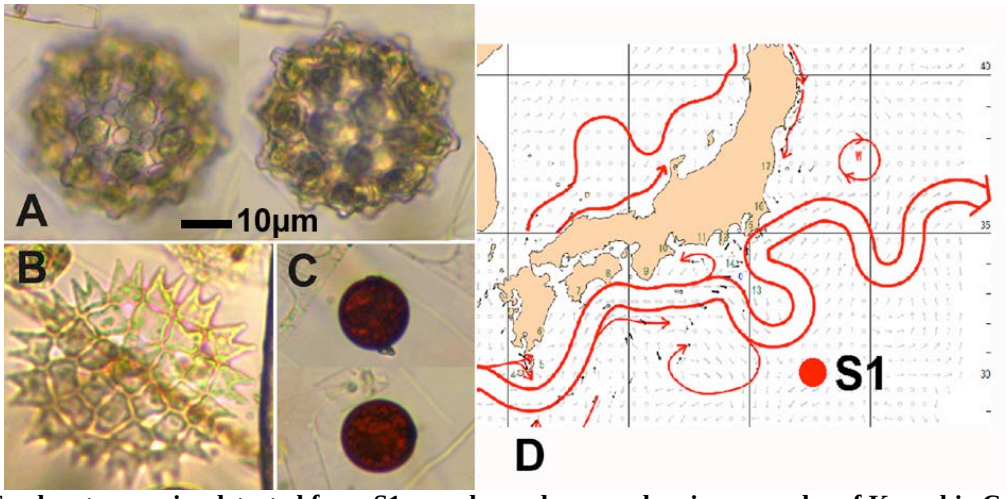

Fig. 1. Freshwater species detected from S1 samples and a map showing meander of Kuroshio Current.
A. *Coelastrum* sp., B. *Pediastrum* sp., C. *Trachelomonas*sp., D. map from Quick Bulletin of Ocean Conditions (17 Jul. 2008, No. 135) reported by Japan Coast Guard.

Coccolithophorids (Haptophyceae) known as one of the dominant phytoplankton in oceans are characterized by calcite cell coverings (called coccolith). In the S1 site, coccolithophorids (Fig. 2) were also recognized as one of the dominant phytoplankton, although light microscopic observations with low magnification allow identifying only limited number of species. In addition to coccolithophorids, other pelagic phytoplankton species (e.g. *Synechococcus*, *Prochlorococcus*, *Halosphaera*, *Thoracosphaera*, etc.) were also observed.

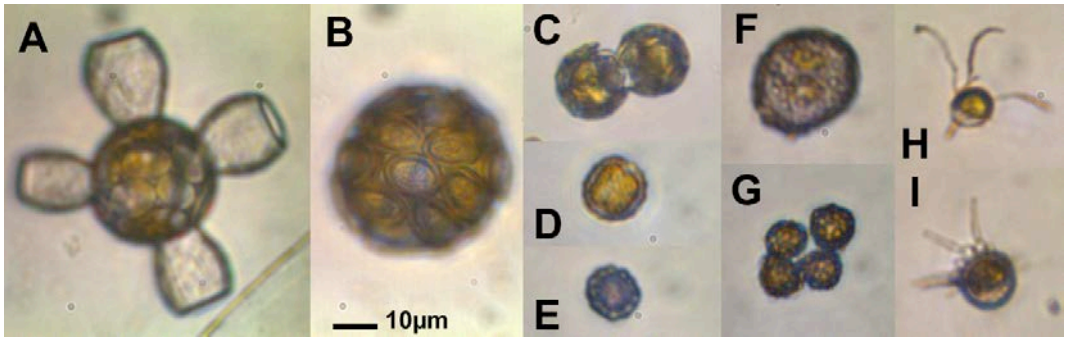

Fig. 2. Various coccolithophorids from S1.
A. *Scyphosphaera apsteinii*, B. *Pontosphaera* sp., C. *Calcidiscus* sp., D. *Calyptrosphaera* sp., E. Algiosphaera sp., F. *Umbilicosphaera sibogae* var. *sibogae*, G. *Gephyrocapsa oceanica*, H-I. *Ophiaster* spp..

Finally it should be noted that some polysaccharide producing phytoplankton species often dominated in sub-culture samples (Fig. 3). At least three species, *Prasinococcus* sp. (Prasinophyceae), *Phaeocystis* sp. (Haptophyceae), and unidentified species (probably Pelagophyceae), have been observed. Bacteria and colorless flagellates seemed to associate with the

polysaccharide matrix, suggesting its contribution to the microbial loop. And also the polysaccharide may be concerned with aggregate formation in water column. Since those species can produce polysaccharide as a photosynthetic reaction even under the nutrient limit (oligotrophic) condition in which cell grow slowly, it is worthwhile to evaluate the ecological roles of such polysaccharide producing phytoplankton species in this site.

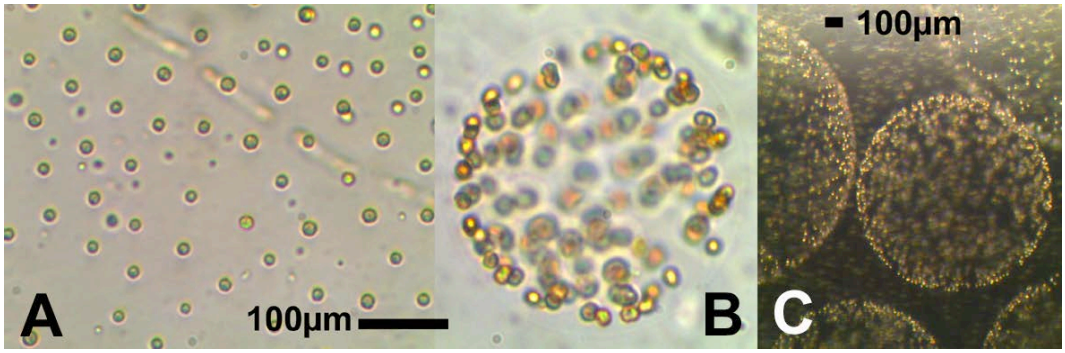

Fig. 3. Polysaccharide producing phytoplankton from S1.
A. *Prasinococcus* sp., B-C. *Phaeocystis* sp..

(4) Phytoplankton diversity at K2 site

Sea water samples at K2 site were collected from 5, 75, 100m in depth during 26 Feb.-2 Mar. 2011. The phytoplankton diversity at K2 site was summarized in Table 1. As for the concentrated samples, almost same phytoplankton species were observed in the investigated depths. As for the sub-culture samples, most species were still initial growth phase at the end of cruise. The time shortage for culturing and observation procedure seems to be one of the reasons why less number of species in K2 than S1 were detected (Table 1).

During this cruise, in addition to major prokaryotic pico-phytoplankton (*Synechococcus* spp. and *Prochlorococcus* sp.), different type of unknown, eukaryotic species distinguished by greenish or yellow-brownish color, pico or nano size, and coccoid or flagellate cell type, were observed from both concentrated and sub-culture samples (Fig. 4). Those tiny and morphologically simple phytoplankton distributed all investigated area including S1 and K2, and this observations coincident with preliminary survey on our samples with flow cytometory (information from Dr. Matsumoto, JAMSTEC). Based on small morphological differences, we have tried to distinguish them as species level and listed in the Table 1. Detail morphological investigation by electron microscopy as well as DNA analysis will reveal those identities resulting accumulation of knowledge on potential biodiversity in both S1 and K2.

Several papers reported dominancy of particular phytoplankton, Parmales species, *Triparma* spp. and *Tetraparma* spp. from K2 area. Cells of *Triparma laevis* sometimes develop spines from the siliceous plate. Then we can distinguish this species from other yellowish coccoid cells (Fig. 4D).

Two haptophyte species, *Corymbellus* (Fig. 4F) like species and *Coccolithus pelagicus* (Fig. 4G) were distinctively observed in K2 samples. Those cannot grow more than 18ºC and apparently adapt to cool temperature. *Corymbellus* like species is characterized by parallel-arranged cells and looks like a colonial haptophyte, *Corymbellus aureus*. But there are some differences, e.g. colony shape, cell size, swimming manner, suggesting a new haptophyte species. Establishment of culture strains is required for more detailed taxonomic studies.

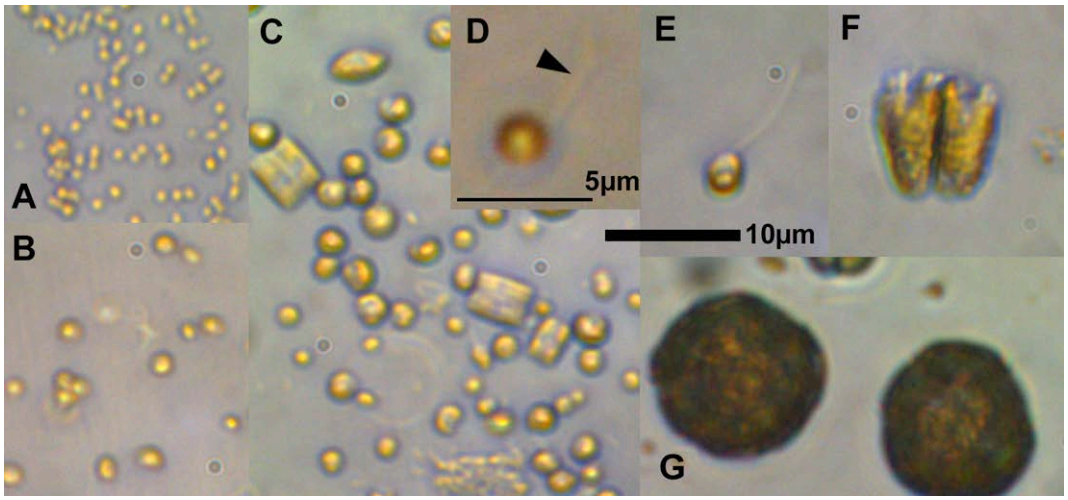

Fig. 4. Pico-nano size phytoplankton and distinctive haptophytes from K2.
A. *Synechococcus*, B-C. Pico-nano size phytoplankton growing in sub-cultures, D. *Triparma* sp. with a long spine (arrowhead), E. Nano-size phytofagellate, *Nephroselmis* sp., F. *Corymbellus* like colonial haptophyte, G. *Coccolithus pelagicus*. A-C, E-G are same scale.

Table 1. Species list confirmed from MR11-02 S1 and K2 samples.

Taxon	Species	S1*	Remarks**	K2*	Remarks**
Cyanobacteria	*Synechococcus* spp.	2	C, D, G	1	C, D, G
Cyanobacteria	*Prochlorococcus* sp.	1	C, D		
Bacillariophyceae (diatom)	*Actinoptychus* sp.			1	
Bacillariophyceae (diatom)	*Asterionellopsis* sp.	1	G	1	
Bacillariophyceae (diatom)	*Asteromphalus* sp.			1	
Bacillariophyceae (diatom)	*Bacteriastrum* sp.	1	G		
Bacillariophyceae (diatom)	*Chaetoceros* spp.	5	C, D, G	5	D, G
Bacillariophyceae (diatom)	*Corethron criophilum*			1	G
Bacillariophyceae (diatom)	*Coscinodiscus* spp.	3	C, G	3	D, G
Bacillariophyceae (diatom)	*Cylindrotheca* sp.	1	G		
Bacillariophyceae (diatom)	*Dactylosolen* sp.	1	C, G		
Bacillariophyceae (diatom)	*Ditylum* sp.	1	C, G		
Bacillariophyceae (diatom)	*Eucampia cornuta*	1	C, G		
Bacillariophyceae (diatom)	*Guinardia* sp.	1	C, G		
Bacillariophyceae (diatom)	*Leptocylindrus danicus*	1	C, G		
Bacillariophyceae (diatom)	*Minidiscus* sp.	1	D, G	1	G
Bacillariophyceae (diatom)	*Navicula* spp.	2	C, D, G	1	D, G
Bacillariophyceae (diatom)	*Pauliella* sp.	1	C, G		
Bacillariophyceae (diatom)	*Pseudonitzschia* spp.	2	C, D, G	1	D, G
Bacillariophyceae (diatom)	*Rhizosolenia* spp.	1	C, G	1	G
Bacillariophyceae (diatom)	*Skeletonema* sp.	1	C, D, G	1	G
Bacillariophyceae (diatom)	*Thalassionema* sp.	1	C, G	1	G
Bacillariophyceae (diatom)	*Thalassiosira* spp.	3	C, G	3	D, G
Bolidophyceae (Parmales)	*Triparma* spp.			3	D, G
Chlorophyceae	*Coelastrum* sp.	1	FW		
Chlorophyceae	*Pediastrum* sp.	1	FW		
Cryptophyceae	*Hillea* spp.	1	G	1	G
Cryptophyceae	*Rhodomonas* spp.	1	C, D, G	2	D, G

Cryptophyceae	*Teleaulax* sp.	1	C, G	1	G
Dictyochophyceae	*Dictyocha speculum*	1	C	1	D
Dictyochophyceae	*Pseudopedinella* sp.	1	C, G		
Dinophyceae	*Ceratium* spp.	3	C, G	2	
Dinophyceae	*Dinophysis* spp.	2	C		
Dinophyceae	*Gymnodinium* spp.	5	C, D, G	5	D
Dinophyceae	*Katodinium* spp.	1	C, G	1	G
Dinophyceae	*Lepidodinium* sp.	1	G		
Dinophyceae	*Prorocentrum dentatum*	1	C, G		
Dinophyceae	*Prorocentrum* spp.	2	G	2	G
Dinophyceae	*Thoracosphaera heimii*	1	G		
Dinophyceae	*Torodinium* sp.	1			
Euglenophyceae	*Trachelomonas* sp.	1	FW		
Haptophyceae	*Algiosphaera* sp.	1			
Haptophyceae	*Braarudosphaera bigelowii*	1			
Haptophyceae	*Calcidiscus* sp.	1	G		
Haptophyceae	*Calcisolenia* sp.	1	G		
Haptophyceae	*Calyptrosphaera* sp.	1	C, G		
Haptophyceae	*Chryaochromulina* spp.	3	C, G	3	G
Haptophyceae	*Coccolithus pelagicus*			1	G
Haptophyceae	*Corymbellus like species*			1	D, G
Haptophyceae	*Emiliania huxleyi*	1	C, D, G	1	G
Haptophyceae	*Gephyrocapsa oceanica*	1	C, D, G	1	G
Haptophyceae	*Helicospahera* sp.	1	G		
Haptophyceae	*Ophiaster* sp.	1			
Haptophyceae	*Phaeocystis* sp.	1	C, D, G	1	G
Haptophyceae	*Pontosphaera* sp.	1			
Haptophyceae	*Scyphosphaera* sp.	1			
Haptophyceae	*Syracosphaera* spp.	2	G	1	
Haptophyceae	*Umbilicosphaera sibogae* var. *foliosa*	1	G		
Haptophyceae	*U. sibogae* var. *sibogae*	1	G		
Pelagophyceae	unidentified species	1	G		
Prasinophyceae	*Halosphaera* spp.	2		2	
Prasinophyceae	*Micromonas* sp.	1	C, D, G	1	
Prasinophyceae	*Nephroselmis* sp.			1	G
Prasinophyceae	*Prasinococcus* sp.	1	C, D, G		
Prasinophyceae	*Pterosperma* spp.	2		2	
Prasinophyceae	*Pyramimonas* spp.	3	D, G	2	G
unknown greenish	nano coccoid	1	D, G	2	G
unknown greenish	pico coccoid	1	D, G	2	G
unknown greenish	pico-nano flagellate	1	G	1	G
unknown yellow-brownish	nano coccoid	1	D, G	4	D, G
unknown yellow-brownish	pico coccoid	2	D, G	3	D, G
unknown yellow-brownish	pico-nano flagellate	1	G	1	G
	Total species no.	**90**		**70**	

*) The number in the S1 and K2 column indicates expected species number. For example, "*Chaetoceros* spp. 5 in S1 column" means 5 species of *Chaetoceros* were observed in S1 samples.

**) Abbreviations in the Remarks column, D: dominant species, G: growth was confirmed in sub-cultured samples, C: cosmopolitan species distributing also in coastal region, FW: fresh water species.

4. Geophysical observation

4.1 Swath Bathymetry

Takeshi MATSUMOTO (University of the Ryukyus) : Principal Investigator（not on-board）
Masao NAKANISHI (Chiba University) : Principal Investigator（not on-board）
Kazuho YOSHIDA (Global Ocean Development Inc.: GODI)
Wataru TOKUNAGA (Mirai Crew)

(1) Introduction

R/V MIRAI is equipped with a Multi narrow Beam Echo Sounding system (MBES), SEABEAM 2112.004 (SeaBeam Instruments Inc.). The main objective of MBES is collecting continuous bathymetric data along ship's track to make a contribution to geological and geophysical investigations and global datasets. We carried out bathymetric survey throughout the MR11-02 cruise

(2) Data Acquisition

The "SEABEAM 2100" on R/V MIRAI was used for bathymetry mapping during the MR11-02 cruise from 11 February to 9 March 2011.

To get accurate sound velocity of water column for ray-path correction of acoustic multibeam, we used Surface Sound Velocimeter (SSV) data to get the sea surface (6.2m) sound velocity, and the deeper depth sound velocity profiles were calculated by temperature and salinity profiles from CTD and XCTD data by the equation in Del Grosso (1974) during the cruise.

Table 4.1-1 shows system configuration and performance of SEABEAM 2112.004 system.

Table 4.1-1 System configuration and performance

SEABEAM 2112.004 (12 kHz system)	
Frequency:	12 kHz
Transmit beam width:	2 degree
Transmit power:	20 kW
Transmit pulse length:	3 to 20 msec.
Depth range:	100 to 11,000 m
Beam spacing:	1 degree athwart ship
Swath width:	150 degree (max) 120 degree to 4,500 m 100 degree to 6,000 m 90 degree to 11,000 m
Depth accuracy:	Within < 0.5% of depth or +/-1m, whichever is greater, over the entire swath. (Nadir beam has greater accuracy; typically within < 0.2% of depth or +/-1m, whichever is greater)

(3) Preliminary Results

The results will be published after primary processing.

(4) Data Archives

Bathymetric data obtained during this cruise will be submitted to the Data Management Group (DMG) in JAMSTEC, and will be archived there.

(5) Remark

4.2 Sea surface gravity

Takeshi MATSUMOTO (University of the Ryukyus) : Principal Investigator（not on-board）
Masao NAKANISHI (Chiba University) : Principal Investigator（not on-board）
Kazuho YOSHIDA (Global Ocean Development Inc.: GODI)
Wataru TOKUNAGA (Mirai Crew)

:

(1) Introduction

The local gravity is an important parameter in geophysics and geodesy. We collected gravity data at the sea surface.

(2) Parameters

Relative Gravity [CU: Counter Unit]
[mGal] = (coef1: 0.9946) * [CU]

(3) Data Acquisition

We measured relative gravity using LaCoste and Romberg air-sea gravity meter S-116 (Micro-g LaCoste, LLC) during the MR11-02 cruise from 11 February to 9 March 2011.

To convert the relative gravity to absolute one, we measured gravity, using portable gravity meter (Scintrex gravity meter CG-3M), at Sekinehama as the reference points.

(4) Preliminary Results

Absolute gravity shown in Tabel 4.2-1

Table 4.2-1

No.	Date	U.T.C.	Port	Absolute Gravity [mGal]	Sea Level [cm]	Draft [cm]	Gravity at Sensor *1 [mGal]	L&R *2 Gravity [mGal]
#1	10 Feb.	00:18	Sekinehama	980371.92	250	650	980372.74	12655.50

*1: Gravity at Sensor = Absolute Gravity + Sea Level*0.3086/100 + (Draft-530)/100*0.0431
*2: LaCoste and Romberg air-sea gravity meter S-116

(5) Data Archives

Surface gravity data obtained during this cruise will be submitted to the Data Management Group (DMG) in JAMSTEC, and will be archived there.

(6) Remark

4.3 Sea Surface three-component magnetic field

Takeshi MATSUMOTO (University of the Ryukyus) : Principal Investigator（not on-board）
Masao NAKANISHI (Chiba University) : Principal Investigator（not on-board）
Kazuho YOSHIDA (Global Ocean Development Inc.: GODI)
Wataru TOKUNAGA (Mirai Crew)

(1) Introduction

Measurements of magnetic force on the sea are required for the geophysical investigations of marine magnetic anomaly caused by magnetization in upper crustal structure. We measured geomagnetic field using a three-component magnetometer during the MR11-02 cruise from 11 February 2011 to 9 March 2011.

(2) Principle of ship-board geomagnetic vector measurement

The relation between a magnetic-field vector observed on-board, **H**ob, (in the ship's fixed coordinate system) and the geomagnetic field vector, **F**, (in the Earth's fixed coordinate system) is expressed as:

Hob = **A R P Y F** + **H**p (a)

where **R**, **R** and **Y** are the matrices of rotation due to roll, pitch and heading of a ship, respectively. $\tilde{\mathbf{A}}$ is a 3 x 3 matrix which represents magnetic susceptibility of the ship, and **H**p is a magnetic field vector produced by a permanent magnetic moment of the ship's body. Rearrangement of Eq. (a) makes

B Hob + **H**bp = **R P Y F** (b)

where $\mathbf{B} = \mathbf{A}^{-1}$, and **H**bp = **-B H**p. The magnetic field, **F**, can be obtained by measuring **R**, **P**, **Y** and **H**ob, if **B** and **H**bp are known. Twelve constants in **B** and **H**bp can be determined by measuring variation of **H**ob with **R**, **P** and **Y** at a place where the geomagnetic field, **F**, is known.

(3) Instruments on *R/V MIRAI*

A shipboard three-component magnetometer system (Tierra Technica SFG1214) is equipped on-board *R/V MIRAI*. Three-axes flux-gate sensors with ring-cored coils are fixed on the fore mast. Outputs of the sensors are digitized by a 20-bit A/D converter (1 nT/LSB), and sampled at 8 times per second. Ship's heading, pitch, and roll are measured utilizing a ring-laser gyro installed for controlling attitude of a Doppler radar. Ship's position (GPS) and speed data are taken from LAN every second.

(4) Data Archives

Magnetic force data obtained during this cruise will be submitted to the Data Management Group (DMG) in JAMSTEC, and will be archived there.

(5) Remarks

1) For calibration of the ship’s magnetic effect, we made a “Figure eight” turn (a pair of clockwise and anti-clockwise rotation). The periods were follows;

i) 06:27UTC - 06:52UTC 14 Feb. 2011 around at 30-00N, 145-00E
ii) 02:19UTC - 02:37UTC 02 Mar. 2011 around at 47-00N, 160-00E

5. Satellite Image Acquisition (MCSST from NOAA/HRPT)

Kazuhiko MATSUMOTO (JAMSTEC): Principal Investigator
Kazuho YOSHIDA (Global Ocean Development Inc.: GODI)
Wataru TOKUNAGA (Mirai Crew)

(1) Objectives

It is our objectives to collect data of sea surface temperature in a high spatial resolution mode from the Advance Very High Resolution Radiometer (AVHRR) on the NOAA polar orbiting satellites and to build a time and depth resolved primary productivity model.

(2) Method

We receive the down link High Resolution Picture Transmission (HRPT) signal from NOAA satellites. We processed the HRPT signal with the in-flight calibration and computed the sea surface temperature by the Multi-Channel Sea Surface Temperature (MCSST) method. A daily composite map of MCSST data is processed for each day on the R/V MIRAI for the area, where the R/V MIRAI located.

We received and processed NOAA data throughout MR11-02 cruise from 11 February 2011 to 9 March 2011.

The sea surface temperature data will be applied for the time and depth resolved primary productivity model to determine a temperature field for the model.

(3) Preliminary results

Fig.5-1 showed MCSST composite image during this cruise from 11 February 2011 to 8 March 2011 at the Northern-west Pacific Ocean.

(4) Data archives

The raw data obtained during this cruise will be submitted to the Data Management Group (DMG) in JAMSTEC, and will be archived there.

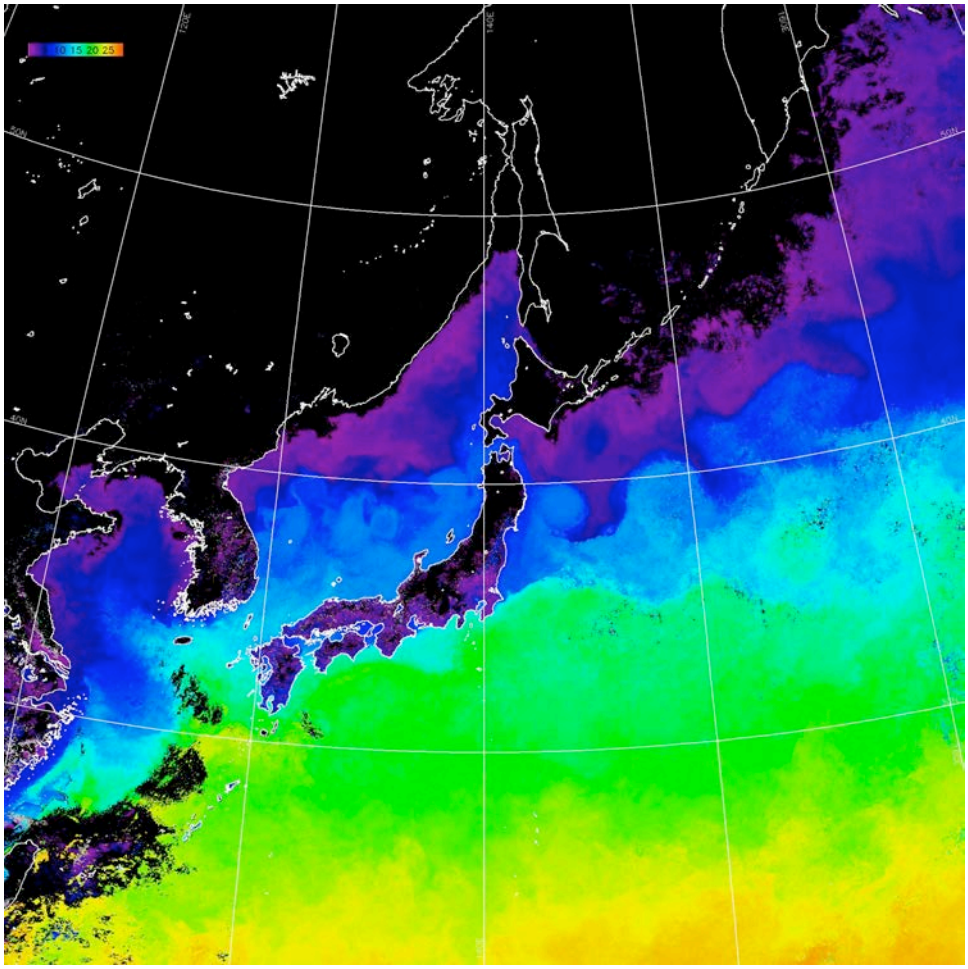

Fig.5-1 MCSST composite image at Northern-west Pacific Ocean.
from 11 February 2011 to 8 March 2011